

ANALOGUE COMPUTATION OF THE IMPEDANCE  
OF A POWERED FLYING CONTROL SYSTEM.

by

S.Q.H. Taqvi. Dip.A.M.(Sheff) G.I.Mech.E.

Submitted in fulfilment of the requirements  
for the degree of Master of Science.  
University of Aston in Birmingham.  
December, 1970

Supervised by

Professor E. Downham. Ph.D. B.Sc.(Eng) A.F.R.Ae.S.

Faculty of Engineering.  
Dept. of Mech. Eng.

Head of Department,  
Professor J. Ede.

*Thesis  
621.0052 TAA*  
11 JUN 71 138241

SYNOPSIS.

This thesis describes an investigation to determine the impedance of a powered flying control system by analogue simulation.

The first stage of this study is concerned with the impedance of a hydraulic servomechanism excited at its output end by a sinusoidal force whilst the input valve was locked in a neutral position. The first part of the analogue simulation investigated the impedance in the presence of the coulomb friction force. The effect on impedance of changes in the bulk modulus of the hydraulic fluid, the leakage across the jack piston and out of the jack, the magnitude of the coulomb friction, the supply pressure and the static valve opening has been determined.

The results from this simulation are compared with the results obtained from laboratory tests on the hydraulic servomechanism and a good agreement is shown to exist between the two results.

The second part of the analogue simulation investigated the impedance of the hydraulic servo in the absence of the coulomb friction force. The results from this simulation are compared with the theoretical results obtained by linearising the valve flow characteristics using the small perturbations technique. A qualitative agreement between these results has been shown to exist.

The second stage of this study investigated a technique for obtaining the impedance of the control system, consisting of the hydraulic servomechanism and the aircraft control surface, from measurements made separately on the hydraulic servomechanism and the aircraft control surface. It is shown that measurements of the direct response or mobility of the servomechanism can be combined with the direct and cross responses or mobilities of the control surface to give the control system response, mobility or impedance by using the sub-system technique.

CONTENTS.

<u>CHAPTER.</u>		<u>PAGE.</u>
1.	Introduction.	1
2.	Impedance and Mobility Methods.	5
3.	Theoretical Analysis of a Hydraulic Servomechanism.	30
4.	The Analogue Computer.	50
5.	Instrumentation.	68
6.	Analogue Simulation of a Hydraulic Servomechanism with Output End Excitation.	73
7.	Correlation of Analogue, Test Rig and Theoretical Results.	91
8.	An Experimental Approach for Obtaining the Control System Impedance by the Sub-System Method.	106
9.	Conclusions.	119
	References.	122
	Acknowledgements.	126

CHAPTER 1

INTRODUCTION.

CHAPTER 1.

INTRODUCTION.

CONTENTS.

PAGE.

1.1. The Hydraulic Servomechanism.	1
1.2. Control Problems Caused by Flutter.	1
1.3. Determination of Impedance of the Control System.	2
1.4. Objectives of the Present Investigation.	3

## CHAPTER 1

### INTRODUCTION.

#### 1.1. The Hydraulic Servomechanism.

The hydraulic servomechanism of the jack type is frequently made use of as a power amplifier in aircraft control systems. This is due to its large power to weight ratio, simplicity of design and the fact that it can be directly coupled to the aircraft control surface without the need for reduction gears as would be the case with rotary servomotors.

The servomechanism investigated in this study is a small hydraulic jack of the type used in a light fighter aircraft with a maximum stalling load of 1,870 lbf at a supply pressure 3,000 lbf/sq.in. It is diagrammatically shown in Fig.1.1. The jack piston is rigidly anchored to the aircraft structure and the jack body is connected to the control surface. To change the control surface position the pilot controls the movement of a fourway spool valve which connects one side of the jack to the pressure supply and the other side to the drain. The valve body being integral to the jack body moves along with it in such a manner as to close the ports and hence the jack body always follows the movement of the spool valve.

Conversely, if the jack body is forced to move by external forces while the position of the spool valve is fixed by the pilot's input, the ports will open connecting the two sides of the jack piston to the pressure supply and the drain respectively. This situation can set up oscillations of the control system and is encountered during flight due to flutter of the control surface.

#### 1.2. Control Problem Caused by Flutter.

Flutter is the aerodynamic excitation of an elastic surface moving through the air. It is caused by turbulence in the boundary

layer which produces fluctuating forces resulting in the oscillations of the surface. This excitation is of a broadband nature where both the low frequency and the high frequency modes of the surface are excited. The control surface structure having a large inertia is insensitive to high frequencies but responds to low frequencies extremely well. In the low frequency range the total sum of the fluctuating forces is tantamount to the application of a large force generator at the output end of the servomechanism and displaces the jack body relative to the piston. The movement of the jack body displaces the valve from its neutral position and hydraulic forces are brought into play to oppose this external force. The action of the hydraulic forces in opposing the external forces gives rise to the concept of impedance.

### 1.3. Determination of the Impedance of the Control System.

In order to predict the response of a powered flying control system to aerodynamic forces the impedance of the control system must be known. The ideal approach would be to excite the control surface of an aircraft on ground in the frequency range of interest and measure the resulting system impedance. This method is not practicable for several reasons. The servomechanism is a very stiff non-linear element and as such would require large force levels at the output end to produce any appreciable response. The control surface is comparatively less stiff and cannot tolerate large force levels unless the forces can be evenly distributed over the entire surface area as is the case during flight. Short of testing the control system in a high speed wind tunnel the only available approach is to carry out impedance measurements on the servomechanism and the control surface separately and to combine these measurements to obtain the overall control system impedance.

The servomechanism may be taken out of the aircraft and tested in a laboratory using commercially available vibrators having large force levels in the desired frequency range. In the absence of the servomechanism the control surface does not require large force levels and can be tested on the aircraft.

Experimental measurements of the impedance of the hydraulic servomechanism were performed in the laboratory by Penny (1). The general arrangement of the test rig for impedance measurement by excitation of the output end is shown in Fig.1.2. The load cell placed between the servo and vibrator was used to measure the force levels and also to provide the force feed back when the vibrator was force controlled. A linear differential transformer was used to measure the servo displacement and provided a feed back when the vibrator was displacement controlled. The effects on impedance of changes in such parameters as pressure supply, static valve opening and excitation amplitude were determined and compared with theoretical calculations of impedance obtained by linearising the flow characteristics through the valve ports. The present investigation is an extension of the experimental work the object of which are described below.

#### 1.4. Objectives of the Present Investigation.

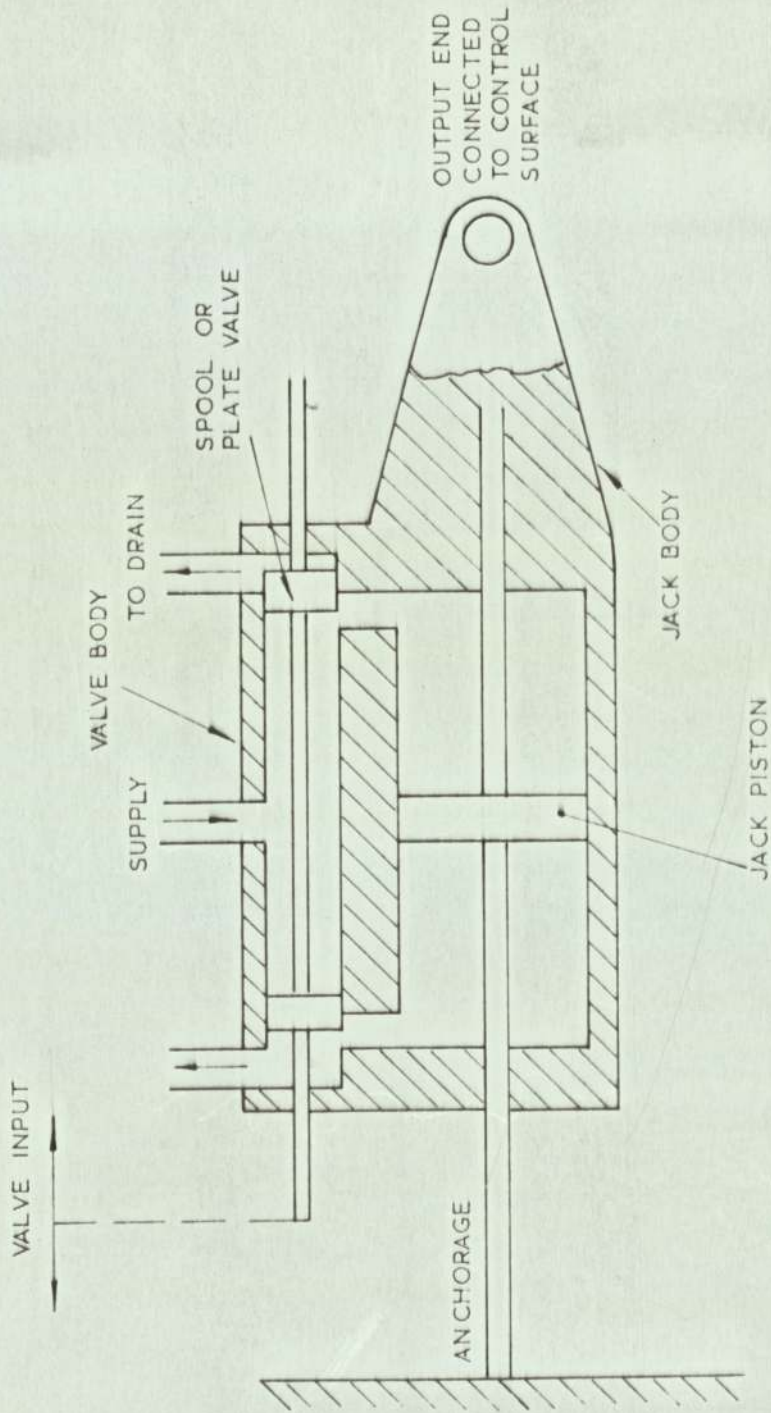
The main objects of the present study were to extend the range of experimental results obtained by Penny by an analogue simulation of the servomechanism, to check the validity of small perturbations technique for analysing non-linear systems, and to establish a technique for obtaining the impedance of the complete control system from separate measurements made on the control surface and the servomechanism.

The first stage of this study has been the analogue simulation of the hydraulic servomechanism for impedance measurements. Particular attention is given to the effects on impedance of changes in bulk modulus of hydraulic fluid, leakage across the jack piston and magnitude of the coulomb friction force since these parameters remain at a fixed value in the physical system. Effects on impedance of changes in static valve opening, excitation amplitude and supply pressure have also been examined.

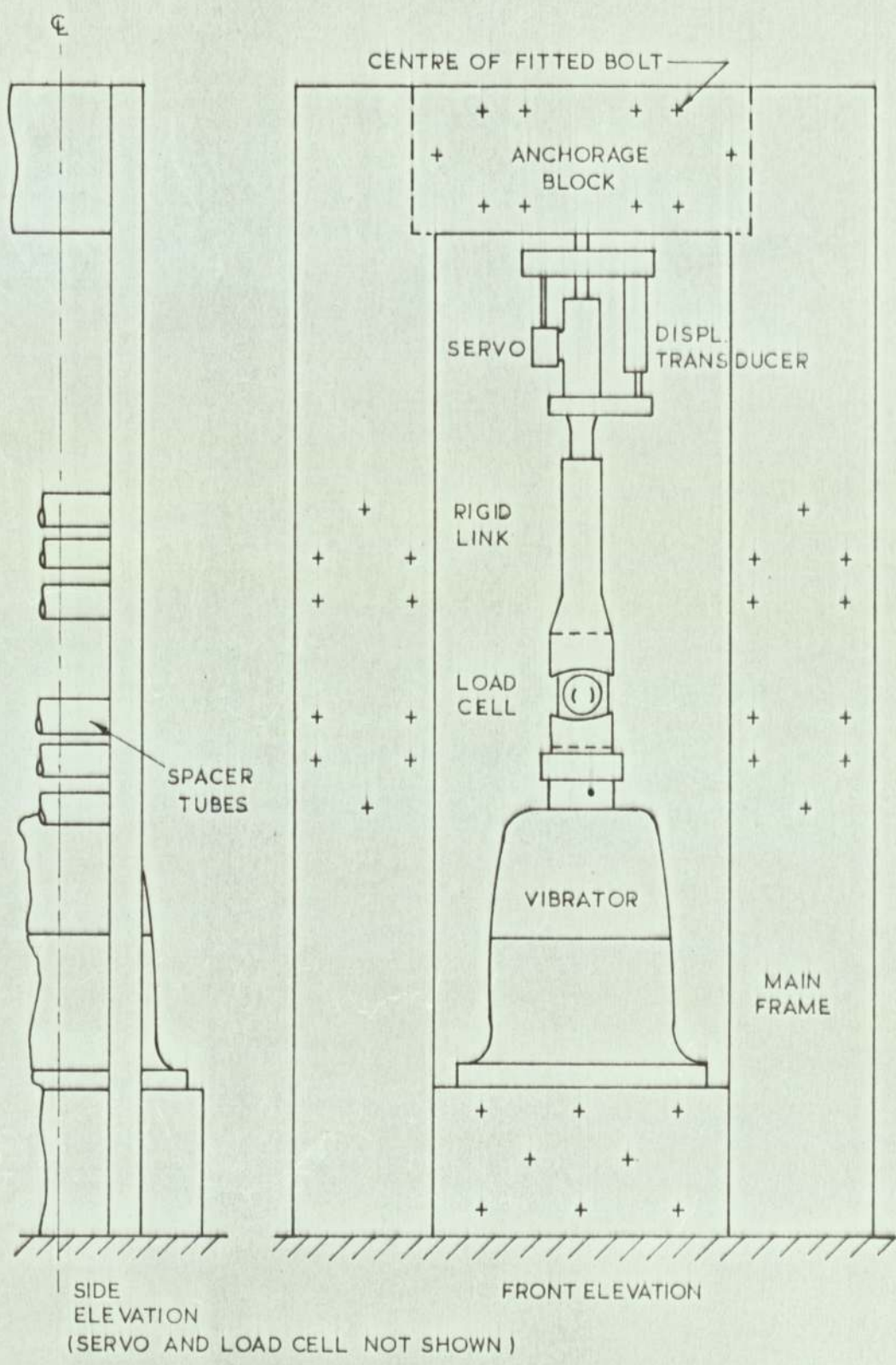
The first part of the simulation forms the study of the non-linear system where coulomb friction represents the principal non-linearity. The results obtained from this simulation are compared with the experimental results obtained on the test rig by Penny, and an estimation is made of such parameters as leakage across the jack piston and the bulk modulus of the hydraulic fluid for the physical system. The second part of the simulation is the study of the servomechanism impedance without the presence of the coulomb friction force. In this case the non-linearity is due to non-linear flow characteristics through the valve ports. Impedance measurements from this study check the validity of results of a digital computation which were obtained by linearising the flow characteristics using the small perturbations technique.

The second stage of this study is concerned with determining the overall control system impedance. A practical method has been devised to obtain the control system impedance by combining the impedances of the servomechanism and the control surface using the sub-system technique. Two simple elastic systems representing the hydraulic servo and the control surface were simulated on the analogue computer and their impedances were recorded on a magnetic tape. These impedances were then combined to obtain the overall control system impedance.

The concepts of impedance and mobility of mechanical systems are introduced and defined as used in vibration analysis in chapter 2.



SCHEMATIC OF A HYDRAULIC SERVOMECHANISM



GENERAL ARRANGEMENT OF TEST RIG  
SERVOMECHANISM IN A RIGID ENVIRONMENT

CHAPTER 2.

IMPEDANCE AND MOBILITY METHODS.

## CHAPTER 2.

### IMPEDANCE AND MOBILITY METHODS.

<u>CONTENTS.</u>	<u>PAGE.</u>
2.1. Notation.	5
2.2. Introduction.	8
2.3. Impedance and Mobility.	9
2.4. Analysis of Mechanical Elements.	10
2.5. Analysis of Mechanical Networks.	13
2.6. The component Mobility Method.	15
2.7. Driving Point and Transfer Response.	19
2.8. Reciprocal Property of Linear Systems.	22
2.9. The Normal Mode Mobility Method.	24

## CHAPTER 2.

2.1. Notation.

The following notation is used in this chapter.

$A_a$	$w/w_{na}$ , the ratio of the frequency of applied force to the natural frequency of the first mode.
$A_b$	$w/w_{nb}$ , the ratio of the frequency of applied force to the natural frequency of the second mode.
$C$	Damping constant (lb.sec/ft).
$F$	Harmonic force (lbf) $F_a$ , $F_b$ etc., denote forces in elements a and b of a system.
$j$	$(-1)^{\frac{1}{2}}$ .
$K$	Spring gradient (lb/in).
$K_i$	Effective spring gradient for a multi-degree of freedom system for mode i.
$M$	Mobility.
$M_D$	Displacement mobility of a system.
$M_V$	Velocity mobility of a system.
$M_A$	Acceleration mobility of a system.

A second subscript refers to mobility of an element in the system i.e.  $M_{Ds}$ ,  $M_{Dd}$ , and  $M_{Dm}$  represent displacement mobilities of a spring, a damper and a mass respectively.

- $M_{Vc}$  = Characteristic velocity mobility.
- $M_{Vc11a}$  = Characteristic velocity mobility of  $m_1$  for the first mode.
- $M_{Vc11b}$  = Characteristic velocity mobility of  $m_1$  for the second mode.
- $M_{Vc21a}$  = Characteristic velocity mobility of  $m_2$  for the first mode.
- $M_{Vc21b}$  = Characteristic velocity mobility of  $m_2$  for the second mode.
- $m$  = Mass (lb.sec<sup>2</sup>/ft.)
- $m_i$  = Effective mass for a multi-degree of freedom system for mode  $i$ .
- $m_{i11}$  = Effective mass for the driving point mobility for mode  $i$ .
- $m_{i21}$  = Effective mass for the transfer mobility for mode  $i$ .
- $R$  = Response (displacement, velocity or acceleration).
- $t$  = Time.
- $w$  = Forcing frequency (radians/second).
- $w_i$  = Natural frequency for mode  $i$ .
- $w_n$  = Natural frequency of a system.
- $w_{na}$  = Natural frequency of the first mode.

- $w_{nb}$  = Natural frequency of the second mode.
- $x$  = Harmonic displacement.
- $x_{1a}$  = Displacement of mass  $m_1$  for the first mode.
- $x_{1b}$  = Displacement of mass  $m_1$  for the second mode.
- $x_{2a}$  = Displacement of mass  $m_2$  for the first mode.
- $x_{2b}$  = Displacement of mass  $m_2$  for the second mode.
- $\dot{x}$  =  $\frac{dx}{dt}$
- $Z$  = Impedance of a system.
- $Z_D$  = Displacement impedance of a system.
- $Z_V$  = Velocity impedance of a system.
- $Z_A$  = Acceleration impedance of a system.

A second subscript refers to impedance of an element in the system, i.e.  $Z_{Ds}$ ,  $Z_{Dd}$ , and  $Z_{Dm}$  represent displacement impedances of a spring, a damper and a mass respectively.

- $Z_{11}$  Driving point impedance for a multi-degree of freedom system for a forced excitation at mass  $m_1$ .
- $Z_{21}$  Transfer impedance or the impedance at mass  $m_2$  for a forced excitation at mass  $m_1$ .
- $Z_{22}$  Driving point impedance at mass  $m_2$  for a forced excitation at  $m_2$ .
- $Z_{12}$  Transfer impedance at mass  $m_1$  for a forced excitation at mass  $m_2$ .

## 2.2. Introduction.

The classical method of vibration analysis of a mechanical system is to apply Newton's laws of motion and solve the resulting differential equations to yield the system response. With an increasing number of degrees of freedom the differential equations become difficult to manipulate and do not easily lend themselves to an interpretation of the system behavior in response to changes in the system parameters. Such systems are experimentally analysed by analogue techniques (2) and (3). A basic study of electrical networks shows the mathematical similarity between these networks and the dynamics systems (4) and (5). Hence extensive use is made of electrical analogies for solution of problems in vibrations and control systems.

Dynamic systems may be simulated either by the mass-capacitance or the mass-inductance analogy. The former is the force-current analogy in which stiffness, damping and inertia are represented by inductance, resistance and capacitance respectively. The latter is the force-voltage analogy in which stiffness, damping and inertia are represented by capacitance, resistance and inductance respectively. The force-current analogy is more direct of the two analogies and forms the basis of impedance and mobility methods.

In the course of analysing linear electric circuits carrying alternating currents, electrical engineers observed that the voltage-current relationship was independent of the amplitude of the applied sinusoidal voltage and a function of frequency only. This ratio was termed the network impedance and led to the development of impedance techniques whereby the response characteristics of complex networks could be obtained by considering the impedance of the individual elements of a network and the manner in which they were connected together. This approach was finally adopted for the analysis of mechanical systems and meant that these systems could

be analysed without recourse to their electrical analogues (6), (7) and (8).

### 2.3. Impedance and Mobility.

#### 2.3.1. Impedance.

Impedance in a mechanical system is the ability of a point to resist motion and as such is defined as the ratio of an applied force to the resulting response. In general the forces are considered to be sinusoidal and the elastic system as being linear. The response to be used can be either displacement, velocity or acceleration depending upon the frequency of the applied force and the nature of the problem. At the lowest frequencies displacement response can be used as the stresses are proportional to displacement. Where impact loading occurs and at higher frequencies when the stresses are more accurately proportional to velocity the velocity response is used. Acceleration response is used when inertia loading is the principal cause of vibration and at higher frequencies when acceleration is more easily measured. The impedance  $Z$  is defined as:-

$$Z = F/R \quad (2.1)$$

where  $F = F \exp j\omega t,$

$$R = R \exp j\omega t.$$

and  $\exp j\omega t = \cos \omega t + j \sin \omega t.$

Hence impedance is a complex quantity.

#### 2.3.2 Mobility.

Mobility in a mechanical system is the ability of a point to respond to an applied force and is defined as the ratio of the response

to the applied force. It is, therefore, the inverse of impedance and is also known as receptance or mechanical admittance (9).

The mobility  $M$  is defined as

$$M = R/F \quad (2.2)$$

where  $R$  is the complex displacement, velocity or acceleration response.

For the analysis of a problem either the mobility or the impedance equations can be used depending on the problem as one will require less algebraic manipulation than the other.

#### 2.4. Analysis of Mechanical Elements.

Mechanical systems have active and passive elements. The active elements are the force and displacement generators and the passive elements are springs, dampers and inertias. In mechanical networks springs and dampers are connected between two other elements or with one end fixed to a rigid support. The mass is a single ended element and when placed between two other elements it is considered to be inparallel with one element and the parallel combination is considered to be placed in series with the other element. The impedances and mobilities of the passive mechanical elements for any type of response can be derived by considering the equations of motion for each element.

##### 2.4.1 Displacement Response.

The ratio of maximum force to maximum displacement is termed the displacement impedance and is represented by  $Z_D$ .

Spring. The equation of motion for a spring is:-

$$F = Kx$$

$$\text{and } Z_{Ds} = \frac{F}{x} = \frac{Kx}{x}$$

$$\therefore Z_{Ds} = K \quad (2.3)$$

Damper. For viscous damping:-

$$\begin{aligned}
 F &= C\dot{x} \\
 &= Cj\omega x \\
 \text{and } Z_{Dd} &= \frac{F}{x} = Cj\omega
 \end{aligned}
 \tag{2.4}$$

Mass. The equation of motion for a mass is:-

$$\begin{aligned}
 F &= m\ddot{x} = -m\omega^2 x \\
 \therefore Z_{Dm} &= \frac{F}{x} = -m\omega^2
 \end{aligned}
 \tag{2.5}$$

The displacement mobility, the ratio of maximum displacement to maximum force, is simply the inverse of displacement impedance. The mobility form of equations (2.3) to (2.5) is:-

$$M_{Ds} = \frac{1}{Z_{Ds}} = \frac{1}{K} \tag{2.6}$$

$$M_{Dd} = \frac{1}{Z_{Dd}} = \frac{-j}{C\omega} \tag{2.7}$$

$$M_{Dm} = \frac{1}{Z_{Dm}} = -\frac{1}{m\omega^2} \tag{2.8}$$

When displacement response is used the real part of the complex impedance represents the energy stored in the system and is termed the stiffness or resistance of the system. The imaginary part of the complex impedance represents the energy dissipated in the system and is termed the damping or reactance of the system.

### 2.4.2 Velocity Response.

The velocity impedance  $Z_V$  is the ratio of maximum force to maximum velocity.

$$\begin{aligned}
 \text{Spring.} \quad F &= Kx \\
 \text{also } x &= \frac{\dot{x}}{j\omega} \\
 \therefore F &= \frac{K\dot{x}}{j\omega} \\
 \text{and } Z_{Vs} &= \frac{F}{\dot{x}} = -\frac{jK}{\omega} \quad (2.9)
 \end{aligned}$$

$$\begin{aligned}
 \text{Damper.} \quad F &= C\dot{x} \\
 \text{and } Z_{Vd} &= \frac{F}{\dot{x}} = C \quad (2.10)
 \end{aligned}$$

$$\begin{aligned}
 \text{Mass.} \quad F &= m\ddot{x} = mj\omega\dot{x} \\
 \text{and } Z_{Vm} &= \frac{F}{\dot{x}} = j\omega m \quad (2.11)
 \end{aligned}$$

With velocity response the stiffness and the damping are represented by imaginary and real parts of the complex impedance respectively.

### 2.4.3 Acceleration Response.

The ratio of maximum force to maximum acceleration is termed the acceleration impedance  $Z_A$ .

Spring.

$$F = Kx$$

$$\text{also } x = - \frac{\ddot{x}}{w^2}$$

$$\therefore F = - \frac{K\ddot{x}}{w^2}$$

$$\text{and } Z_{As} = \frac{F}{\ddot{x}} = - \frac{K}{w^2} \quad (2.12)$$

Damper.

$$F = C\dot{x}$$

$$\text{also } \dot{x} = \frac{\ddot{x}}{jw}$$

$$\therefore F = \frac{C\ddot{x}}{jw}$$

$$\text{and } Z_{Ad} = \frac{F}{\ddot{x}} = - \frac{Cj}{w} \quad (2.13)$$

Mass.

$$F = m\ddot{x}$$

$$Z_{Am} = \frac{F}{\ddot{x}} = m \quad (2.14)$$

## 2.5. Analysis of Mechanical Networks.

Mechanical networks may be formed by connecting together any number of mechanical elements in series, parallel, and a series-parallel combination. The networks impedance is obtained by combining the impedances of individual elements according to series or parallel laws of impedance addition.

### 2.5.1. Elements Connected in Series.

In a series arrangement of a mechanical network the same force acts through all the elements and the system response is the sum of the responses of the individual elements. Referring to Fig.2.1a and considering displacement response

$$F = F_1 = F_2 = F_3 \quad (2.15)$$

$$x = x_1 + x_2 + x_3 \quad (2.16)$$

$$\text{now } Z = \frac{F}{x} = \frac{F}{(x_1 + x_2 + x_3)}$$

$$\text{or } \frac{1}{Z} = \frac{(x_1 + x_2 + x_3)}{F}$$

$$\therefore \frac{1}{Z} = \frac{1}{Z_1} + \frac{1}{Z_2} + \frac{1}{Z_3} \quad (2.17)$$

also  $\frac{1}{Z}$  is the mobility  $M$

$$\therefore M = M_1 + M_2 + M_3 \quad (2.18)$$

In a series arrangement the system mobility is the direct sum of the element mobilities.

### 2.5.2. Elements Connected in Parallel.

In a parallel arrangement of a mechanical network the response is the same for all the elements but the force acting on the system is the sum of the forces acting on individual elements.

Referring to Fig.2.1b

$$F = F_1 + F_2 + F_3 \quad (2.19)$$

$$x = x_1 = x_2 = x_3 \quad (2.20)$$

and 
$$Z = \frac{(F_1 + F_2 + F_3)}{x}$$

$$\therefore Z = Z_1 + Z_2 + Z_3 \quad (2.21)$$

but 
$$Z = \frac{1}{M}$$

$$\therefore \frac{1}{M} = \frac{1}{M_1} + \frac{1}{M_2} + \frac{1}{M_3} \quad (2.22)$$

In a parallel arrangement the system impedance is the direct sum of the element impedances and the reciprocal mobility is the sum of the element reciprocal mobilities.

Mechanical networks are not always in a pure series or a pure parallel arrangement. They are generally a combination of both the arrangements. There are two methods available for impedance and mobility analysis of mechanical networks; these are the component mobility method and the normal mode mobility method (8) and are described in sections 2.6 and 2.9 respectively.

## 2.6. The Component Mobility Method.

The component mobility method consists essentially of calculating the mobilities of the elements of a system and combining these according to parallel or series laws of addition to obtain

the system mobility or impedance. This technique is very useful for the analysis of simple mechanical systems.

Consider the single degree of freedom system consisting of a mass supported by a spring and a damper, Fig.2.2a. The diagram in Fig.2.2b is a schematic representation of the mechanical system and shows the manner in which the elements are connected. The force  $F \exp j\omega t$  is applied to the mass  $M$  and causes it to oscillate at a frequency  $\omega$ (rad/sec.) of the applied force. The ends of the spring and the damper attached to the rigid support have zero deflections and are shown grounded in the schematic diagram. The other two ends connected to the mass have the same deflection as that of the mass and hence the three elements are connected in a parallel arrangement as explained in 2.5.3. Since the motion of the mass and the applied force must be measured with reference to an inertial frame they are also shown grounded.

The point of application of the force changes the mode of connection between the elements. This can be demonstrated by applying the force to the support of the mechanical system of Fig.2.2a as shown in Fig.2.3a. The mobility schematic, Fig.2.3b, shows how the elements are connected. The ends of the spring and the damper connected to the support share the displacement experienced by the support and as such are connected in parallel. The other two ends connected to the mass have a displacement in common with the mass but different to that of the support. Alternately, the points attached to the mass share the force experienced by the mass and, hence, are connected in series. Therefore the parallel spring-damper combination acts in series with the mass.

The combined velocity mobility,  $M_v$ , of the system of Fig.2.2a can be determined by considering the mobility schematic diagram. Since the elements are in parallel the system impedance is the direct sum of the element impedances:-

$$Z_V = Z_{Vd} + Z_{Vs} + Z_{Vm} \quad \text{from (2.21)}$$

$$\text{and } M_V = \frac{1}{Z_V} = \frac{1}{Z_{Vd} + Z_{Vs} + Z_{Vm}} \quad (2.23)$$

Substituting the values of elements in impedances from equations (2.9) to (2.11) into (2.23),

$$M_V = \frac{1}{C + \frac{K}{j\omega} + j\omega m}$$

or 
$$M_V = \frac{j\omega (K - m\omega^2) + C\omega^2}{(K - m\omega^2)^2 + C^2\omega^2} \quad (2.24)$$

Equations (2.24) represents the complex velocity mobility which may be separated into its real and imaginary parts.

$$M_V \text{ Rl} = \frac{C\omega^2}{(K - m\omega^2)^2 + C^2\omega^2} \quad (2.25)$$

$$M_V \text{ Imag.} = \frac{j\omega (K - m\omega^2)}{(K - m\omega^2)^2 + C^2\omega^2} \quad (2.26)$$

Equations (2.25) and (2.26) can be vectorially represented on an Argand diagram as shown in Fig.2.4. The modulus of the velocity mobility is obtained in the following manner

$$M_V = \left[ (M_V \text{ Rl})^2 + (M_V \text{ Imag.})^2 \right]^{\frac{1}{2}}$$

$$M_V = \frac{\omega}{\left[ (C\omega)^2 + (K - m\omega^2)^2 \right]^{\frac{1}{2}}} \quad (2.27)$$

$$\text{and the argument } \theta = \tan^{-1} \left[ \frac{M_V \text{ imag.}}{M_V \text{ Rl.}} \right]$$

$$\theta = \tan^{-1} \left[ \frac{K - m\omega^2}{C\omega} \right] \quad (2.28)$$

One of the advantages of velocity mobility is that it can be plotted on a special log-log graph paper as shown in Fig.2.5. The straight lines represent the element mobilities. The combined velocity mobility (solid line) is asymptotic to the spring mobility line at frequencies below the system natural frequency. This means that the system is spring controlled at these frequencies and the effect of inertia is negligible. At frequencies above the natural frequency the system is controlled entirely by the inertia and the combined mobility line is now asymptotic to the mass mobility line. At resonance the magnitude of the combined mobility is limited by the damping force, which in the absence of damping tends to infinity as shown by the broken line, and the curve is tangential to the damper mobility line or the system is damper controlled. This condition is obtained when the angle  $\theta$  is zero, that is, the imaginary part of the combined mobility is zero. The point of intersection of the mass and the spring mobilities is located at the undamped natural frequency of the system and is known as the characteristic mobility  $M_{Vc}$ . At this point the spring and the mass mobilities are equal in magnitude but of opposite signs, thus,

$$M_{Vs} - M_{Vm} = 0 \quad (2.29)$$

Substituting the values of spring and mass mobilities in equation (2.29) gives:-

$$\frac{j\omega}{K} - \frac{j}{m\omega} = 0 \quad (2.30)$$

Solution of (2.30) for  $\omega$  yields the well known expression for the natural frequency,  $\omega = (K/m)^{\frac{1}{2}}$ .

## 2.7. Driving Point and Transfer Response.

In a multi-degree of freedom system there exists a response for each degree of freedom or for each mass. To help simplify the analysis of such systems it is necessary to define and label these responses. The two degree of freedom system, Fig.2.6a, will have a response for each of the masses  $m_1$  and  $m_2$  if displaced from its equilibrium position. If a harmonic forcing function  $F \cos \omega t$  is applied at mass  $m_1$ , the displacement response of this mass is called the 'direct response' or the 'driving point' response and is labeled as  $x_{11}$ . The response of the mass  $m_2$  due to excitation at mass  $m_1$  is called the 'cross response' or the transfer response and is labeled as  $x_{21}$ . This convention is also applied to mobilities and impedances. Thus the driving point impedance  $Z_{11}$  is the impedance at mass  $m_1$  for excitation at  $m_1$  and the transfer impedance  $Z_{21}$  is the impedance at mass  $m_2$  for excitation at  $m_1$ . In general, the first subscript refers to the point where the response is measured and the second subscript refers to the point where the exciting force is applied. In the system of Fig.2.6a if the harmonic force is now applied at mass  $m_2$ , the driving point impedance will be defined as  $Z_{22}$  and the transfer impedance as  $Z_{12}$ .

The driving point and transfer impedances for systems having more than one degree of freedom may be calculated by the component method. For the two degree of freedom system of Fig.2.6a the displacement impedances for the elements are:-

$$Z_{K1} = K_1$$

$$Z_{K2} = K_2$$

$$Z_{m1} = -m_1 \omega^2$$

$$Z_{m2} = -m_2 \omega^2$$

For the exciting force applied at mass  $m_1$ , Fig.2.6b represents the schematic diagram. In branch C the mass  $m_1$  and the spring  $K_1$

act in parallel and the impedance at C is given by

$$Z_C = Z_{K1} + Z_{m1}$$

$$Z_C = K_1 - m_1 w^2 \quad (2.31)$$

In branch b the spring  $K_2$  and the mass  $m_2$  act in series and, hence, the impedance at b is given by:-

$$\frac{1}{Z_b} = \frac{1}{Z_{K2}} + \frac{1}{Z_{m2}}$$

$$Z_b = \frac{Z_{K2} \cdot Z_{m2}}{Z_{K2} + Z_{m2}}$$

$$\therefore Z_b = - \frac{K_2 m_2 w^2}{K_2 - m_2 w^2} \quad (2.32)$$

The impedance at point a, which is the driving point impedance  $Z_{11}$ , is the sum of the impedances of the branches b and c. Since the two branches act in parallel,

$$Z_{11} = Z_a = Z_c + Z_b$$

$$= K_1 - m_1 w^2 - \frac{K_2 m_2 w^2}{K_2 - m_2 w^2}$$

$$\therefore Z_{11} = \frac{m_1 m_2^2 w^4 - m_1 [K_1 m_2 + K_2 (m_1 + m_2)] \cdot w^2 + K_1 K_2}{K_2 - m_2 w^2} \quad (2.33)$$

For the transfer impedance,  $Z_{21}$ , consider the force acting on branch b in the schematic diagram. Let this force be denoted by  $F_b$  then,

$$F_b = \frac{F_b}{F} F$$

dividing top and bottom of the R.H.S. of this expression by  $x_1$ , the displacement of  $m_1$  which is common to both the branches

$$F_b = \frac{Z_b}{Z_{11}} F \quad (2.34)$$

Now  $x_2$ , the displacement of the mass  $m_2$ , is:-

$$x_2 = \frac{F_b}{Z_{m2}} \quad (2.35)$$

Substituting equation (2.34) in (2.35):-

$$x_2 = \frac{Z_b}{Z_{11} \cdot Z_{m2}} \cdot F \quad (2.36)$$

$$\text{Now } Z_{21} = \frac{F}{x_2} = \frac{Z_{11} \cdot Z_{m2}}{Z_b} \quad (2.37)$$

Substituting the values of  $Z_{11}$ , and  $Z_{m2}$  and  $Z_b$  in equation (2.37) and simplifying gives:-

$$Z_{21} = \frac{m_1 m_2 w^4 - K_1 m_2 + K_2 (m_1 + m_2) w^2 + K_1 K_2}{K_2} \quad (2.38)$$

Comparing the equations for the driving point and the transfer impedances, equations (2.33) and (2.38), it is seen that the numerator in both the cases is the same. This is a property of the impedance and mobility equations. If the numerator is equated to zero, it gives the frequency equation of the system which may be solved to obtain the values of the natural frequencies.

## 2.8. Reciprocal Property of Linear Systems.

Consider the two degree of freedom system with a harmonic force applied to mass  $m_2$  as shown in Fig.2.7a. The schematic diagram showing the mode of connection of the components (Fig.2.7b) is different to the schematic of Fig.2.6b which represents the case for the harmonic force applied at mass  $m_1$ . Using the laws of impedance addition the driving point impedance  $Z_{22}$  is given by:-

$$Z_{22} = Z_a = Z_c + Z_b$$

and

$$Z_c = \frac{Z_{K2} \cdot Z_d}{Z_{K2} + Z_d}$$

$$Z_c = \frac{K_2 (K_1 - m_1 \omega^2)}{K_1 + K_2 - m_1 \omega^2} \quad (2.39)$$

$$\text{since } Z_d = K_1 - m_1 \omega^2$$

$$\text{and } Z_b = Z_{m2} = -m_2 \omega^2$$

Substituting the values of  $Z_c$  and  $Z_b$  in equation (2.39)

$$Z_{22} = \frac{m_1 m_2 \omega^4 - [K_1 m_2 + K_2 (m_1 + m_2)] \omega^2 + K_1 K_2}{K_1 + K_2 - m_1 \omega^2} \quad (2.40)$$

For the transfer impedance,  $Z_{12}$ , consider the force acting on branch c and let it be denoted by  $F_c$ . Since  $K_2$  and the sub-branch d act in series, the same force acts at points c and d, that is:-

$$F_d = F_c = \frac{F_c}{F} \cdot F \quad (2.41)$$

Multiplying top and bottom of R.H.S. of equation (2.41) by  $x_2$ , the displacement of mass  $m_2$  which is common to both the branches b and c

gives 
$$F_d = \frac{Z_c}{Z_{22}} \cdot F \quad (2.42)$$

also 
$$F_d = F_{K1} + F_{m1} = (K_1 - m_1 \omega^2) x_1$$

$\therefore$  
$$x_1 = \frac{F_d}{K_1 - m_1 \omega^2} = \frac{F_d}{Z_d} \quad (2.43)$$

Substituting for  $F_d$  in equation (2.43) from (2.42)

$$x_1 = \frac{Z_c}{Z_{22} \cdot Z_d} F$$

but 
$$Z_{12} = \frac{F}{x_1} = \frac{Z_{22} \cdot Z_d}{Z_c} \quad (2.44)$$

inserting in equation (2.44) the values of  $Z_c$ ,  $Z_{22}$  and  $Z_d$  from equations (2.39), (2.40) and (2.43) and simplifying gives

$$Z_{12} = \frac{m_1 m_2 \omega^4 - [K_1 m_2 + K_2 (m_1 + m_2)] \omega^2 + K_1 K_2}{K_2} \quad (2.45)$$

Comparing equations (2.45) and (2.38), it is seen that the transfer impedance with the harmonic force applied at mass  $m_2$  is equal to the transfer impedance with the harmonic force applied at mass  $m_1$ , or

$$Z_{12} = Z_{21} \quad (2.46)$$

Equation (2.46) defines an important property of linear systems which is known as the reciprocal property or simply as the reciprocity of linear systems. The existence of this property

has long been appreciated and has been dealt with in terms of mobilities in (10); where as Rayleigh (11) has provided a proof of reciprocity in terms of lagrange equations. The impedance and mobility techniques can be used to show that the transfer impedance or mobility between any pair of co-ordinates in a system are equal. In general, if a system has multi-degrees of freedom, the reciprocity can be expressed as:-

$$Z_{ij} = Z_{ji} \quad (2.47)$$

Equation (2.47) means that the impedance at station i due to an excitation at station j equals the impedance at station j due to an excitation at station i. This statement holds for a system with any number of degrees of freedom as long as the condition of linearity is fulfilled.

### 2.9. The normal Mode Mobility Method.

For systems having more than one degree of freedom the normal mode mobility is used for simplified analysis. It is based on the concept of modes of vibration of a system. A system having n degrees of freedom has associated with it n natural frequencies or resonances. At each natural frequency there exists a unique amplitude ratio between the displacements of the masses,  $x_2/x_1$  etc., and is termed the normal mode of vibration. If a multi-degree of freedom system is excited by a harmonic force then the response of each mass in the system is the algebraic sum of the responses produced due to each mode. The system of Fig.2.6a will have two natural frequencies and, hence, two normal modes of vibration. The two natural frequencies may be found by equating to zero the numerator of equation (2.33):-

$$m_1 m_2 w^4 - [K_1 m_2 + K_2 (m_1 + m_2)] w^2 + K_1 K_2 = 0$$

or

$$w_n^2 = \frac{K_1 + K_2}{2m_1} + \frac{K_2}{2m_2} \pm \left[ \left( \frac{K_1 + K_2}{2m_1} + \frac{K_2}{2m_2} \right)^2 - \frac{K_1 K_2}{m_1 m_2} \right]^{\frac{1}{2}} \quad (2.48)$$

The lower value of  $w_n$  may be designated to the first mode and the higher value of  $w_n$  to the second mode. Denoting the first mode by subscript a and the second mode by the subscript b the displacements and velocities of the masses  $m_1$  and  $m_2$  due to excitation of the mass  $m_1$  will be

$$x_1 = x_{1a} + x_{1b} \quad (2.49)$$

$$x_2 = x_{2a} + x_{2b}$$

$$\text{and } \dot{x}_1 = \dot{x}_{1a} + \dot{x}_{1b} \quad (2.50)$$

$$\dot{x}_2 = \dot{x}_{2a} + \dot{x}_{2b}$$

The driving point and the transfer velocity mobilities can be obtained by dividing equations (2.50) by maximum value of the applied force, thus

$$M_{V11} = \frac{\dot{x}_1}{F} = \frac{\dot{x}_{1a}}{F} + \frac{\dot{x}_{1b}}{F}$$

$$\text{or } M_{V11} = M_{V11a} + M_{V11b} \quad (2.51)$$

$$M_{V21} = \frac{\dot{x}_2}{F} = \frac{\dot{x}_{2a}}{F} + \frac{\dot{x}_{2b}}{F}$$

$$\text{or } M_{V21} = M_{V21a} + M_{V21b} \quad (2.52)$$

The modulus of the driving point and transfer mobilities can be written in terms of the characteristic mobilities and the ratio

of the frequency of the applied force to the natural frequency relating to each mode (8)

$$M_{V11} = \frac{M_{Vc11a}}{A_a - \frac{1}{A_a}} + \frac{M_{Vc11b}}{A_b - \frac{1}{A_b}} \quad (2.53)$$

$$M_{V21} = \frac{M_{Vc21a}}{A_a - \frac{1}{A_a}} + \frac{M_{Vc21b}}{A_b - \frac{1}{A_b}} \quad (2.54)$$

where  $M_{Vc}$  is the characteristic mobility

$A_a = w/w_{na}$ , the ratio of the forcing frequency to the natural frequency of the first mode.

$A_b = w/w_{nb}$ , the ratio of the forcing frequency to the natural frequency of the second mode.

The characteristic velocity mobility was defined with reference to Fig.2.5 as the point of intersection of the spring and the mass mobility lines. Hence the value of characteristic mobility equals that of either the mass mobility or the spring mobility at the natural frequency, thus

$$M_{Vc} = \frac{j}{mw} = \frac{jw}{K} \quad (2.55)$$

replacing  $w$  by  $w_n = (K/m)^{\frac{1}{2}}$  in the above equation and noting that  $j$  merely indicates direction,

$$M_{Vc} = \frac{1}{(Km)^{\frac{1}{2}}} \quad (2.56)$$

For a multi-degree of freedom system equation (2.56) may be written in terms of effective mass  $m_i$  and effective spring gradient  $K_i$  for mode  $i$ , where  $i$  is any integer, as:-

$$M_{Vc} = \frac{1}{(K_i m_i)^{\frac{1}{2}}} \quad (2.57)$$

The effective mass  $m_i$  for any normal mode of a system is a single mass that has the same kinetic energy as the system itself at the natural frequency pertaining to the normal mode under consideration, and is referred to the point where the response is measured. It may be obtained by equating kinetic energies at a natural frequency. The expression for the effective mass,  $m_{ill}$ , for the driving point velocity mobility, equation (2.53), will be:-

$$\frac{1}{2} m_{ill} V_1^2 = \frac{1}{2} m_1 V_1^2 + \frac{1}{2} m_2 V_2^2$$

$$\therefore m_{ill} = \frac{m_1 V_1^2 + m_2 V_2^2}{V_1^2}$$

replacing  $V$  by  $wx$ , where  $x$  are the amplitudes of the masses at the natural frequency of the mode under consideration:-

$$m_{ill} = \frac{m_1 x_1^2 + m_2 x_2^2}{x_1^2} \quad (2.58)$$

and hence, the effective masses for the driving point characteristic mobilities,  $M_{Vc11a}$  and  $M_{Vc11b}$ , are respectively:-

$$m_{illa} = \frac{m_1 x_{1a}^2 + m_2 x_{2a}^2}{x_{1a}^2} \quad (2.59)$$

$$m_{illb} = \frac{m_1 x_{1b}^2 + m_2 x_{2b}^2}{x_{1b}^2} \quad (2.60)$$

The effective mass,  $m_{i2l}$ , for the transfer mobility is referred to the transfer point and may be obtained as follows

$$\frac{1}{2} (m_{i2l} V_1^2) \frac{V_2}{V_1} = \frac{1}{2} m_1 V_1^2 + \frac{1}{2} m_2 V_2^2$$

putting  $V = wx$ , we get

$$m_{i2l} = \frac{m_1 x_1^2 + m_2 x_2^2}{x_1 \cdot x_2} \quad (2.61)$$

and the effective masses for the transfer mobilities  $M_{Vc21a}$  and  $M_{Vc21b}$ , are

$$m_{i21a} = \frac{m_1 x_{1a}^2 + m_2 x_{2a}^2}{x_{1a} \cdot x_{2a}} \quad (2.62)$$

$$m_{i21b} = \frac{m_1 x_{1b}^2 + m_2 x_{2b}^2}{x_{1b} \cdot x_{2b}} \quad (2.63)$$

The effective spring gradient  $K_i$  can be calculated from the frequency equation

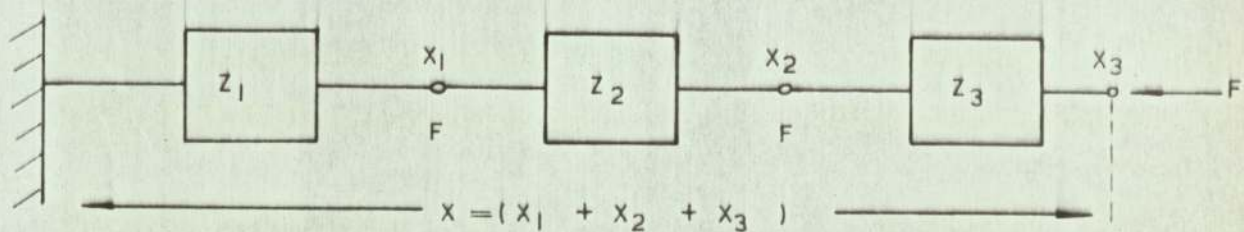
$$w_i^2 = K_i / m_i$$

$$\text{or } K_i = m_i w_i^2 \quad (2.64)$$

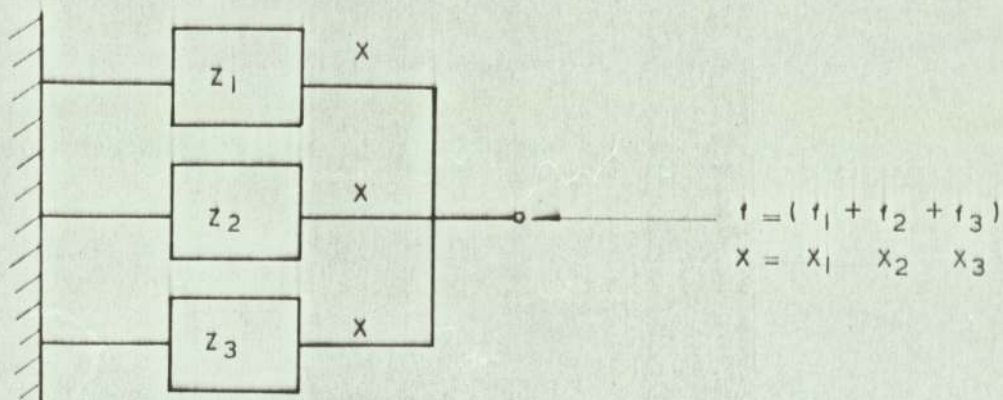
Substituting equation (2.64) in equation (2.57) the characteristic velocity mobility can be expressed in terms of the natural frequency and the effective mass as

$$M_{Vc} = \frac{1}{m_i w_i} \quad (2.65)$$

Chapter 3 contains the theoretical analysis of a hydraulic servomechanism. Response and impedance equations are derived from the basic considerations and evaluation of flow parameters is discussed.

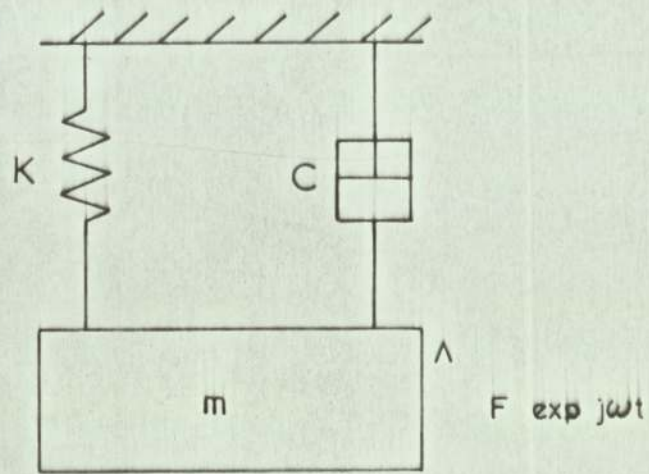


d) SERIES ARRANGEMENT OF IMPEDANCE ELEMENTS

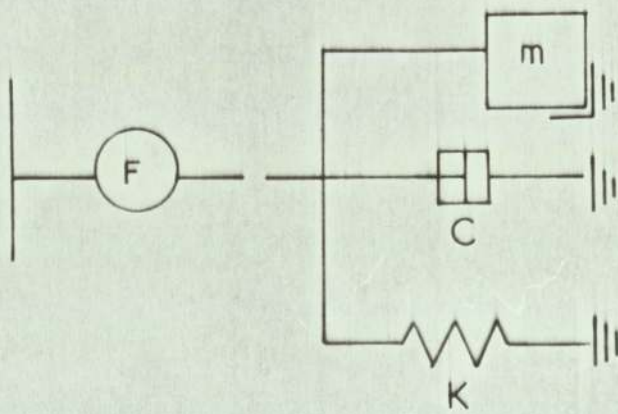


b) PARALLEL ARRANGEMENT OF IMPEDANCE ELEMENTS

SERIES AND PARALLEL ARRANGEMENT  
OF IMPEDANCE ELEMENTS

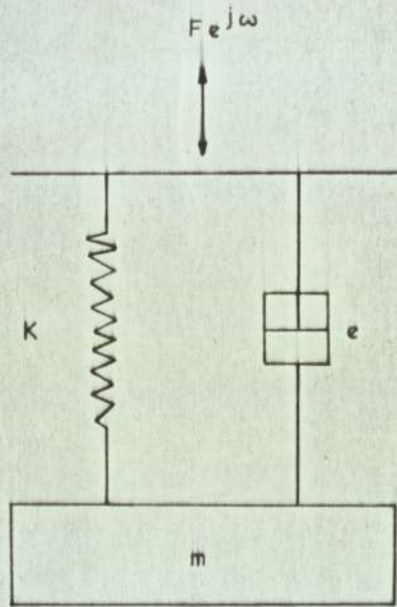


a) MECHANICAL SYSTEM

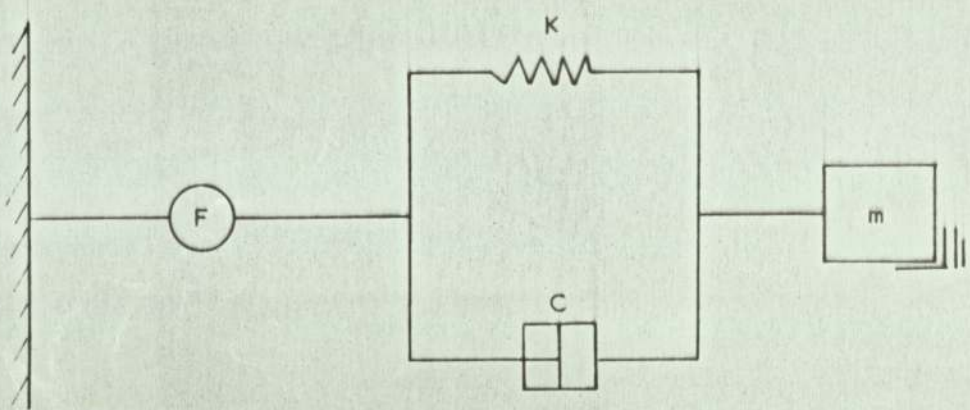


b) SCHEMATIC REPRESENTATION

A SINGLE DEGREE OF FREEDOM SYSTEM

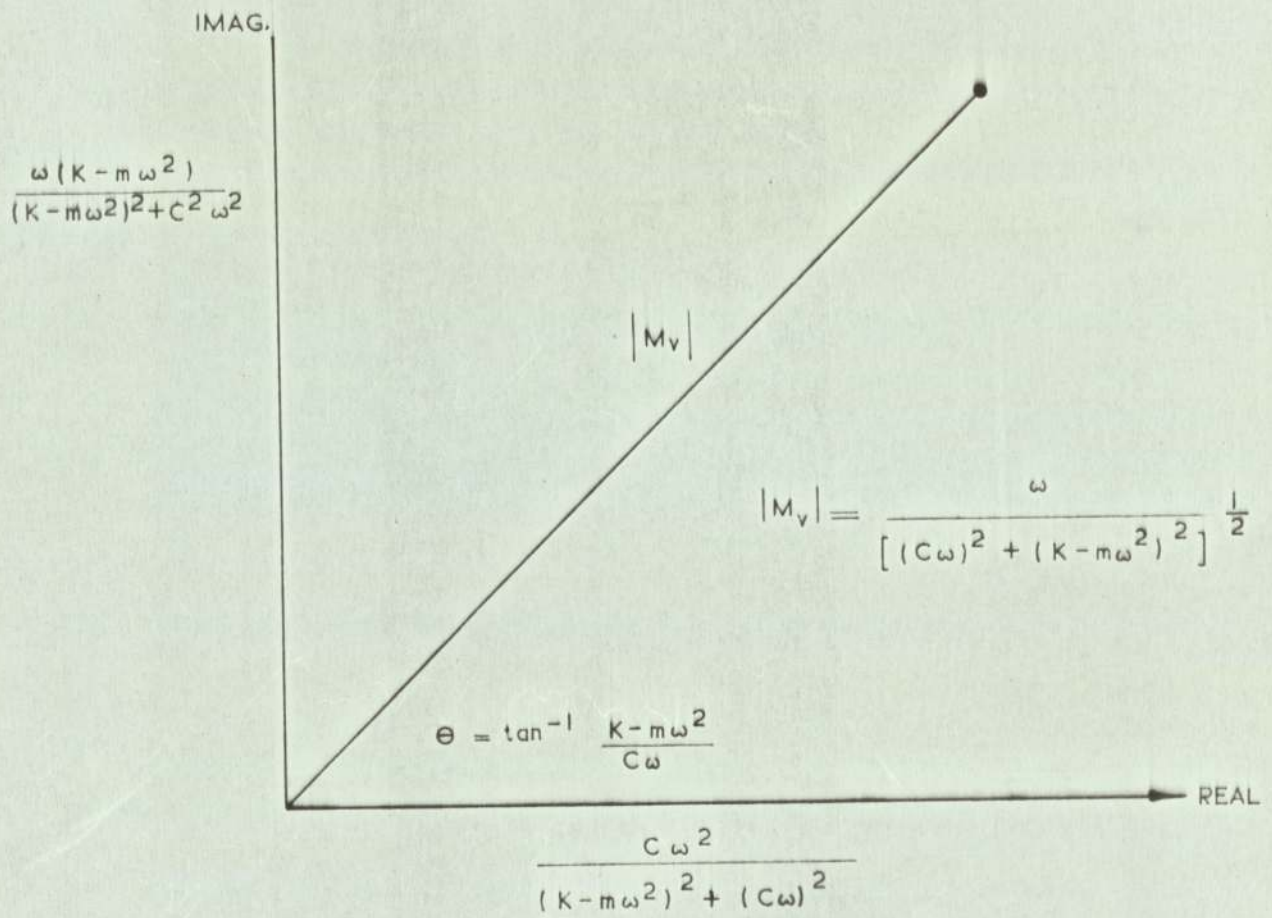


d) MECHANICAL SYSTEM OF FIG 2·2d WITH FORCE APPLIED TO THE SUPPORT.

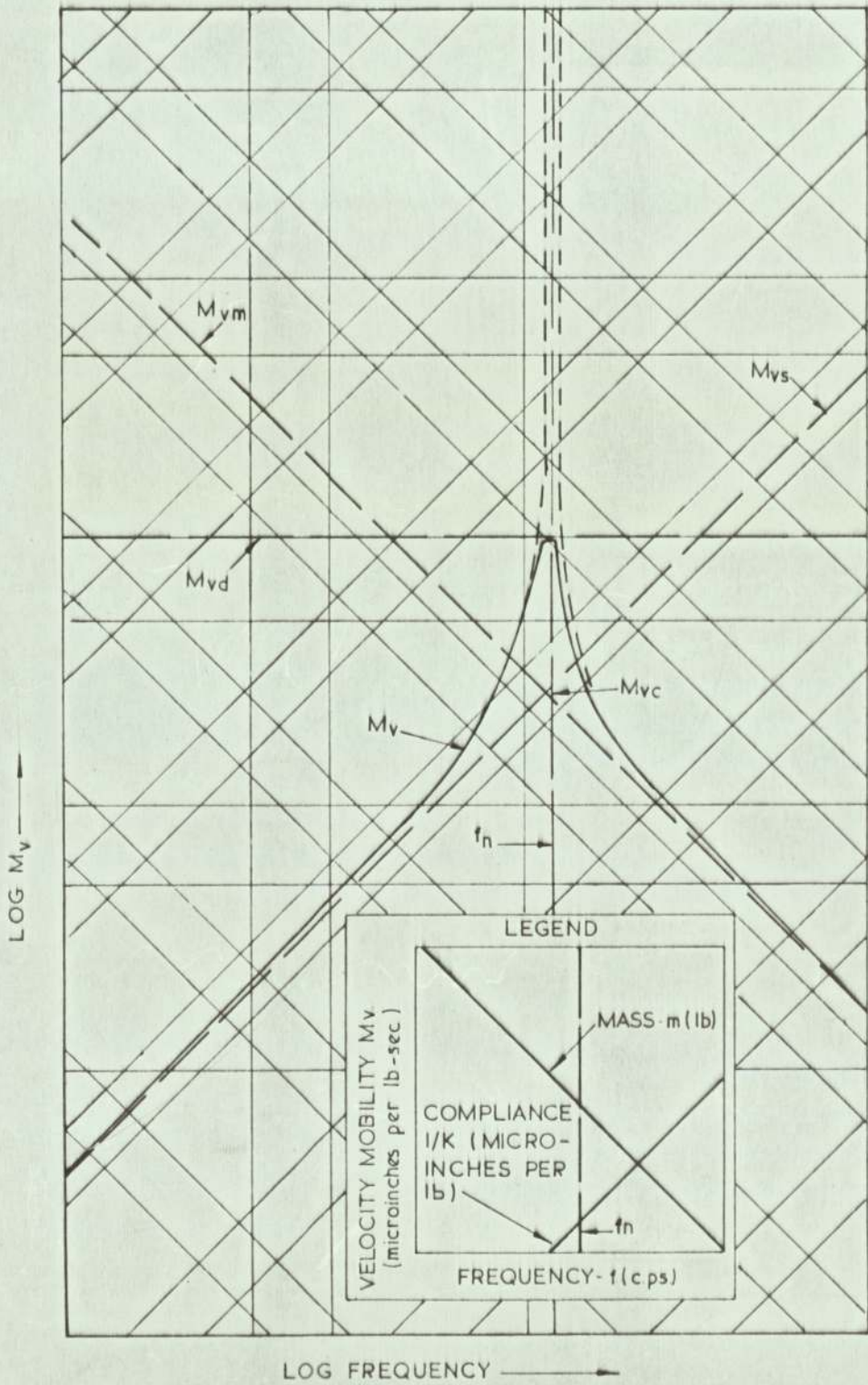


b). SCHEMATIC FOR THE SYSTEM OF a)

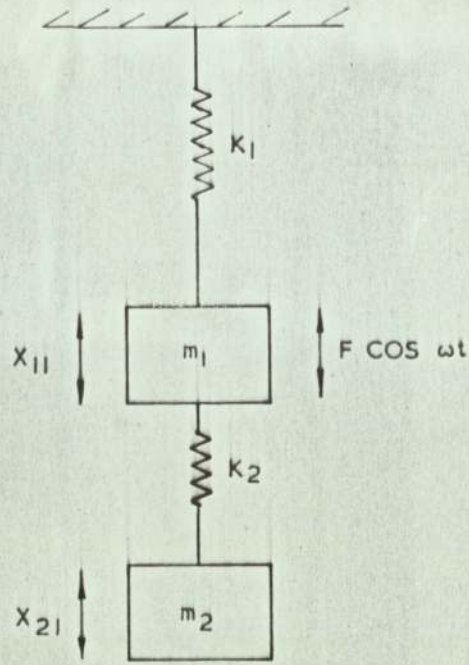
SYSTEM OF FIG 2·2 WITH FORCE APPLIED TO THE SUPPORT



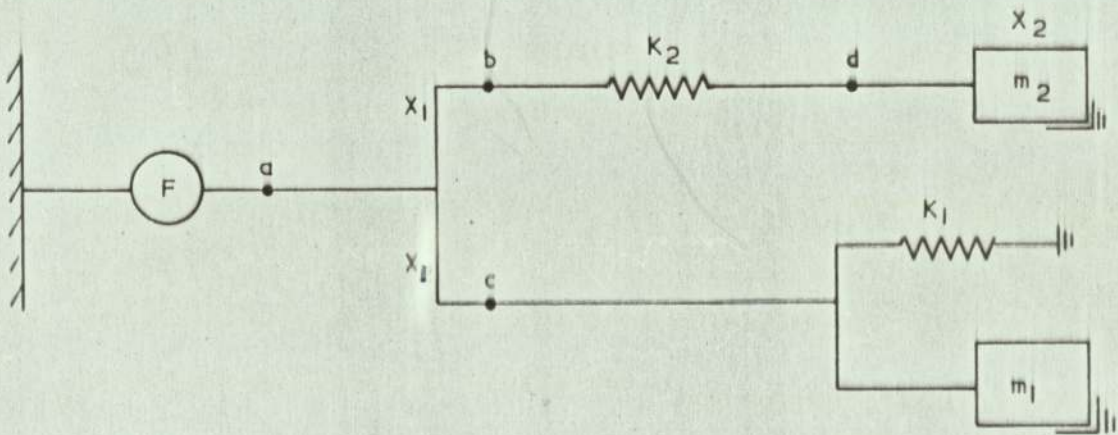
VECTOR REPRESENTATION OF VELOCITY MOBILITY



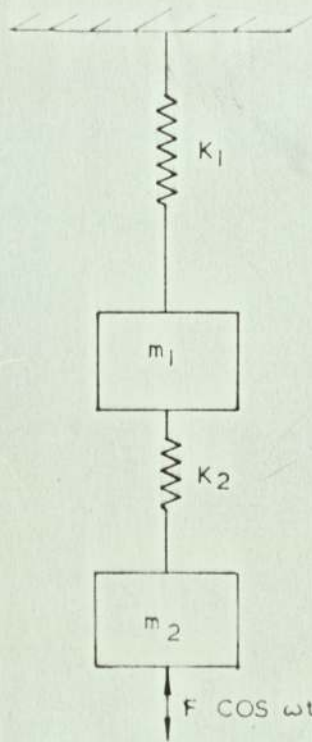
VELOCITY MOBILITY vs FREQUENCY FOR SYSTEM OF FIG 2.2a  
( ref. 8)



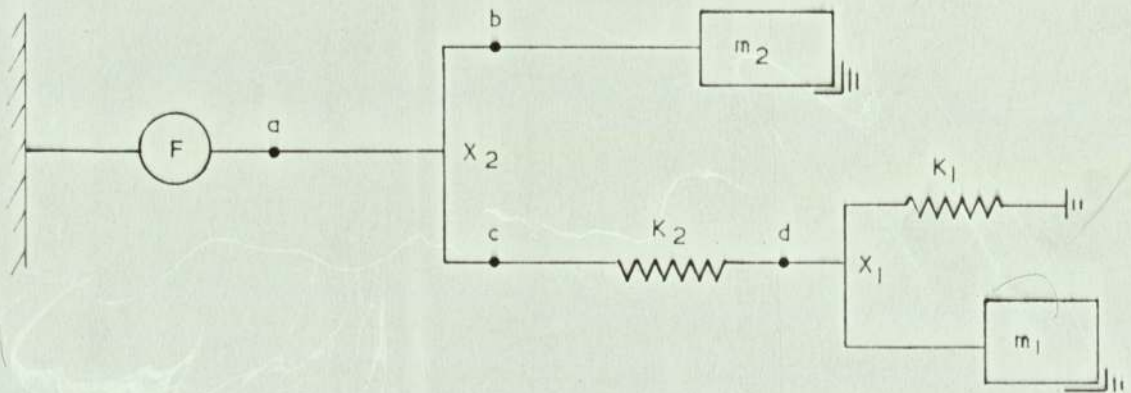
d) MECHANICAL SYSTEM.



b) MOBILITY SCHEMATIC FOR THE SYSTEM IN (a)



a) SYSTEM OF FIG 2.6 a WITH EXCITATION FORCE APPLIED AT MASS  $m_2$



b) SCHEMATIC DIAGRAM FOR THE SYSTEM IN (a).

CHAPTER 3.

THEORETICAL ANALYSIS OF A HYDRAULIC SERVOMECHANISM.

## CHAPTER 3.

### THEORETICAL ANALYSIS OF A HYDRAULIC SERVOMECHANISM.

<u>CONTENTS.</u>	<u>PAGE.</u>
3.1. Notation.	30
3.2. Introduction.	32
3.3. Equations of Motion of a Hydraulic Servomechanism.	33
3.4. Frequency Response Equation for the Servomechanism.	37
3.5. Impedance Equation for the Servomechanism.	39
3.6. Evaluation of Servo Valve Coefficients.	43
3.7. Effect of Coulomb Friction on Impedance.	46

## CHAPTER 3.

3.1. Notation.

A	Cross Sectional area of jack piston.
$C_e$	Valve flow coefficient $\partial Q/E$ .
$C_p$	Valve flow coefficient $2\partial Q/P_v$ .
$C_{jp}$	Leakage coefficient around jack piston $dQ_j/dP_j$ .
$C_{op}$	Leakage coefficient out of jack $dQ_o/dP_1$ , $dQ_o/dP_j$ .
$C_p'$	$= C_p + 2C_{jp} + C_{op}$ .
C	Viscous damping coefficient.
$E_b$	Boundary value of E.
$F_c$	Coulomb friction force.
j	$(-1)^{\frac{1}{2}}$ .
$K_e$	$= Aw$ .
$K_p$	$= Vw/2N$ .
$K_j$	Leakage constant around jack piston.
$K_o$	Leakage constant out of jack.
$K_v$	valve flow coefficient.
M	Equivalent mass of the control surface referred to the servomechanism.
N	Bulk modulus of fluid.
$Q_{j1}$	Leakage around piston out of No.1 chamber.
$Q_{j2}$	Leakage around piston into No.2 chamber.
$Q_{o1}$	Leakage from No.1 chamber (out of jack).
$Q_{o2}$	Leakage from No.2 chamber (out of jack).

$P_s$	Supply pressure.
$t$	Time.
$V$	Swept volume of jack.
$W$	Energy dissipated/cycle.
$X_{ob}$	Initial or boundary value of $X_o$ .
$Z$	Impedance.
$Z_s$	Impedance of a particular system.
$Z_u$	Impedance of servomechanism unit.
$\omega$	Excitation frequency.

In the following notation the upper case letters refer to the steady state condition, and the lower case letters refer to the small perturbations about the steady state condition.

$E$	$e$	Valve error or opening.
$F_o$	$f_o$	Applied force in the direction of $X_o$ .
$Q_1$	$q_1$	Flow into one side of jack (No.1 chamber).
$Q_2$	$q_2$	Flow out of other side of jack (No.2 chamber).
$P_1$	$p_1$	Pressure in No.1 chamber.
$P_2$	$p_2$	Pressure in No.2 chamber.
$P_j$	$p_j$	Pressure drop across jack piston, $(P_1 - P_2)$ .
$P_v$	$p_v$	Total pressure drop across valves, $(P_s - P_j)$ .
$X_i$	$x_i$	Input displacement.
$X_o$	$x_o$	Output displacement.

### 3.2. Introduction.

The hydraulic jack servomechanism is essentially a non-linear element. The most basic of the non-linearities is due to dependence of flow through valve ports on the square root of the pressure drop. Other factors contributing to the non-linearity of this type of servomechanism are the coulomb friction force, valve port area if it is not a linear function of the valve displacement, and discharge coefficient which may vary with the orifice area and the pressure drop across it.

The equations of motion for the servomechanism may be solved by graphical methods (12), by analysis of the response to various input functions (13), or by the small perturbations technique. The one most frequently used is the small perturbations technique in which the non-linear equations are linearised by considering small oscillations about a steadystate condition. This method is based on development of work by McRuer (14) and was used by Conway and Collinson (15) and Harpur (16). Harpur developed the usual response equations as well as the impedance equation for the servomechanism by considering the excitation of the output end, and took into account the effects of oil compressibility. This analysis was extended by Sung and Waterhabe (17) who included the effects of internal friction and oil leakages in the response equations. The effects of oil momentum forces on the valve were included in the equations of motion by Williams (18) who solved these equations using the same technique as that employed by Harpur. Lambert and Davies (19) and Glaze (20) have solved the response equations, which included the effects of coulomb friction and leakages, using an analogue computer.

Penny (1) has developed the impedance equations for the hydraulic servomechanism using Harpur's method but has included the effects of coulomb friction and oil leakages. He has also investigated the effects on impedance of flexibilities in the anchorage,

the valve input and the output stages. The theoretical analysis of the hydraulic servomechanism in this chapter is based on the work of Harpur and Penny.

### 3.3. Equations of Motion of a Hydraulic Servomechanism.

This analysis assumes that the servomechanism is of symmetrical design and there is no leakage from the valve ports due to an underlap. Account is taken of leakages across the piston and out of the jack. The supply pressure is assumed to remain constant and the return pressure zero.

The servo error  $E$  is defined as:-

$$E = X_i - X_o \quad (3.1)$$

where  $X_i$  and  $X_o$  are measured in such a way that  $E = 0$  when the valve is in a neutral position. The flow through the valve ports, with reference to Fig.3.1 may be defined as:-

$$Q_1 = f(E, P_1) \quad (3.2)$$

and the flow out of jack:-

$$Q_2 = f(E, P_2) \quad (3.3)$$

The bulk modulus of a fluid is defined as:-

$$N = \frac{VdP}{dV} \quad (3.4)$$

Now consider the effect of compressing the fluid confined to one side of the jack piston, differentiating w.r.t. time:-

$$\frac{dV}{dt} = \frac{V}{N} \frac{dP}{dt}$$

The total volume flow into one side of the jack piston is:-

$$Q_1 = \frac{V_1}{N} \frac{dP}{dt} + A \frac{dX_o}{dt} + Q_{j1} + Q_{o1} \quad (3.5)$$

where  $\frac{V_1}{N} \frac{dP}{dt} =$  flow to compress fluid confined to one side of jack piston.

$A \frac{dX_o}{dt} =$  flow corresponding to jack velocity.

$Q_{j1} =$  leakage flow across jack, out of chamber 1.

$Q_{o1} =$  leakage flow out of jack, chamber 1.

with  $Q_{j1} = f_{j1} (P_1 - P_2) = f_{j1} (P_j)$ .

and  $Q_{o1} = f_{o1} (P_1)$ .

Similarly flow out of jack may be written as:-

$$Q_2 = -\frac{V_2}{N} \frac{dP_2}{dt} + A \frac{dX_o}{dt} + Q_{j2} - Q_{o2} \quad (3.6)$$

where  $Q_{j2} = f_{j2} (P_1 - P_2) = f_{j2} (P_j)$

and  $Q_{o2} = f_{o2} (P_2)$ .

Equations (3.10 to (3.6) define the motion of the servo-mechanism and their solution is obtained by considering small perturbations about a steady state condition. Replacing  $X_1, X_o, Q_1$  etc., by  $X_1 + x_1, X_o + x_o,$  and  $Q_1 + q_1$  etc., the equations

of motion become:-

$$E + e = X_i - X_o = x_i - x_o. \quad (3.7)$$

$$Q_1 + q_1 = f(E, P_1) + \frac{\partial Q_1}{\partial E} e + \frac{\partial Q_1}{\partial P_1} p_1 \quad (3.8)$$

$$Q_2 + q_2 = f(E, P_2) + \frac{\partial Q_2}{\partial E} e + \frac{\partial Q_2}{\partial P_2} p_2 \quad (3.9)$$

$$Q_1 + q_1 = \frac{V_1}{N} \frac{dP_1}{dt} + A \frac{dX_o}{dt} + Q_{j1} + Q_{o1} + \frac{V_1}{N} \frac{dp_1}{dt} \\ + A \frac{dx_o}{dt} + \frac{dQ_{j1}}{dP_j} p_j + \frac{dQ_{o1}}{dP_1} p_1 \quad (3.10)$$

$$Q_2 + q_2 = \frac{V_2}{N} \frac{dP_2}{dt} + A \frac{dX_o}{dt} + Q_{j2} + Q_{o2} - \frac{V_1}{N} \frac{dp_2}{dt} \\ + A \frac{dx_o}{dt} + \frac{dQ_{j2}}{dP_j} p_j - \frac{dQ_{o2}}{dP_2} p_2 \quad (3.11)$$

Equations (3.8) and (3.9) are obtained by using Taylor series expansion for two variables and neglecting all powers in the expansion above the first. Eliminating the steady state from equations (3.7) to (3.11) gives the equations in perturbation terms only:-

$$e = x_1 + x_o \quad (3.12)$$

$$q_1 = \frac{\partial Q_1}{\partial E} e + \frac{\partial Q_1}{\partial P_1} p_1 \quad (3.13)$$

$$q_2 = \frac{\partial Q_2}{\partial E} e + \frac{\partial Q_2}{\partial P_2} p_2 \quad (3.14)$$

$$q_1 = \frac{V_1}{N} \frac{dp_1}{dt} + A \frac{dx_o}{dt} + \frac{dQ_{j1}}{dP_j} p_j + \frac{dQ_{o1}}{dP_1} p_1 \quad (3.15)$$

$$q_2 = - \frac{V_2}{N} \frac{dp_2}{dt} + A \frac{dx_o}{dt} + \frac{dQ_{j2}}{dP_j} p_j - \frac{dQ_{o2}}{dP_2} p_2 \quad (3.16)$$

Since the valve ports are assumed to be symmetrical

$$\text{Let} \quad \frac{\partial Q_1}{\partial E} = \frac{\partial Q_2}{\partial E} = C_e \quad (3.17)$$

$$- \frac{\partial Q_1}{\partial P_1} = \frac{\partial Q_2}{\partial P_2} = C_p \quad (3.18)$$

$$\frac{dQ_{j1}}{dP_j} = \frac{Q_{j2}}{P_j} = C_{jp} \quad (3.19)$$

$$\frac{dQ_{o1}}{dP_1} = \frac{dQ_{o2}}{dP_2} = C_{op} \quad (3.20)$$

If the piston is in mid-stroke position, then:-

$$V_1 = V_2 = V/2$$

Equating equations (3.13) & (3.15) and (3.14) & (3.16) and substituting from equations (3.17) to (3.20),

$$q_1 = -C_p p_1 + C_e e = \frac{V}{2N} \frac{dp_1}{dt} + A \frac{dx_o}{dt} + C_{jp} p_j + C_{op} p_1 \quad (3.21)$$

$$q_2 = C_p p_2 + C_e e = -\frac{V}{2N} \frac{dp_2}{dt} + A \frac{dx_o}{dt} + C_{jp} p_j - C_{op} p_2 \quad (3.22)$$

Adding equations(3.21) and (3.22)

$$-C_p (p_1 - p_2) + 2C_e e = \frac{V}{2N} \frac{d}{dt} (p_1 - p_2) + 2A \frac{dx_o}{dt} + 2C_{jp} p_j$$

$$+ C_{op} (p_1 - p_2)$$

$$\text{or } 2C_e e - p_j (C_p + 2C_{jp} + C_{op}) = \frac{V}{2N} \frac{dp_j}{dt} + 2A \frac{dx_o}{dt}$$

Putting  $C_p' = C_p + 2C_{jp} + C_{op}$

$$2C_e e - p_j C_p' = \frac{V}{2N} \frac{dp_j}{dt} + 2A \frac{dx_o}{dt} \quad (3.23)$$

This is the performance equation for the servomechanism for the steady state condition at which the values of  $C_e$  and  $C_p'$  have been calculated. The frequency response and the impedance equations are developed from equation (3.23) in sections 3.4 and 3.5 respectively.

#### 3.4. Frequency Response Equation for the Servomechanism.

Considering the load produced on the servomechanism by the inertia of the control surface

$$F_o = m \frac{d^2 X_o}{dt^2}$$

where  $m$  is the equivalent mass of the control surface referred to the servomechanism. The external forces on the servomechanism will be balanced by the pressure drop across the jack. Considering small perturbations of  $F_o$  :-

$$A (p_1 - p_2) = f_o$$

$$\text{or } p_j = \frac{m}{A} \frac{d^2 x_o}{dt^2} \quad (3.24)$$

Substituting equations (3.12) & (3.24) into (3.23):-

$$2C_e (x_i - x_o) - \frac{C_p^m}{A} \frac{d^2 x_o}{dt^2} = \frac{V_m}{2NA} \frac{d^3 x_o}{dt^3} + 2A \frac{dx_o}{dt}$$

$$\text{Or } \frac{V_m}{2NA} \frac{d^3 x_o}{dt^3} + \frac{C_p^m}{A} \frac{d^2 x_o}{dt^2} + 2A \frac{dx_o}{dt} + 2C_e x_o = 2C_e x_i \quad (3.25)$$

If the perturbations are sinusoidal, then by putting  $x_i = x_i \exp j\omega t$  and  $x_o = x_o \exp j\omega t$  the transfer function of the servomechanism in terms of the forcing frequency is obtained as:-

$$\frac{x_o}{x_i} = \frac{2C_e}{- \frac{V_m}{2NA} j\omega^3 - \frac{C_p^m}{A} \omega^2 + 2A j\omega + 2C_e}$$

From which the amplitude ratio is:-

$$\frac{x_o}{x_i} = \frac{2C_e}{\left[ \left( 2C_e - \frac{C_p^m}{A} \omega^2 \right)^2 + \omega^2 \left( 2A - \frac{V_m}{2NA} \omega^2 \right)^2 \right]^{\frac{1}{2}}} \quad (3.26)$$

and the phase lag is:-

$$\theta = \tan^{-1} \left( \frac{4NA^2 \omega - V_m \omega^2}{2AC_e - C_p^m \omega^2} \right) \quad (3.27)$$

The above equations are the frequency response equations from which can be calculated the values of system parameters to give a response characteristics of the system for a fast or slow response to suit the function for which the aircraft has been designed.

### 3.4.1. Condition for Stability.

The Routh-Hyrwitz criterion for stability, when applied to equation (3.25), requires that for the servomechanism to be stable

$$\left( \frac{C'_m}{A} \right) 2A - \left( \frac{V_m}{2NA} \right) 2C_e > 0$$

or that, 
$$C'_p/C_e > \frac{V}{2NA} \quad (3.28)$$

The servomechanism will be stable over the operating range for which equation (3.28) is satisfied. The effect of leakage, included in  $C'_p$ , is to improved stability.

### 3.5. Impedance Equation for the Servomechanism.

The impedance of the servomechanism is defined as the ratio of force to displacement. This force is that applied to the output end while the displacement is measured with the valve input locked, that is  $x_i = 0$  and hence the servo error  $e = -x_o$ . The force  $f_o$  causing the jack to move in the direction of  $x_o$  is balanced by the jack pressure differential:-

$$f_o = -p_j A$$

or 
$$\frac{f_o}{A} = -p_j$$

Substituting for  $e$  and  $p_j$  in the performance equation (3.23) we obtain:-

$$-2C_e x_o + \frac{f_o}{A} C_p' = -\frac{V}{2NA} \frac{df_o}{dt} + 2A \frac{dx_o}{dt} \quad (3.29)$$

Since the above equation is in small perturbation terms only it will be linear over the perturbed range, and, if the exciting force is sinusoidal the resulting response will be sinusoidal also.

$$\text{Putting } f_o = f_o \exp j\omega t, \quad x_o = x_o \exp j\omega t.$$

$$\text{and } \frac{df_o}{dt} = j\omega f_o \exp j\omega t, \quad \frac{dx_o}{dt} = j\omega x_o \exp j\omega t.$$

equation (3.29) becomes:-

$$\left( j \frac{V\omega}{2N} + C_p' \right) \frac{f_o}{A} = 2(jA\omega + C_e) x_o$$

$$\text{or } \frac{f_o}{x_o} = \frac{2A(jA\omega + C_e)}{\left( j \frac{V\omega}{2N} + C_p' \right)}$$

Resolving this equation into its real and imaginary parts gives:-

$$\frac{f_o}{x_o} = \frac{2A}{C_p'^2 + K_p^2} \left( C_e C_p' + \left( \frac{AV\omega^2}{2N} \right) + j \left( A\omega C_p' - \frac{V\omega C_e}{2N} \right) \right)$$

$$\text{or } Z_u = \frac{2A}{C_p'^2 + K_p^2} \left[ (C_e C_p' + K_e K_p) + j(C_p' K_e - C_e K_p) \right] \quad (3.30)$$

where  $Z_u$  = Impedance of the servomechanism:-

$$K_p = \frac{V\omega}{2N}$$

$$K_e = A\omega$$

Equation (3.30) is the impedance equation for the servomechanism. The real term represents stiffness and the imaginary term represents damping.

### 3.5.1 Static Stiffness.

The static stiffness of the servomechanism is defined as the stiffness when the frequency tends to zero, that is, when  $K_e = K_p = 0$ . From equation (3.30).

$$Z_u \text{ (static)} = \frac{2AC_e}{C'_p} \quad (3.31)$$

The damping will be zero and the effect of leakage is to reduce the static stiffness (since  $C'_p = C_p + 2C_{pj} + C_{op}$ ).

### 3.5.2 Infinite Frequency Stiffness.

As the frequency of excitation increases from zero the stiffness of the servomechanism increases from its static value (equation 3.31). At higher frequencies  $C_e$  and  $C'_p$  become insignificant compared with  $K_e$  and  $K_p$ , and hence from equation (3.30),

$$Z_u \text{ (inf.freq.)} = \frac{2A K_e}{K_p} = \frac{4A^2 V}{N} \quad (3.32)$$

The damping is once again zero and oil in the jack acts as a plain spring of stiffness  $4A^2 V/N$ . That is, the valve motion is insignificant and the piston is bouncing on the oil in the jack.

### 3.5.3 Maximum damping.

It can be seen from equations (3.31) & (3.32) that the damping is zero both at zero frequency and at infinite frequency, It

increases as the frequency is increased from zero and reaches its maximum value at some higher frequency and then falls back to zero at infinite frequency. The maximum value of damping and the frequency at which it occurs can be determined by differentiating the imaginary term of the impedance equation w.r.t.w.

$$Z_u \text{ (imag.)} = \frac{2Aw}{C_p'^2 + \left(\frac{Vw}{2N}\right)^2} \left( AC_p' - \frac{VC_e}{2N} \right) \quad (3.33)$$

$$\frac{dZ_u}{dw} \text{ (imag.)} = \frac{2A \left[ AC_p' - \frac{VC_e}{2N} \right] \left[ C_p' + \left(\frac{Vw}{2N}\right)^2 - w \left(\frac{V}{2N}\right)^2 2w \right]}{\left[ C_p'^2 + \left(\frac{Vw}{2N}\right)^2 \right]^2}$$

For maximum condition:-

$$C_p'^2 - \left(\frac{Vw}{2N}\right)^2 = 0$$

$$\text{and } w = \frac{2NC_p'}{V} \quad (3.34)$$

This is the value of frequency at which the maximum damping occurs. The value of this damping can be obtained by substituting equations (3.34) in (3.33).

$$Z_u \text{ (imag.) max} = A \left( \frac{2NA}{V} - \frac{C_e}{C_p'} \right) \quad (3.35)$$

If the bulk modulus  $N$  is assumed constant then the maximum damping depends on the ratio  $C_e/C_p'$ . The damping and, hence, stability can be increased by decreasing this ratio but this would reduce the static stiffness of the servo unit (eqn. 3.31). Therefore the choice lies between a highly damped system with a low static stiffness or a lightly damped system with a high static stiffness. For flutter

prevention a high stiffness is desirable but the actual values of stiffness and damping can best be determined when the flutter characteristics of a control surface are known.

### 3.6. Evaluation of the Servo Valve Flow Coefficients.

The response characteristics of the servomechanism and the servo impedance can be determined from equations (3.26) and (3.30) respectively for the steady state condition for which the values of  $C_e$  and  $C_p$  are known. These parameters can best be determined experimentally for a particular unit. But in the absence of experimental data, as would be the case at pre-design stages, approximate values of  $C_e$  and  $C_p$  may be evaluated.

#### 3.6.1 Approximate Evaluation of $C_e$ and $C_p$ .

The flow through an orifice is a function of the square root of the pressure drop across it, the orifice area and the losses due to friction. As a first approximation the flow through one side of jack piston may be defined as:-

$$Q_1 = K_V E (P_S - P_1)^{\frac{1}{2}}$$

where  $K_V$  is a constant for the valve which includes the discharge coefficient and the effect of non-linear relationship between the flow area and the valve error  $E$ .

$$\begin{aligned} \frac{\partial Q_1}{\partial E} &= K_V (P_S - P_1)^{\frac{1}{2}} \quad \text{since } P_S - P_1 = P_V/2 \\ \frac{\partial Q_1}{\partial E} &= K_V (P_V/2)^{\frac{1}{2}} \end{aligned} \quad (3.36)$$

Similarly,

$$\begin{aligned} Q_2 &= K_V E (P_2)^{\frac{1}{2}} \\ &= K_V E (P_V/2)^{\frac{1}{2}} \quad \text{since } P_2 = P_V/2 \end{aligned}$$

$$\text{and } \frac{\partial Q_2}{\partial E} = K_V (P_V/2)^{\frac{1}{2}} \quad (3.37)$$

From equations (3.36) and (3.37):-

$$C_e = \frac{\partial Q_1}{\partial E} = \frac{\partial Q_2}{\partial E} = K_v (P_v/2)^{\frac{1}{2}} \quad (3.38)$$

$$\begin{aligned} \text{Now - } \frac{\partial Q_1}{\partial P_1} &= K_v E^{\frac{1}{2}} (P_s - P_1)^{\frac{1}{2}} \\ - \frac{\partial Q_1}{\partial P_1} &= \frac{K_v E}{2(P_v/2)^{\frac{1}{2}}} \end{aligned} \quad (3.39)$$

$$\begin{aligned} \text{and } \frac{\partial Q_2}{\partial P_2} &= \frac{K_v E}{2(P_2)^{\frac{1}{2}}} \\ \frac{\partial Q_2}{\partial P_2} &= \frac{K_v E}{2(P_v/2)^{\frac{1}{2}}} \end{aligned} \quad (3.40)$$

From equation (3.39) and (3.40):-

$$\begin{aligned} C_p &= -\frac{\partial Q_1}{\partial P_1} = \frac{\partial Q_2}{\partial P_2} \\ \therefore C_p &= \frac{K_v E}{2(P_v/2)^{\frac{1}{2}}} \end{aligned} \quad (3.41)$$

### 3.6.2. Experimental Evaluation of $C_e$ and $C_p$ .

The experimental values of  $C_e$  and  $C_p$  for a hydraulic jack may be evaluated from the data supplied by the manufacturer. This data consists of the flow characteristics against valve opening for lines of constant pressure drop across the valve as shown in

Fig.3.3. The slope of these lines at any instant represents  $\partial Q/\partial E$ , or  $C_e$ , for a constant pressure drop. To obtain values of  $C_p$  the data in Fig.3.3 is cross plotted to give flow characteristic against pressure drop across the valve for lines of constant valve opening as shown in Fig.3.4. The slope of these lines represents  $\partial Q/\partial P_v$  or  $C_p/2$ . The dependence of  $C_p$  and  $C_e$  on valve opening for constant pressure drop and on pressure drop for constant valve opening is shown in Figures 3.5 and 3.6.

Figure 3.6 shows a plot of  $C_p$  against  $C_e$  for constant valve pressure drop and valve opening. The diagonal lines represent the ratio  $C_e/C_p$  which help indicate the high stability and static stiffness regions on the diagram. The criterion for stability (eqn. 3.28) was found to be:-

$$C_p/C_e > \frac{V}{2NA}$$

Therefore a high degree of stability is obtained for low values of  $C_e/C_p$  and a low stability for high values of this ratio. It was stated earlier that stiffness and stability are related in such a manner that an increase in one parameter is accompanied by a decrease in the other. From equation 3.31

$$Z_u \text{ (static)} = 2A \frac{C_e}{C_p}$$

or that the static stiffness is proportional to the ratio  $C_e/C_p$  that is, a high static stiffness is obtained for a high value of  $C_e/C_p$ . Hence the region of high static stiffness is also the region of low stability and vice versa.

### 3.7. Effect of Coulomb Friction on Impedance.

Coulomb friction in a servomechanism forms a principal non-linearity and has to be linearised for its effect to be included in an analysis. The linearised coulomb damping force is then equated with a viscous damping force of equal magnitude to give an equivalent viscous damping coefficient in which the damping force is a linear function of velocity.

The equivalent damping coefficient can be determined either by a Fourier analysis or by energy dissipation considerations as follows.

#### 3.7.1 Fourier Analysis.

The response of a system with coulomb friction to a sinusoidal excitation will be a square wave the Fourier expansion of which is given by,

$$\frac{4}{\pi} F_c \left( \sin wt + \frac{1}{3} \sin 3 wt + \frac{1}{5} \sin 5 wt + \dots \right)$$

where  $F_c$  is the magnitude of the coulomb friction force opposing the motion. Neglecting all terms except the first in the above expression gives the amplitude of the fundamental component which varies sinusoidally and gives approximately the linearised coulomb damping force.

∴ Approximate coulomb damping force

$$= \frac{4}{\pi} F_c \sin wt.$$

The viscous damping force

$$= C \frac{dx}{dt}$$

$$= Cwx \sin wt.$$

Equating the viscous and coulomb damping forces

$$\frac{4}{\pi} F_c \sin wt = Cwx \sin wt.$$

$$\therefore C = \frac{4F_c}{\pi wx} \quad (3.42)$$

where C is the equivalent viscous damping coefficient.

### 3.7.2 Energy Dissipation.

In this analysis the equivalent viscous damping coefficient is determined by equating the energy dissipated by viscous damping force to the energy dissipated by the coulomb damping force.

$$\text{The viscous damping force} = C \dot{x}$$

and the energy dissipated per cycle by this force,

$$W = \oint (C \dot{x}) dx$$

$$= \int_0^{2\pi/w} (C \dot{x}) \dot{x} dt \quad \text{since } dx = \frac{dx}{dt} dt$$

$$= Cwx^2 \int_0^{2\pi} (\cos^2 wt) d(wt)$$

$$= Cwx^2 \int_0^{2\pi} \frac{1}{2} (1 + \frac{1}{2} \cos 2wt) d(wt)$$

$$= \frac{1}{2} Cwx^2 (wt + \frac{1}{2} \sin 2wt) \Big|_0^{2\pi}$$

$$W = \pi Cwx^2 \quad (3.43)$$

Coulomb damping force =  $F_c (\text{sgn } \dot{x})$

and energy dissipated per cycle,

$$\begin{aligned}
 W &= \oint F_c (\text{sgn } \dot{x}) dx \\
 &= \int_0^{2\pi/\omega} F_c (\text{sgn } \dot{x}) \dot{x} dt \\
 &= x \int_0^{2\pi} F_c (\text{sgn } \dot{x}) \cos \omega t d(\omega t) \\
 &= x F_c \left[ \int_{3\pi/2}^{\pi/2} \cos \omega t d(\omega t) + \int_{3\pi/2}^{5\pi/2} \cos \omega t d(\omega t) \right] \\
 W &= 4 F_c x \tag{3.44}
 \end{aligned}$$

equating equations (3.43) and (3.44) the equivalent viscous damping coefficient is given as:-

$$\begin{aligned}
 \pi C \omega x^2 &= 4 F_c x \\
 \therefore C &= \frac{4 F_c}{\pi \omega x}
 \end{aligned}$$

The effect of coulomb damping may be included in the analysis by considering a damper placed in parallel with the servomechanism as shown in Fig.3.2.

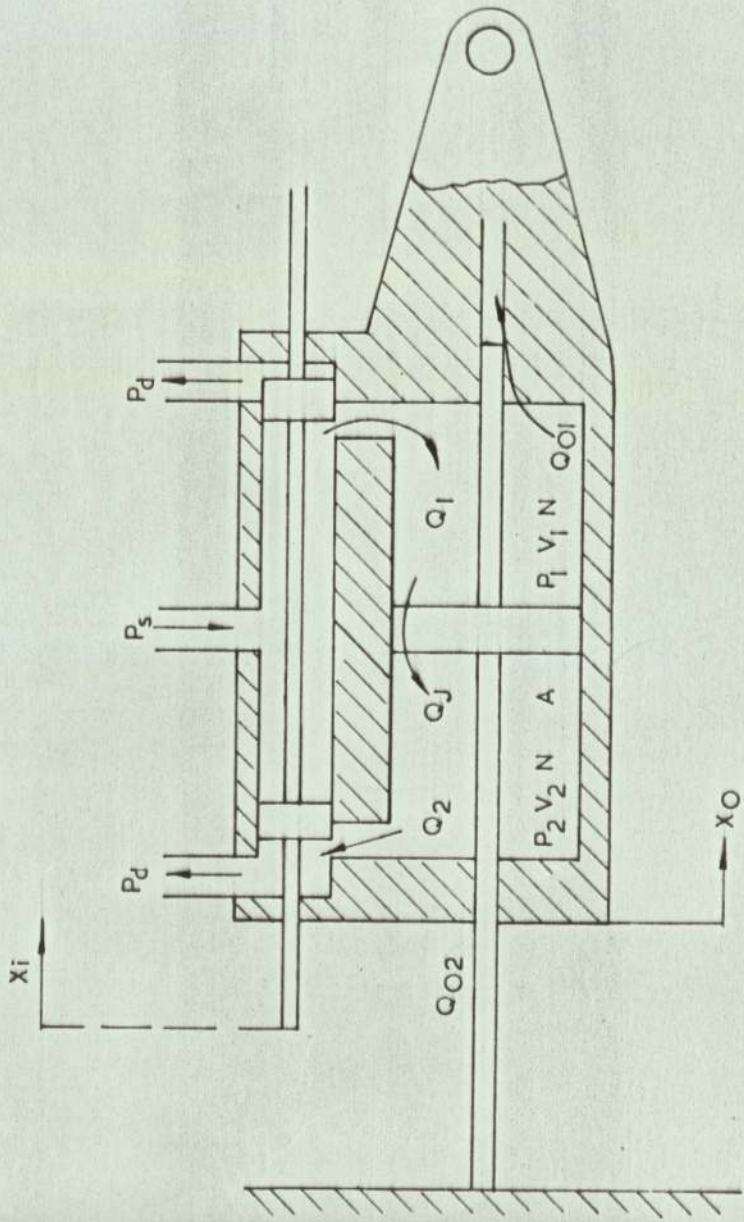
Let  $Z_u$  be the impedance of the servomechanism and let  $Z_d$  be the impedance of the damper.

Using the laws of impedance addition for elements in parallel, the total system impedance  $Z_s$  is,

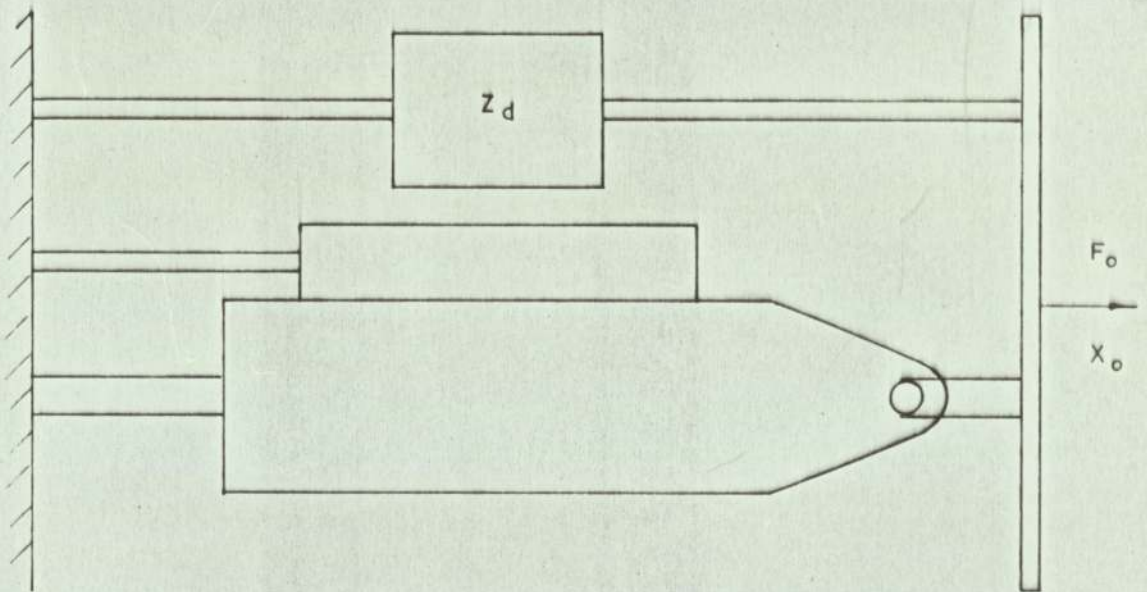
$$\begin{aligned} Z_s &= Z_u + Z_d \\ &= Z_u + j \frac{4F_c}{\pi W X} \end{aligned} \quad (3.45)$$

where  $Z_u$  is represented by eqn. 3.30.

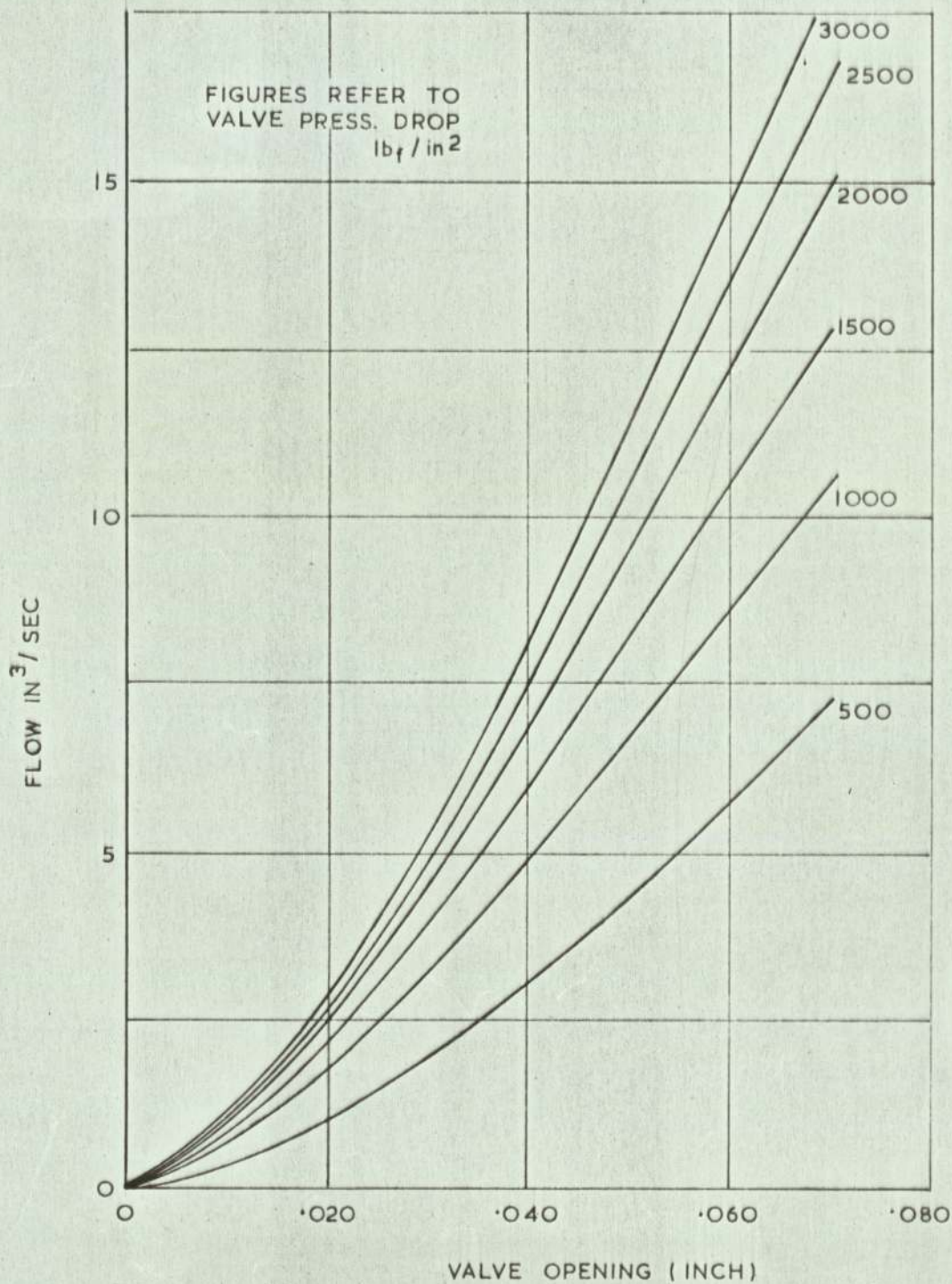
Chapter 4 introduces the fundamental concepts of analogue computing together with the networks that form a general purpose analogue computer.



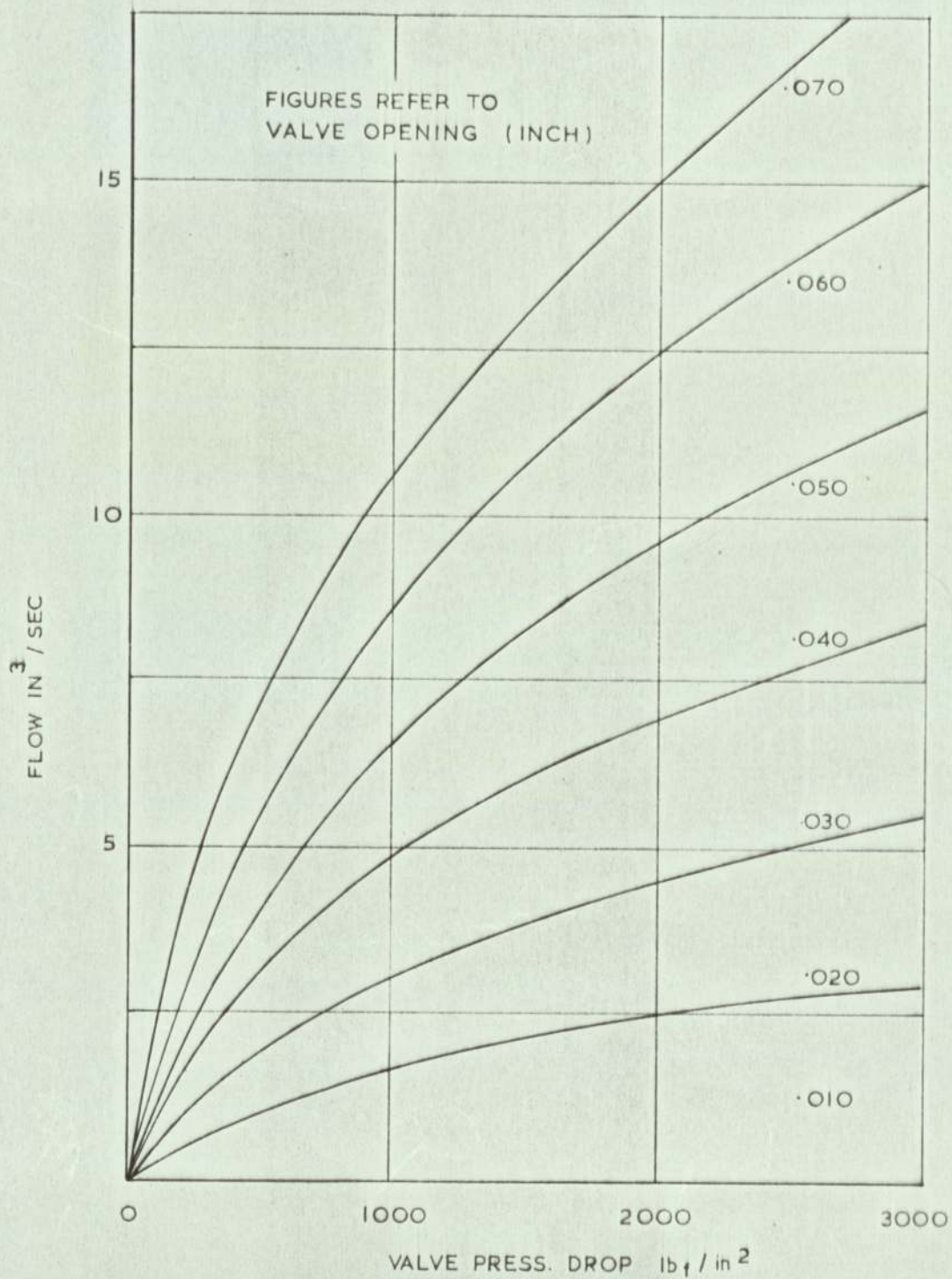
SCHEMATIC OF A HYDRAULIC SERVOMECHANISM



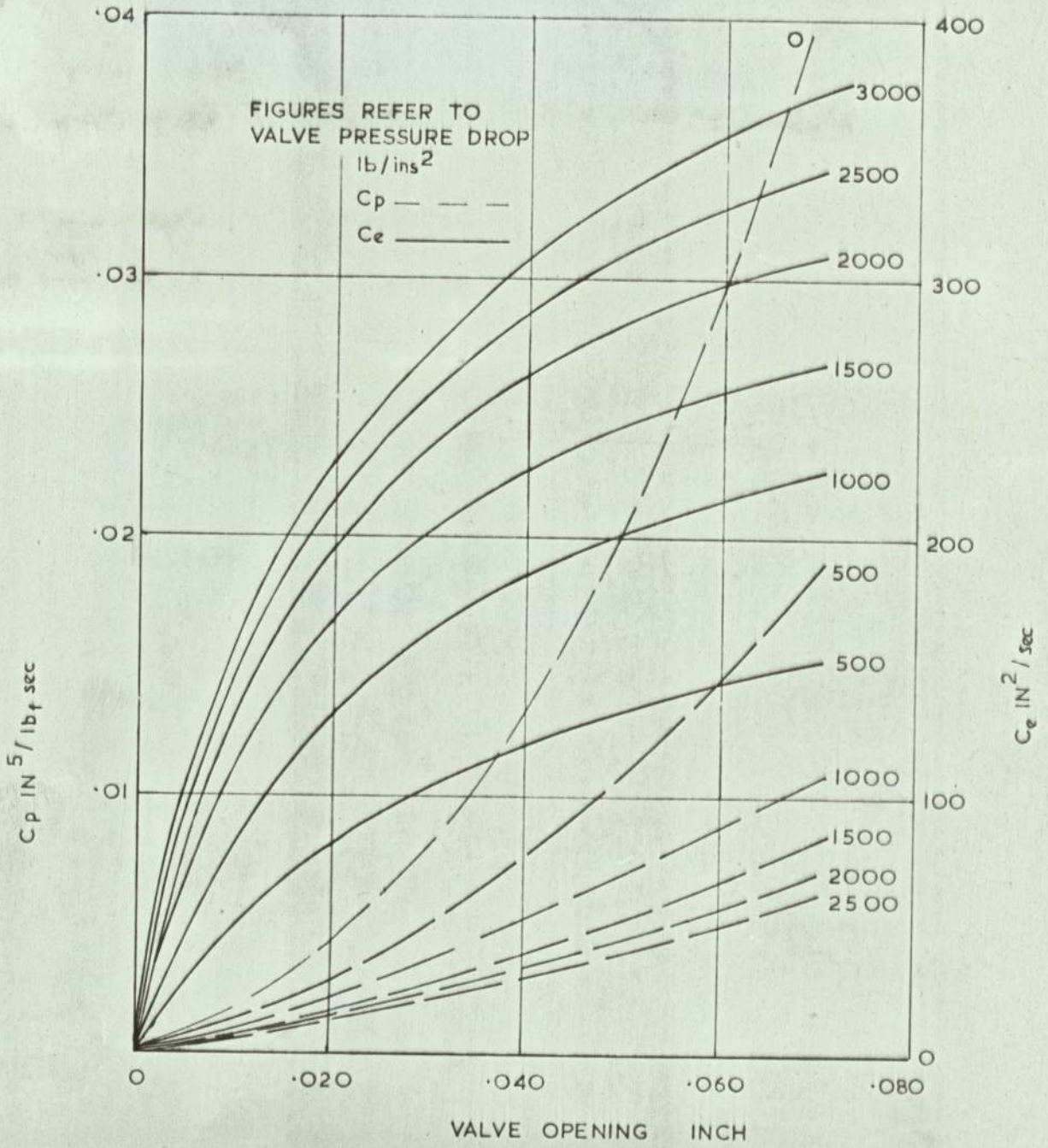
HYDRAULIC SERVOMECHANISM WITH  
A DAMPER CONNECTED IN PARALLEL



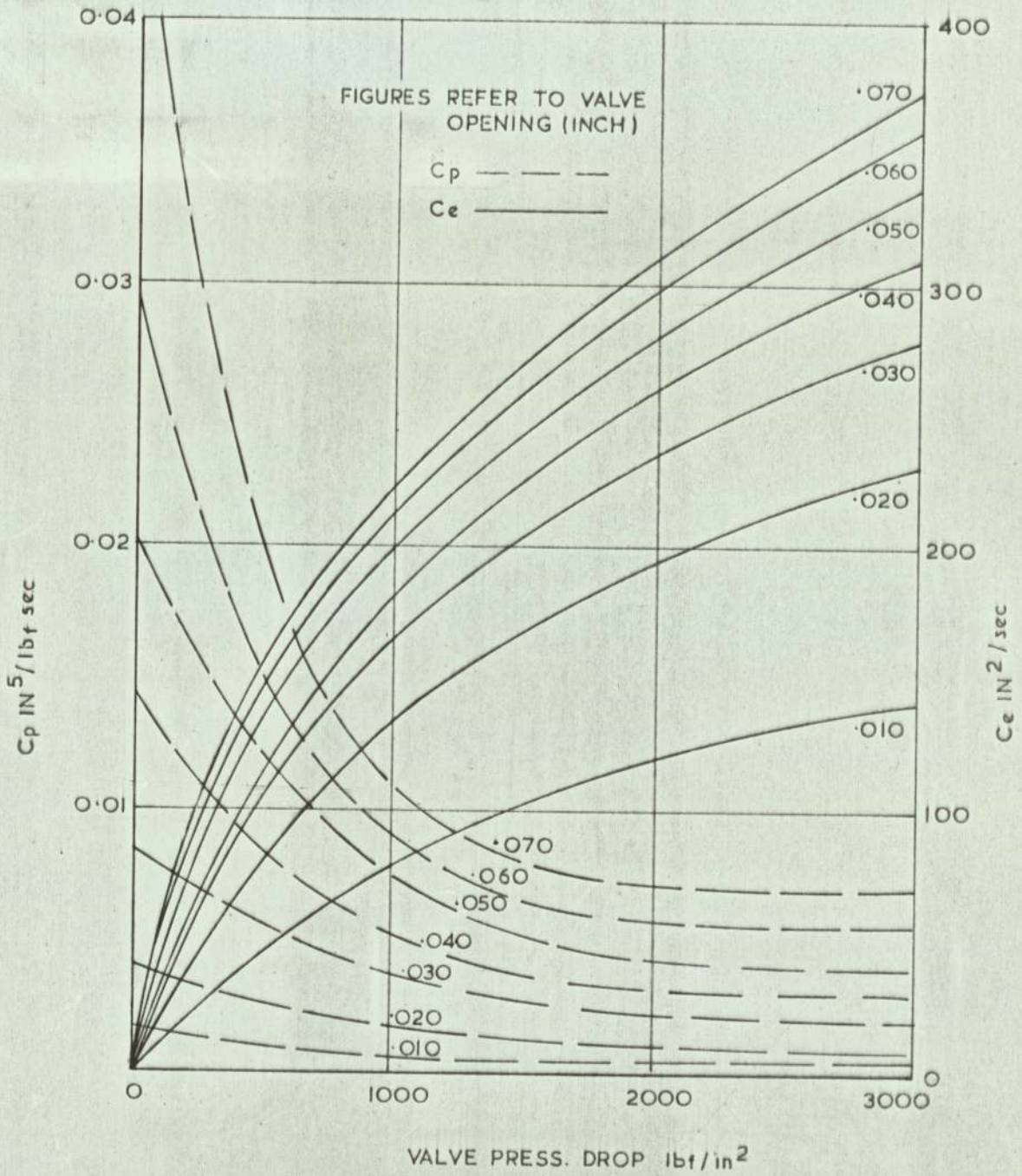
VALVE FLOW / OPENING CHARACTERISTICS



VALVE FLOW/PRESS. DROP CHARACTERISTIC



VALVE FLOW COEFFICIENTS / OPENING



VALVE FLOW COEFFICIENTS / PRESS. DROP

CHAPTER 4.

THE ANALOGUE COMPUTER.

## CHAPTER 4.

### THE ANALOGUE COMPUTER.

<u>CONTENTS.</u>	<u>PAGE.</u>
4.1. Notation.	50
4.2. Introduction.	51
4.3. Basic Elements of the Analogue Computer.	51
4.4. The Use of a High Gain Operational Amplifier.	55
4.5. Mathematical Operations Performed With the Operational Amplifier.	59
4.6. Integration.	60
4.7. Differentiation.	61
4.8. Multiplication of Two Variables.	62
4.9. Generating Functions of a Variable.	63
4.10. Control Modes of the Computer.	64

CHAPTER 4.THE ANALOGUE COMPUTER.4.1. Notation.

- A Operational amplifier gain.
- C Capacitance (Farads).
- D Differential operator ( $\frac{d}{dt}$ ).
- i Instantaneous current.
- M Problem variable.
- R Resistance (ohms).
- t Time (sec).
- T Time constant of a network (RC).
- V Voltage.
- w Frequency of the input signal (radians/sec).
- x,y Problem variables.
- Z Impedance element, resistance or capacitance.

The subscripts i, o and f denote input, output and feedback respectively.

## 4.2. Introduction.

The analogue computer is a useful aid for the solution of problems governed by ordinary differential equations. It is particularly useful for the analysis and synthesis of non-linear control systems which are otherwise treated by the phase plane and the describing function techniques. These analytical methods though useful are laborious and can be used only for input signals which are not of a statistical nature. The great advantage of an analogue computer is that once a problem is simulated a comprehensive analysis can be performed with great speed for any type of input signal and for any combination of system parameters. This makes the process of optimising the values of system parameters a relatively easy exercise. The results are presented in a graphical form and hence easily interpreted.

This chapter introduces the fundamental concepts of analogue computing and describes briefly operations of the basic elements that form an analogue computer. Only the operations and computing units used in this research are discussed. Detailed information on simulation and design of computing elements is well presented in the published text (21) (22) and (23).

## 4.3. Basic Elements of an Analogue Computer.

The analogue computer is a voltage operated device in which the variables of a physical problem are represented by voltages in the computer. It is built around the concept of blocks or elements which are connected together to perform various mathematical operations required for the solution of a problem. Only a few basic elements are needed in order to solve a wide range of problems. These elements consist mostly of passive electrical networks used in conjunction with the high gain operational amplifiers and provide

the following mathematical operations

1. Algebraic summation of two or more variables.
2. Multiplication of a variable by a constant.
3. Integration of a variable with respect to time.
4. Differentiation of a variable with respect to time.
5. Multiplication of two variables.
6. Generating functions of a variable.

The first four operations can be obtained simply by a combination of resistors and capacitors. The last two operations are achieved by means of special units known as 'Multipliers' and 'Function generators' respectively.

#### 4.3.1 Algebraic Summation.

The resistance network of Fig.4.1 can be used as a summing device. The resistances  $R_1$  and  $R_2$  are termed the input resistances while  $R_f$  is termed the feedback resistance. Applying Kirchhoff's current law to point N the nodal equation for the network is:-

$$i_1 + i_2 + i_f = 0 \quad (4.1.)$$

$$\text{or} \quad \frac{-V_o + V_1}{R_1} + \frac{-V_o + V_2}{R_2} + \frac{V_o}{R_f} = 0$$

$$\therefore V_o = \left( \frac{R_f}{R_1} V_1 + \frac{R_f}{R_2} V_2 \right) / R_f \left( \frac{1}{R_1} + \frac{1}{R_2} \right) - 1 \quad (4.2)$$

If the ratio of feedback resistance to input resistances is chosen to be unity then  $V_o$  is obtained as a sum of the input voltages.

#### 4.3.2. Multiplication by a Constant.

Consider the network shown in Fig.4.2, the nodal equation for which is given by:-

$$i_1 + i_f = 0$$

$$\text{or } \frac{V_o - V_1}{R_1} + \frac{V_o}{R_f} = 0$$

$$\therefore V_o = \frac{R_f}{R_1 + R_f} V_1 \quad (4.3)$$

Thus by varying the values of input and feedback resistances the input voltage can be multiplied by a constant less than unity.

#### 4.3.3. Integrating Network.

Integration in an electrical network is made possible due to the property of a capacitor that the current through it is proportional to the time derivative of the applied voltage:-

$$i = C \frac{d}{dt} V \quad (4.4)$$

Using the operator notation

$$i = CDV$$

$$\therefore V = \frac{i}{CD} = \frac{1}{C} \int_0^t i dt \quad (4.5)$$

Referring to Fig.4.3 the input voltage  $V_i$  causes a current to flow through the resistance  $R$  and charges the capacitor in a manner which approximates integration. But the output voltage  $V_o$  which builds up across the capacitor makes the charging current proportional to  $(V_i - V_o)$  rather than to input voltage alone. It is this proportionality of the charging current to  $(V_i - V_o)$  which prevents true integration. The transfer function of the network is given by:-

$$\frac{V_o - V_i}{R} + C D V_o = 0 \quad (4.6)$$

$$\text{and } V_o = \frac{1}{1 + RCD} V_i$$

Putting  $RC = T$ , the time constant,

$$V_o = \frac{1}{1 + TD} V_i \quad (4.7)$$

For the value of  $T$  much greater than unity eqn. (4.7) can be written as:-

$$V_o = \frac{1}{TD} V_i$$

$$\text{or } V_o = \frac{1}{T} \int V_i dt \quad (4.8)$$

#### 4.3.4. Differentiating Network.

A differentiator is rarely used in analogue computing due to its inherent ability to amplify the noise content of a signal. This introduces errors in the solution of a problem and makes

analysis more difficult. There are occasions when differentiating circuits can be beneficially used. They are often used to improve the response of control systems by way of phase advance networks and as elements for velocity and acceleration feedback and for error rate damping.

A basic differentiating network is shown in Fig.4.4 consisting of a capacitor C and a resistor R. If  $i$  is the current in the network the following relationships are obtained:-

$$\begin{aligned}
 i &= CD (V_i - V_o) \\
 V_o &= Ri \\
 &= RCD (V_i - V_o) \\
 \therefore V_o &= \frac{RCD}{1 + RCD} V_i \quad \text{putting } RC = T, \\
 V_o &= \frac{TD}{1 + TD} \qquad (4.9)
 \end{aligned}$$

If the value of  $T$  is much smaller than unity, the equation (4.9) reduces to:-

$$V_o = TD V_i \qquad (4.10)$$

Thus for a small value of time constant,  $T$ , the output voltage will be proportional to the time derivative of the input voltage and the network will act as a differentiating element.

#### 4.4. The Use of a High Gain Operational Amplifier.

##### 4.4.1. Limitations of Electrical Networks.

The electrical networks discussed above work well providing

there is no load connected across the output terminals. This is a serious limitation since during simulation of a problem several such networks may have to be connected together. This causes elements of one network to act in series or in parallel with the elements of other networks thus changing the nodal equations which were derived assuming no current flow across the output terminals. This condition is known as loading and can be overcome if the networks being connected together have a very high input impedance and a very low output impedance. It is also necessary for the source supplying the input voltage  $V_i$  to have a low impedance, that is the drawing of a current from the source must not have any significant effect on the value of  $V_i$  across the input terminals. Let the L - network of Fig.4.5 represent the network under discussion and let  $Z_1$  and  $Z_2$  be the impedances of the resistance and capacitance elements. If we now consider the current flow, then for current  $i$ :-

$$V_i = i Z_1 + i Z_2 \quad (4.11)$$

Consider now, the circuit of Fig.4.6 in which the source supplying  $V_i$  has a high internal resistance  $R$ , and a current is drawn from  $Z_2$  by the resistance  $R_3$  connected across the terminals. The equation for  $V_i$  now becomes:-

$$V_i = Ri + Z_1 i + \frac{Z_2 R_3 i}{Z_2 + R_3} \quad (4.12)$$

Comparing eqn. (4.11) and (4.12) it is clear that to prevent loading of networks some device is required to isolate the stages by offering a high input impedance to the output terminals of the first stage and a low output impedance to the input terminals of the second stage.

The high gain operational amplifier is such a device and is briefly described in the following section.

#### 4.4.2. The High Gain Operational Amplifier.

A block representation of an operational amplifier is shown in Fig.4.7. All voltages are measured with respect to a ground reference known as the signal ground. The quantity  $-A$  represents the gain of the amplifier which is very high, being of the order of  $10^6$  to  $10^8$  for amplifiers used in analogue computers. The symbolic representation of the operational amplifier is shown in Fig.4.8. The ground connections are usually omitted for the sake of clarity. These amplifiers are normally used in a closed loop configuration (Fig.4.9), that is, with a feedback from the output to the input and this accounts for the negative gain of the amplifier. A positive feedback would result in an unstable system.

The input and feedback impedances are represented by  $Z_i$  and  $Z_f$  respectively. The point SJ is the summing junction where all inputs to the amplifier are summed before going to the grid of the amplifier. This point is also known as the 'virtual earth' because the voltage  $V$  at the summing junction is given by:-

$$V = -\frac{V_o}{A} \quad (4.13)$$

The maximum value of  $V_o$  being the full swing computer voltage which in a valve machine is of the order of 100 volts. If the gain of the amplifier is  $10^8$ , then:-

$$V = -\frac{100}{10^8} = -10^{-6} \text{ volts.}$$

and hence the summing junction is virtually at the ground potential. Equation (4.13) assumes the output voltage  $V_o$  to be independent of the amplifier output current. This demands that the amplifier be

regarded as a voltage source with zero output impedance. In practice operational amplifiers are designed to have an output impedance of few ohms and input impedances of the order of mega-ohms thus satisfying the above condition.

The role played by the large gain ( $-A$ ) of an amplifier can be demonstrated in the following manner. Assuming no current flow from SJ (Fig.4.9) to the amplifier input, the nodal equation at SJ becomes:-

$$\frac{V - V_i}{Z_i} + \frac{V - V_o}{Z_f} = 0 \quad (4.14)$$

or 
$$\left( \frac{1}{Z_i} + \frac{1}{Z_f} \right) V - \frac{V_o}{Z_f} = \frac{V_i}{Z_i}$$

Substituting eqn. (4.13) in the above expression:-

$$- \frac{1}{A} \left( \frac{1}{Z_i} + \frac{1}{Z_f} \right) V_o - \frac{V_o}{Z_f} = \frac{V_i}{Z_i}$$

$$\text{or } V_o = - \frac{Z_f}{Z_i} \cdot V_i \left[ 1 + \frac{1}{A} \left( \frac{Z_f}{Z_i} + 1 \right) \right] \quad (4.15)$$

but  $A$  is very large and the equation (4.15) reduces to:-

$$V_o = - \frac{Z_f}{Z_i} V_i \quad (4.16)$$

It can be seen that the very large gain of an amplifier makes the various operations dependent solely on the ratio of feedback and input impedances.

#### 4.5. Mathematical Operations Performed with the Operational Amplifier.

##### 4.5.1. Sign Change.

The negative gain of an operational amplifier makes it possible to invert the sign of an input voltage by choosing the values of  $Z_i$  and  $Z_f$  such that their ratio is unity. This is shown in Fig.4.10a where both  $Z_i$  and  $Z_f$  are replaced by resistances  $R$  of equal value, giving:-

$$V_i = -V_o$$

The symbolic representation of a sign changer is shown in Fig.4.10b.

##### 4.5.2. Multiplication by a Constant.

Multiplication of a variable by a constant can simply be obtained by adjusting the ratio  $Z_f/Z_i$  to the required value. Since in most analogue computers these ratios are available only in steps of 10 it is necessary to use coefficient potentiometers. Figure 4.11 shows multiplication by a constant less than unity and Figure 4.12 shows multiplication by a constant greater than unity.

##### 4.5.3. Algebraic Summation.

An operational amplifier permits the summation of any number of voltages or variables without loading effects. The circuit diagram of Fig.4.13 illustrates the principle of addition. The polarity of variables to be summed can be either negative or positive. Assuming no current flow from SJ to the amplifier input the nodal equation becomes

$$\left(\frac{V_o}{A} - V_1\right) \frac{1}{R_1} + \left(\frac{V_o}{A} - V_2\right) \frac{1}{R_2} + \left(\frac{V_o}{A} + V_3\right) \frac{1}{R_3} + \left(\frac{V_o}{A} - V_o\right) \frac{1}{R_f} = 0$$

$$\text{or } V_o = -R_f \left( \frac{V_1}{R_1} + \frac{V_2}{R_2} - \frac{V_3}{R_3} \right) \left( 1 - \frac{1}{1 - Aa} \right) \quad (4.17)$$

where A is the amplifier gain

$$\text{and } a = \left( 1 + \frac{R_f}{R_1} + \frac{R_f}{R_2} + \frac{R_f}{R_3} \right)^{-1}$$

since the amplifier gain is very large, Aa is much greater than unity and may be neglected, Thus equation (4.17) reduces to:-

$$V_o = -R_f \left( \frac{V_1}{R_1} + \frac{V_2}{R_2} - \frac{V_3}{R_3} \right) \quad (4.18)$$

Each of the variables  $V_1$ ,  $V_2$  and  $V_3$  can be multiplied by a constant smaller or greater than unity by adjusting the ratio of input resistors to the feedback resistor  $R_f$  thus combining the two operations.

#### 4.6. Integration.

In the integration circuit shown in Fig.4.14 the voltage V opposing the capacitor charging current is very small ( $V = -V_o/A$ ) and hence the rate of charge on the capacitor is very nearly proportional to the input voltage  $V_i$ . This makes the output voltage directly proportional to the time integral of the input voltage resulting in accurate integration.

The nodal equation at SJ is:-

$$\left(\frac{V_o}{A} - V_1\right) \frac{1}{R} + CD \left(\frac{V_o}{A} - V_o\right) = 0 \quad (4.19)$$

since A is very large, and assuming no leakage across the capacitor, equation (4.19) can be written as:-

$$\frac{V_i}{R} + CD V_o = 0$$

or 
$$V_o = - \frac{1}{RCD} V_i$$

$\therefore$  
$$V_o = - \frac{1}{T} \int_0^T V_i \cdot dt \quad (4.20)$$

#### 4.7. Differentiation.

The network of Fig.4.4 when used with an operational amplifier represents the ideal or true differentiator. Consider Fig.4.15 the nodal equation for this circuit simplifies to give the transfer function:-

$$\frac{V_o}{V_i} = - RCD \quad (4.21)$$

and the modulus of this transfer function will be simply:-

$$\frac{V_o}{V_i} = - RCw \quad (4.22)$$

where w is the radian frequency of the input signal. It can be seen from eqn. (4.22) that the gain of the differentiator increases directly with the frequency of the input signal. Therefore the

noise content of the signal is also amplified. For this reason a true differentiator is often referred to as a 'noise amplifier'. In analogue computers approximate differentiating circuits are used to overcome the disadvantage of a true differentiator. A few approximate differentiating circuits are shown in Fig.4.16. The choice of the differentiator is governed by the quality and the frequency of the input signal and the requirements of accuracy.

#### 4.8. Multiplication of Two Variables.

Multiplication of one variable by another requires the use of special units known as multipliers. Many types of multipliers are available each making use of a different technique (25) (26) (27) (28) and (29). Since an electronic quarter-square multiplier was used during the course of this study, it is briefly described below.

##### The Electronic Quarter-Square Multiplier.

The quarter-square multipliers use electronic function generators in conjunction with operational amplifiers to perform multiplication. The function generators consist of biased diode networks or 'squaring cards' that produce a current proportional to the sum of the input voltages and generate a segmented straight line approximation to a square law. Thus the operation of multiplication is reduced to summing and squaring and is based on the identity

$$xy = \frac{1}{4} (x + y)^2 - \frac{1}{4} (x - y)^2 \quad (4.23)$$

For a four quadrant multiplication four squaring cards are used to form the product  $xy$  from inputs of  $+x$ ,  $-x$ ,  $+y$  and  $-y$ . The

positive squaring cards conduct when the sum of the input voltages has a positive polarity and produce the relationship:-

$$\frac{1}{4} (x + y)^2$$

The negative squaring cards conduct only when the sum of the input voltages has a negative polarity and generate the function:-

$$-\frac{1}{4} (x - y)^2$$

The outputs of the positive and the negative squaring cards are summed in an amplifier to give the relationship of eqn. (4.27). The schematic arrangement of a quarter-square multiplier, as used in a E.A.L. TR-20R analogue computer, is shown in Fig.4.17. The output is shown as  $-xy/V$ , where  $V$  represents the maximum computer voltage.

#### 4.9. Generating Functions Of a Variable.

Function generation is performed by special units called the diode function generators (DFG). A DFG is an electrical network consisting of diodes and resistors. It is based on the concept of straight line segmented approximation of arbitrary functions. The diodes are simply used as voltage sensitive switches which, when properly biased, switch a number of resistances at predetermined values of an input voltage. This switching action generates straight line segments which are added together to form the desired function.

Consider the diode circuit of Fig.4.18, the input voltage  $V_i$  sees an infinite resistance until its value equals  $V_b$ , the bias voltage. When  $V_i$  becomes greater than  $V_b$  the diode conducts and the

voltage drop due to the diode current appears across R as the output voltage  $V_o$ . The relationship between the input and the output voltages is of the form:-

$$V_o = \frac{V_i - V_b}{R} \quad (4.24)$$

A combination of such circuits can be used to generate monotonic functions giving any desirable relationship between the input and the output voltages. Two basic diode function generator circuits (30) together with their voltage-current characteristics are shown in Fig.4.19a and b. The former circuit gives a non-linear resistance which decreases with increasing value of  $V_i$ , and the later circuit gives a non-linear resistance which increases for increasing value of  $V_i$ . Practical D.F.G. circuits are connected to a load resistance which is usually the input resistance of an operational amplifier (Fig.4.20) and, hence, account must be taken of the load resistance when calculating the slopes after successive breakpoints. Non-monotonic functions are generated by subtracting two monotonic functions in an operational amplifier.

#### 4.10. Control Modes of the Computer.

Once a problem has been simulated on the computer it is necessary to adjust coefficient values and initial conditions of the problem before a computation can be started. This is done by setting the computer in one of its control modes. The control modes allow an operator to adjust, compute and hold a problem at any instant in time for checking and recording purposes. There are three basic control modes in the general purpose computer and these may be described as follows.

#### 4.10.1. Reset Control Mode.

It is in this control mode that the coefficient values are adjusted on the potentiometers and the initial condition voltages are applied to the integrators.

#### Coefficient Setting.

The transfer function of a potentiometer was shown to be in Fig.4.11a as:-

$$\frac{V_o}{V_i} = \frac{R_2}{R_1} \quad (4.25)$$

This relationship holds only if the output of the potentiometer is not connected to a load resistance. In practice the potentiometer will be loaded by the input resistance of an operational amplifier (Fig.4.21). The transfer function of a loaded potentiometer is given by:-

$$\frac{V_o}{V_i} = \frac{R_2/R_1}{1 + R_2/R_L - R_2^2/R_1 R_L} \quad (4.35)$$

To avoid loading errors coefficient potentiometers are set under load conditions by comparison to a precision reference potentiometer having an accuracy of .01 per cent or better. The reference potentiometer is adjusted to the value to be set on the coefficient potentiometer. The computer reference voltages are applied to both the potentiometers and the coefficient potentiometer is adjusted with its slider arm connected to the load resistance. The outputs of the two potentiometers are compared on a null indicating meter.

When the reading on the null meter is zero the coefficient potentiometer is accurately set (Fig.4.22).

#### Initial Conditions.

The initial conditions of a problem require that the integrators used in the simulation be charged to voltages representing the values of the dependent variables at a time  $t = 0$ . This operation is performed with the computer in the reset mode. Figure 4.23 shows a typical integrator circuit which includes two relays  $L_1$  and  $L_2$  labeled reset relay and hold relay respectively. In reset mode the relay  $L_1$  is energised and connects the initial condition voltage to the capacitor through the resistance  $R$ . The relay  $L_2$  connects the inputs  $Z_1$  and  $Z_2$  of the integrator to earth ensuring that the only voltage on the capacitor is that representing the initial conditions.

#### 4.10.2. Computer Mode.

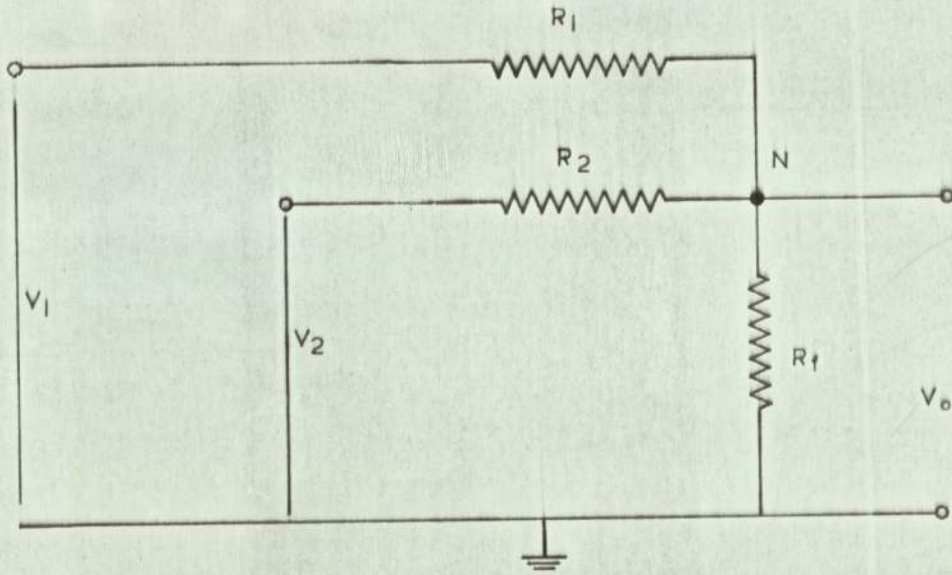
When the initial conditions have been set the solution of a problem can be started at the instant of zero time. This is done by changing the state of the computer from reset to compute mode. In the basic analogue computer the only elements that change state when the compute mode is operated are the integrators. Referring to Fig.4.23, both the reset and hold relays are de-energised in the compute mode. The relay  $L_1$  grounds the initial condition voltages and the relay  $L_2$  connects the inputs  $Z_1$  and  $Z_2$  to the integrator.

#### 4.10.3. Hold Mode.

The hold mode affords the facility for holding or "freezing" the solution at any instant of time. Once the hold mode is operated the integrators are disabled and the voltages across the computing

elements are held at a constant value. This facility is useful when checks are required at a particular time or for recording the output of the computing elements through analogue to digital converters. The hold mode is also made use of as an analogue memory element in track-hold circuits for iterative computing. In the hold mode the relay  $L_1$  remains open and the relay  $L_2$  is energised grounding inputs to the integrator which causes the capacitor to hold its voltage at a constant level (Fig.4.23). The solution in time can be recommenced by simply placing the computer in the compute mode.

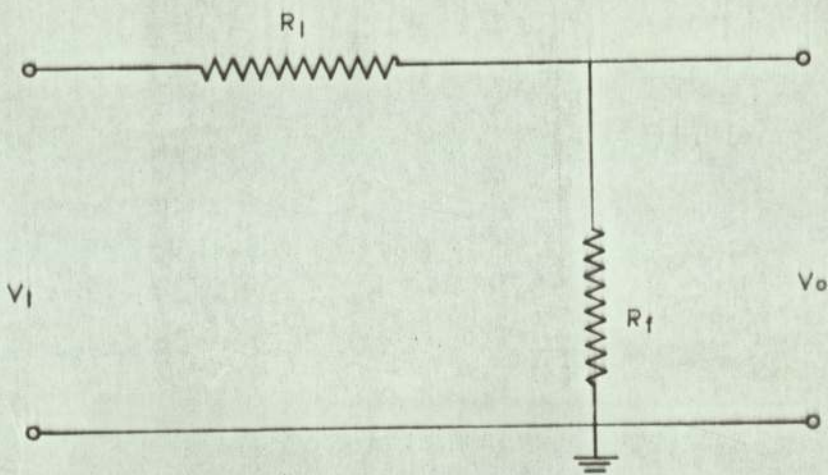
Chapter 5 contains a description of the analogue computer and the instrumentation used for impedance analysis.



$$V_o = \left( \frac{R_f}{R_1} V_1 + \frac{R_f}{R_2} V_2 \right) \left[ R_f \left( \frac{1}{R_1} + \frac{1}{R_2} \right) \right]^{-1}$$

SUMMING NETWORK

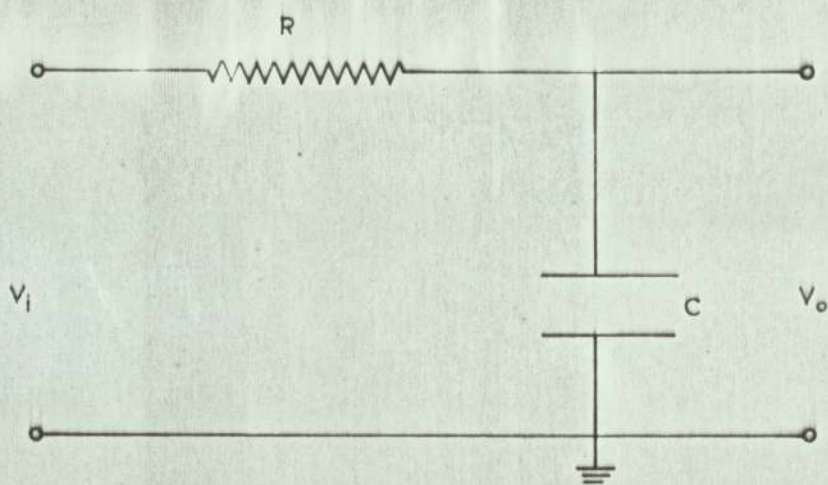
FIG 4.1



$$V_o = \frac{R_f}{R_1 + R_f} V_1$$

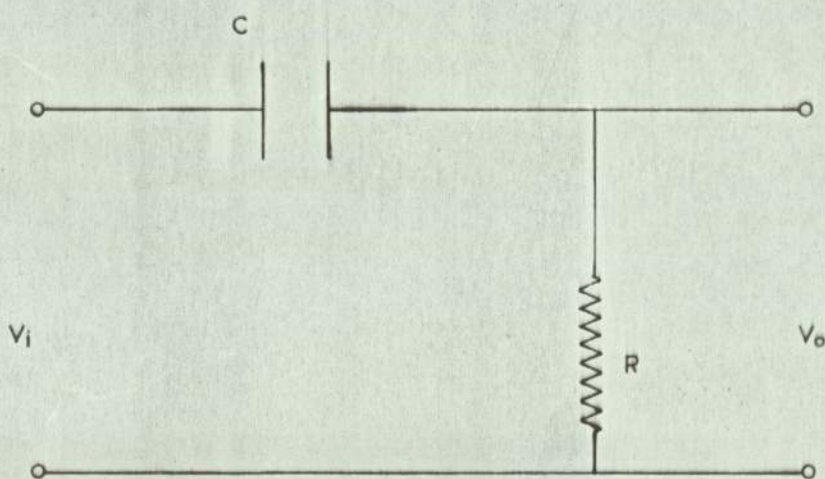
MULTIPLICATION BY A CONSTANT

FIG 4.2



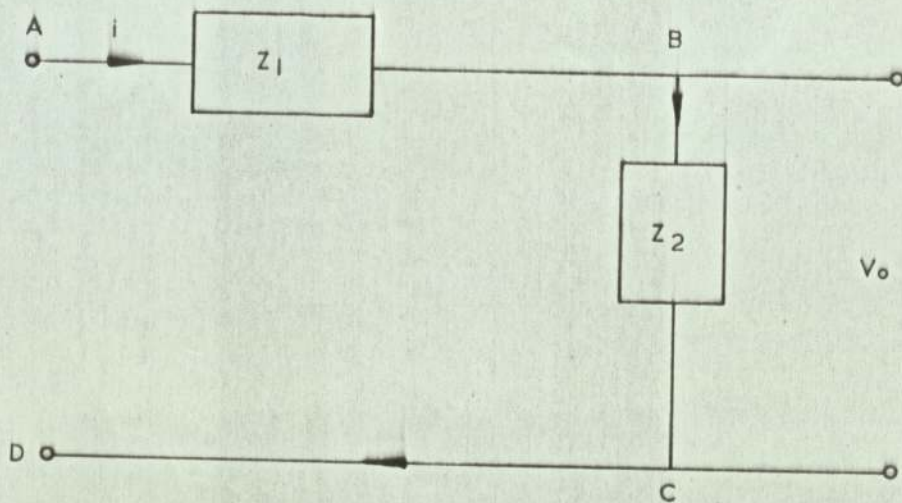
INTEGRATING NETWORK

FIG 4.3



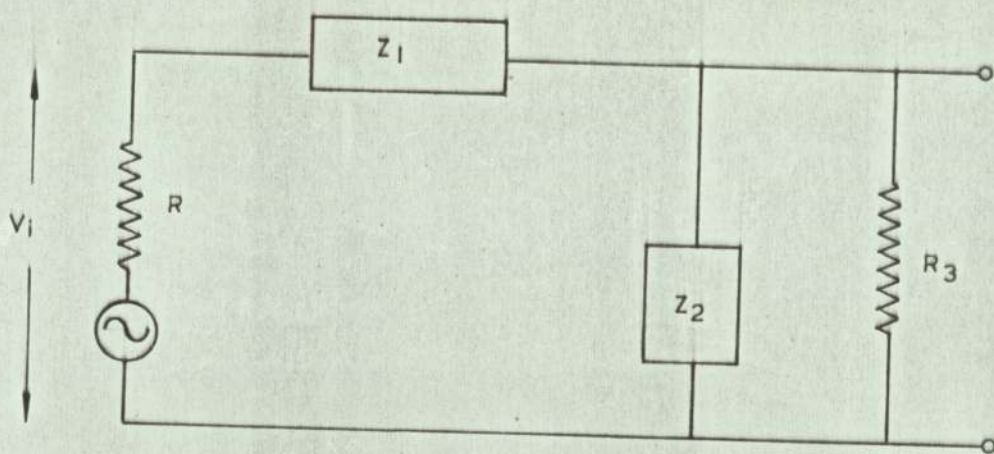
DIFFERENTIATING NETWORK

FIG 4.4



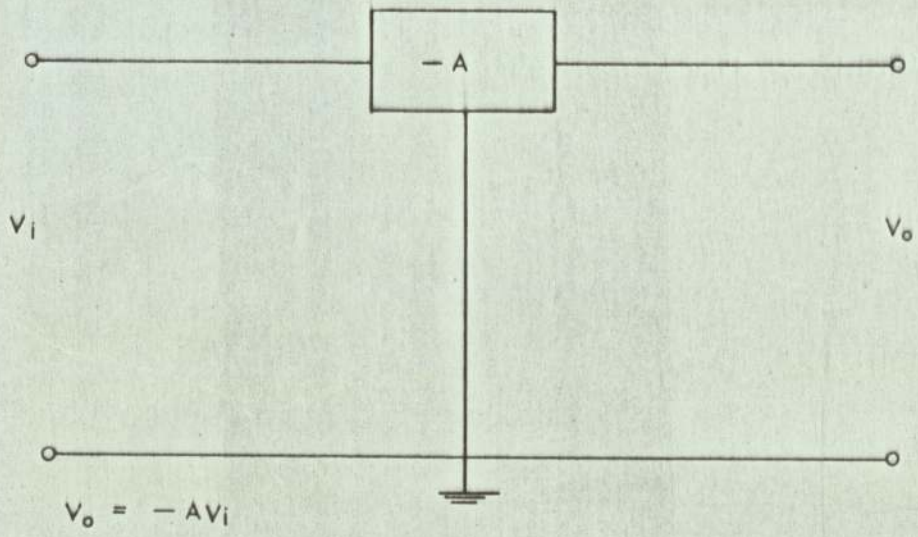
L - NETWORK

FIG 4.5



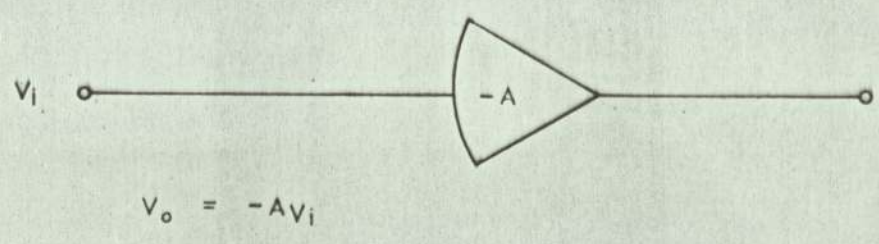
$$V_i = R_i + Z_i + \frac{Z_1 R_3 i}{Z_1 + R_3}$$

A LOADED L-NETWORK



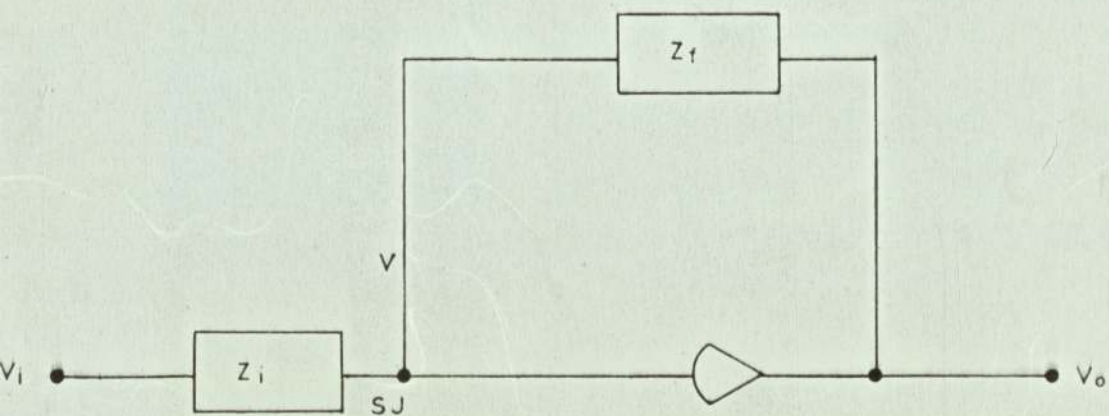
BLOCK REPRESENTATION OF AN OPERATIONAL AMPLIFIER

FIG 4.7



SYMBOL FOR AN OPERATIONAL AMPLIFIER

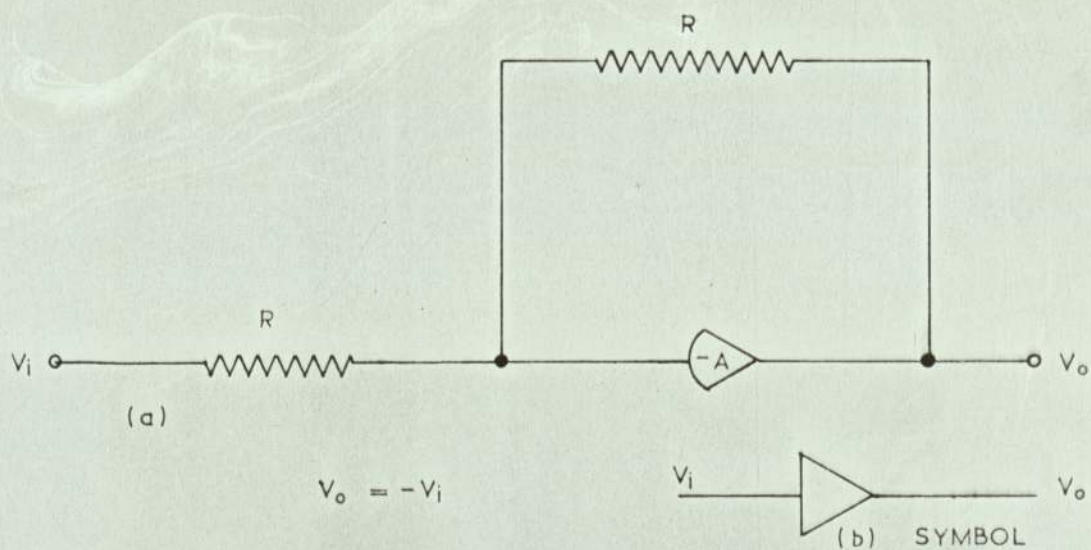
FIG 4.8



$$V_o = -AV = -\frac{Z_f}{Z_i} V_i$$

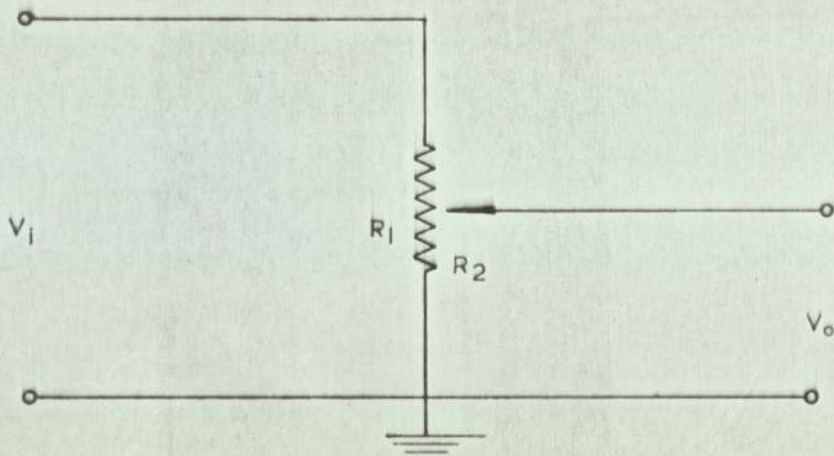
OPERATIONAL AMPLIFIER IN A CLOSED LOOP

FIG 4-9



SIGN INVERSION OPERATIONAL AMPLIFIER

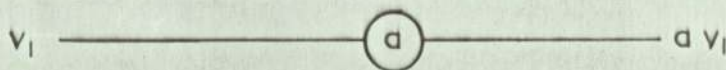
FIG 4-10



$$V_o = a V_i \quad \text{WHERE } a = \frac{R_2}{R_1} \leq 1$$

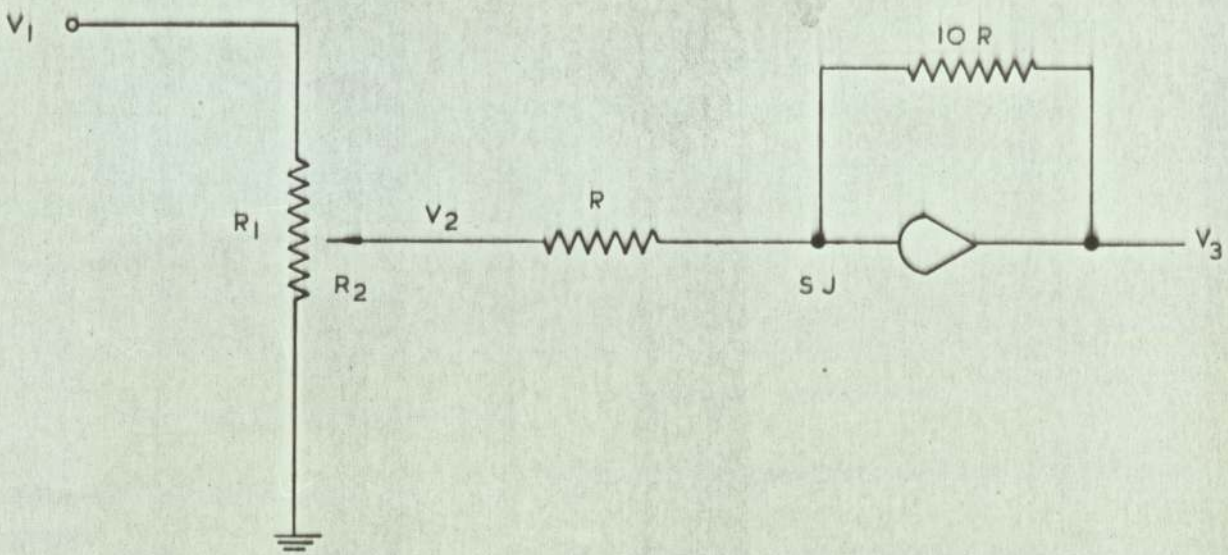
SCHEMATIC OF A COEFFICIENT POTENTIOMETER

FIG 4-II.a.



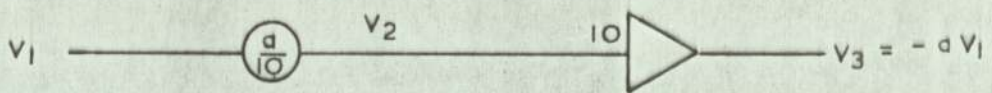
SYMBOL FOR A COEFFICIENT POTENTIOMETER

FIG 4-II.b.



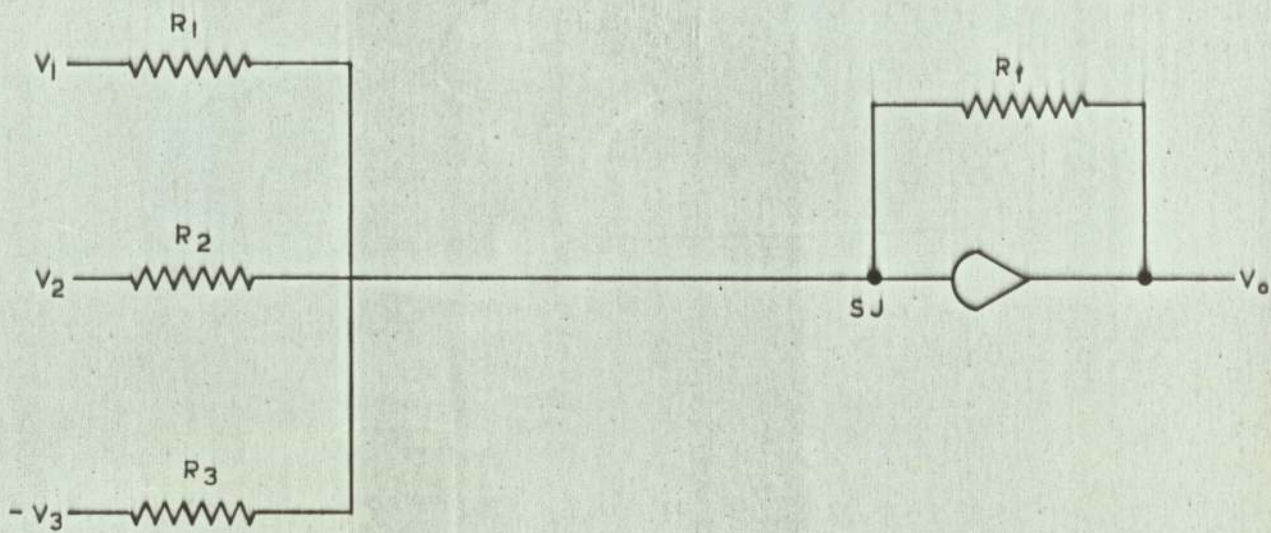
$$\left. \begin{aligned} V_2 &= \frac{R_2}{R_1} V_1 = \frac{a}{10} V_1 \\ V_3 &= \frac{R_2}{R_1} V_1 = a V_1 \end{aligned} \right\} \text{ASSUMING NO CURRENT FLOW}$$

(a) SCHEMATIC



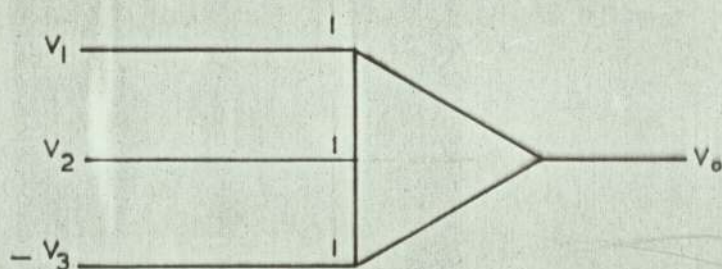
(b) SYMBOL

MULTIPLICATION BY A CONSTANT GREATER THAN UNITY



$$V_o = -R_f \left( \frac{V_1}{R_1} + \frac{V_2}{R_2} - \frac{V_3}{R} \right)$$

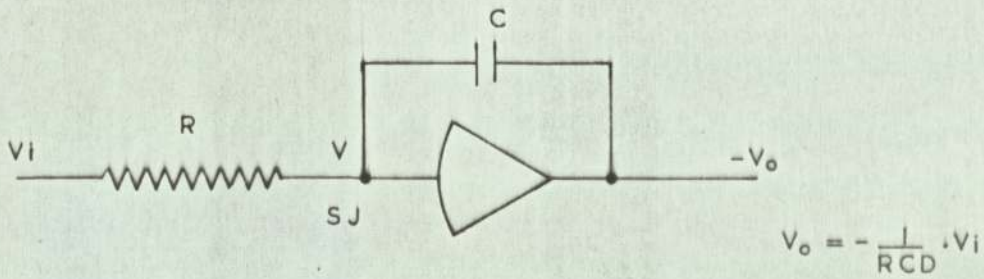
(a) CIRCUIT DIAGRAM FOR SUMMATION



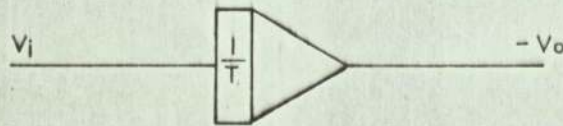
$$V_o = -(V_1 + V_2 - V_3)$$

(b) SYMBOL FOR SUMMATION

ALGEBRAIC SUMMATION OF VARIABLES



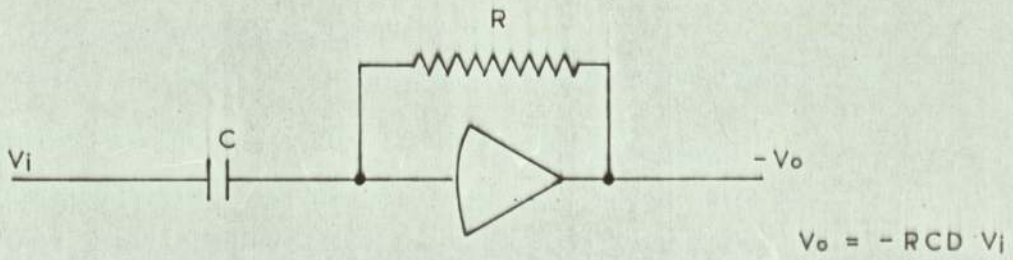
(d) CIRCUIT DIAGRAM



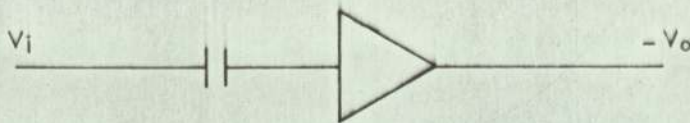
(b) SYMBOL FOR AN INTEGRATOR

INTEGRATION USING AN OPERATIONAL AMPLIFIER

FIG 4.14



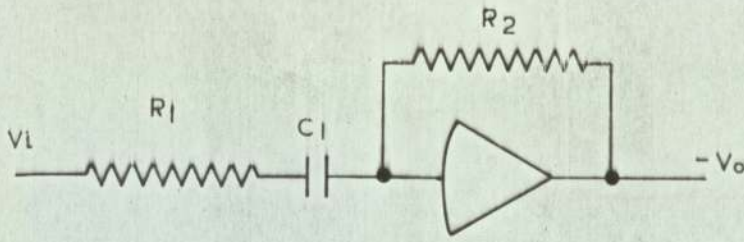
(d) CIRCUIT DIAGRAM



(b) SYMBOL FOR A DIFFERENTIATOR

DIFFERENTIATION USING AN OPERATIONAL AMPLIFIER

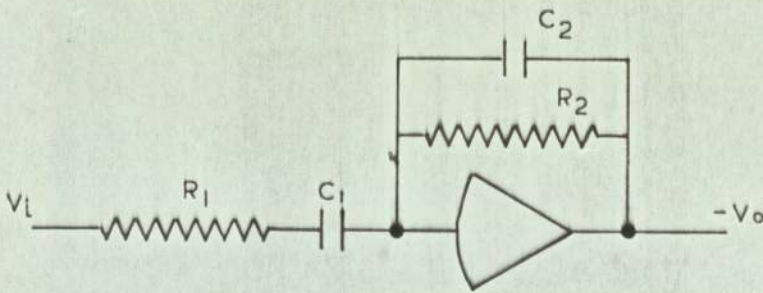
FIG 4.15



$$T_2 = R_2 C$$

$$T_1 = R_1 C$$

d) 
$$\frac{V_o}{V_i} = - \frac{T_2 D}{1 + T_1 D}$$

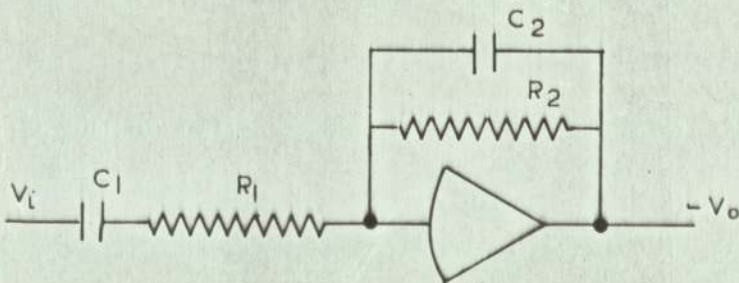


$$T_3 = R_2 C_1$$

$$T_2 = R_2 C_2$$

$$T_1 = R_1 C_1$$

b) 
$$\frac{V_o}{V_i} = - \frac{T_3 D}{(1 + T_1 D) (1 + T_2 D)}$$



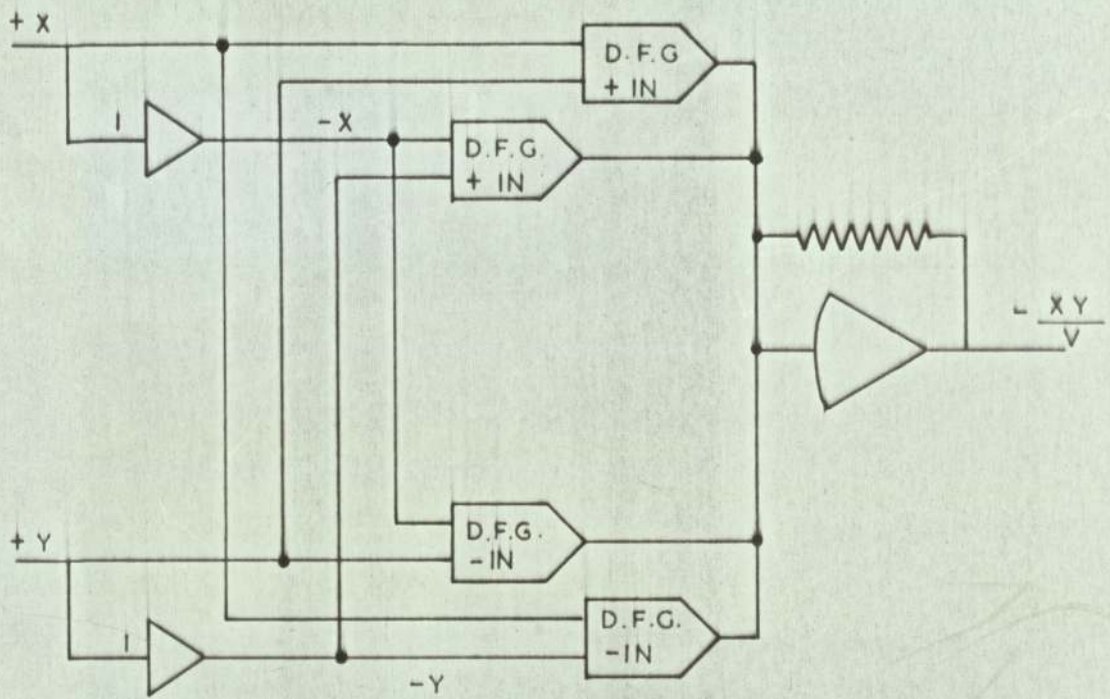
$$T_3 = R_1 C_2$$

$$T_2 = R_2 C_2$$

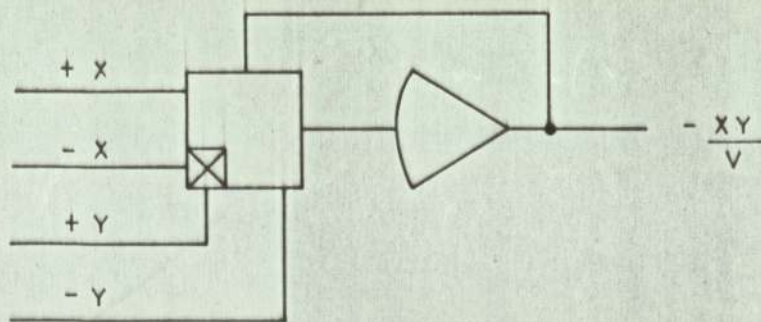
$$T_1 = R_1 C_1$$

c) 
$$\frac{V_o}{V_i} = - \frac{T_3 D}{(1 + T_1 D) (1 + T_2 D)}$$

### APPROXIMATE DIFFERENTIATING CIRCUITS

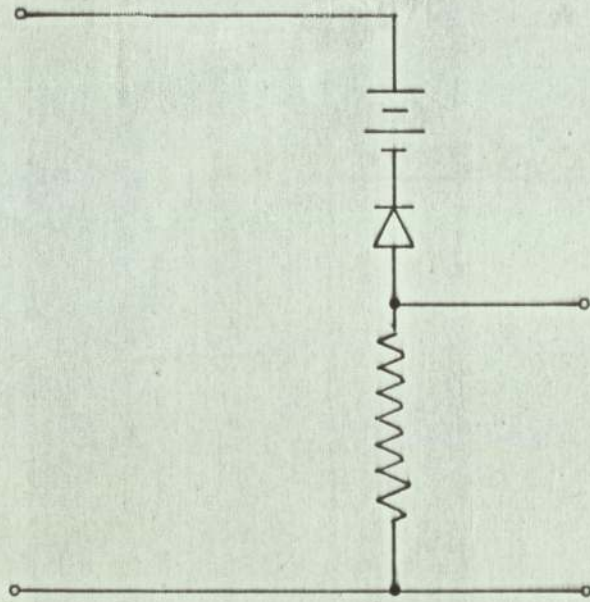


d) SCHEMATIC ARRANGEMENT OF A QUARTER - SQUARE MULTIPLIER

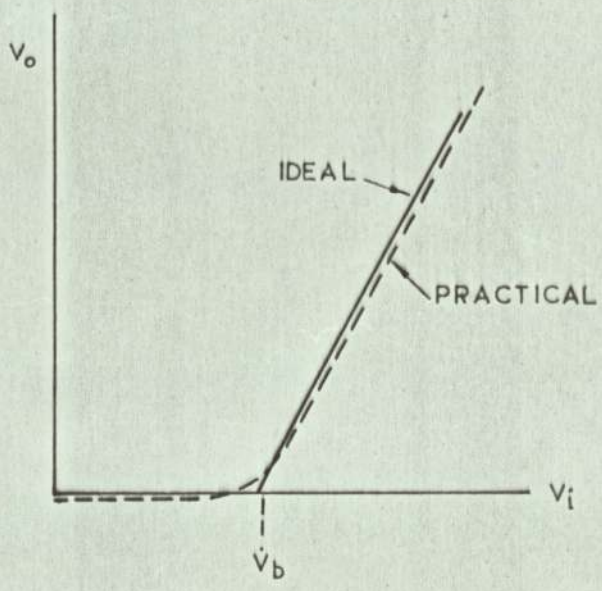


d) SYMBOL FOR A QUARTER - SQUARE MULTIPLIER

QUARTER - SQUARE MULTIPLIER

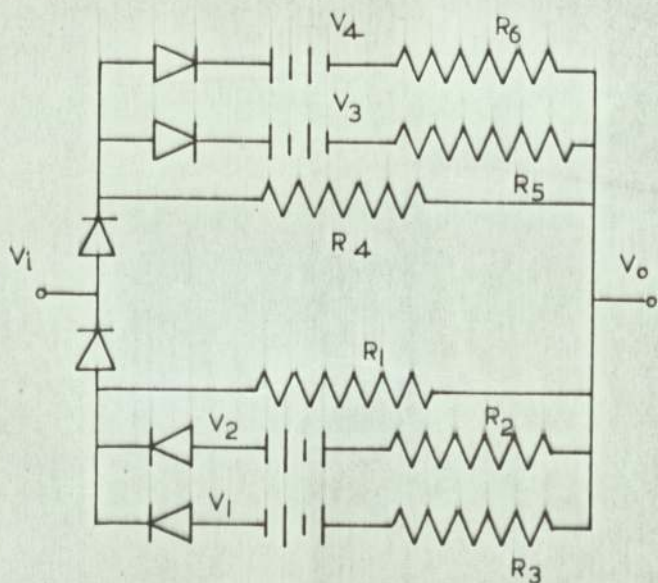


a) DIODE CIRCUIT

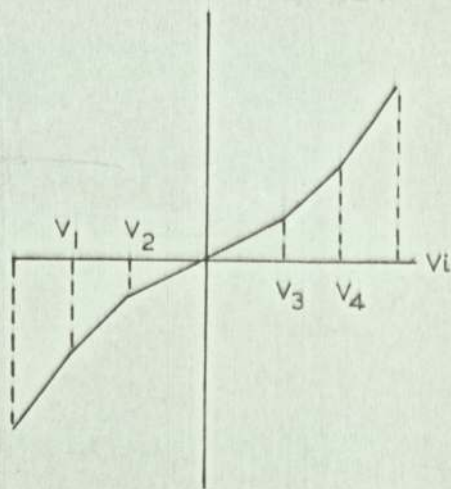


b) DIODE CHARACTERISTICS

A BASIC DIODE CIRCUIT

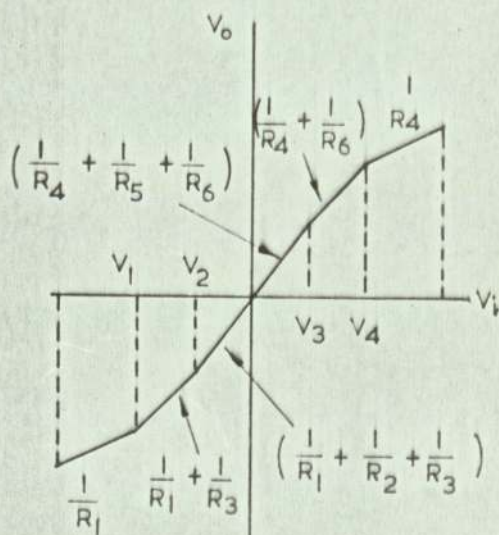
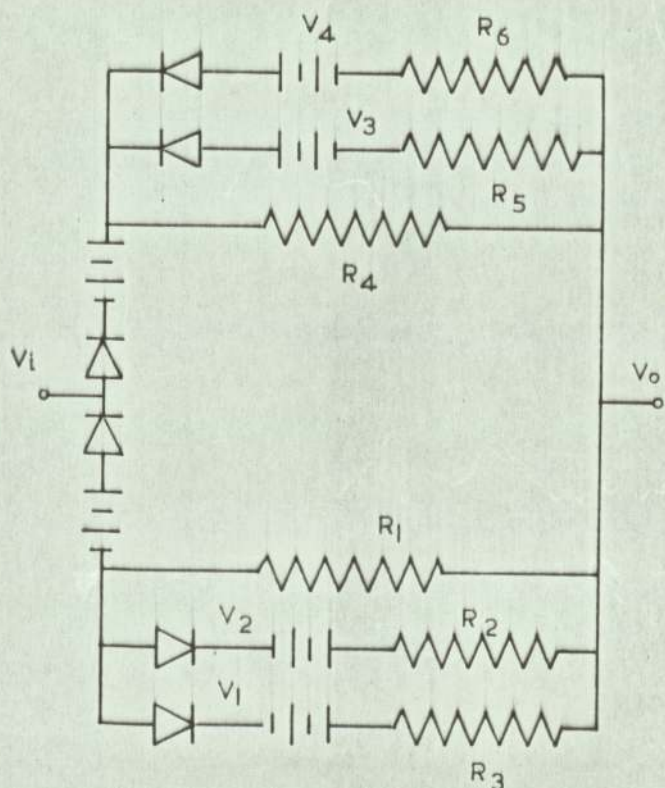


DIODE CIRCUIT



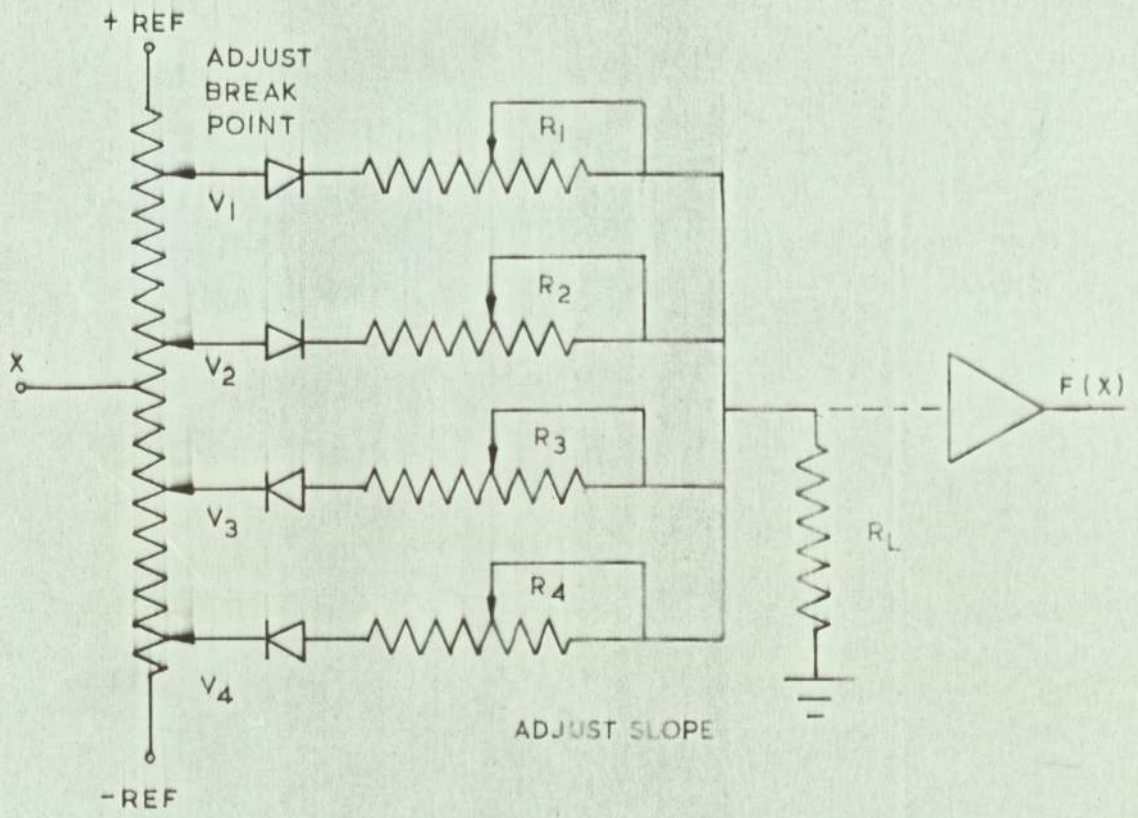
CHARACTERISTICS

d) DECREASING NON-LINEAR RESISTANCE

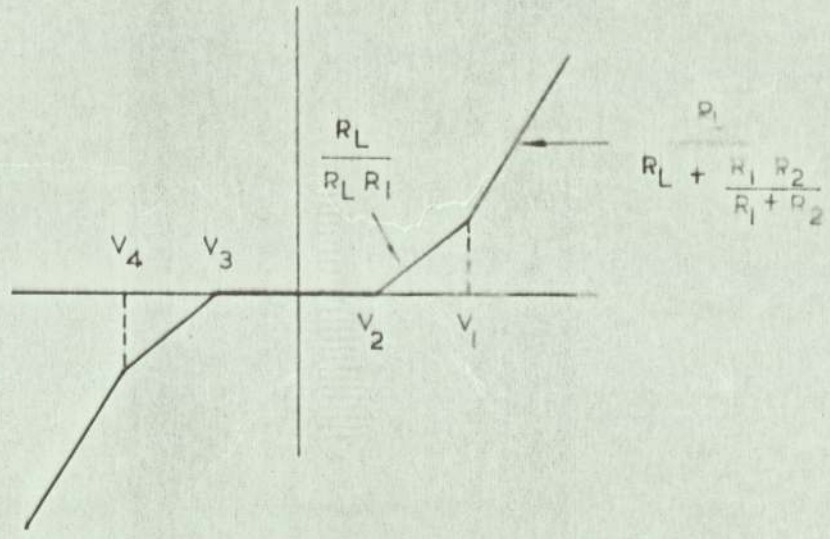


b) INCREASING NON-LINEAR RESISTANCE

BASIC DIODE FUNCTION GENERATOR CIRCUITS

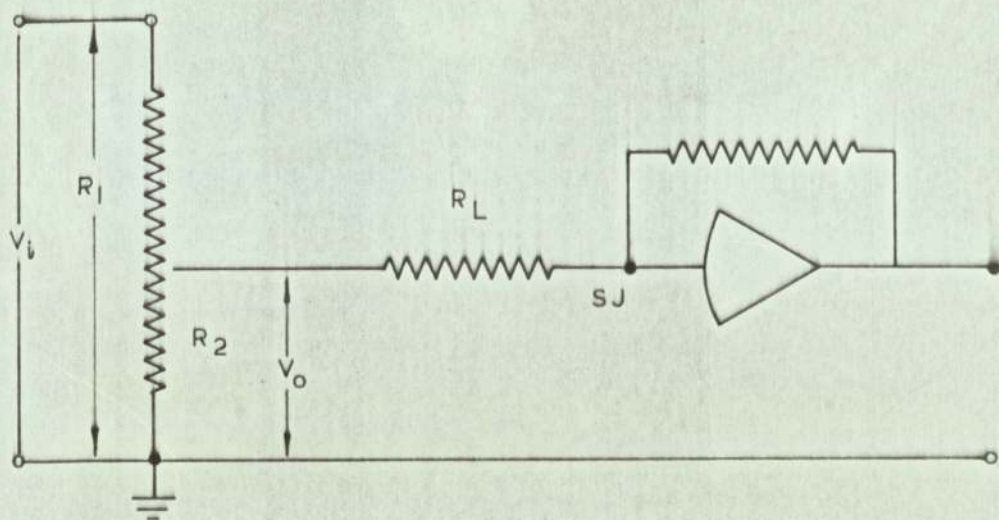


a) PRACTICAL CIRCUIT



b) CHARACTERISTIC

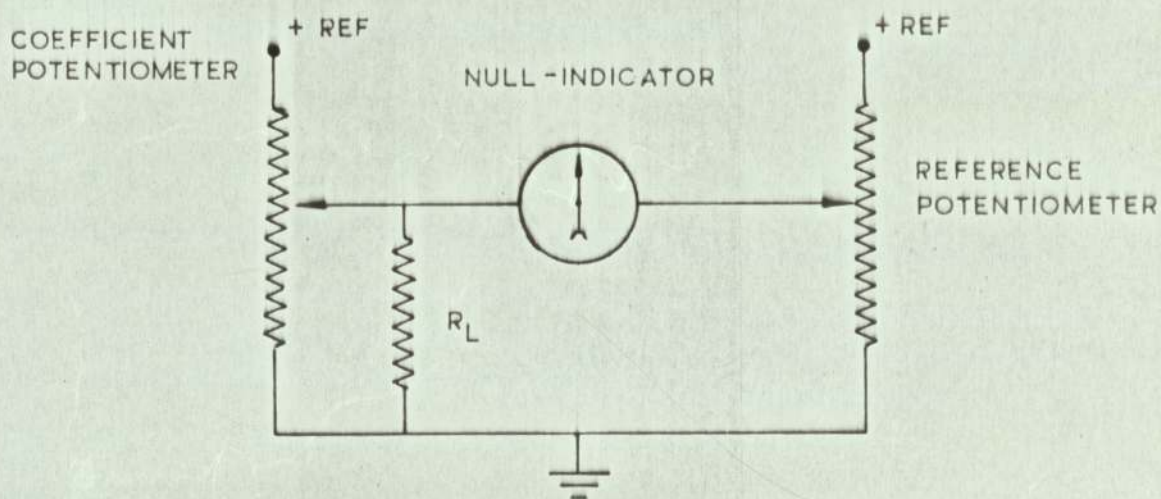
A PRACTICAL DIODE FUNCTION GENERATOR



$$\frac{V_o}{V_i} = \frac{R_2 / R_1}{1 + \frac{R_2}{R_L} - \frac{R_2^2}{R_1 R_L}}$$

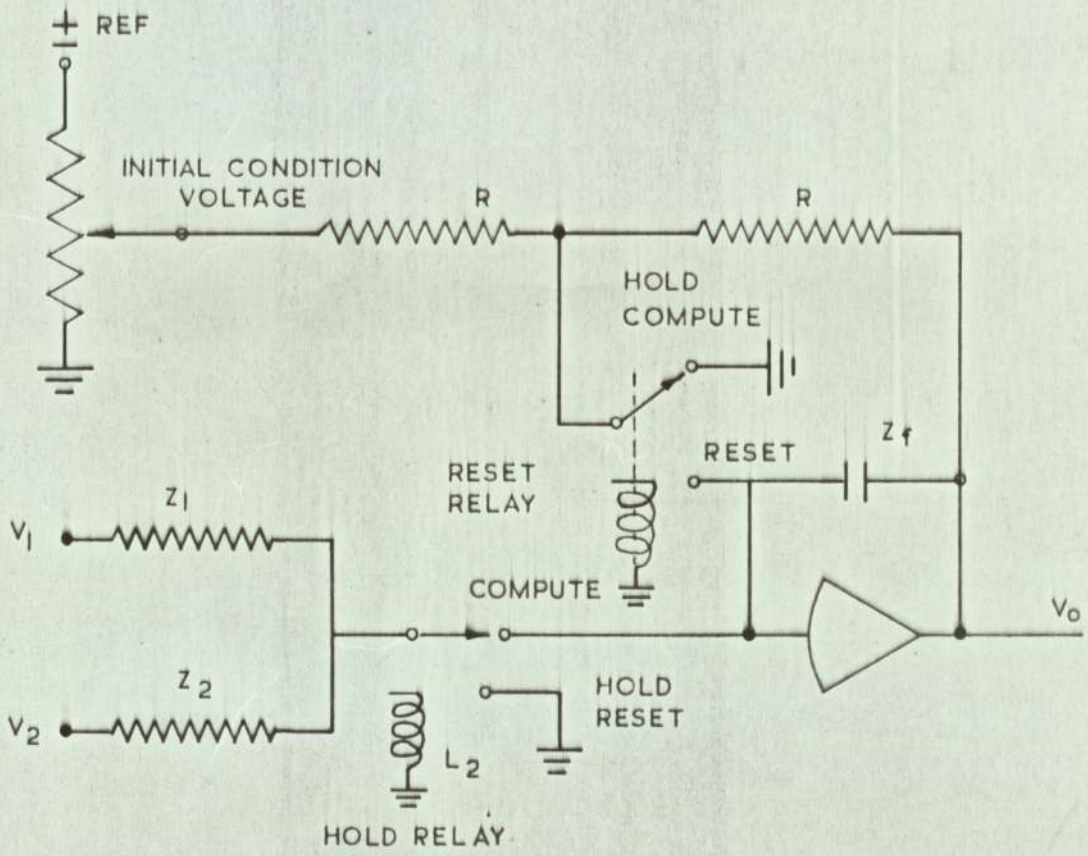
A LOADED COEFFICIENT POTENTIOMETER

FIG 4.21



COEFFICIENT SETTING UNDER LOAD CONDITIONS

FIG 4.22



RELAY CONTROL OF AN INTEGRATOR

CHAPTER 5.

INSTRUMENTATION.

CHAPTER 5.

INSTRUMENTATION.

CONTENTS.

PAGE.

5.1.	The Analogue Computer.	68
5.2.	The Automatic Mechanical Impedance Analyser.	70

## CHAPTER 5.

INSTRUMENTATION.5.1. The Analogue Computer.

The Analogue Computer used for the present study was an EAL 'PACE' model TR-20r. It was a transistorised machine with a full swing computer voltage of  $\pm 10$  volts and an overload voltage of  $\pm 13.5$  volts. It had the following complement of plug-in computing elements.

Operational amplifiers (24 off)

The high gain operational amplifiers had an open loop gain of better than  $5 \times 10^7$ . Each amplifier having five input resistors, three at 100 kil $\Omega$ -ohms and two at 10 kil $\Omega$ -ohms. Either the 100 kil $\Omega$ -ohm or the 10 kil $\Omega$ -ohm resistor could be used as the feedback element to the amplifier thus providing gains of 10 and 1 or 1 and 0.1. All resistors had an accuracy of .01 percent. The output impedances of the operational amplifiers were each less than 0.5 ohms. The amplifier output current was rated at 20 ma which was more than adequate to drive an x-y plotter or a U-V recorder.

Coefficient potentiometers. (28 off)

Four of the 28 potentiometers were precision attenuators with calibrated dials and a resolution of .001. The remaining 24 potentiometers had to be set with reference to a precision potentiometer and a null indicating meter. Twelve of these potentiometers were grounded and the other twelve were left open ended with an earth terminal located near each.

### Integrators (8 off)

Each integrator unit had two built in circuits. One circuit had a 10 micro-farad capacitor and was used with the manual operation of the computer to provide integrator gains of the 1 and 10 depending on the value of the input resistor. The other circuit was normally used with the automatic repetition unit and had a .02 micro-farad capacitor to provide gains of 500 and 5,000 for the fast repetitive operation. Any integrator unit could be used as a feed-back element to any of the 24 operational amplifiers. The relays for the reset hold and compute modes were incorporated in each of the units.

### Multipliers (2 off)

These were electronic quarter-square multipliers and were used as feed forward elements to an operational amplifier to perform multiplication of two variables or to square a single variable. For accurate multiplication the output of the multiplier was required to be one volt and above. This was found to be a serious limitation. These units were also found to be unstable when used as feedback elements to an operational amplifier for division or root extraction of periodic or complex signals.

### Variable diode function generators (2 off)

One unit was a + V.D.F.G. and the other a - V.D.F.G. Each unit had 10 segments for generating functions of a single variable, by straight line approximation, in conjunction with an operational amplifier.

### Relay comparators (2 off)

These were electro - mechanical devices that changed state by comparing two input signals and could be made to switch on or off at a predetermined voltage level.

These units were, however, found to malfunction above a frequency of 20 C/S and caused a great deal of trouble in the initial

stages of the simulation. It was finally decided not to use these units.

#### Function switches (2 off)

These were manual switches that could select one of the two applied signals to them.

#### Log x units (2 off)

When used as feed forward elements to an operational amplifier these units provided the logarithm to the base of 10 of a constant or a variable.

### 5.2. The Automatic Mechanical Impedance Analyser.

The force and displacement signals from the analogue computer were fed to the "spectral Dynamics" automatic-mechanical impedance analyser which operated upon these signals and produced at its output d.c. voltages representing the logarithm of the impedance, the phase difference between the force and displacement signals, and the logarithm of the frequency (Fig.5.1). The operation of the impedance analyser, in terms of its modules, is described below.

#### Dynamic analyser.

The dynamic analyser is a frequency tuned tracking filter of a constant narrow band width the frequency of which is automatically tuned to the frequency of the signal being analysed. A functional diagram of the dynamic analyser elements is shown in block form in Fig.5.2 and the concept of operation in Fig.5.3. Plug-in filters having bandwidth of 2,5, 10 and 20 C/S were available but the filters used for this study had a bandwidth of 5 C/S and a shape factor of 4 as shown in Fig.5.4. This gave a rejection of 22 dB for the first harmonic at a filter centre frequency of 5 C/S. At a centre frequency of 10 C/S and above the harmonic rejection was better than 60 dB (Fig.5.5).

### Log converter.

The log converters operate upon the output of the dynamic analysers and generate a d.c. proportional to the logarithm of the input signals thus providing the ability to plot a wide range of impedances or mobilities. The meters on the log converters display the r.m.s. value of the input signal on a logarithmic scale.

### Phase meter.

The phase meter compares the constant 100 KC/S amplitude and phase coherent signals, generated by the dynamic analysers, and gives a d.c. output proportional to the phase difference between the two signals. It operates very accurately at this particular frequency.

### Sweep oscillator.

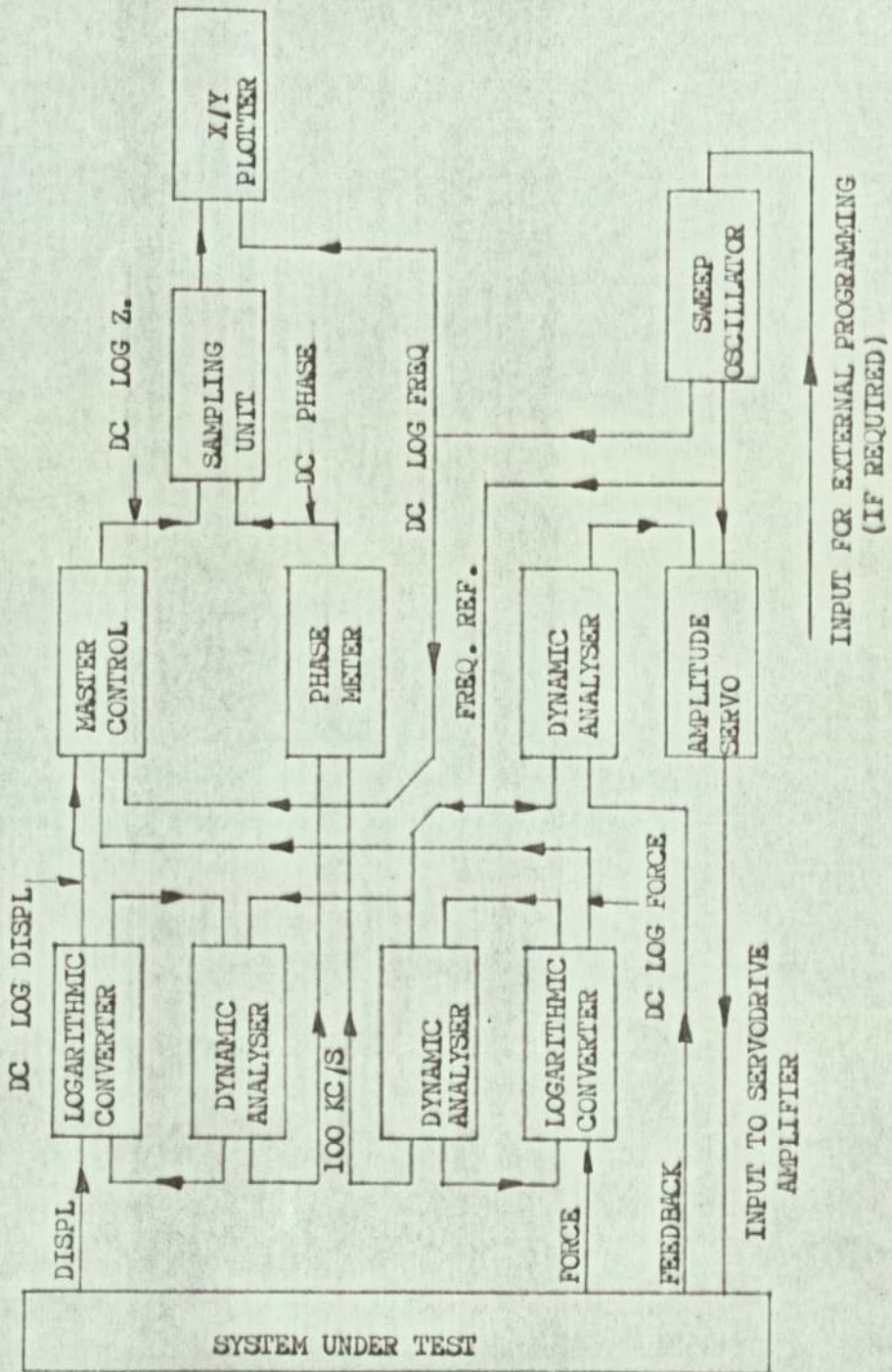
The sweep oscillator provides a constant amplitude sinusoidal signal for system excitation the frequency of which can be continuously varied at a predetermined rate. It also provides reference signals for tuning the frequency of the dynamic analysers and linear and logarithmic d.c. signals proportional to frequency. The frequency sweep rate can be either linear or logarithmic. The oscillator can be remotely controlled by an external d.c. input proportional to the frequency,

### Amplitude servo monitor.

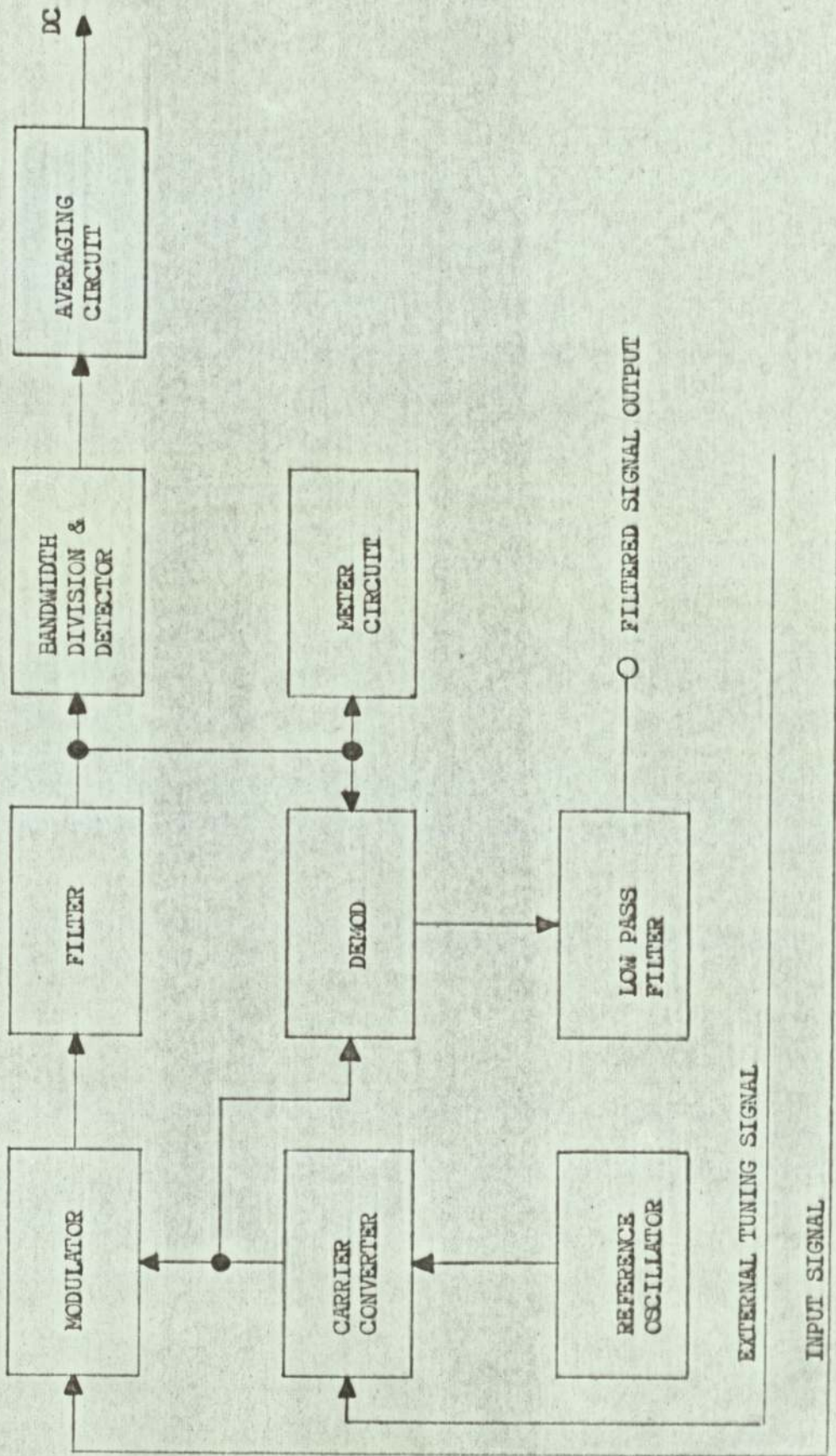
The amplitude servo monitor (compressor) keeps the force or displacement signal to the system under test at a constant level by comparing a feedback from the system with the oscillator output. The system feedback is first filtered by a dynamic analyser in the servo loop so that the servo monitor operates on a clean sinusoidal signal and compares only the fundamental component with the oscillator output.

Master control unit.

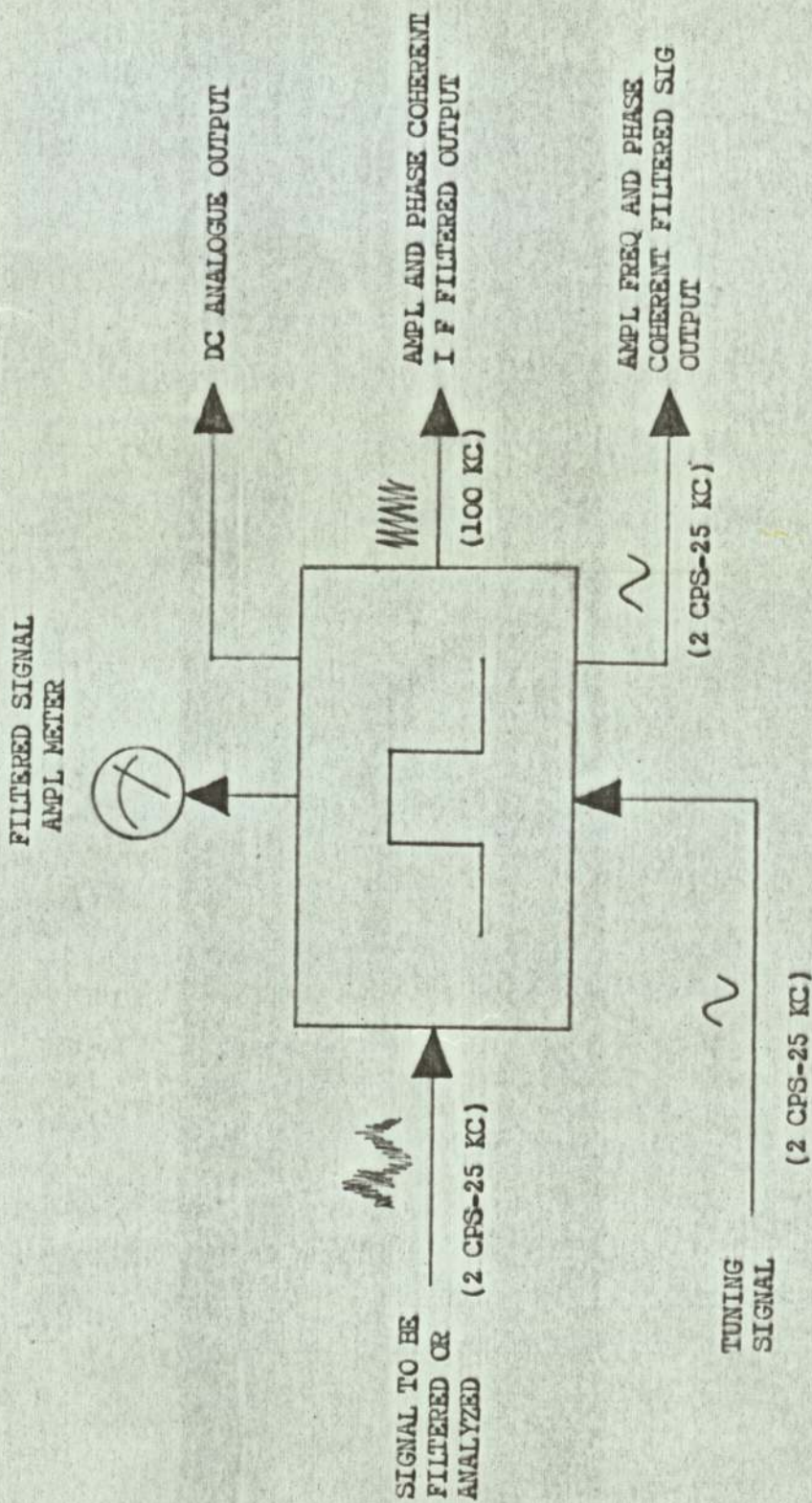
The master control unit operates upon the force and response signals from the log converters and give a d.c. proportional to the difference of two logarithms which is the impedance or mobility depending upon the settings of the controls on this unit. It is also capable of integrating and differentiating the input signals and, hence, given an acceleration response can provide a velocity or a displacement response and vice versa.



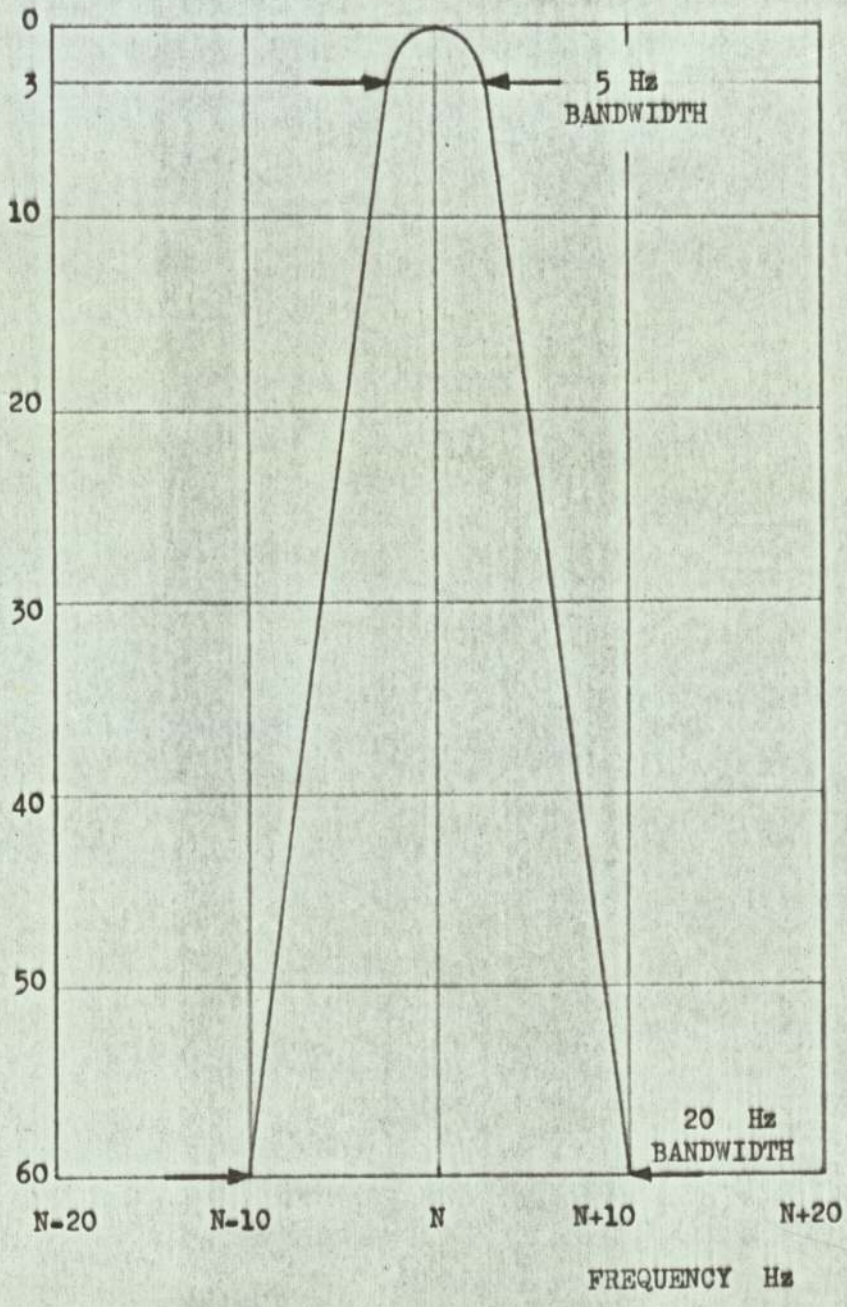
AUTOMATIC MECHANICAL IMPEDANCE ANALYSIS SYSTEM



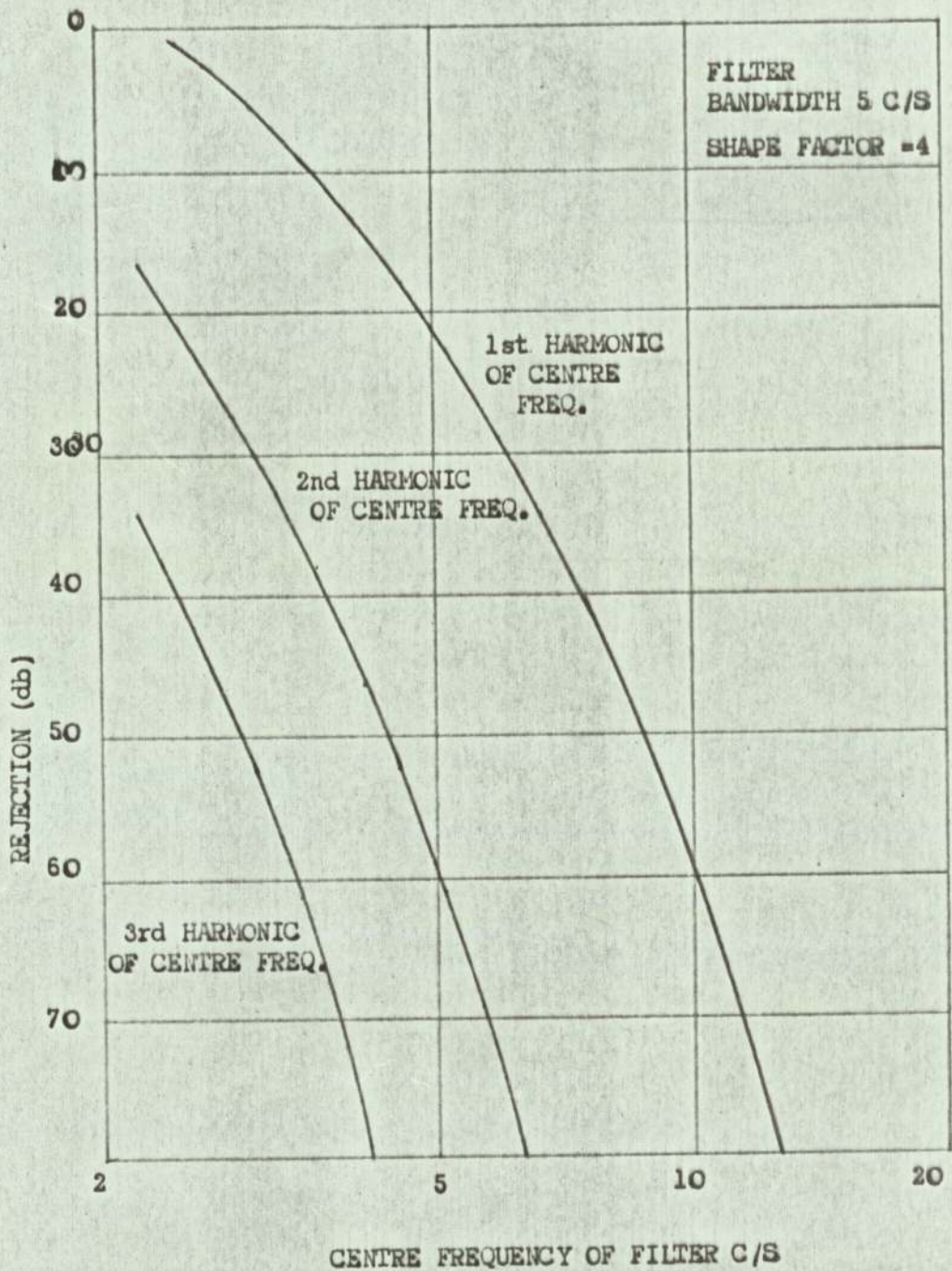
DYNAMIC ANALYSER - FUNCTIONAL DIAGRAM



DYNAMIC ANALYSER - CONCEPT OF OPERATION



RESPONSE OF A CONSTANT BANDWIDTH FILTER



HARMONIC FREQUENCY OF REJECTION OF A CONSTANT BANDWIDTH FILTER

CHAPTER 6.

ANALOGUE SIMULATION OF A HYDRAULIC SERVOMECHANISM  
WITH OUTPUT END EXCITATION.

CHAPTER 6.

ANALOGUE SIMULATION OF A HYDRAULIC SERVOMECHANISM  
WITH OUTPUT END EXCITATION.

<u>CONTENTS.</u>	<u>PAGE.</u>
6.1. Equations of Motion in a form suitable for simulation.	73
6.2. Coefficient Values.	76
6.3. Problem variables and Scale Factor Equations.	78
6.4. The Analogue Computer Circuit.	83

## CHAPTER 6.

ANALOGUE SIMULATION OF A HYDRAULIC  
SERVOMECHANISM WITH OUTPUT END EXCITATION.

6.1. Equations of Motion in a Form Suitable for Simulation.

The equations of motion for a hydraulic servomechanism were developed in chapter 3 and are here modified into a form suitable for analogue simulation. The flow into one side of jack piston was defined as:-

(Flow to compress fluid confined to one side of jack piston).

+ (Flow corresponding to jack velocity).

+ (Leakage flow across the jack, out of chamber 1).

+ (Leakage flow out of jack).

$$\therefore Q_1 = \frac{V_1}{N} \frac{dP_1}{dt} + A \frac{dx_o}{dt} + Q_{j1} + Q_{o1}$$

where  $Q_{j1} = K_j(P_1 - P_2)$  and  $Q_{o1} = K_o(P_1)$

Putting  $V_1 = V_2 = V/2$  and  $dx_o/dt$  as  $\dot{x}$  etc.,

$$Q_1 = \frac{V}{2N} \dot{P}_1 + A\dot{x}_o + K_j(P_1 - P_2) + K_o(P_1) \quad (6.1)$$

Similarly the flow out of the other side of jack will be:-

$$Q_2 = -\frac{V}{2N} \dot{P}_2 + A\dot{x} + K_j(P_1 - P_2) - K_o(P_2) \quad (6.2)$$

Also from equations (3.40) and (3.41)

$$Q_1 = Q_2 = K_V E (P_V/2)^{\frac{1}{2}} \quad (6.3)$$

Substituting for  $Q_1$  and  $Q_2$  into equations (6.1) and (6.2) and adding for total flow through the valve,

$$2K_V E (P_V/2)^{\frac{1}{2}} = \frac{V}{2N} (\dot{P}_1 - \dot{P}_2) + 2A\dot{x} + 2K_j(P_1 - P_2) + K_o(P_1 - P_2)$$

But  $(P_1 - P_2) = P_j$ , the pressure drop across the jack, and  $P_V = P_s - P_j$ , where  $P_s$  is the supply pressure.

$$\therefore K_V E [2(P_s - P_j)]^{\frac{1}{2}} = \frac{V}{2N} \dot{P}_j + 2A\dot{x} + 2K_j P_j + K_o P_j \quad (6.4)$$

Both the valve error  $E$  and the valve constant  $K_V$  are functions of the valve displacement from the neutral position. With the valve input locked for impedance testing  $K_V E$  can be expressed as a function of  $X_o$ , the displacement of the output end of the jack.

$$\therefore K_V E = f(X_o)$$

$$\text{and } P_j = F/A$$

where  $F$  is the external force on the jack and  $A$  is the effective area of jack piston. Substituting for  $K_V E$  and  $P_j$  equation (6.4)

$$f(X_o) [2(P_s - F/A)]^{\frac{1}{2}} = \frac{V}{2NA} \dot{F} + 2A\dot{x} + 2K_j \frac{F}{A} + K_o \frac{F}{A} \quad (6.5)$$

Furthermore, the leakage terms can be combined to give one leakage coefficient

$$\begin{aligned} 2K_j \frac{F}{A} + K_o \frac{F}{A} &= 2\left(K_j + \frac{K_o}{2}\right) \frac{F}{A} \\ &= 2K_c \frac{F}{A} \end{aligned}$$

where  $K_c = K_j + \frac{K_o}{2}$  is the combined leakage coefficient

$$\therefore f(X_o) \left[2(P_s - F/A)\right]^{\frac{1}{2}} = \frac{V}{2NA} \dot{F} + 2A\dot{x}_o + 2K_c \frac{F}{A} \quad (6.6)$$

$$\text{or } \frac{V}{2NA} \dot{F} = f(X_o) \left[2(P_s - F/A)\right]^{\frac{1}{2}} - 2A\dot{x}_o - 2K_c \frac{F}{A} \quad (6.7a)$$

$$\text{and } 2A\dot{x}_o = f(X_o) \left[2(P_s - F/A)\right]^{\frac{1}{2}} - \frac{V}{2NA} \dot{F} - 2K_c \frac{F}{A} \quad (6.7b)$$

Equations (6.7a) and (6.7b) are now in a form suitable for simulation on an analogue computer and will yield force or displacement depending upon whether the system is excited by a sinusoidal displacement or by a sinusoidal force.

The value of  $f(X_o)$  may be evaluated by considering the total volume flow  $Q$  through the valve

$$Q = f(X_o) (P_v)^{\frac{1}{2}}$$

$$\therefore f(X_o) = \frac{Q}{(P_v)^{\frac{1}{2}}} \quad (6.8)$$

The values of  $f(X_o)$  were calculated for valve pressure drop of 3,000, 2,000 and 1,000 lbf/in<sup>2</sup> respectively using values of  $Q$  and  $P_v$  against valve opening as supplied by the valve manufacture (Fig.3.3). The three values of  $f(X_o)$  thus obtained

for each of the valve opening (Table 6.1) were averaged and are shown plotted against  $X_0$  in Fig 6.1.

## 6.2. Coefficient Values.

The mathematical analysis of a practical hydraulic serve is usually performed by assigning constant values to parameters such as jack piston area, swept volume, bulk modulus of the hydraulic fluid, leakage coefficient, and the system supply pressure. These parameters appear as coefficients in equations (6.7) and any change in their value may effect the system impedance in the following manner.

### Area and Swept Volume.

The small changes in area, and hence the volume, which may occur due to dilation of the jack body under pressure or due to wear will effect the bulk modulus of the fluid (By definition,  $N = -V \cdot dP/dV$ ).

### Bulk Modulus (N).

The bulk modulus of a fluid is independent of fluid pressure if there is no air present in the fluid. But any air in the fluid will reduce the bulk modulus, particularly at low pressures. Different values of  $N$  have been used in the analysis of hydraulic servos by different investigators. Lambert and Davies (19) used a value of  $N = 50,000 \text{ lbf/in}^2$ , where as Penny (1) has used a value of  $N = 120,000 \text{ lbf/in}^2$ . Since the bulk modulus constitutes an important parameter in the performance of the system, equation (6.6), a range of values of  $N$  were used in the analogue simulation to study the effects on impedance of changes in bulk modulus.

### Leakage Coefficient ( $K_c$ ).

The leakage across the jack piston and out of the jack will tend to increase as the number of reversals the jack piston undergoes increase. once again there is no agreement among investigators as to the value of  $K_c$  to be used in the analysis. Therefore a range of values for  $K_c$  have been used during this study.

### Supply Pressure ( $P_s$ ).

The supply pressure in a system normally remains constant. But there may be occasions when due to defective or worn out seals the system pressure may drop to a lower value. A study is made of the effects of changes in supply pressure for constant values of  $N$  and  $K_c$ .

The following parameter values have been used in this study.

$$A = .623 \text{ in}^2.$$

$$K_c = 0-20 \times 10^{-5} \text{ in}^5/\text{lb} \cdot \text{sec}.$$

$$N = 20,000 - 200,000 \text{ lbf}/\text{in}^2.$$

$$P_s = 500 - 3,000 \text{ lbf}/\text{in}^2.$$

$$V = 1.63 \text{ in}^3.$$

Furthermore, let  $N = \frac{n}{a}$  where  $n$  is the maximum value of bulk modulus used in the simulation (200,000 lbf/in<sup>2</sup>).

$$\left. \begin{array}{l} \text{Then for } N = n, \quad a = 1 \\ \quad \quad \quad N < n, \quad a > 1 \end{array} \right\} \quad (6.8)$$

Also, let  $K_o = bk_c$  and let  $k_c = 16 \times 10^{-5} \text{ in}^5/\text{lbf. sec.}$

$$\begin{aligned} \text{Then for } K_o &= 16 \times 10^{-5} \text{ in}^5/\text{lbf. sec, } b = 1 \\ K_o &> 16 \times 10^{-5} \text{ in}^5/\text{lbf. sec, } b > 1 \\ K_o &< 16 \times 10^{-5} \text{ in}^5/\text{lbf. sec, } b < 1 \end{aligned} \quad (6.9)$$

The coefficient values for equation (6.7) may now be defined as follows:-

$$\left(\frac{V}{2NA}\right)_{\max} = (6.55 \times 10^{-6}) a \dot{F} \text{ for } N = 200,000 \text{ lbf/in.}^2$$

$$\left(\frac{2K_c}{A}\right)_{\max} = (5 \times 10^{-4}) b \text{ in}^3/\text{lbf. for } K_c = 16 \times 10^{-5} \text{ in}^5/\text{lbf. sec.}$$

$$(2A)_{\max} = 1.246 \text{ in.}^2$$

Substituting the coefficient values in equation (6.7a) gives:-

$$\begin{aligned} 6.55 \times 10^{-6} \left(\frac{\text{in}^3}{\text{lbf}}\right) a \dot{F} &= 1.414f(X_o) (P_s - F/A)^{\frac{1}{2}} - 1.246 (\text{in}^2) \dot{x} - \\ 5 \times 10^{-4} \left(\frac{\text{in}^3}{\text{lbf. sec.}}\right) bF & \end{aligned} \quad (6.10)$$

### 6.3. Problem Variables and Scale Factor Equations.

The maximum values of the problem variables (time dependent parameters in the equation of motion) must now be defined and scale factor equations worked out to transform the problem variables into voltages in order to mechanise the equation of motion of the servo on the analogue computer.

Frequency range of tests.

During the laboratory tests on the hydraulic jack servo Penny (1) had found that at a frequency of 70 C/S the valve motion was no longer significant and the piston was bouncing on the oil in the jack. Hence this frequency may be taken as an upper limit for the servomechanism. A lower limit of 5 C/S was dictated by the automatic impedance analysis equipment being the lower limit of the dynamic analysers. Therefore the frequency range for the servo simulation was chosen to be 5-70 C/S.

Maximum values of problem variables.

Maximum displacement.

Maximum steady state displacement,  $X_{os} = .045$  in.

Maximum sinusoidal displacement,  $x_o = \pm .005$  in.

Total maximum displacement,  $X_o = (X_{os} + x_o) = .05$  in.

Maximum velocity.

$$\begin{aligned} \text{Velocity} &= \frac{d}{dt} (X_o + x_o) \\ &= \frac{dx_o}{dt} \\ &= \dot{x}_o \end{aligned}$$

$$\begin{aligned} \text{Also } \dot{x}_o &= w x_o \\ &= 500 \times .005 \text{ in/sec.} \end{aligned}$$

$$\therefore \dot{x}_o = 2.5 \text{ in/sec.}$$

The value  $w = 500$  radian/sec. has been chosen for ease of scaling. This would give an upper frequency of 78.5 C/S.

Maximum force.

$$\begin{aligned}\text{Maximum steady state force } F_s &= P_s \cdot A \\ &= 1869 \text{ lbf.}\end{aligned}$$

$$\text{Maximum sinusoidal force } F = \underline{+} 1,000 \text{ lbf.}$$

$$\text{Total maximum force } (F_s + F) = (1869 + 1,000) \text{ lbf.}$$

say 3,000 lbf.

Maximum  $\dot{F}$ 

$$\frac{d}{dt} (F_s + F) = \dot{F}$$

$$\begin{aligned}\text{but } \dot{F} &= wF \\ &= 500 \times 1,000 \text{ lbf/sec.}\end{aligned}$$

$$\therefore \dot{F} = 500,000 \text{ lbf./sec.}$$

Maximum value of  $(P_s - F/A)^{\frac{1}{2}}$ 

$$(P_s - F/A)^{\frac{1}{2}}_{\text{max}} = (3,000)^{\frac{1}{2}} \text{ for } F = 0$$

$$\therefore (P_s - F/A)^{\frac{1}{2}} = 54.77 \text{ lbf}^{\frac{1}{2}}/\text{in.}$$

$$\approx 55 \text{ lbf}^{\frac{1}{2}}/\text{in.}$$

Maximum value of  $f(X)$ 

The maximum value of  $f(X_0)$  occurs at a valve opening of .05 in. and from table 6.1 it is 0.211. But to avoid multiplication by a large constant in the computer the values of this function were multiplied by a factor of 40 and  $40 f(X)$  was simulated.

$$\therefore 40 f(X_0) = 8.44 \text{ say } = 10 \text{ in}^4/\text{lbf}^{\frac{1}{2}} \text{ sec.}$$

Scale factor equations.

A scale factor equation may be defined as:-

$$x = \frac{(x)_{\max}}{(c)_{\max}} \cdot \bar{x} \quad (6.11)$$

where  $x$  represents the problem variable.

( $x$ )  $\max$  represents the maximum of the absolute value of  $x$ .

( $c$ )  $\max$  represents the maximum voltage output of the computing elements (10 volts for the analogue computer used).

$\bar{x}$  is the voltage representing  $x$  in the computer.

Using equation (6.11) the problem variable may be transformed into voltages as follows:-

$$X_o = \frac{.05}{10} \left( \frac{\text{in}}{\text{volt}} \right) \bar{X}_o \quad (6.12)$$

$$\dot{x}_o = \frac{2.5}{10} \left( \frac{\text{in}}{\text{sec.volt}} \right) \dot{\bar{x}}_o \quad (6.13)$$

$$F = \frac{3,000}{10} \left( \frac{\text{lbf}}{\text{volt}} \right) \bar{F} \quad (6.14)$$

$$\dot{F} = \frac{500,000}{10} \left( \frac{\text{lbf}}{\text{sec.volt}} \right) \dot{\bar{F}} \quad (6.15)$$

$$(P_s - F/A)^{\frac{1}{2}} = \frac{55}{10} \left( \frac{\text{lbf}^{\frac{1}{2}}}{\text{in.volt}} \right) (\bar{P}_s - \bar{F}/A)^{\frac{1}{2}} \quad (6.16)$$

$$f(X_o) = \frac{10}{10} \left( \frac{\text{in}^4}{\text{lbf}^{\frac{1}{2}} \text{sec.volt}} \right) f(\bar{X}_o) \quad (6.17)$$

Substituting the scale factor equations (6.12) to (6.17) in equation (6.10) and simplifying gives:-

$$a\bar{F} = 23.866 f(\bar{X}_o) (\bar{P}_s - \bar{F}/A)^{\frac{1}{2}} - .9526 \dot{\bar{x}}_o - .2356 b\bar{F} \quad (6.18a)$$

$$\text{or } \dot{\bar{x}}_o = 25.1 f(\bar{X}_o) (\bar{P}_s - \frac{\bar{F}}{A})^{\frac{1}{2}} - 1.05a \dot{\bar{F}} - .2356 b\bar{F} \quad (6.18b)$$

The problem variables are now voltages that will be operated upon by the computing elements in a manner governed by equation (6.18).

#### Inclusion of coulomb friction.

Let  $F_c$  be the coulomb friction force of a constant amplitude. Since this force always opposes motion it may be represented as  $F_c (\text{sign } \dot{x})$ . With coulomb friction present the force  $F$  at the output end of the hydraulic jack will be:-

$$F = P_j A + F_c (\text{sign } \dot{x})$$

$$\text{or } P_j = \frac{F}{A} - \frac{F_c}{A} (\text{sign } \dot{x}) \quad (6.19)$$

Substituting the above expression for  $P_j$  in equation (6.6) yields:-

$$f(X_o) \left[ 2 \left( P_s - \frac{F}{A} + \frac{F_c}{A} (\text{sign } \dot{x}) \right) \right]^{\frac{1}{2}} = \frac{V}{2NA} \dot{\bar{F}} + 2A\dot{\bar{x}}_o + \frac{2K_c}{A} \cdot \left[ \bar{F} - \frac{F_c}{A} (\text{sign } \dot{\bar{x}}_o) \right] \quad (6.20)$$

The values of scale factor equations and coefficients remain unaltered by addition of the coulomb friction force:-

$$\therefore a\ddot{\bar{F}} = 23.866 f(\bar{X}_0) \left[ P_s - \frac{\bar{F}}{A} + \frac{F_c}{A} (\text{sign } \dot{\bar{x}}_0) \right]^{\frac{1}{2}} - .9526 \dot{\bar{x}}_0 - .2356b \left[ \bar{F} - F_c (\text{sign } \dot{\bar{x}}_0) \right] \quad (6.21a)$$

$$\ddot{\bar{x}}_0 = 23.866f(\bar{X}_0) \left[ P_s - \frac{\bar{F}}{A} + \frac{F_c}{A} (\text{sign } \dot{\bar{x}}_0) \right]^{\frac{1}{2}} - 1.05a\ddot{\bar{F}} - .2356b \left[ \bar{F} - F_c (\text{sign } \dot{\bar{x}}_0) \right] \quad (6.21b)$$

#### 6.4. The Analogue Computer Circuit.

##### 6.4.1 Simulation of hydraulic servo without coulomb friction.

The analogue computer simulation was arranged to allow computation of either the output force for a displacement excitation or the output displacement for a force excitation of the output end of the hydraulic jack. Initially the hydraulic servo without the coulomb friction force was simulated in order to check the simulation and correct functioning of the computing elements. The basic computer circuit diagram is shown in Fig.6.2.

The differentiation of a waveform other than a pure sinusoid generates noise by amplifying the harmonic contents of the waveform. For this reason the exciting signal, derived from an external signal generator, is taken either as  $\dot{\bar{x}}_0$  or as  $\ddot{\bar{F}}$  in order to avoid differentiation of the sum of variables which will not be pure sinusoids. The signal from the generator is taken through a compressor circuit and after integration is feedback to the compressor through the switch S3 in order to maintain  $\bar{x}_0$  or  $\bar{F}$  at a constant level when the signal frequency is changed. When the system is displacement excited the switches S1 and S2 are in 'up' position and the switch S3 is in 'down' position. For a force excitation the positions of these switches are reversed. The switch S4 connects either potentiometer P3 or integrator 7 to amplifier 2 for dynamic or steady state solution.

The functions performed by the computing elements in the circuit diagram of Fig.6.2 may be defined as follows.

### V.D.F.G.

The variable diode function generator takes an input  $\bar{X}_o = \bar{X}_{os} + \bar{x}_o$  and generates  $40 f(\bar{X}_o)$  in conjunction with amplifiers 3 and 4 which are used here as high gain amplifiers.

### Multiplier (Q.S.M.)

The quarter-square multiplier performs a four-quadrant multiplication for bipolar inputs of two variables. It takes as input variables  $\pm 40f(\bar{X}_o)$  and  $\pm (\bar{P}_s - \frac{\bar{F}}{A})^{\frac{1}{2}}$  and produces at its output the quantity  $4f(\bar{X}_o) (\bar{P}_s - \frac{\bar{F}}{A})^{\frac{1}{2}}$ . A scale of  $\frac{1}{10}$  is incorporated in Q.S.M. circuitry to avoid overloading of the high gain amplifier.

### Square rooter.

The square root is obtained by using a Q.S.M. as a feedback element to high gain amplifier 10. Due to built-in scaling in the circuitry the Q.S.M. generates  $(10)^{\frac{1}{2}} (\bar{P}_s - \frac{\bar{F}}{A})^{\frac{1}{2}}$  for the input  $-(\bar{P}_s - \frac{\bar{F}}{A})$ .

$$\text{Integrator 1} \quad -\bar{x}_o/5 = -10 \int_0^t \bar{x}_o dt \quad (6.22)$$

$$\text{Amplifier 2} \quad \bar{X}_o = (-1) \left[ 10(-0.1 \bar{x}_o) - \bar{X}_{os} \right] \quad (6.23)$$

$$\text{Amplifier 5} \quad -40 f(\bar{X}_o) = (-1) \left[ 40f(\bar{X}_o) \right] \quad (6.24)$$

$$\text{Integrator 7} \quad -\bar{x}_{os} = - \int_0^t v \cdot dt \quad (6.25)$$

$$\text{Integrator 8} \quad -\bar{F} = - 500 \int_0^t \cdot 333 \dot{F} dt \quad (6.26)$$

$$\text{Amplifier 9} \quad - \left( \bar{P}_s - \frac{\bar{F}}{A} \right) = (-1) \left( \bar{P}_s - \frac{\bar{F}}{A} \right) \quad (6.27)$$

$$\text{Amplifier 11} \quad - \left( \bar{P}_s - \bar{F}/A \right)^{\frac{1}{2}} = (-1) \left( \bar{P}_s - \frac{\bar{F}}{A} \right)^{\frac{1}{2}} \quad (6.28)$$

$$\text{Amplifier 12} \quad \left( \bar{P}_s - \bar{F}/A \right)^{\frac{1}{2}} = (-1) \left[ - \left( \bar{P}_s - \frac{\bar{F}}{A} \right)^{\frac{1}{2}} \right] \quad (6.29)$$

$$\text{Amplifier 13} \quad + b \bar{F} = (-1) (-b \bar{F}) \quad (6.30)$$

$$\begin{aligned} \text{Amplifier 14} \quad + \bar{x}_o &= (-10) \left[ \cdot 622(-4) f(\bar{x}_o) \left( \bar{P}_s - \bar{F}/A \right)^{\frac{1}{2}} \right] \\ &+ (-1) \left[ \cdot 2473 (+b\bar{F}) \right] + (-10) \left[ \cdot 105 (+a\dot{F}) \right] \end{aligned} \quad (6.31)$$

$$\begin{aligned} \text{Amplifier 15} \quad + a\dot{F} &= (-1) \left[ \cdot 953 (+\bar{x}_o) \right] + (-1) \left[ \cdot 2356 (+b\bar{F}) \right] \\ &+ (-10) \left[ \cdot 592 (-4) f(\bar{x}_o) \left( \bar{P}_s - \bar{F}/A \right)^{\frac{1}{2}} \right] \end{aligned} \quad (6.32)$$

#### Values of integrator gains.

The relationship between the input and the output of an integrator is defined as:-

$$x = \frac{1}{T} \int_0^t \dot{x} dt \quad (6.33)$$

where  $T = RC$  is the time constant of an integrator with  $R$  and  $C$  being the input resistant and the feedback capacitance respectively. The inverse of time constant  $T$  is the gain of an integrator and has units of  $(\text{sec})^{-1}$ . The values of gains for integrators 1 and 8 may be determined by substitution of appropriate scale factor equations in equation (6.33).

### Integrator 1

Substituting the scale factor equations (6.12 and (6.13) in equation (6.33)

$$\frac{.05}{10} \left( \frac{\text{in}}{\text{volt}} \right) \bar{X}_0 = \frac{2.5}{10} \left( \frac{\text{in}}{\text{sec.volt}} \right) \int_0^t \dot{\bar{x}}_0 dt$$

$$\text{or } \bar{X}_0 = \frac{50}{\text{sec}} \int_0^t \dot{\bar{x}}_0 dt \quad (6.34)$$

From equation (6.34) the gain for integrator 1 is found to be 50/sec. In the analogue computer used integrator gains of 1, 10, 500 and 5,000 were available. To obtain a gain of 50 the variable would have to be divided by 10 with an integrator gain of 500/sec. Since this integrator does not form a closed loop, in the displacement excitation mode, with the rest of the computing elements any drift voltages in the integrator would be multiplied by 500/sec. and would overload the amplifiers in a matter of seconds. For this reason an integrator gain of 10/sec. was chosen (equation 6.22) and the output was multiplied by 5 in amplifier 2.

### Integrator 8

From equation (6.19) and (6.20)

$$\frac{3,000}{10} \left( \frac{\text{lb.f}}{\text{volt}} \right) \bar{F} = \frac{500,000}{10} \left( \frac{\text{lb.f}}{\text{sec.volt}} \right) \int_0^t \dot{\bar{F}} dt$$

$$\text{or } \bar{F} = \frac{166.7}{\text{sec}} \int_0^t \dot{\bar{F}} dt \quad (6.35)$$

The integrator gain is found to be 166.7/sec. (eqn.6.35). This value of gain is obtained by multiplying  $\dot{\bar{F}}$  by .333 in potentiometer P11 and setting the integrator gain at 500/sec. as defined by equation (6.26). When the system is force excited this integrator operates in an open loop mode and a gain of 500/sec would be unacceptable for overload reasons. In this mode an integrator gain of 10/sec. is used and the output of the integrator is multiplied by 16.67 in amplifier 17 and inverted in amplifier 18 as shown in Fig.6.3.

#### 6.4.2. Trial Runs On The Computer.

To check the ability of the computing elements to perform required mathematical operations trial runs were made on the computer. The trial runs were made both for the steady state operation of hydraulic servo and for the sinusoidal excitation.

##### Steady state operation.

For the steady state condition the equation (6.6) reduces to:-

$$f(X_0) \left[ 2(P_s - F/A) \right]^{\frac{1}{2}} = 2 K_c \frac{F}{A}$$

$$\text{or } 2 \left( \frac{K_c}{A} \right)^2 \cdot \frac{1}{\left[ f(X_0) \right]^2} \cdot F^2 + \frac{F}{A} - P_s = 0 \quad (6.36)$$

Equation (6.36) gives a quadratic in F which was solved for values of  $X_0$  using the information contained in Fig.6.1, and the results are plotted in Fig.6.4.

For steady state solution on the analogue computer the switches S1 and S3 were put in neutral position. Switch S2 connected the

output of amplifier 15 to potentiometer 10 while S1 applied a slow ramp (output of integrator 1) to amplifier 2. The computed graph of  $\bar{F}$  against  $\bar{X}_{os}$  is plotted in Fig.6.5. The irregularities in the computed graph gave errors of up to 30% in the value of  $\bar{F}$ . A check of the output of each of the computing elements revealed the multiplier as the source of error. This unit was found to be incapable of accurate computation if its output was less than 1 volt. The inputs to the multiplier  $40f(X_o)$  and  $(\bar{P}_s - F/A)^{\frac{1}{2}}$  are so related that an increase in one function is accompanied by a decrease in the other as shown by Fig.6.6, and hence their product in the steady state is always less than 1 volt.

This problem was overcome by multiplying first the quantity  $40 f(\bar{X}_{os})$  by a factor of 5 until it reached a value of 2.2 volts and then multiplying  $(\bar{P}_s - F/A)^{\frac{1}{2}}$  by 5 whose value had by now decreased to 2.2 volts. This represents the intersection point of the two functions in Fig.6.6. The multiplication of the functions by a constant was performed by means of two relay comparators  $L_1$  and  $L_2$  as shown in Fig.6.7. A relay comparator is a voltage sensitive switch which changes state at a predetermined voltage level. With this modification the steady state solution was accurately computed.

### Dynamic operation.

For the dynamic solution the switch S1 connected the signal generator through the compressor circuit to integrator 1 whose output was feedback to the compressor through S3. The switch S2 connected the output of amplifier to integrator 8 and S4 connected the steady state displacement from potentiometer P3 to amplifier 2. On selecting the compute mode all amplifiers showed an overload and a solution was not possible for the following reasons.

1. The relay comparators failed to operate correctly above 20 HZ.
2. The quarter-square multiplier when used as a feed back element

for square rooting was found to be unstable and generated parasitic oscillations from 5 KHZ to 100 KHZ depending on the magnitude of the input signal.

3. The signal generator had a small d.c. voltage at its output which was multiplied by a factor of 10 every second in integrator 1 and soon overloaded the amplifier.

It was found that the relay comparators were not required during dynamic solution as the voltage representing the product of the functions  $(\bar{P}_s - \bar{F}/A)^{\frac{1}{2}}$  and  $40 f(\bar{X}_0)$  had sufficiently high value to allow for accurate computation by the multiplying unit. Hence the relay comparators were not needed. The difficulty presented by the square rooter was overcome by using a variable diode function generator as a square rooter. The d.c. voltage from the signal generator was eliminated by using a differentiating circuit as described below.

#### A unity gain - zero phase shift differentiator.

The differentiating circuit shown in Fig.6.8 was used to eliminate the d.c. voltage from the signal generator. This circuit was placed between the compressor output and the potentiometer P1.

The transfer function of the differentiator with reference to Figure 6.8 is defined as:-

$$\frac{V_o}{V_i} = - \frac{DCR_2}{1+DCR_1} \quad \text{where D is the differential operator.}$$

Let  $R_1 = R_2 = R$  and  $RC = T$ , the time constant

$$\text{Then } \frac{V_o}{V_i} = - \frac{TD}{1 + TD}$$

Now if  $R = 10^5$  ohms and  $C = 10$  micro-Farad

Then  $T = RC = 10^5 \times 10 \times 10^{-6} = 1 \text{ sec.}$

$$\therefore \frac{V_o}{V_i} = - \frac{D}{1 + D} = - \frac{jw}{1 + jw} \quad (6.37)$$

$$\text{and Gain} = \frac{w}{(1^2 + w^2)^{\frac{1}{2}}} \quad \text{but } w \gg 1$$

$$\therefore \text{Gain} = 1$$

and phase shift is given by:-

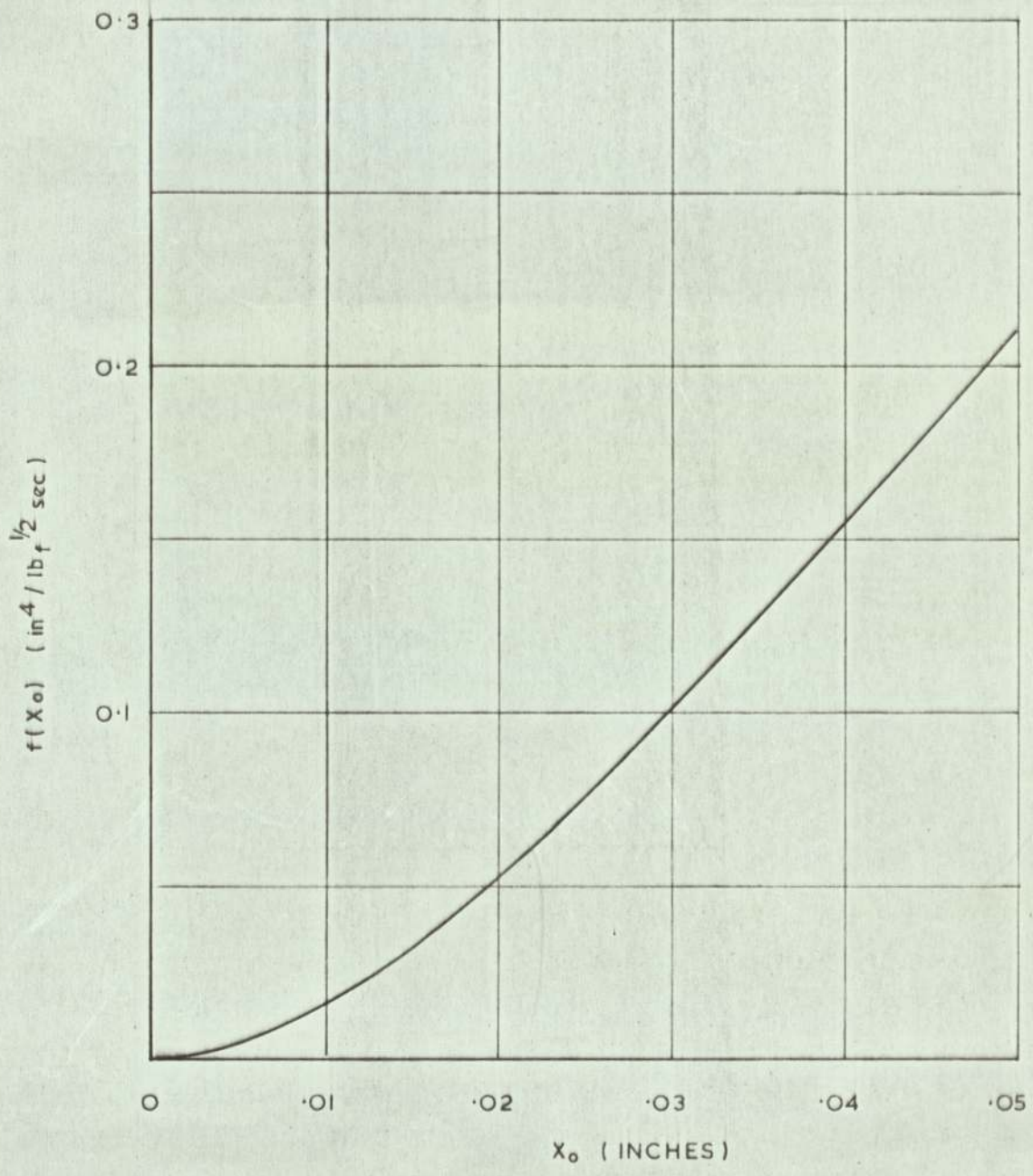
$$\phi = - (\tan^{-1} w - \tan^{-1} w) = 0$$

Hence the difference has a unity gain and a zero phase shift at all frequencies of interest.

#### 6.4.3 Simulation of Coulomb Friction Force.

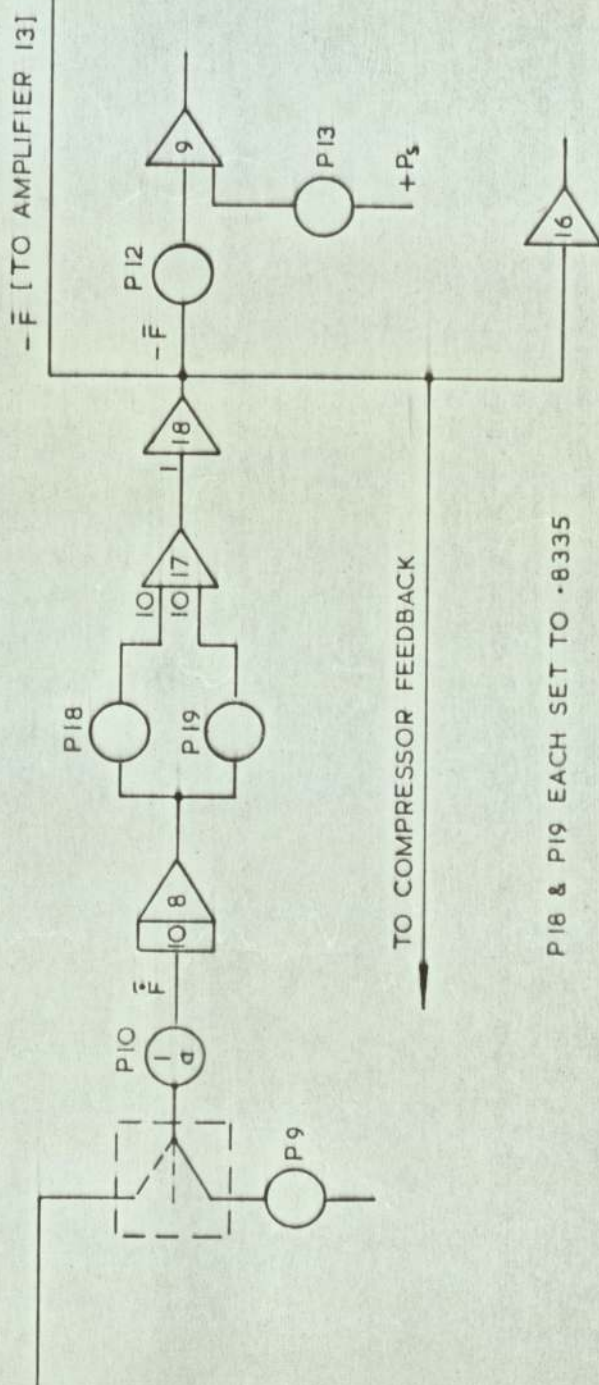
The coulomb friction was simply simulated by using two high quality diodes as feedback elements to a high gain amplifier. The diodes were biased by two potentiometers connected at their top ends to the computer positive and negative reference supplies respectively, and their bottom ends connected to the amplifier output. Due to the high gain of the amplifier a rise time of less than 1 micro-second was obtained for the output waveform. The output of the high friction force the same as that of  $\dot{X}_o$ . The circuit diagram is shown in Fig.6.9.

The final circuit diagram simulating the servomechanism including the coulomb friction and modifications mentioned above is shown in Fig.6.10. The value of potentiometer settings are given in Fig.6.11.



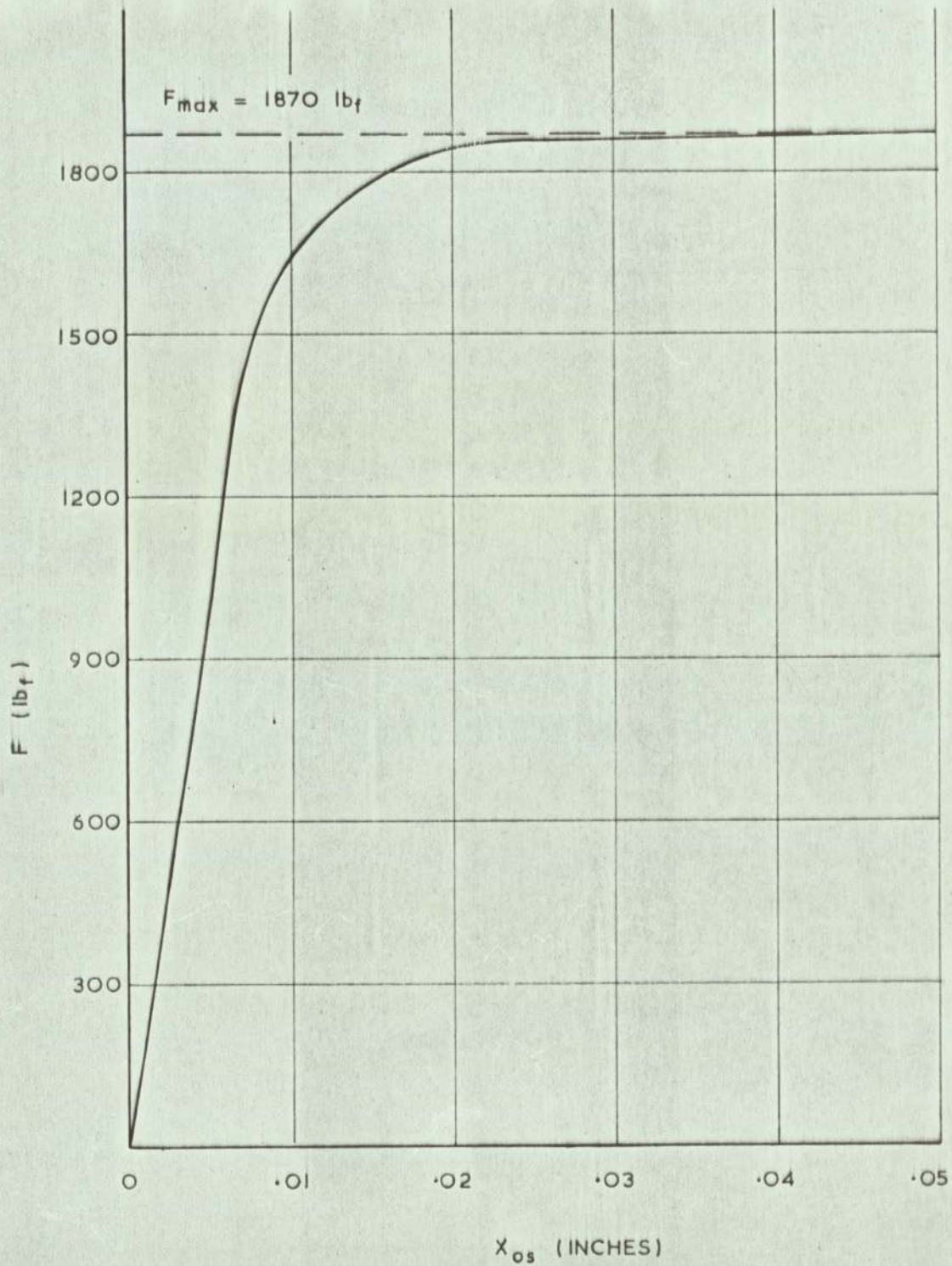
RELATIONSHIP BETWEEN  $f(x_0)$  AND  $x_0$



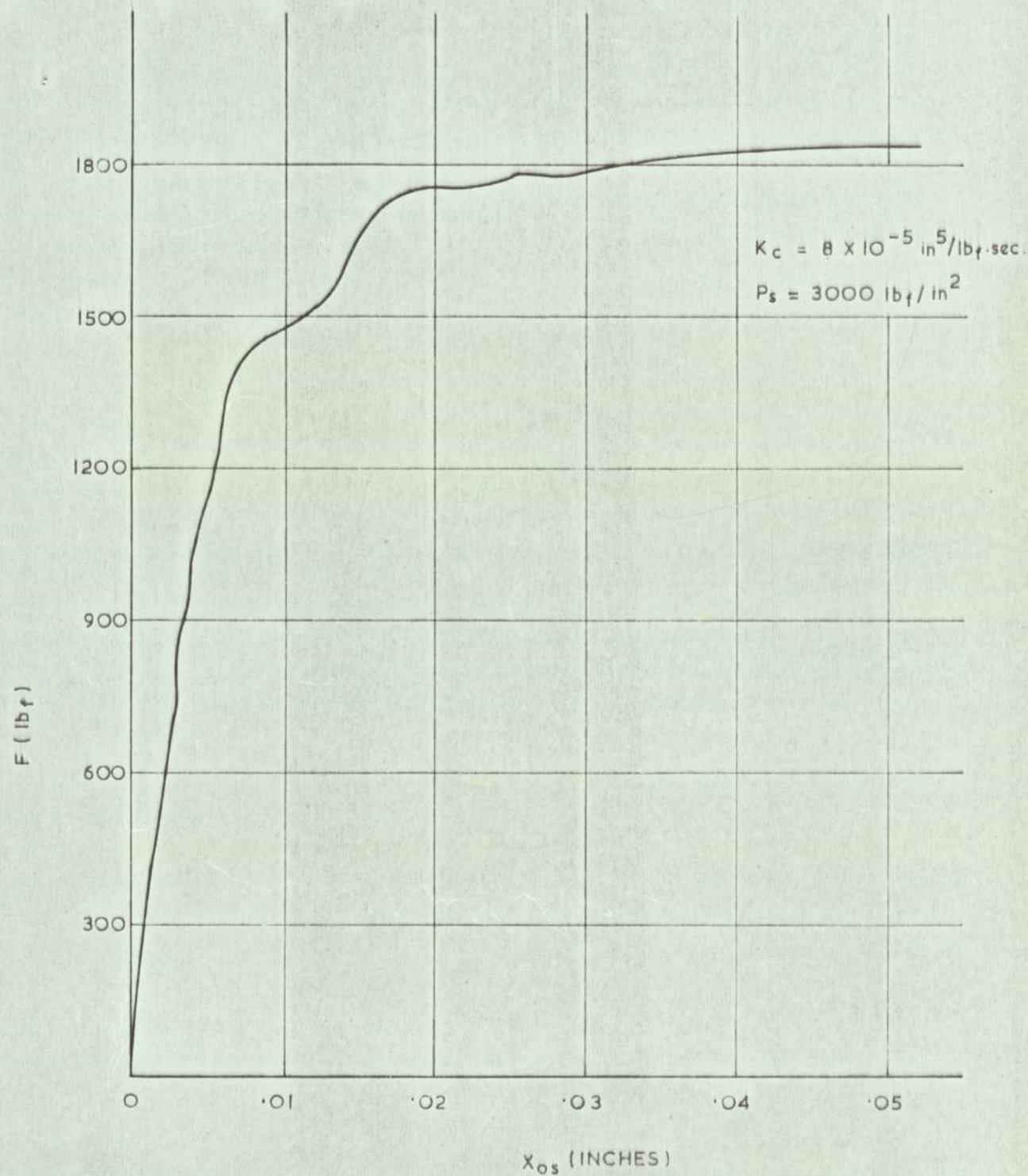


P18 & P19 EACH SET TO .8335

MODIFICATION TO ANALOGUE CIRCUIT FOR FORCE EXCITATION



RELATIONSHIP BETWEEN FORCE AND DISPLACEMENT  
FOR STEADY STATE OPERATION (CALCULATED RESULTS)



RELATIONSHIP BETWEEN FORCE AND DISPLACEMENT  
FOR STEADY STATE OPERATION (ANALOGUE RESULTS)

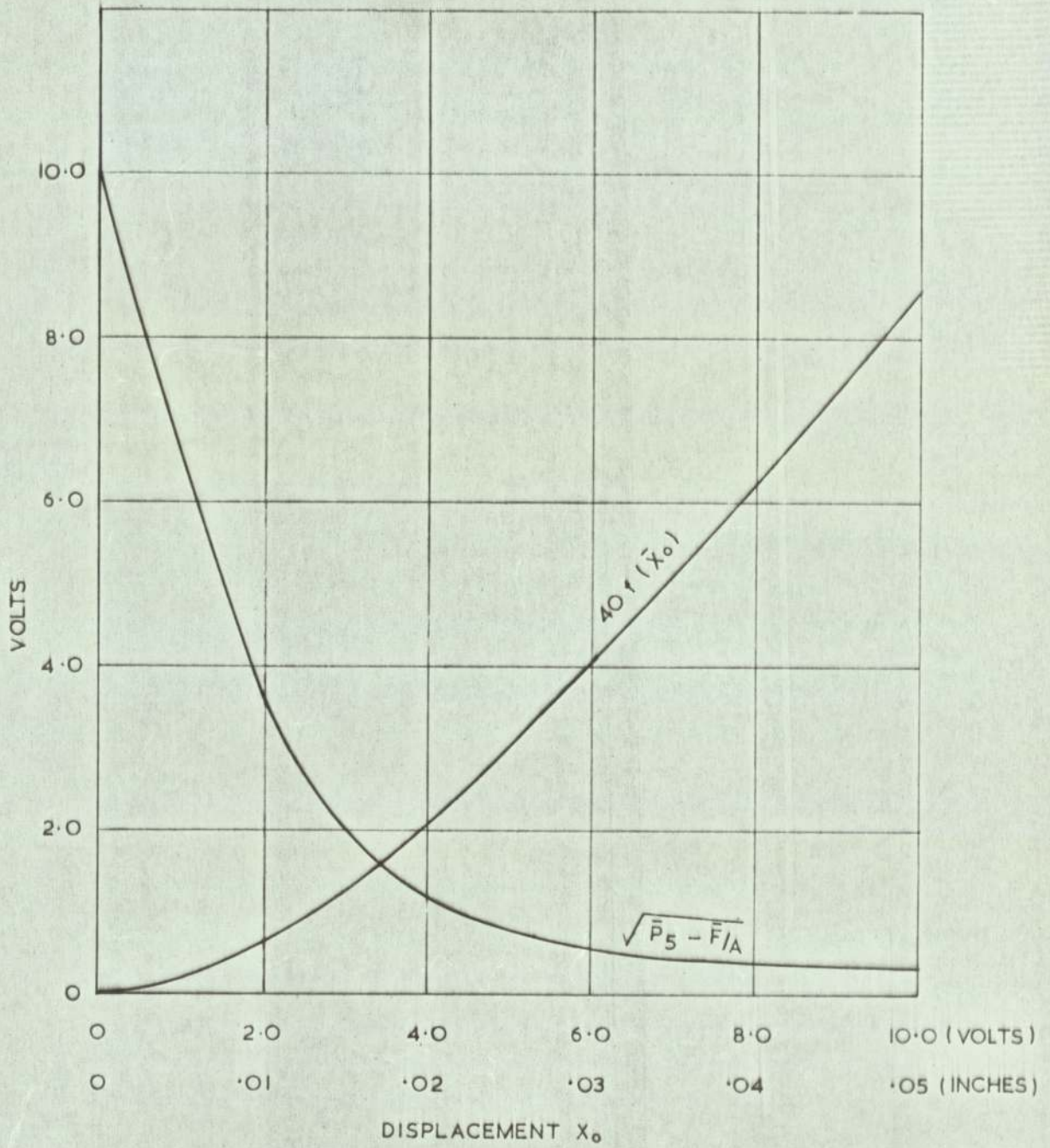
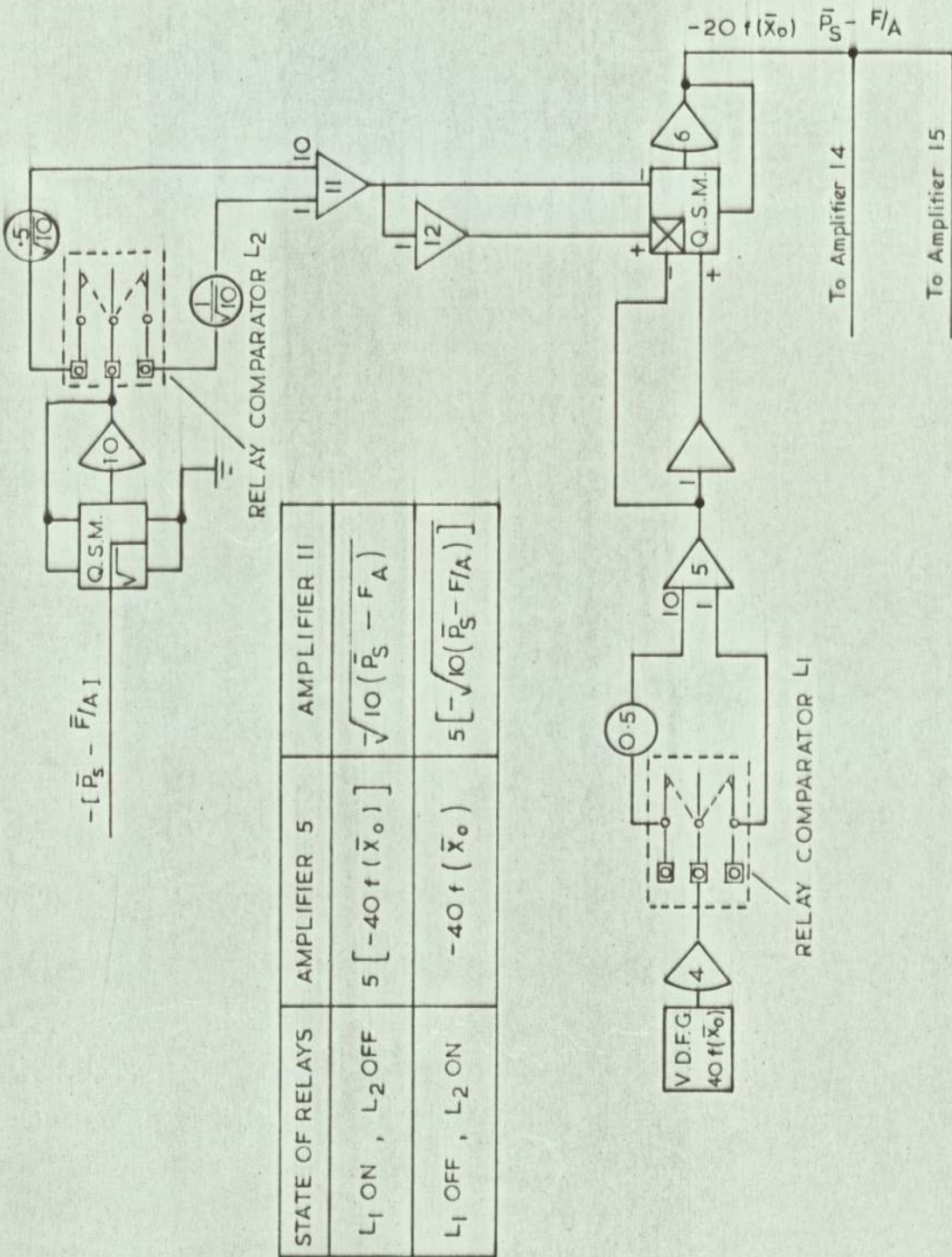
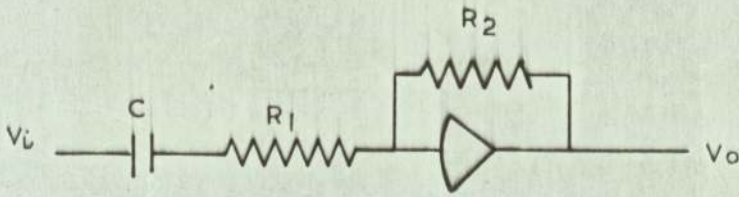


FIG 6.6



MODIFICATION OF SIGNALS TO THE MULTIPLIER USING RELAY COMPARATORS

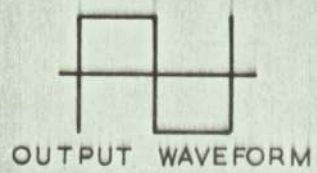
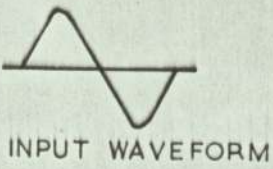
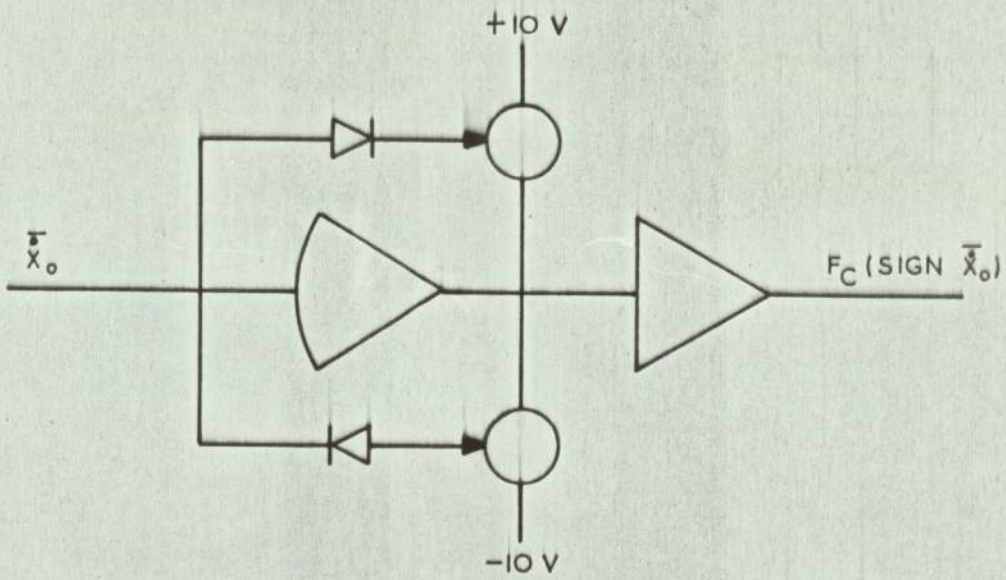


$$R_1 = R_2 = 100 \text{ K } \Omega$$

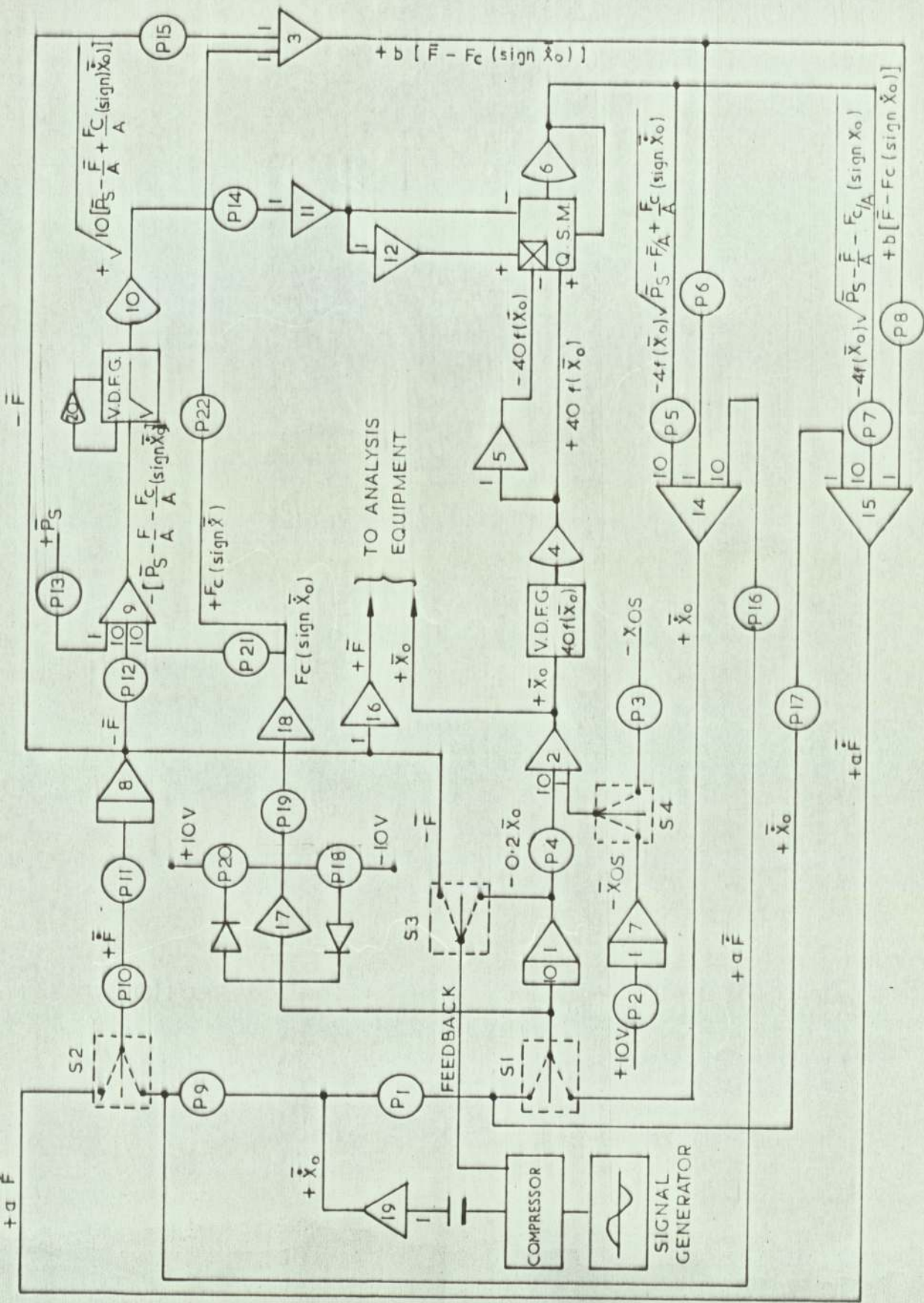
$$C = 10 \mu \text{ F}$$

$$\frac{V_o}{V_L} = - \frac{R_2 C D}{1 + R_1 C D}$$

A UNITY GAIN - ZERO PHASE SHIFT DIFFERENTIATOR



SIMULATION OF COULOMB FRICTION



SIMULATION OF HYDRAULIC SERVO - FINAL COMPUTER DIAGRAM

Potentiometer No	Settings	Remarks
P1	Variable	Controls sinusoidal valve displacement
P2	Variable	Controls ramp amplitude for static operation
P3	Variable	Controls static valve opening
P4	0.5	
P5	0.6216	
P6	0.2473	
P7	0.5922	
P8	0.2356	
P9	Variable	Controls sinusoidal force amplitude
P10	Variable	Controls amplitude of Bulk modules
P11	0.3333	Sets integrator gain
P12	0.1604	
P13	Variable	Controls the amplitude of hydraulic supply pressure
P14	1 10	
P15	Variable	Controls leakage coefficient by changing value 'b'
P16	0.105	
P17	0.9526	
P18	0.04	
P19	Variable	Controls the amplitude of coulomb force
P20	0.04	
P21	0.1604	
P22	Variable	Same function as potentiometer 15

CHAPTER 7.

CORRELATION OF ANALOGUE,  
TEST RIG AND THEORETICAL RESULTS.

CHAPTER 7.

CORRELATION OF ANALOGUE,  
TEST RIG AND THEORETICAL RESULTS.

<u>CONTENTS.</u>	<u>PAGE.</u>
7.1. Introduction.	91
7.2. Impedance of The Hydraulic Servo With Coulomb Friction.	91
7.3. Correlation of Analogue and Rig Results.	97
7.4. Impedance of The Hydraulic Servo Without Coulomb Friction.	98
7.5. Correlation of Analogue and Theoretical Results.	102

## CHAPTER 7.

CORRELATION OF ANALOGUE  
TEST RIG AND THEORETICAL RESULTS.

7.1. Introduction.

The measurements of impedance from the analogue computer simulation of the hydraulic servo (Chapter 6) are presented in this chapter. The simulation with coulomb friction represents the physical system and hence the results from this simulation are compared with those obtained from the test rig (Fig.1.2) by Penny (1). The effects on impedance of variations in the bulk modulus, the leakage across the jack piston and the coulomb friction force, all of which cannot be varied or controlled on a test rig, are presented.

The impedance of the servo with the coulomb friction removed is presented for changes in various parameters and a comparison is made with theoretical results obtained by Penny by linearising the flow characteristics based on the small perturbation technique as discussed in chapter 3.

The phase meter in the analysis equipment (chapter 5) was found to malfunction at times. During this malfunction it was not possible to obtain the same phase relationship if a test was repeated. Also the phase meter tended to reverse the polarity of the phase for small angles. It was, however, consistent for relative phase changes with changes in the value of a parameter. Therefore the shapes of the damping curves or the amount by which the damping varies in response to changes in a parameter remain unaltered. Whenever a malfunction of the phase meter is suspected this fact has been stated in the text or a comparison between two results is made on a basis of impedance.

7.2. Impedance of The Hydraulic Servo With Coulomb Friction.

The simulation of the hydraulic servo with coulomb friction is represented by the analogue computer diagram Fig.6.10. The force,

and displacement signals were fed to the analysis equipment described in chapter 5 which gave plots of the logarithm of impedance and the linear phase difference between the two signals against the logarithm of the frequency. The parameter values were varied by the settings of the potentiometers as shown in Fig.6.11.

### 7.2.1 The Effect of Coulomb Friction On Impedance.

Coulomb friction forms the principal non-linearity in the hydraulic servo and helps to stabilise the servo particularly at small values of the valve opening when it is theoretically predicted to be unstable. Values of the coulomb friction force,  $F_c$ , from 0-180 lbf. in steps of 60 lbf. were tested to evaluate its effects on impedance. Figures 7.1 to 7.5 show the effect of coulomb friction on stiffness. Figure 7.1 shows the variation in stiffness against frequency for constant lines of  $F_c$ . The effect of coulomb friction is to increase the stiffness. This increase is constant for the frequency range of the test for any particular static valve opening. The variation in stiffness with and without coulomb friction at 5 C/S and 70 C/S for changes in the static valve opening is compared in Figure 7.2. It is seen that at small valve opening the contribution of  $F_c$  to stiffness is very little. This contribution increases with increasing values of the valve opening. Also the increase in stiffness due to  $F_c$  is greater at 70 C/S than it is at 5 C/S for the same valve opening. The figures 7.3, 7.4 and 7.5 compare the variation in stiffness for 20, 40 and 60 C/S respectively.

The effect of coulomb friction on damping against frequency is shown in Fig.7.6. The negative damping at  $F_c = 0$  changes to positive damping as the value of  $F_c$  is increased. The maximum increase in damping occurs at 5 C/S and gradually decreases to zero at a frequency of about 35 C/S when the value of damping is not influenced by coulomb friction. It is this large increase in damping that accounts for substantial increases in impedance at low frequencies. The variation in damping with and without  $F_c$  at 5 C/S and 70 C/S for changes

in the static valve opening is shown in Fig.7.7. At a frequency of 5 C/S the increase in damping due to  $F_c$  is a maximum for small valve openings. But at a frequency of 70 C/S there is no increase in damping until the valve opening is .015 in. and the maximum increase is obtained at .035 in. At other frequencies, Figures 7.8 to 7.10, there is a range of valve openings for which coulomb friction does not increase the damping.

### 7.2.2 The Effect of Bulk Modulus on Impedance.

The bulk modulus,  $N$ , of a hydraulic fluid is an important parameter in determining the impedance of the servomechanism. Particularly at the higher frequencies of excitation a change in bulk modulus has more effect on impedance than a change in any other parameter. It was found that at higher frequencies and small valve openings the impedances tended to reach a value close to the value of the bulk modulus and that a change in impedance could be linearly related to a change in bulk modulus. The values of bulk modulus in the range 40,000 - 200,000 lbf/sq.in. were tested during this study. The effects on impedance for changes in  $N$  are shown in Figures 7.11 to 7.14. Figure 7.11 shows a plot of stiffness against bulk modulus for constant lines of frequency. The values of  $N$  from 40,000 - 70,000 lbf/sq.in. makes very little difference to stiffness on a frequency basis. In fact, the stiffness is constant for all frequencies at  $N = 64,000$  lbf/sq.in. As the value of  $N$  increases beyond 100,000 lbf/sq.in. the change in stiffness with frequency becomes greater until at  $N = 200,000$  lbf/sq.in. the stiffness at 60 C/S is twice the value of the stiffness at 5 C/S.

The effect of bulk modulus on stiffness with changes in the valve opening is shown in Fig.7.12 for 5 C/S and 70 C/S. At 5 C/S the stiffness is very high for small valve opening but decreases rapidly as the valve opening is increased. Doubling the value of  $N$  increases the stiffness by about one hundred percent at a valve opening of .005 in. but

this rapidly reduces to zero at a valve opening of just over .010 in. At 70 C/S the picture is somewhat encouraging. The stiffness initially increases with the valve opening and reaches a maximum at .015 in. when it gradually decreases to about three times the value of stiffness at 5 C/S for a valve opening of .035. Doubling the value of N at 70 C/S causes large increases in stiffness which is maintained for larger valve openings than is the case for 5 C/S.

Figure 7.13 shows the variation of damping with frequency for changes in the bulk modulus N. The damping remains constant for all frequencies at  $N = 60,000$  lbf/sq.in. as was the case for stiffness. Below this value of N the negative damping decreases for higher frequencies and above this value of N the negative damping increases for higher frequencies. The maximum increase taking place from 20 - 60 C/S. The effect of changing the value of the bulk modulus on a displacement basis is shown in Fig.7.14. At 5 C/S the doubling of the value of N has virtually no effect on damping until the valve opening is just over .020 in. when the increase in N reduces the damping slightly. At 70 C/S the increase in N causes a large increase in the negative damping at a valve opening of .005 in. which rapidly decreases and changes into a positive increase at about .013 in.

### 7.2.3 The Effect of Leakage on Impedance.

Leakage across the jack piston or to the atmosphere out of the jack is undesirable from the static stiffness point of view, and also the fact that it makes heavier demands of the hydraulic pump depending on the amount of leakage. But it does increase the dynamic impedance in the manner of a viscous damper and hence leakage is often introduced in hydraulic servos to improve stability particularly at very small valve openings and at low frequencies. Values of the leakage coefficient  $K_c$  in the range  $0-20 \times 10^{-5}$  in<sup>5</sup>/lbf.sec. have been tested and the effect on stiffness and damping is shown in Figures 7.15 and 7.16 respectively. The stiffness at low frequencies increases as the

value of  $K_c$  is increased. For higher frequencies, however, the effect of leakage becomes smaller until at 70 C/S an increase in  $K_c$  from 0 to  $20 \times 10^{-5} \text{ in}^5/\text{lb} \cdot \text{sec}$ . causes an increase in stiffness of the order of only 6 percent.

The effect of leakage on damping, however, is more pronounced throughout the frequency range (Fig.7.16) and the increase in negative damping at 5 C/S is of the same order of magnitude as that at 70 C/S. The combined effect of increases in stiffness and damping with leakage is to give a large increase in impedance at the low frequencies which gradually decreases for the higher frequencies of excitation (Fig.7.17).

#### 7.2.4 Effect of Supply Pressure on Impedance.

The supply pressure remains at a constant value in a hydraulic system unless there is a malfunction in one of the pressure regulating devices when the system pressure can be either less than or in excess of the normal operating pressure. Generally a decrease in the supply pressure is followed by a decrease in the servo impedance but the effect on stiffness and damping are somewhat different. Supply pressure,  $P_s$ , in the range 500 lbf/sq.in. to 3000 lbf/sq.in. was tested at one value of the static valve opening. The results are presented in Figures 7.18 and 7.19. When examined on the basis of frequency a decrease in  $P_s$  causes an increase in the stiffness (Fig.7.18). Maximum stiffness in the frequency range 5-30 C/S is obtained for  $P_s = 2400 \text{ lbf/sq.in.}$  For the frequency range 30-70 C/S  $P_s = 1500 \text{ lbf/sq.in.}$  gives the maximum stiffness. Change in the value of  $P_s$  changes the frequency at which the maximum stiffness occurs.

Figure 7.19 shows the effect of supply pressure on damping. An increase in  $P_s$  causes the damping to go negative while increasing its absolute value. Hence, the maximum negative damping occurs at  $P_s = 3000 \text{ lbf/sq.in.}$  The increase in negative damping is also frequency dependant and the maximum increase occurs at the highest frequency.

### 7.2.5 The Effect of Static Valve Opening On Impedance.

The effect of static valve opening is to decrease the impedance of the hydraulic servo particularly at the low frequencies. Figure 7.20 shows the effect of valve opening on stiffness for various frequencies. Except for 5 C/S, the stiffness initially rises to a maximum value before it rapidly decreases. Each frequency has its maximum stiffness at a difference value of the valve opening and also the decrease in stiffness is larger at the lower frequencies. The damping behaves in a different manner to changes in the valve opening. It is seen that as the valve opening increases the value of the negative damping decreases and finally becomes positive at a certain valve opening depending upon the frequency. (Fig.7.21). The graph also shows that higher the frequency the larger the valve opening at which the damping becomes positive. This is probably due to the malfunction of the phase meter as explained earlier. In fact, the higher frequencies are expected to reach positive damping for smaller valve openings than is the case for the lower frequencies, but the general shape of the curves remains valid.

### 7.2.6 The Effect of Perturbation Amplitude.

The effect of increasing the perturbation amplitude is to decrease the impedance of the servo. Unlike a change in other parameters, an increase in the perturbation amplitude reduces both the stiffness and the damping in the entire frequency range. Figures 7.22 and 7.23 show plots of stiffness and damping, respectively, against the frequency for static valve openings of .015in. and .025in. at perturbation amplitude of  $\pm .002$ in. and  $\pm .005$ in. It will be seen that both the stiffness and the damping vary in the same manner to changes in the perturbation amplitude. For the smaller valve opening the decrease in the stiffness and the damping due to an increase in the perturbation amplitude is not very large and is very nearly constant in the frequency range except at the higher frequencies when it tends to be smaller. For the larger valve opening the decrease in the stiffness and the damping

is considerably more and increases for the higher frequencies.

### 7.3. Correlation of Analogue and Rig Results.

The impedance of the hydraulic servo measured by analogue simulation is compared with that obtained by Penny(1) on the test rig. Figure 7.24 shows the variation of impedance with frequency for static valve openings of .005in. and .015in. The broken line represents the analogue result and the solid line represents the rig result. At the valve opening of .005in. the analogue results shows a very high impedance at 5 C/S which rapidly decreases and at 10 C/S is about 10 percent higher than the impedance obtained from the test rig. Above 50 C/S the analogue results again gives higher values of impedance but the difference is only of the order of about 6 percent at a frequency of 70 C/S. The value of the bulk modulus for this test point was 120,000 lbf/sq.in. which corresponds to the value estimated for the test rig at small valve openings and high frequencies. The lower set of curves on Fig.7.24 compares the impedance at a valve opening of .015in. An excellent correlation is obtained between the analogue and the rig results. The value of the bulk modulus for the analogue was, however, only 40,000 lbf/sq.in. for this test point. Higher value of  $N$  for analogue simulation gave much higher values of impedance when compared to the test rig. This would suggest that the value of  $N$  in the physical system does not remain constant as the valve opening increases.

The variation of stiffness with frequency for changes in the valve opening for the test rig and the analogue simulation is presented in Figures 7.25 and 7.26 respectively. The general shapes of the curves for the two cases are similar. The stiffness decreases as the valve opening is increased. For any particular setting of the valve opening the stiffness increases with the frequency. Once again the analogue results give a higher value for stiffness compared to rig results except at a valve opening of .005in.

The variation in stiffness with the valve opening for selected frequencies from the test rig is shown in Fig.7.27. Comparing it with the analogue result (Fig.7.20) it is seen that the two results are similar except for rapid decrease in stiffness with the valve opening predicted by rig results. Comparing Figures 7.28 and 7.21, which show the variation of damping with the valve opening for the test rig and analogue simulation respectively, it is seen that the damping increases from a negative to a positive value as the valve opening increases. The analogue result differs from the rig result that it shows the damping at higher frequencies to have a greater negative value than that at the low frequencies. This difference is believed to be due to the inaccuracy of the phase meter. The general trends in the two results are nevertheless very similar. Figures 7.29 and 7.30 compare the stiffness from the test rig and the analogue simulation for a perturbation amplitude of  $\pm .005$ in. and again good correlation is seen to exist.

#### 7.4. Impedance of The Hydraulic Servo without Coulomb Friction.

In the absence of coulomb friction the non-linearity in the servo is due to the flow characteristics through the valve ports. It is this non-linear flow characteristic that is linearised when theoretical calculations of the servo response are made. To study the impedance of the servo without coulomb friction on the analogue computer the circuit diagram of Fig.6.10 was used. To remove  $F_c$  the input to amplifiers 3 and 8 from amplifier 18 were removed. The values of the parameters were changed by potentiometer settings as shown in Fig.6.11.

##### 7.4.1 The Effect of Bulk Modulus on Impedance.

The effect of bulk modulus on stiffness and damping is shown in Figures 7.31 to 7.34. A change in the value of  $N$  from 40,000 lbf/sq.in. makes very little difference to stiffness on a basis of frequency (Fig.7.31). Further increase in  $N$  causes larger increases in stiffness as the frequency goes up. Comparing Fig.7.31 with Fig.7.11 shows

that in the absence of coulomb friction higher values of stiffness are obtained, but the increase in stiffness with frequency is not so pronounced. The absence of coulomb friction also increases the value of  $N$  at which all frequencies have the same stiffness. The effect of bulk modulus on stiffness for changes in static valve opening is shown in Fig.7.32. At a frequency of 5 C/S doubling the value of  $N$  causes a very large increase in stiffness at a valve opening of .005 in. At a valve opening of just over .010 in the effect of increased value of  $N$  becomes almost insignificant. At 70 C/S, however, the effect of the increased value of  $N$  on stiffness remains significant for much larger valve openings. Comparing Fig.7.32 with Fig.7.12 shows that while the absence of coulomb friction substantially reduces the stiffness for large valve opening, it allows for larger increase in stiffness for an increase in the value of  $N$ . The basic shape of the curves in the two figures being compared remains unchanged.

Figure 7.33 shows the effect on damping for increases in the value of  $N$  for selected frequencies. Initially, at  $N = 40,000$  lbf./sq.in. The damping is more negative for the low frequency than it is for the high frequency. Increasing the value of  $N$  reduces the negative damping for low frequencies but causes large increase in negative damping for the high frequencies. At  $N = 110,000$  lbf/sq.in. the value of damping remains constant at all frequencies. Below this value of  $N$  the high frequency damping is more positive and above this value of  $N$  the low frequency damping is more positive. Comparing this figure with Fig.7.13 shows that the absence of coulomb friction makes the damping more negative at all frequencies, and gives a higher value of  $N$  at which the damping remains constant for all frequencies. The effect of  $N$  on damping with valve opening is shown in Fig.7.34. Doubling the value of  $N$  decreases the negative damping at 5 C/S but as the valve opening gets larger this difference gets progressively smaller until it is insignificant at and above a valve opening of .020 in. At a frequency of 70 C/S the picture is somewhat different. Doubling the value of  $N$  increases the amount of negative damping for small values of the valve opening. At a valve opening of .005in. the amount of neg-

ative damping is almost doubled. This large increase in the negative damping rapidly reduces with the valve opening until at .0135 in the damping is the same for the two values of  $N$ . Above this value of the valve opening the damping is less negative for the higher value of  $N$  and changes into a large positive increase at .0175 in. As the valve opening increases further the effect of bulk modulus reduces until at .030 in. this effect is insignificant. The effect of removing the coulomb friction (Compare Fig.7.34 with 7.14) is to decrease the positive damping through out the frequency range.

#### 7.4.2. The Effect of Leakage on Impedance.

The effect of leakage on impedance in the absence of coulomb friction is shown in Figures 7.35 to 7.37. An increase in the leakage causes an increase in the stiffness at all frequencies (Fig.7.35). The largest increase is obtained at 5 C/S which gradually decreases as the frequency is increased until at 70 C/S the stiffness increases by 7 percent for a leakage coefficient,  $K_c 4 \times 10^{-5} \text{ in}^5/\text{lb} \cdot \text{sec}$ . compared with no leakage. Further increase in leakage does not change the value of stiffness at 70 C/S. Comparison of Fig.7.35 with 7.15 shows that the absence of coulomb friction reduces the stiffness, particularly at the higher frequencies.

The variation of damping with leakage against frequency is shown in Fig.7.36. An increase in leakage increases the negative damping throughout the frequency range. Comparison of this figure with Fig.7.16 shows that coulomb friction substantially reduces the negative damping. The leakage increases the impedance of the servo (Fig.7.37) by a considerable amount, the increase being larger for the lower frequencies.

#### 7.4.3 The Effect of Supply Pressure on Impedance.

A decrease in supply pressure decreases the impedance of the servomechanism. This decrease is linearly proportional to the supply

pressure at very low frequencies but this is not the case at the higher frequencies where the effect of supply pressure is much reduced. Referring to Fig.7.38 it can be seen that at 5 C/S reducing the supply pressure by a factor of 6 reduces the impedance by the same factor. At a frequency of 70 C/S reducing the supply pressure by a factor 6 reduces the impedance only by 15.5 percent. The variation in stiffness with frequency for changes in the supply pressure is shown in Fig.7.39. At low frequencies a substantial reduction in stiffness follows a reduction in the supply pressure but the high frequency stiffness is much less effected. Comparing this figure with Fig.7.18 shows that the presence of coulomb friction generally increases the stiffness for increased supply pressure except at  $P_s = 3000$  lbf/sq.in. when the presence of coulomb friction drastically lowers the stiffness particularly at the higher frequencies. Also in the presence of coulomb friction the maximum stiffness in the frequency range 5-35 C/S is obtained at  $P_s = 2400$  lbf/sq.in. and the maximum stiffness for frequencies above 35 C/S is obtained at  $P_s = 1500$  lbf/sq.in.

The effect on damping of changes in  $P_s$  can be seen in Fig.7.40. An increase in the supply pressure causes an increase in the negative damping. This increase is more pronounced at the higher frequencies. Comparing this figure with Fig.7.19 it is seen that the presence of coulomb friction makes the damping positive for low frequencies at  $P_s = 1500$  lbf/sq.in. But at higher values of the supply pressure coulomb friction causes large increases in the negative damping particularly at the higher frequencies.

#### 7.4.4 The Effect of Static Valve Opening on Impedance.

The Effect of increasing the valve opening is to decrease the impedance of the servo. Fig.7.41 shows the variation of stiffness with the valve opening. It is seen that the low frequency stiffness suffers larger decreases than the high frequency stiffness as the valve opening increases. At a valve opening of .008 in. the stiffness remains constant for all frequencies except at 5 C/S which tends to reach the

value of static stiffness for the hydraulic servo. The variation of damping with the valve opening is shown in Fig.7.42. At small valve openings the higher frequencies have a larger negative damping than the lower frequencies. For all frequencies the negative damping decreases for larger valve opening. At a valve opening of .020 in. and above the higher frequencies have a larger positive damping than the lower frequencies. Comparing Figures 7.41 and 7.42 with Figures 7.20 and 7.21 it is seen that coulomb friction increases both the stiffness and the positive damping. Except for the higher values of the stiffness and damping the shapes of the curves with and without coulomb friction are similar.

#### 7.5. Correlation of Analogue and Theoretical Results.

The results of the analogue simulation of the hydraulic servo without the coulomb friction are compared with theoretical results obtained by linearising the valve flow characteristics using the small perturbations technique.

The effect of static valve opening on impedance for 5,40 and 70 C/S is compared in Fig.7.43. The solid line and the broken line represent the analogue and the theoretical results respectively. There is a qualitative agreement between the results inasmuch as they both show a decrease in impedance for larger valve openings and an increase in impedance for the higher frequencies. The magnitude of the theoretical impedance is considerably less compared to the analogue result except for the higher frequencies at very small valve openings. Figure 7.44 compares the variation of impedance with frequency for valve openings of .005 in. and .030 in. for  $N = 200,000 \text{ lbf/sq.in.}$  For the smaller valve opening a good qualitative and quantitative correlation exists between the analogue and the theoretical impedance. For the larger valve opening there is good agreement between the two results for the lower frequencies. At the higher end of the frequency range the analogue result gives a much higher value of impedance than the theoretical result. Figure 7.45 presents information similar to Fig.7.44 but for a value of  $N=120,000 \text{ lbf/sq.in.}$  Here the picture has changed in that the theoretical imped-

ance has a higher value at the smaller valve opening, but for the larger valve opening the analogue result still shows large increase in impedance for the higher frequencies.

The effect of valve opening on the theoretical stiffness for selected frequencies is shown in Fig.7.46. Comparing this figure with Fig.7.41, which is the analogue result, it is seen that there is a qualitative agreement between the two results but the theoretical stiffness decreases very rapidly and falls to a value of about 350 lbf/in at a valve opening of .035in. for the highest frequency. Comparing the variation of the theoretical damping against the valve opening with the damping obtained from the analogue simulation, Figures 7.47 and 7.42 respectively, shows that the two results differ considerably. The analogue results predict a large negative damping for all frequencies up to a valve opening of .016in. when the damping becomes positive. The theoretical result, on the other hand, show a small amount of negative damping which becomes positive at a velve opening of .006in. when there is a large increase in the positive damping. The two results agree well for the values of the valve opening above .020in.

Figures 7.48 and 7.49 show the effect of bulk modulus on theoretical stiffness and damping, respectively, for changes in the static valve opening. At a frequency of 5 C/S an increase in the value of the bulk modulus from 80,000lbf/sq.in. to 200,000 lbf/sq.in. makes a slight difference in stiffness only for the values of the valve openings below .010in. At 70 C/S the increased value of N causes a very large increase in stiffness for valve openings of up to .010in. when the value of stiffness for  $N = 80,000$  lbf/sq.in. At a valve opening of .020 the stiffness is not effected by changes in the bulk modulus. Comparing Figures 7.48 and 7.32 shows that the effect on stiffness for changes in the bulk modulus is more pronounced in the analogue result which not only shows larger increases in the stiffness for increase in the value of N but also covers a wide range of the valve openings for which a change in N effects the stiffness.

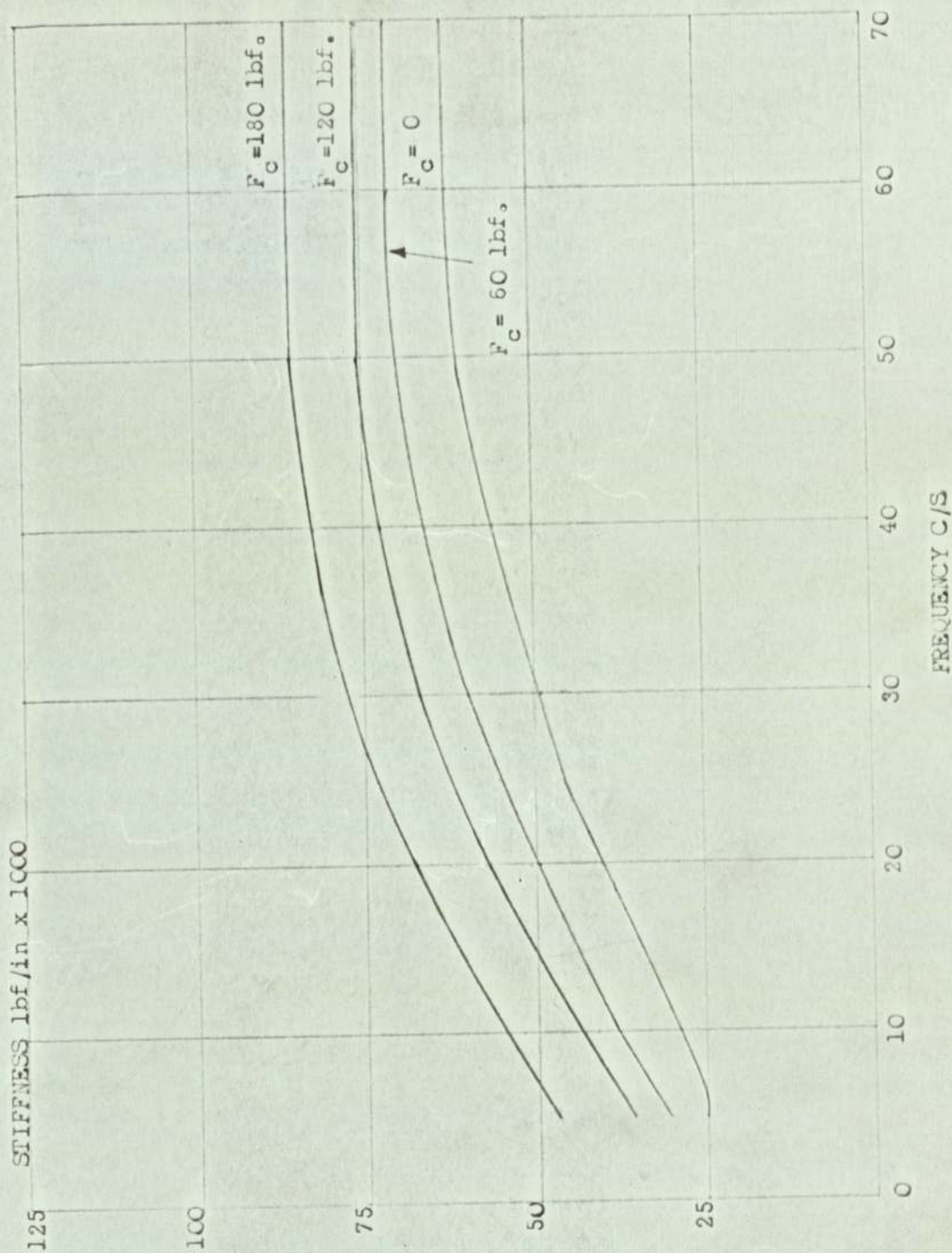
The effect of bulk modulus on theoretical damping is shown in Fig.7.49. It is seen that at 5 C/S an increase in the value of N

changes the large negative damping to a positive value for a valve opening of .005in. Beyond a valve opening of about .012, a change in the value of  $N$  does not effect the damping at this frequency. At 70 C/S the increased value of  $N$  causes a very large increase in positive damping which peaks at a valve opening of .010 in. and rapidly decreases. At a valve opening of .020in. the effect of  $N$  on damping is negligible. Comparing Figs.7.49 and 7.34 shows that the analogue result gives a large negative damping at small valve openings and that the increased value of  $N$  initially increases the negative damping at 70 C/S. Also the range of valve openings for negative damping is much greater in the analogue result than it is for the theoretical result.

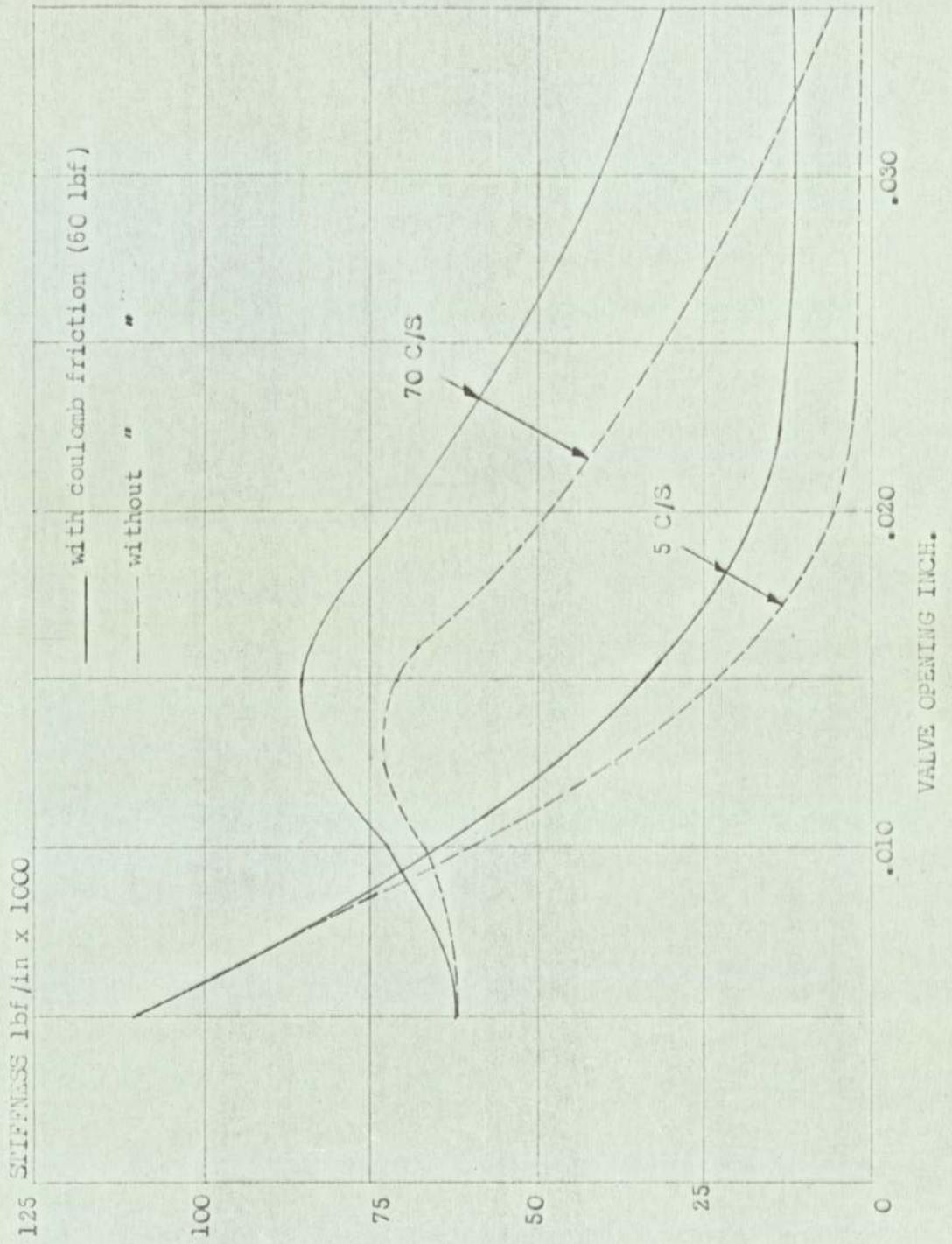
The effect of leakage on impedance against frequency is shown in Fig.7.50. The solid line and the broken line represent the analogue and the theoretical results respectively. The two results shows that the impedance increases as the leakage increases. The theoretical result gives small increases in impedance at low frequencies and large increases at high frequencies. But the analogue result shows large increases in impedance at the low frequencies and small increases at the high frequencies. The same pattern is shown when the effect of leakage on theoretical stiffness is compared with the analogue result, Figures7.51 and 7.35 respectively. The theoretical damping (Fig.7.52) is positive for all values of the leakage coefficient  $K_c$ , and an increase in  $K_c$  increases the amount of positive damping particularly at the higher frequencies. The analogue result, however, shows a negative damping (Fig.7.36) which increase in magnitude as the leakage is increased. This contrast in the two results may partly be due to the malfunction of the phase meter used for analysis of signals from the analogue computer.

The variation of theoretical stiffness and damping for changes in the supply pressure is shown in Figures 7.53 and 7.54. respectively. As the supply pressure increases the stiffness of the servo also increases. Comparison of Fig.7.53 with 7.39 shows the agreement between the analogue and the theoretical results. The damping, however,

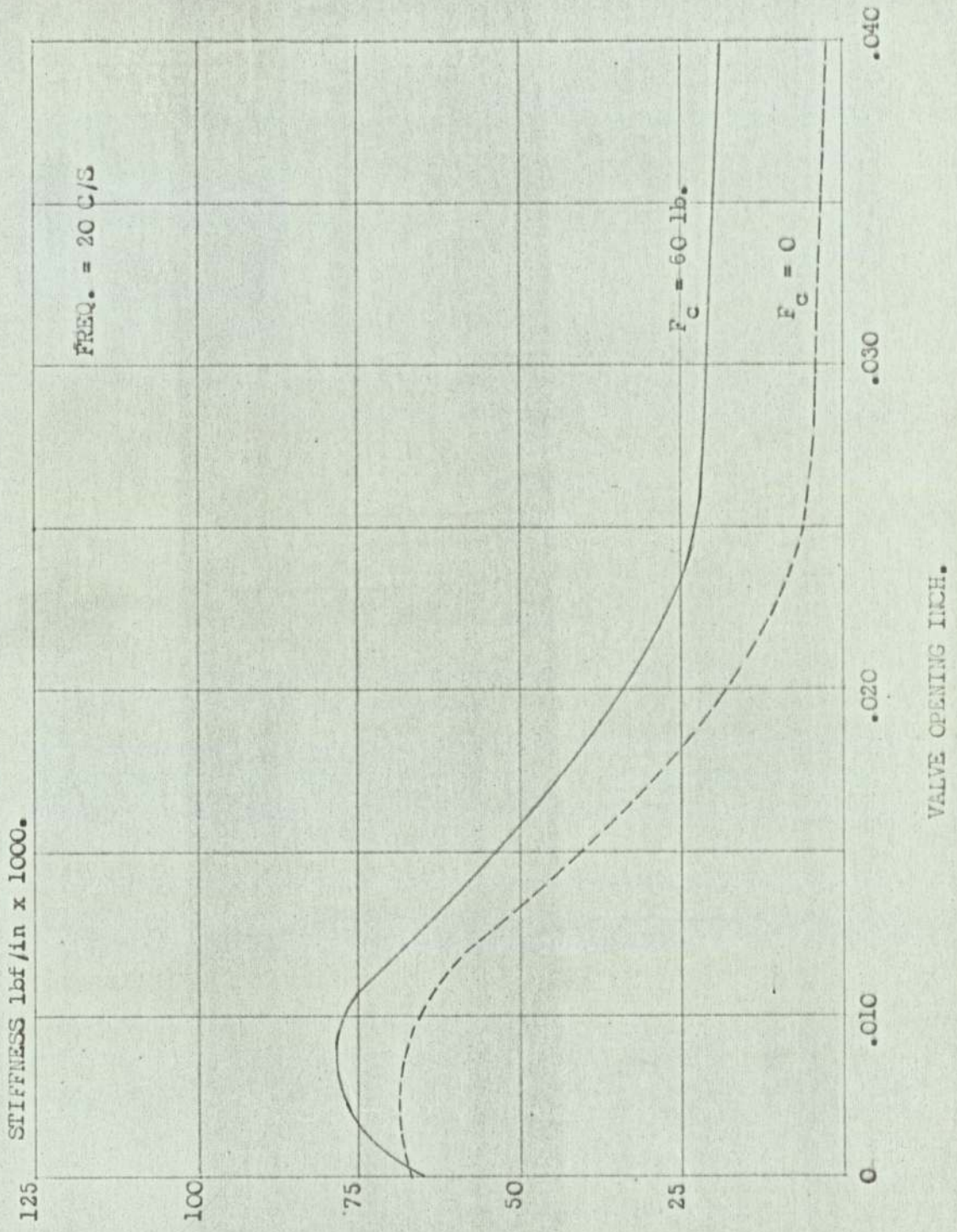
becomes less positive for higher values of the supply pressure, Figures 7.54 and 7.40. The negative damping for the theoretical results occurs only at very small valve openings but the positive phase angle at the higher valve openings decreases for an increase in the supply pressure. Therefore a qualitative agreement between the analogue and the theoretical results exists.



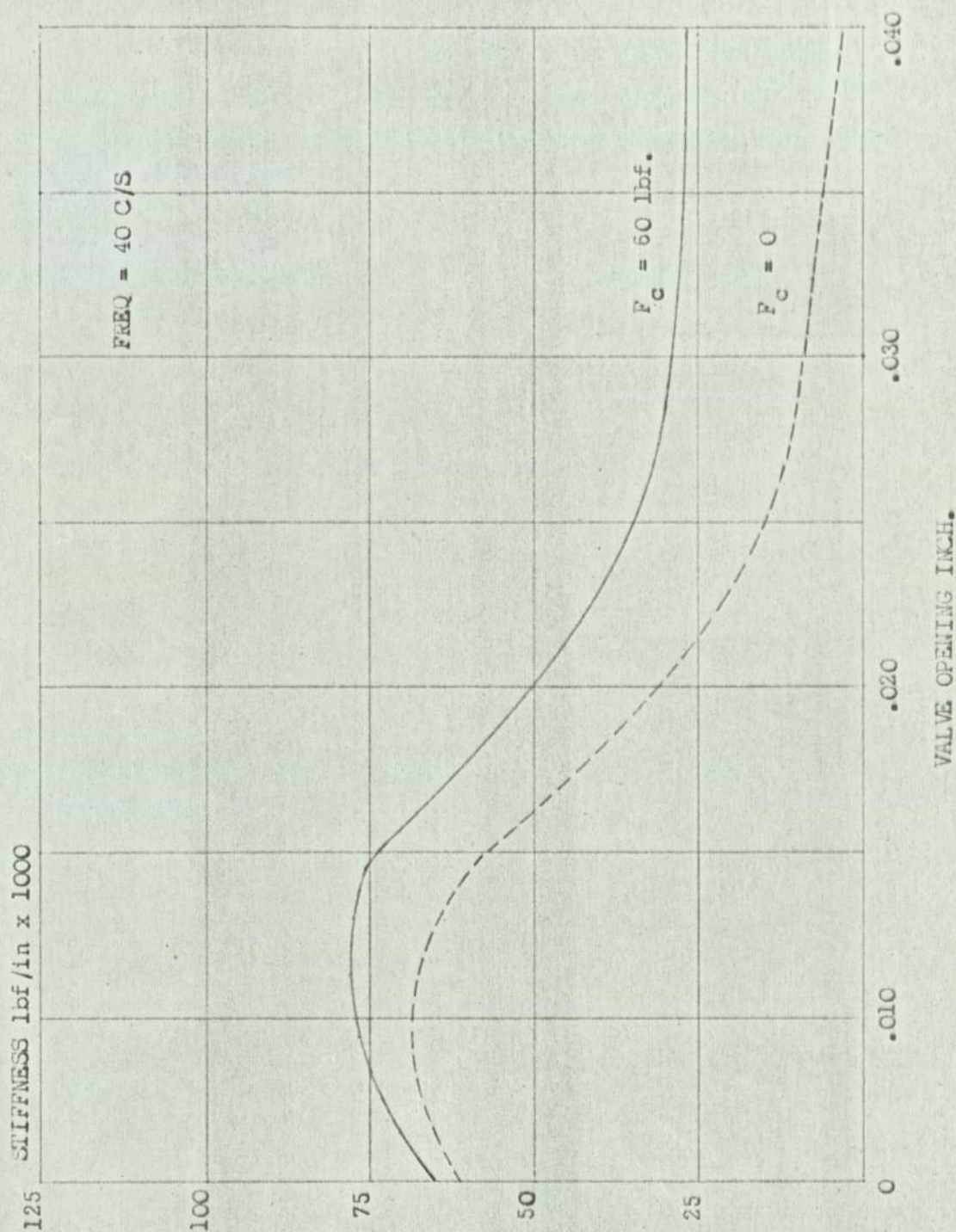
VARIATION OF STIFFNESS WITH COULOMB FRICTION  
 VALVE OPENING = .015 in. PERTURBATION AMPLITUDE =  $1.005$  in.



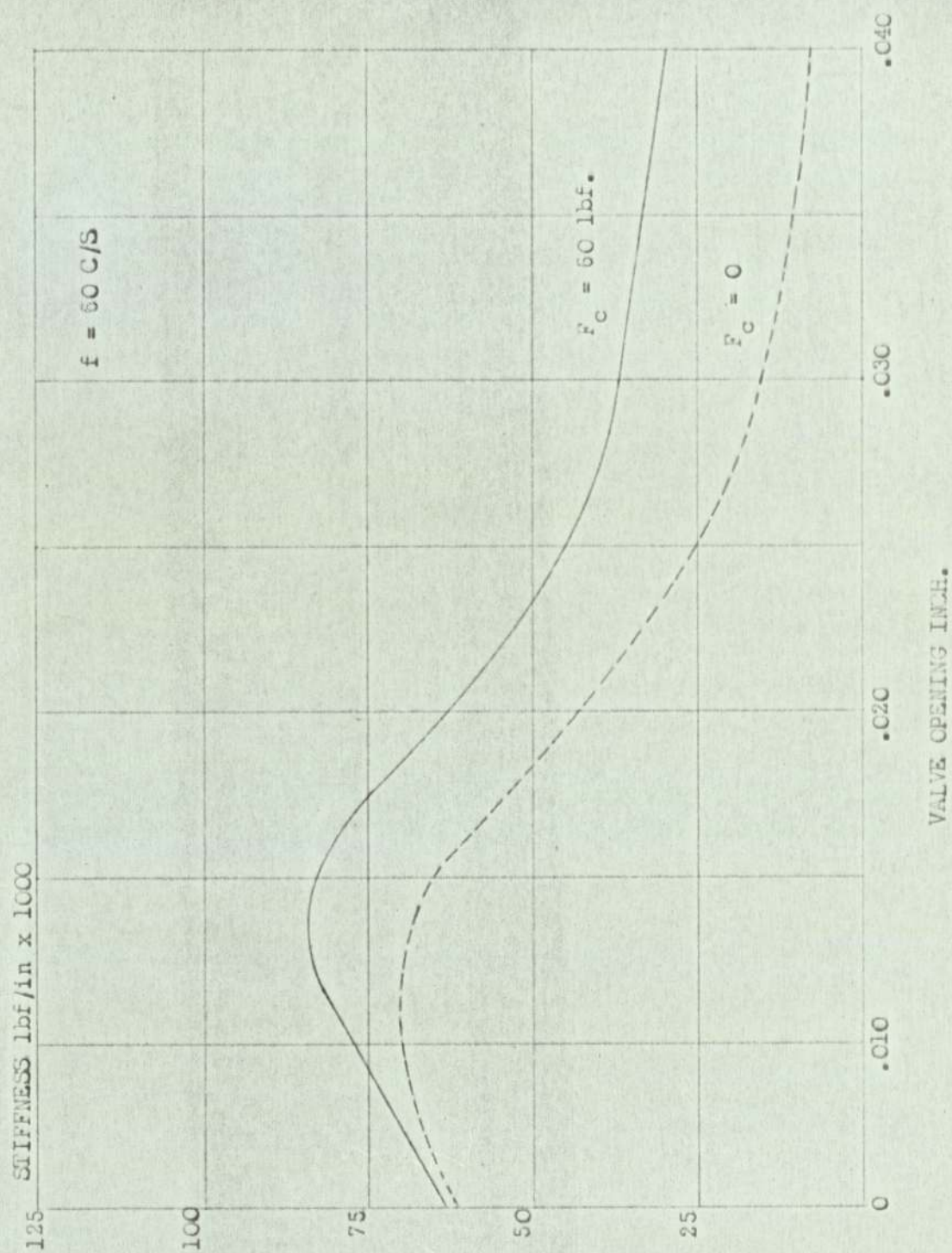
EFFECT OF COULOMB FRICTION ON STIFFNESS FOR CHANGES  
IN STATIC VALVE OPENING. PERTURBATION AMPLITUDE =  $\pm$ .003 inch.



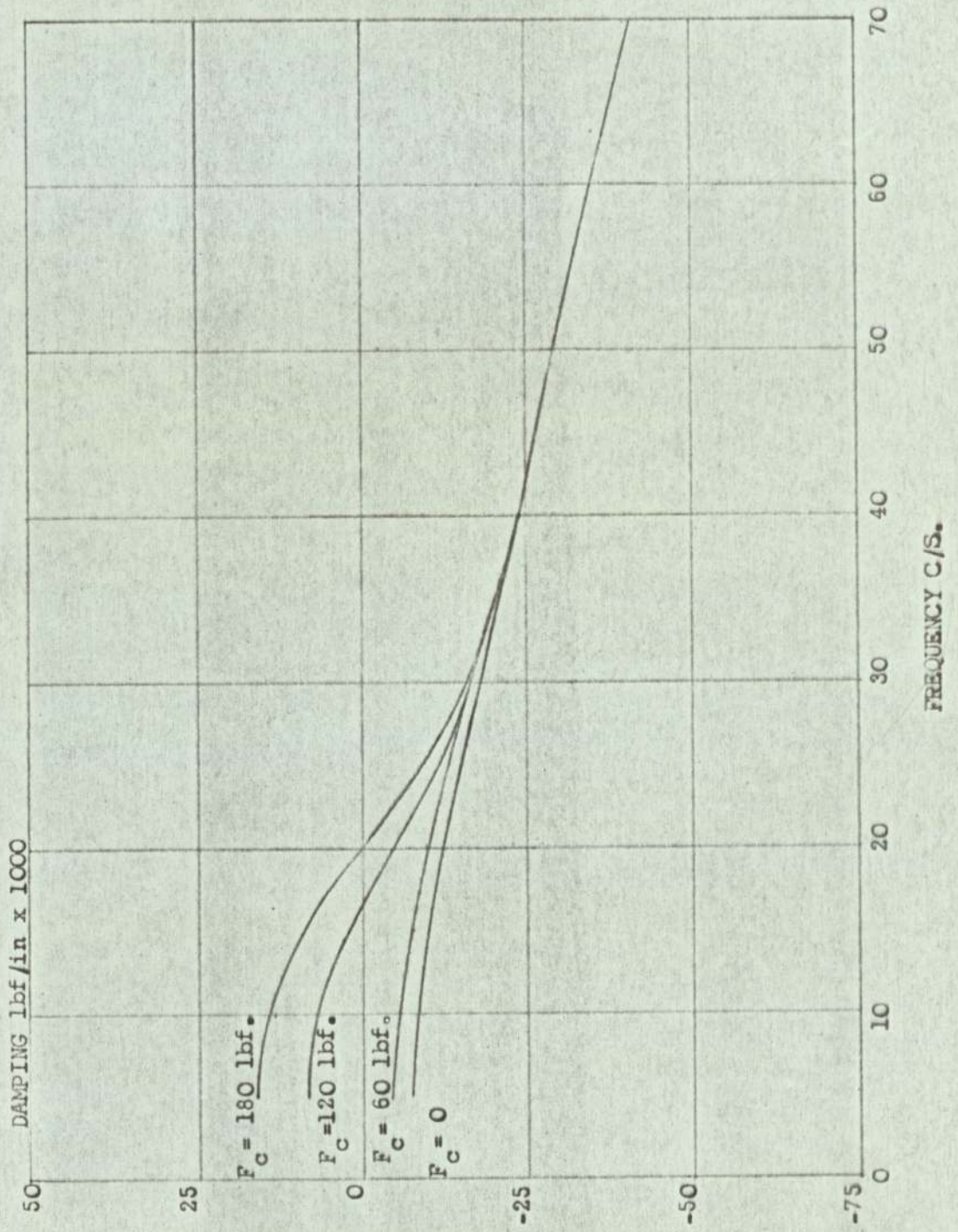
EFFECT OF COULOMB FRICTION ON STIFFNESS FOR CHANGES  
IN STATIC VALVE OPENING. PERTURBATION AMPLITUDE =  $\pm .003$  inch.



EFFECT OF COULOMB FRICTION ON STIFFNESS FOR CHANGES  
IN STATIC VALVE OPENING. PERTURBATION AMPLITUDE =  $\pm .003$  inch.

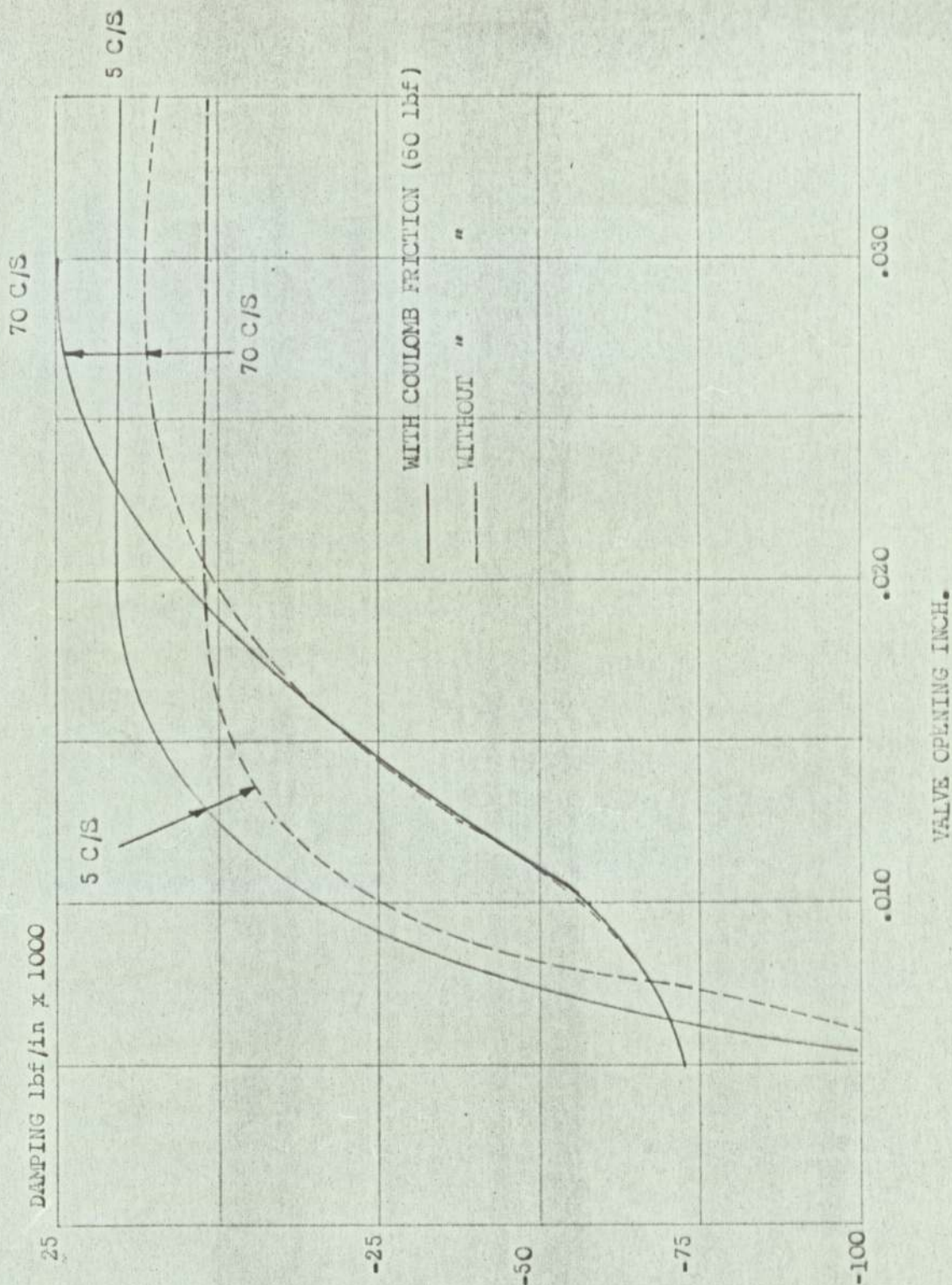


EFFECT OF COULOMB FRICTION ON STIFFNESS FOR CHANGES  
IN STATIC VALVE OPENING. PERTURBATION AMPLITUDE =  $\pm 1.003$  inch.

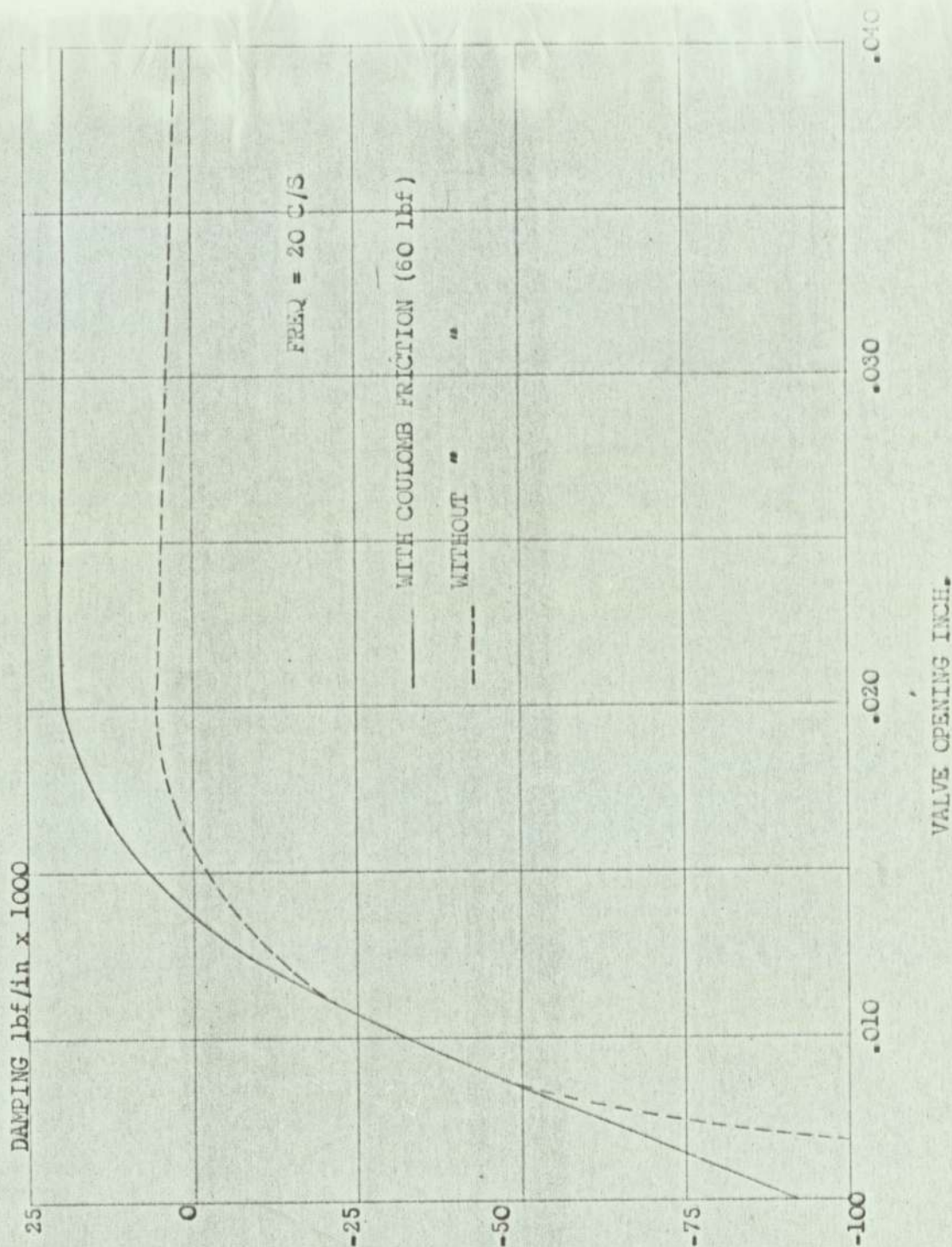


VARIATION OF DAMPING WITH COULOMB FRICTION

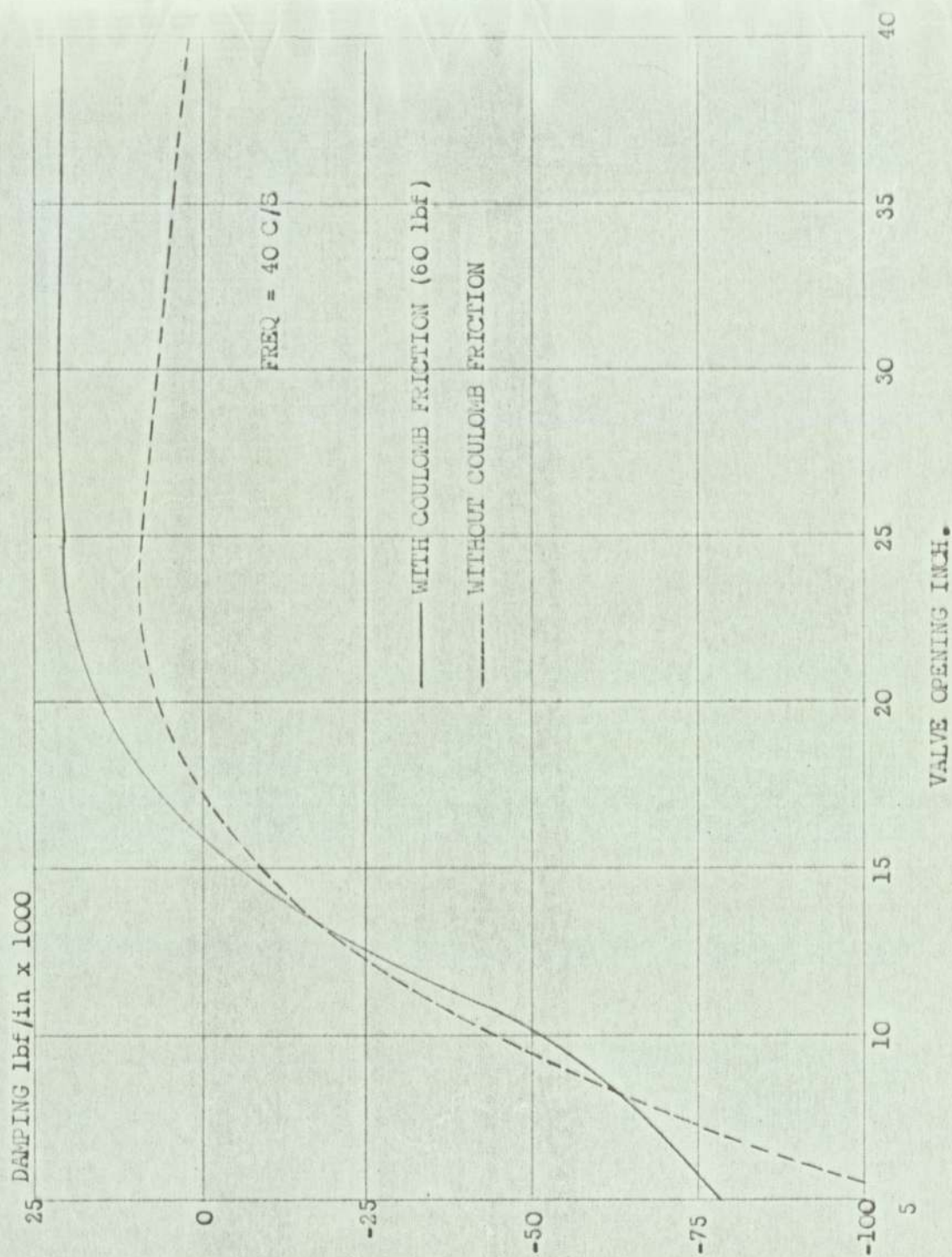
VALVE OPENING = .015 in. PERTURBATION AMPLITUDE =  $\pm$  .005 in.



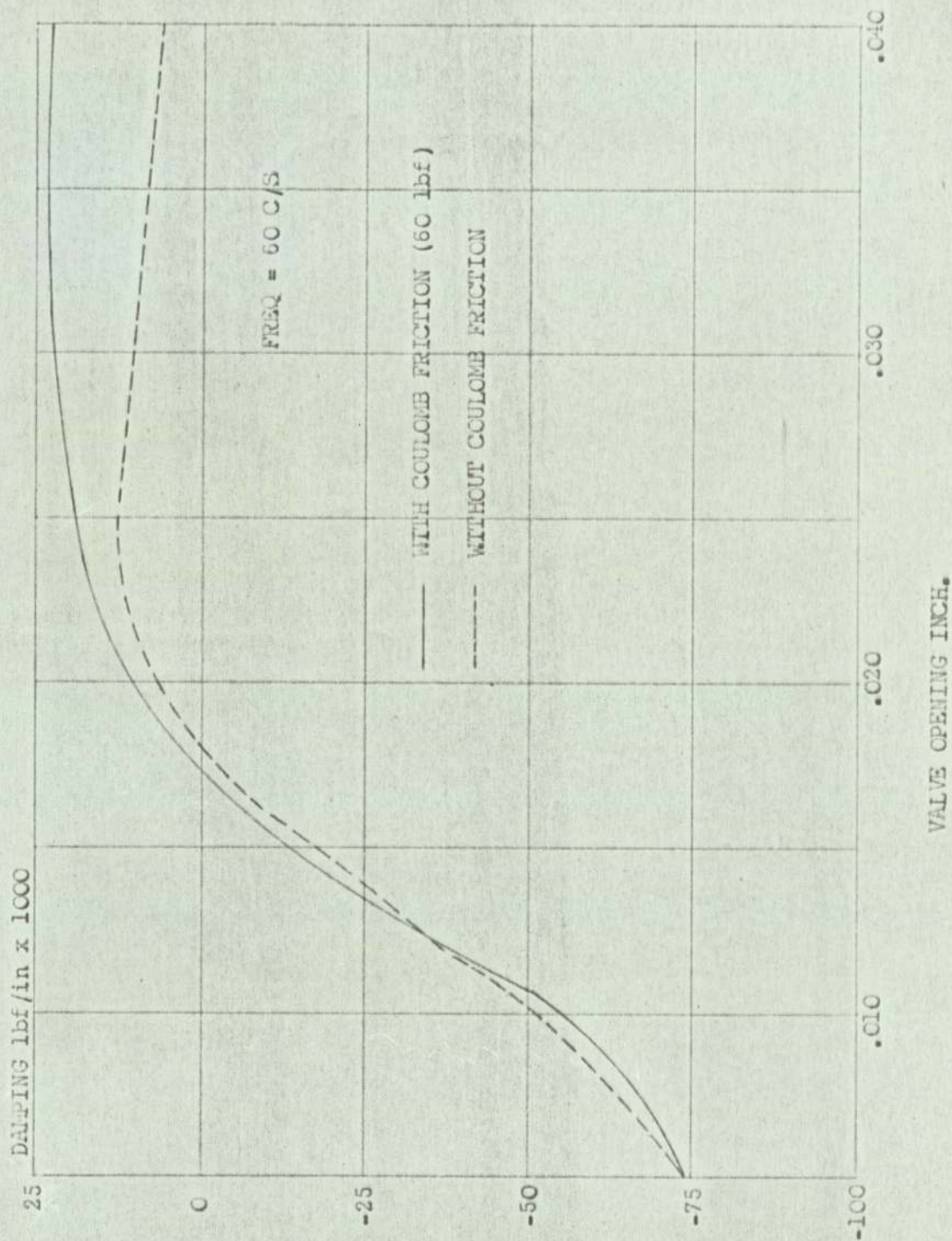
EFFECT OF COULOMB FRICTION ON DAMPING FOR CHANGES  
 IN STATIC VALVE OPENING. PERTURBATION AMPLITUDE =  $1.003$  in.



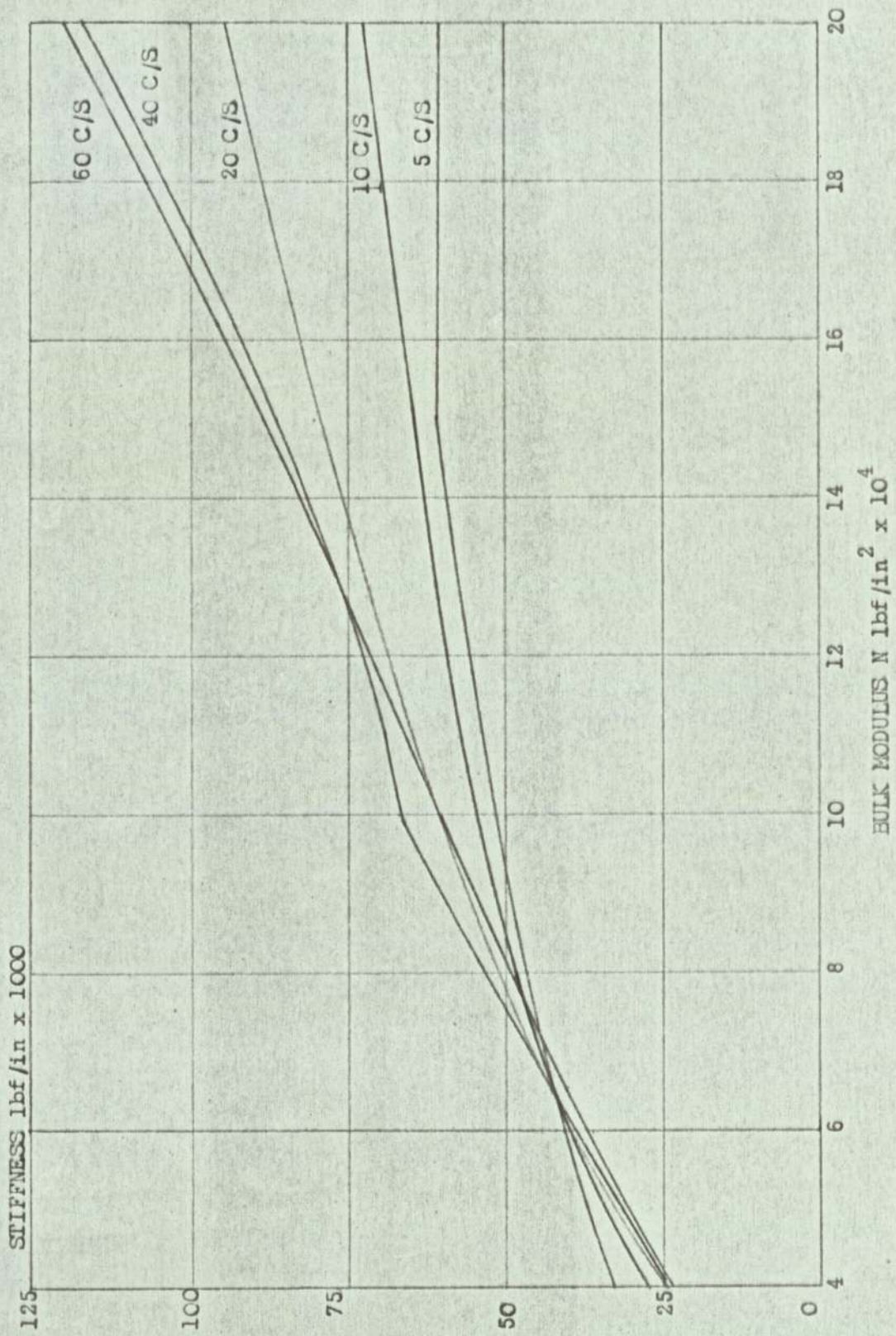
EFFECT OF COULOMB FRICTION ON DAMPING FOR CHANGES  
IN STATIC VALVE OPENING. PERTURBATION AMPLITUDE =  $\frac{+}{-} .003$  in.



EFFECT OF COULOMB FRICTION ON DAMPING FOR CHANGES  
IN STATIC VALVE OPENING. PERTURBATION AMPLITUDE =  $\pm .003$  in.

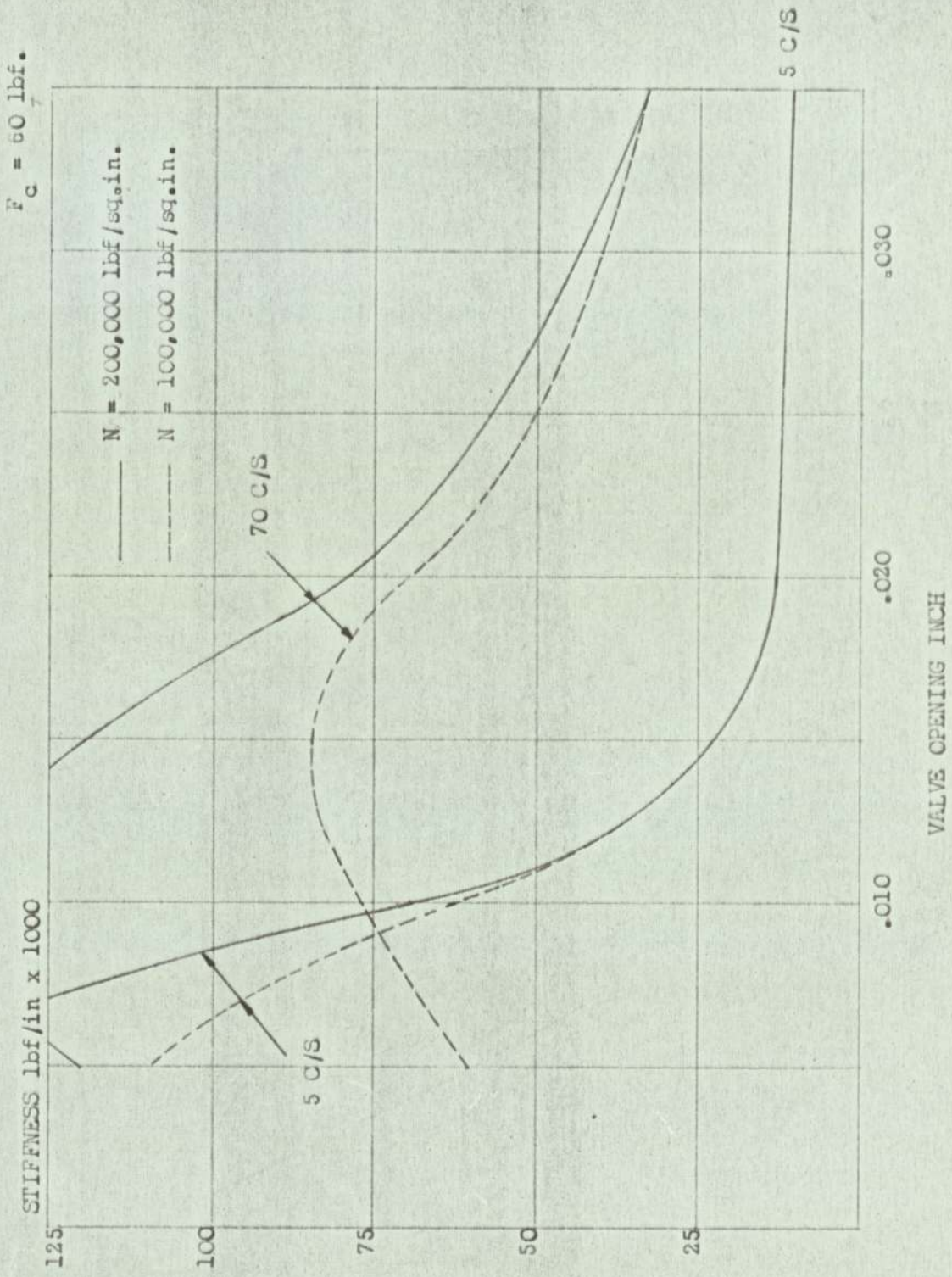


EFFECT OF COULOMB FRICTION ON DAMPING FOR CHANGES  
IN STATIC VALVE OPENING. PERTURBATION AMPLITUDE =  $\pm 0.003$  in.



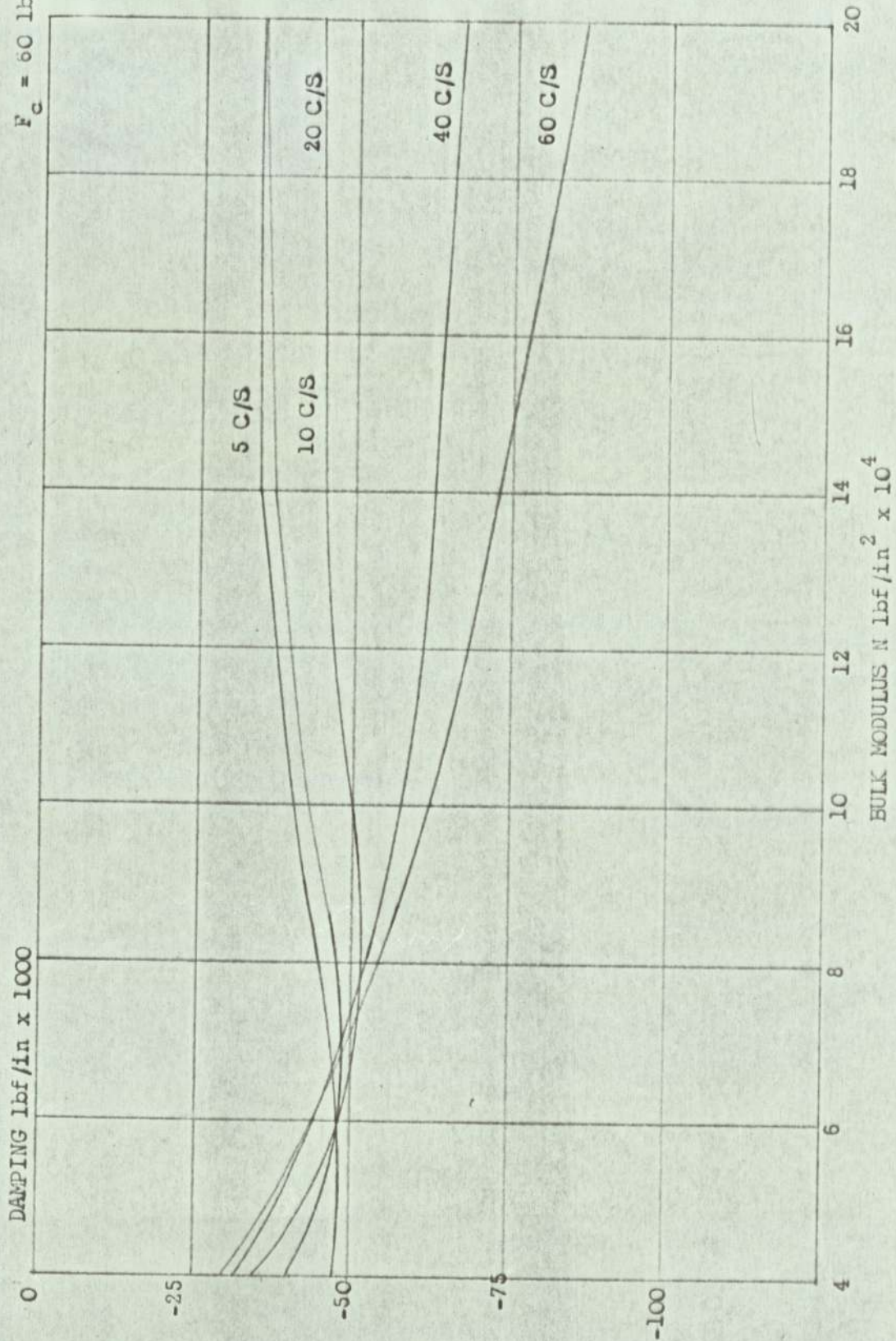
EFFECT OF BULK MODULUS ON STIFFNESS FOR CHANGES

FREQUENCY VALVE OPENING = .010 in. PERTURBATION AMPLITUDE = .005 in.

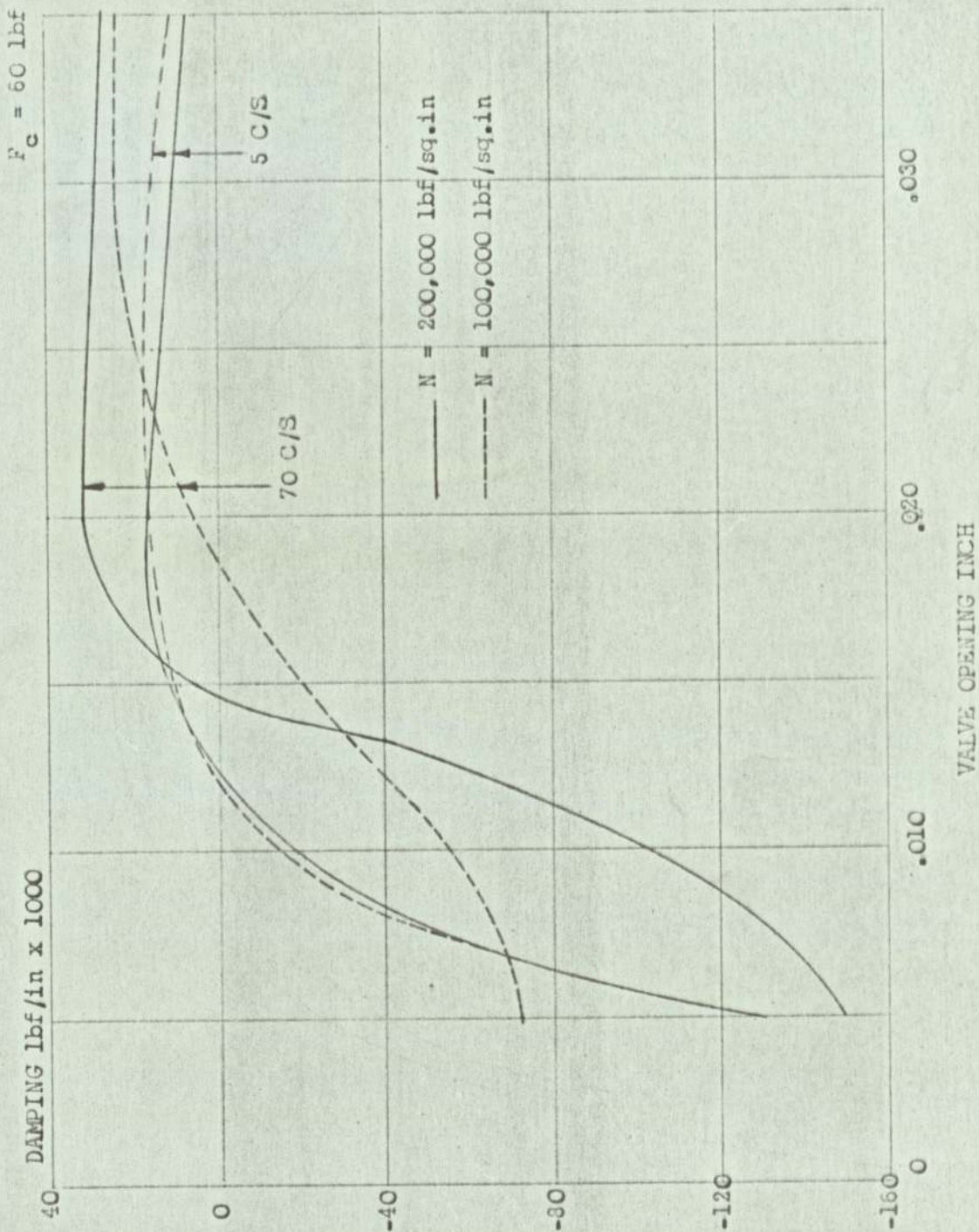


EFFECT OF BULK MODULUS ON STIFFNESS FOR CHANGES  
IN STATIC VALVE OPENING. PERTURBATION AMPLITUDE =  $\pm .003 \text{ in.}$

$F_c = 60 \text{ lbf.}$



EFFECT OF BULK MODULUS ON DAMPING FOR CHANGES IN  
FREQUENCY VALVE OPENING. 0.10 in. PERTURBATION AMPLITUDE =  $\pm .006$  in.

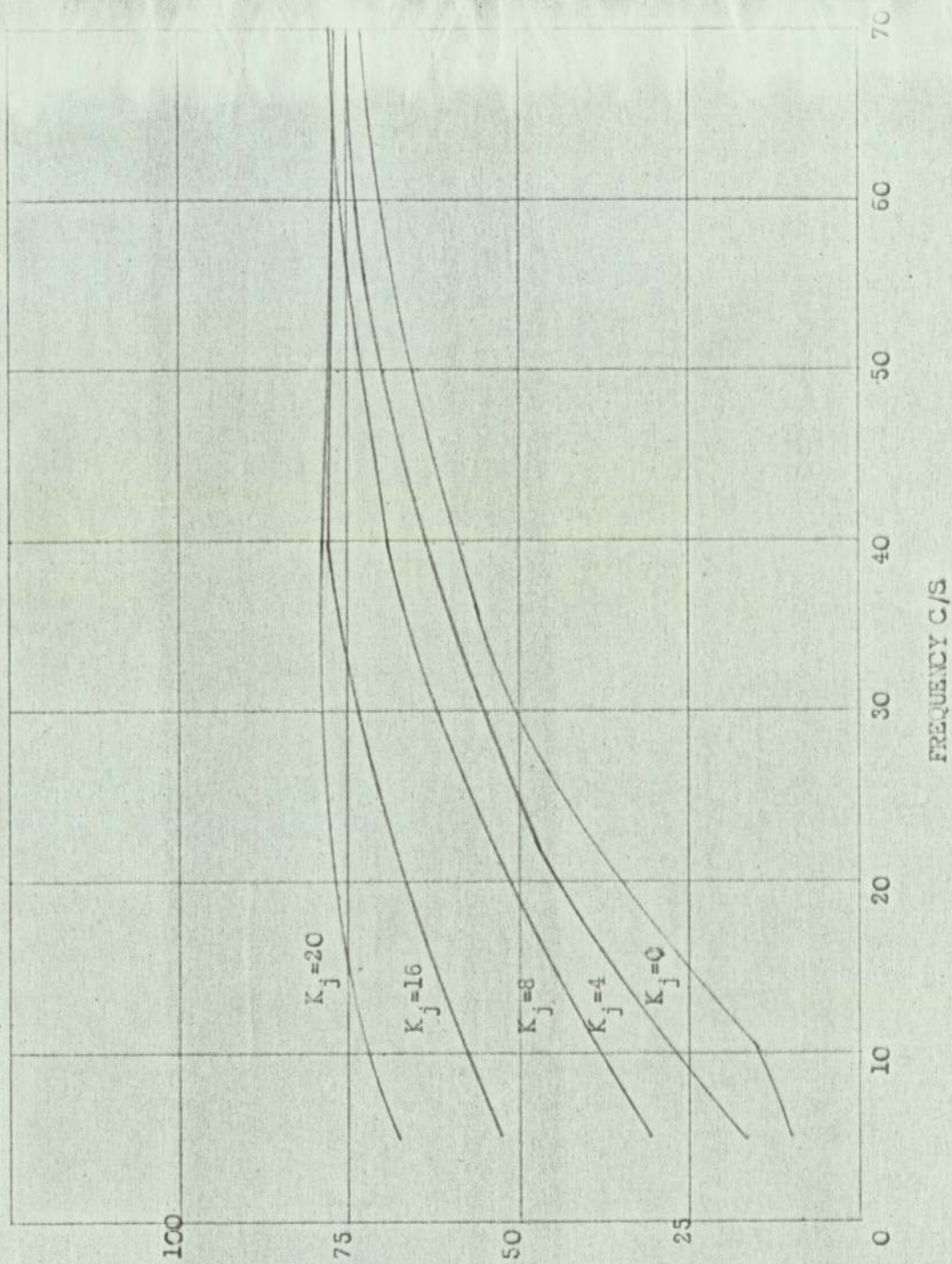


EFFECT OF BULK MODULUS ON DAMPING FOR CHANGES IN  
STATIC VALVE OPENING. PERTURBATION AMPLITUDE =  $\pm .003 \text{ in.}$

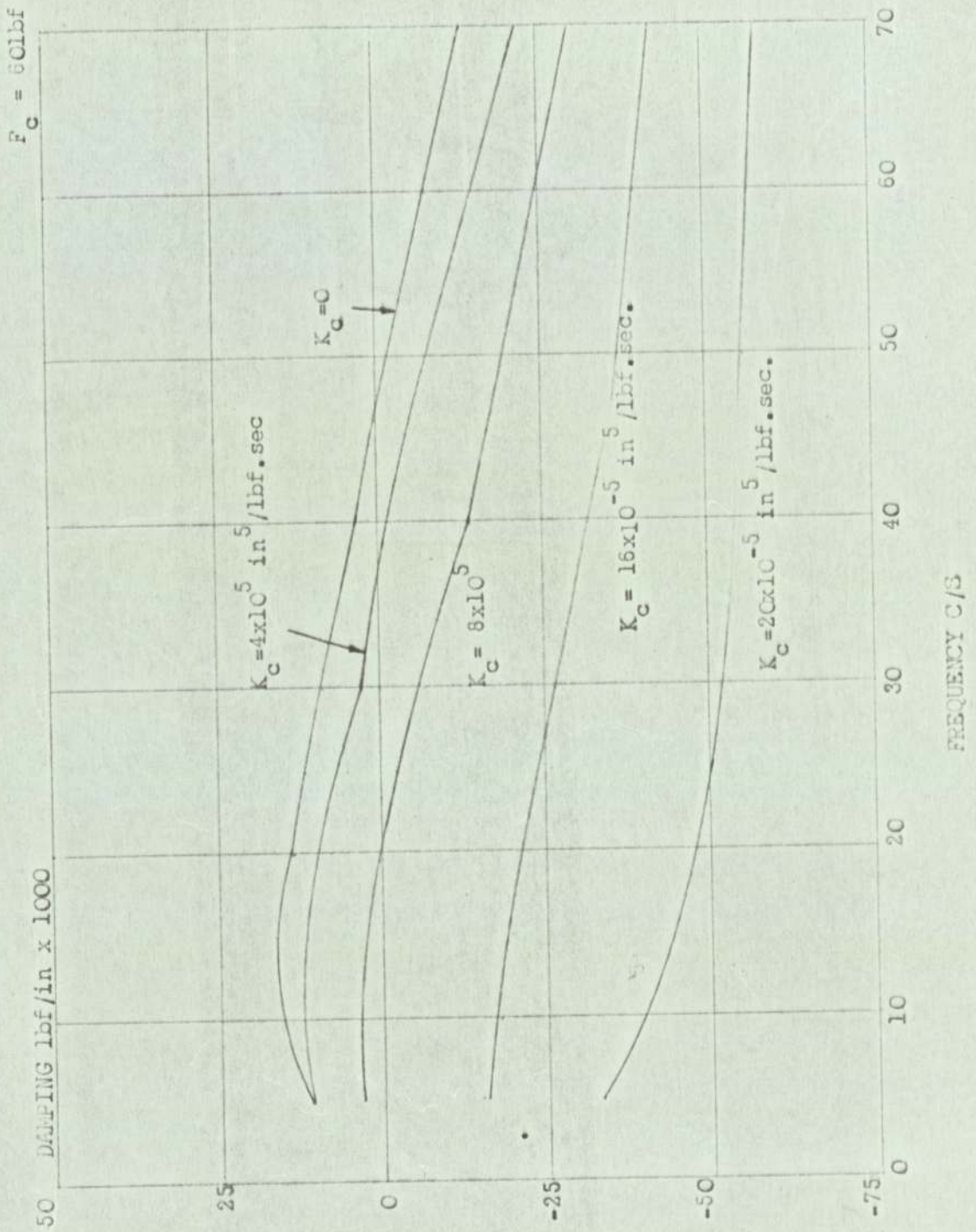
FIG. 7.14

$F_c = 60 \text{ lbf.}$

STIFFNESS lbf/in. x 1000

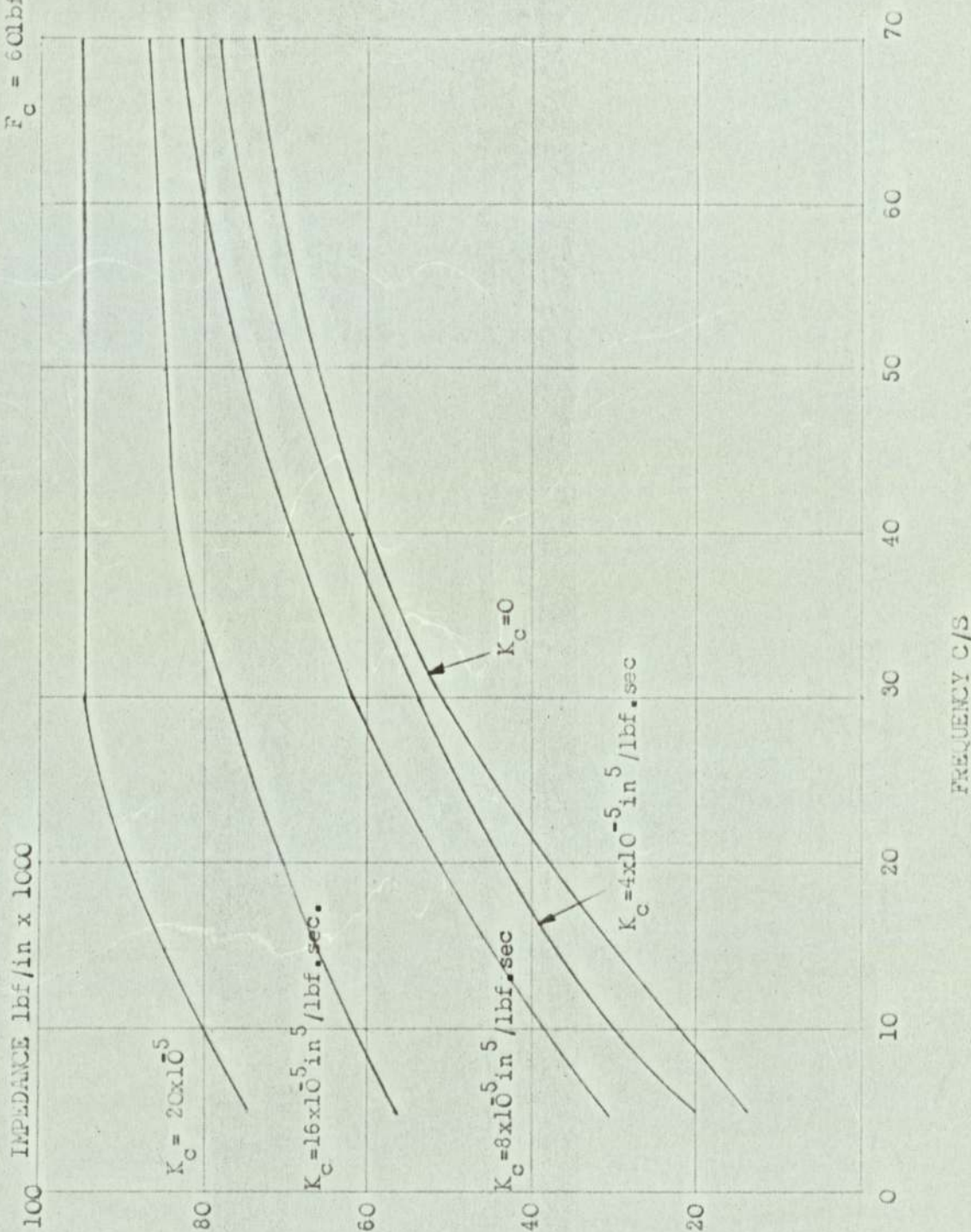


EFFECT OF LEAKAGE ON STIFFNESS STATIC VALVE OPENING =  $\pm .015$  in  
PERTURBATION AMPLITUDE =  $\pm .005$  in



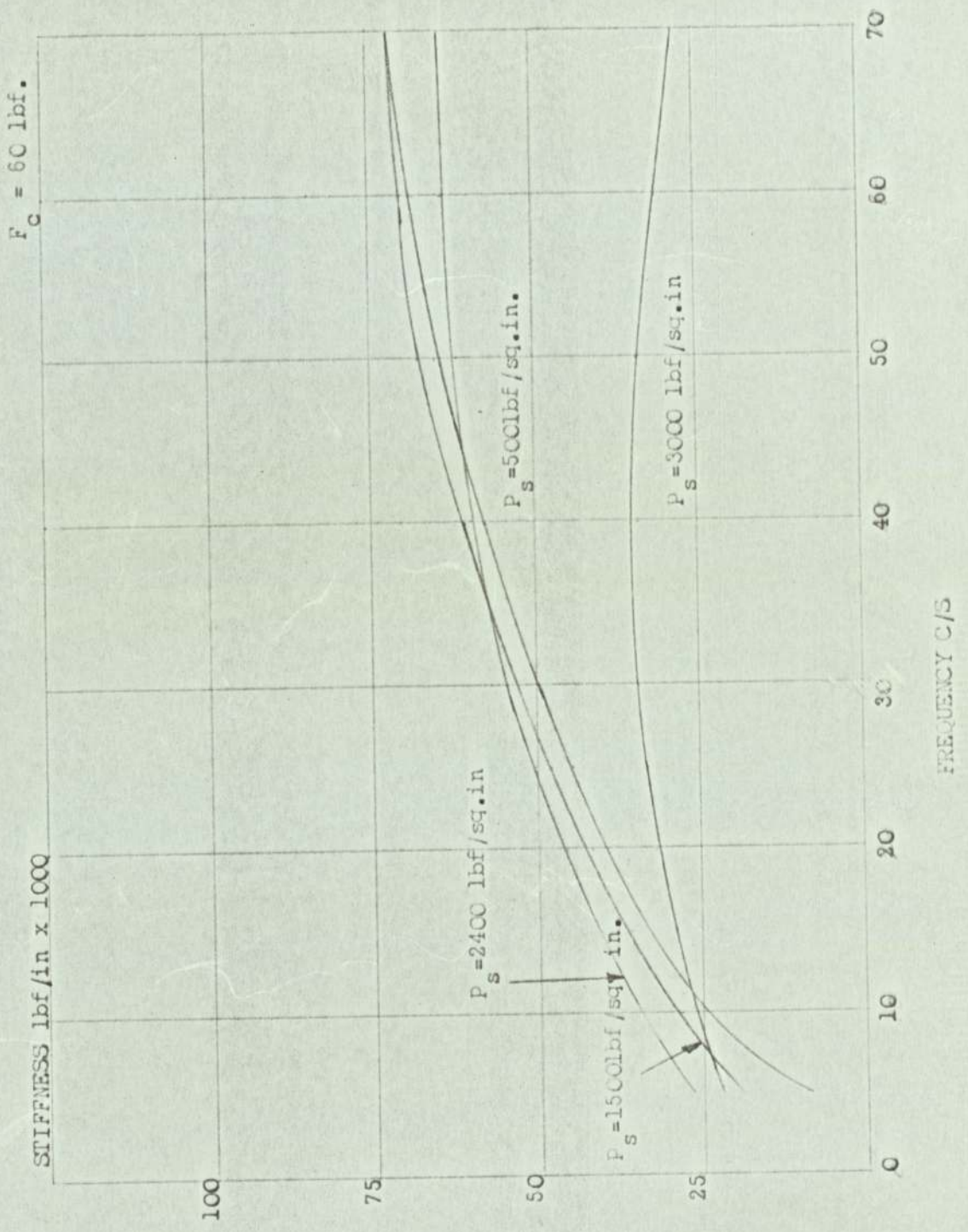
EFFECT OF LEAKAGE ON DAMPING STATIC VALVE OPENING =  $\pm .015 \text{ in}$   
PERTURBATION AMPLITUDE =  $\pm .005 \text{ in}.$

$F_c = 60 \text{ lbf.}$



EFFECT OF LEAKAGE ON IMPEDANCE. STATIC VALVE OPENING = .015 in.  
PERTURBATION AMPLITUDE =  $\pm$  .005 in.

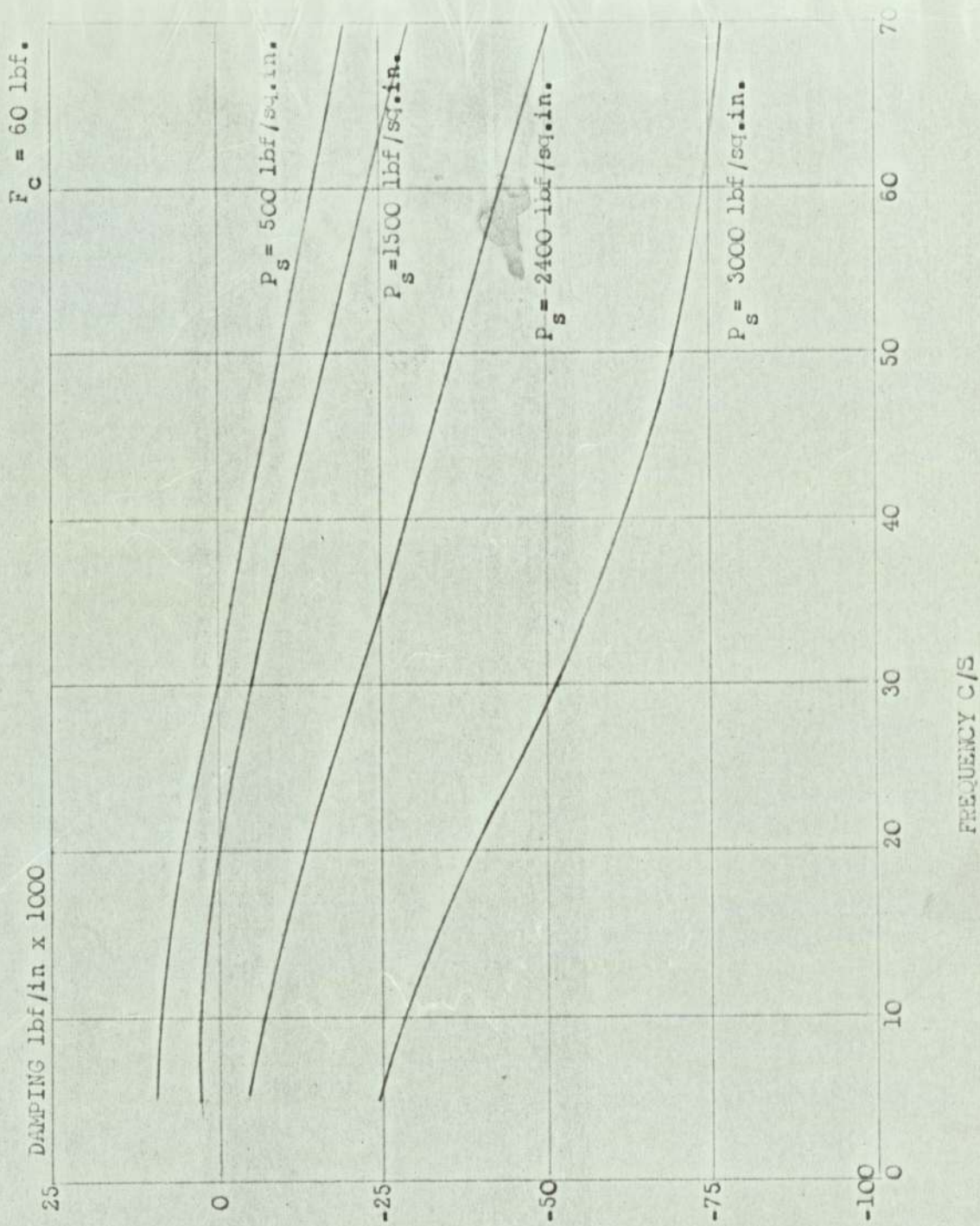
FIG. 7.17



EFFECT OF SUPPLY PRESURE ON STIFFNESS

STATIC VALVE OPENING = .015 in. PERTURBATION AMPLITUDE =  $\pm$  .005 in.

FIG.7.18

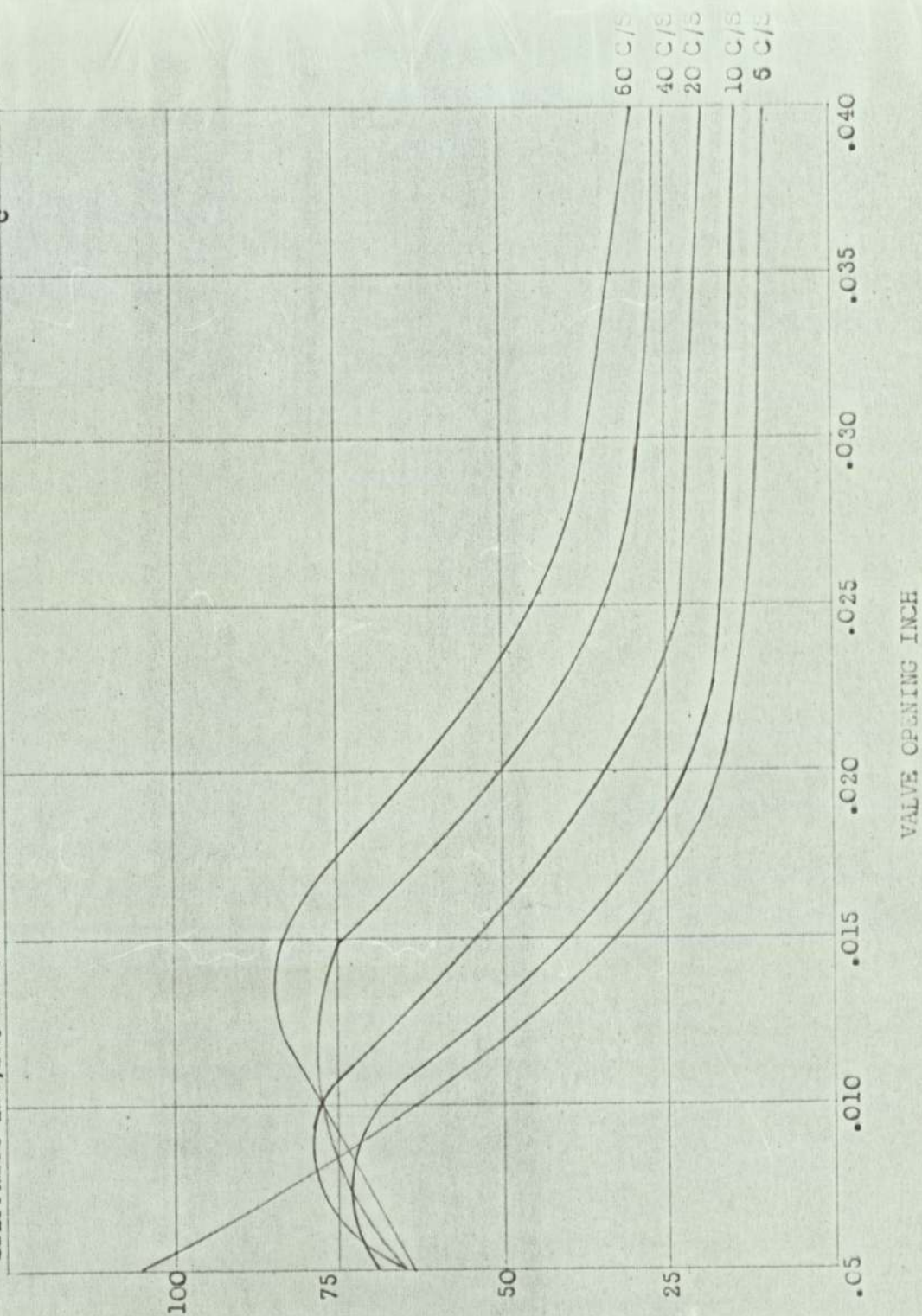


EFFECT OF SUPPLY PRESSURE ON DAMPING

STATIC VALVE OPENING = .015 in. PERTURBATION AMPLITUDE =  $\pm$  .005 in.

$F_c = 60 \text{ lbf.}$

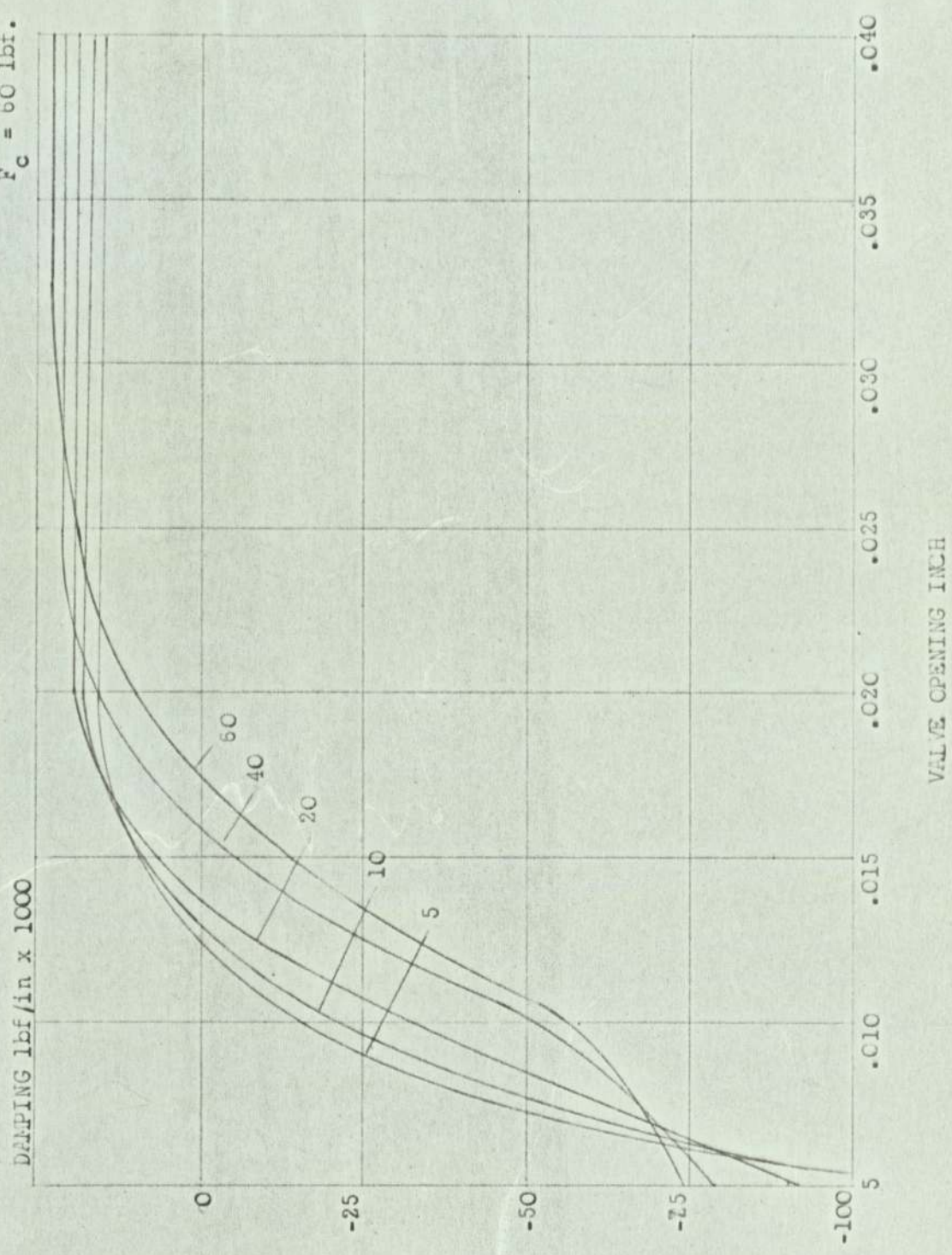
STIFFNESS lbf/in. x 1000



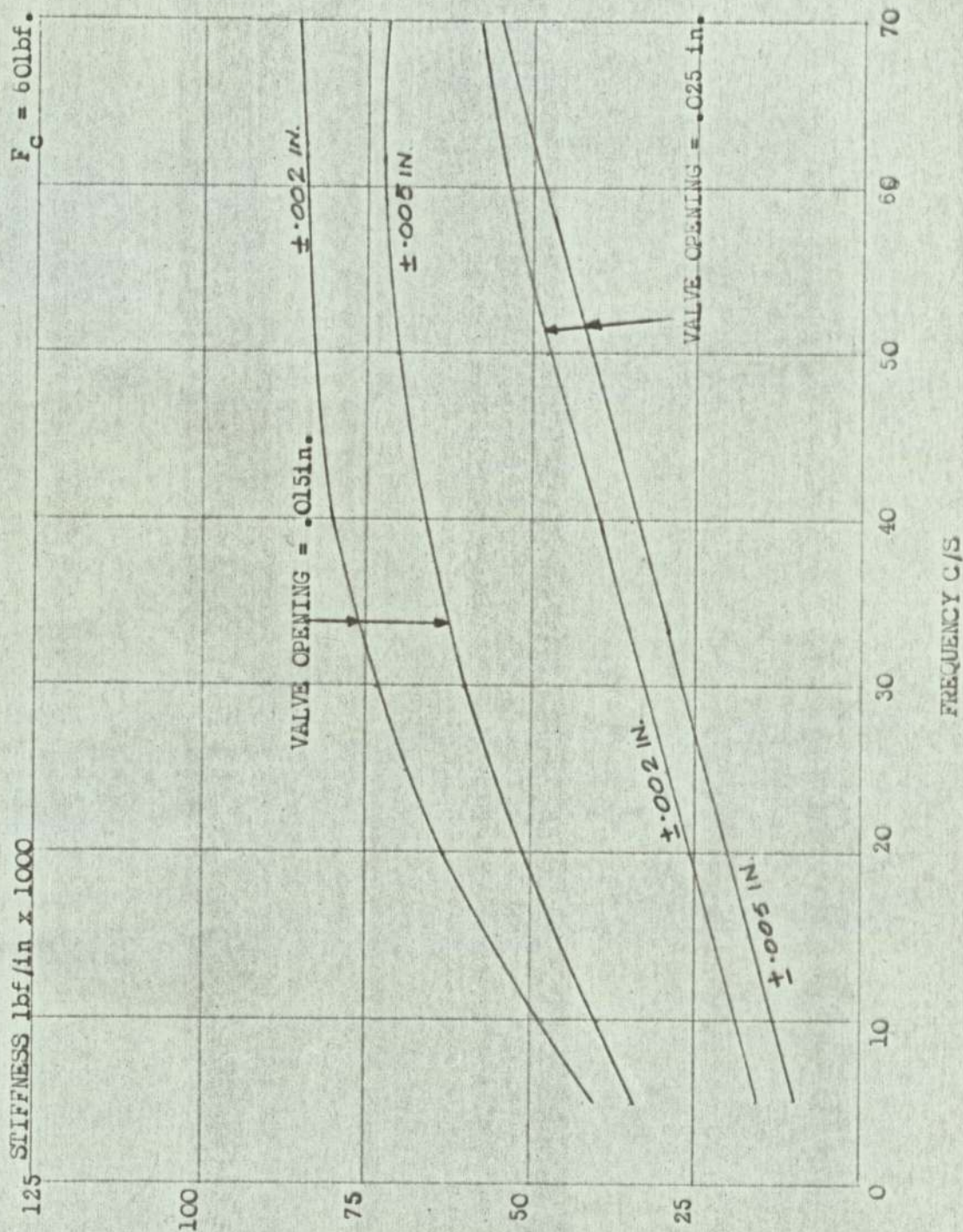
EFFECT OF STATIC VALVE OPENING ON STIFFNESS

PERTURBATION AMPLITUDE =  $\pm .003 \text{ in.}$

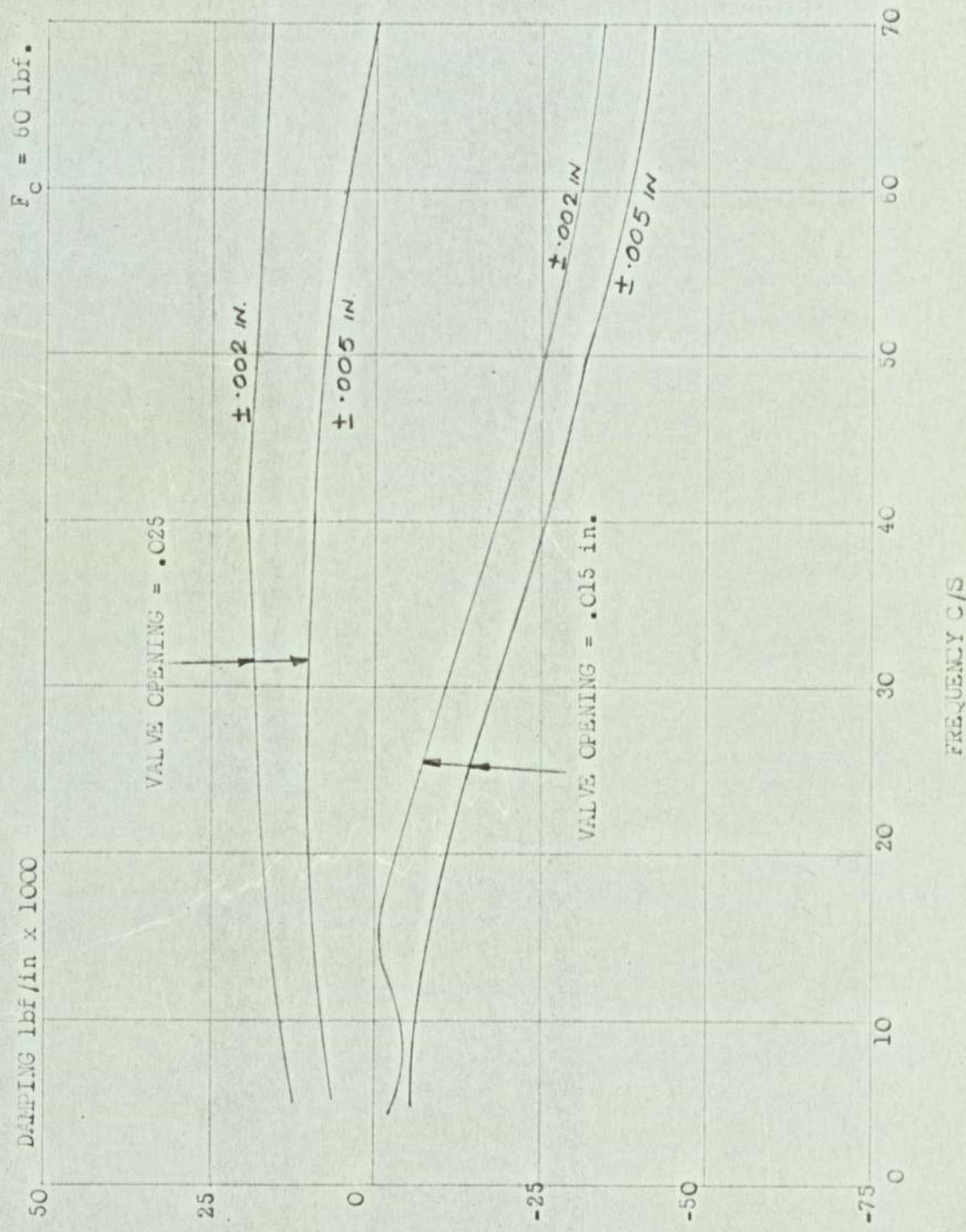
$F_c = 60 \text{ lbf.}$



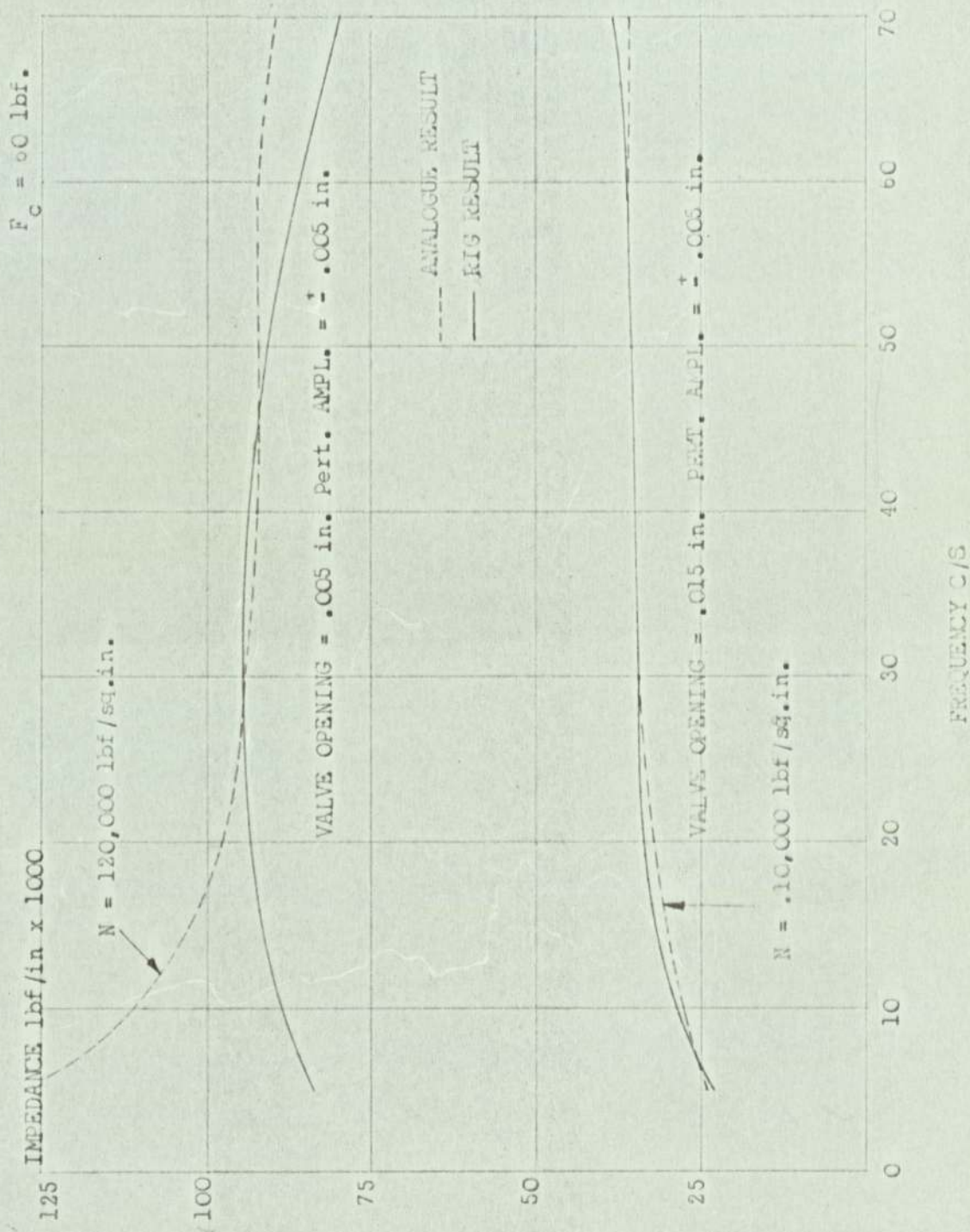
EFFECT OF STATIC VALVE OPENING ON DAMPING  
PERTURBATION AMPLITUDE =  $\pm .003 \text{ in.}$



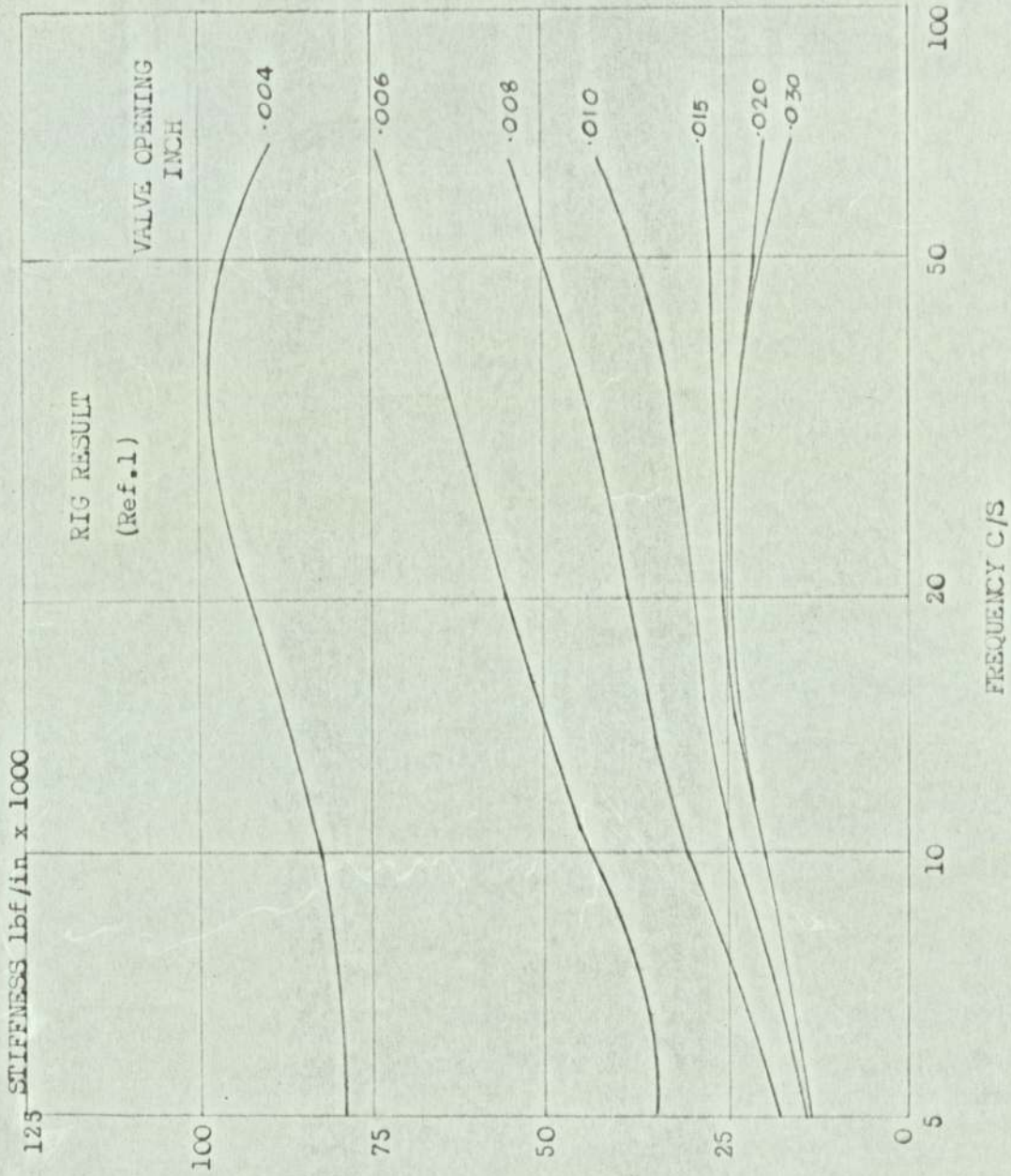
EFFECT OF PERTURBATION AMPLITUDE STIFFNESS.



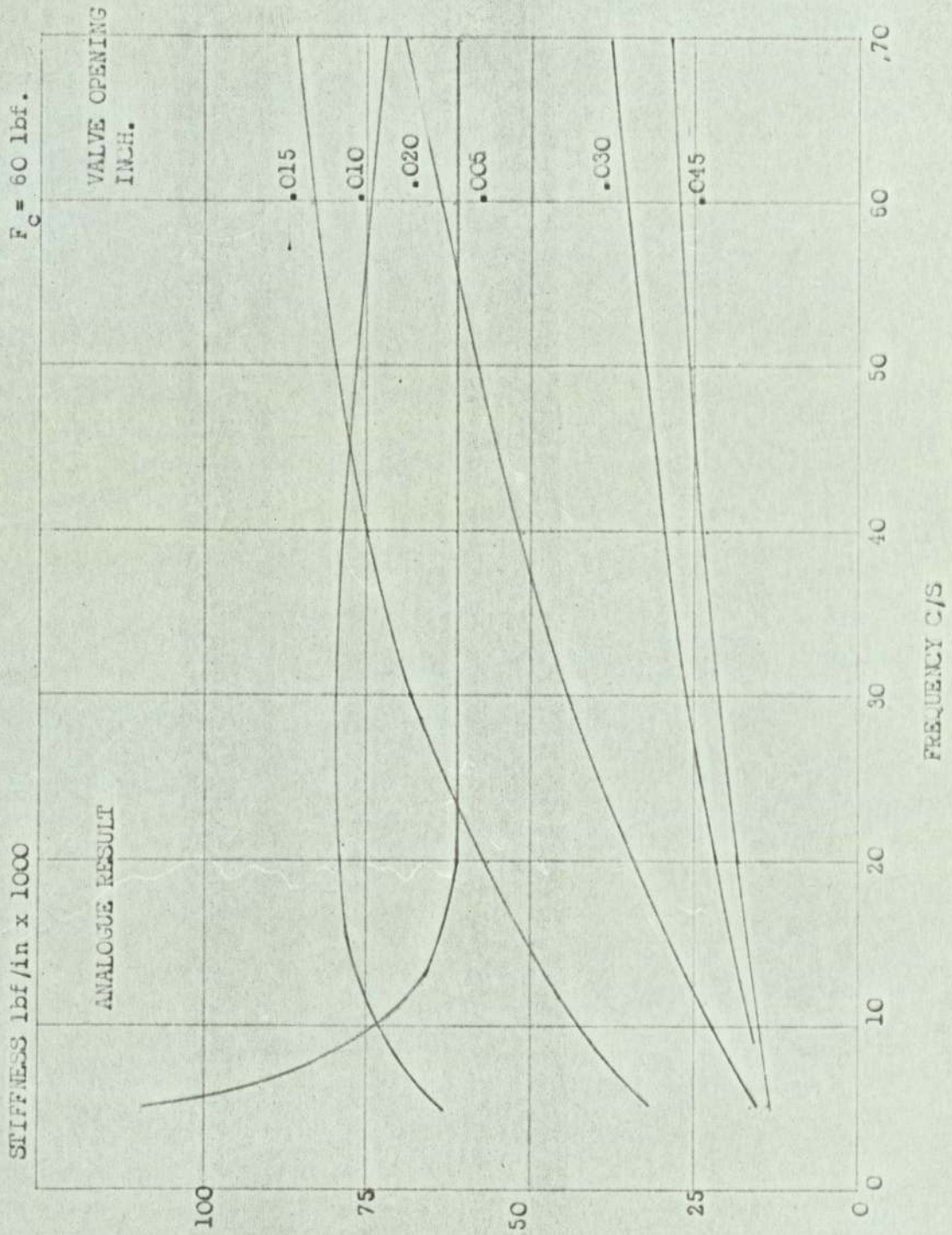
EFFECT OF PERTURBATION AMPLITUDE ON DAMPING.



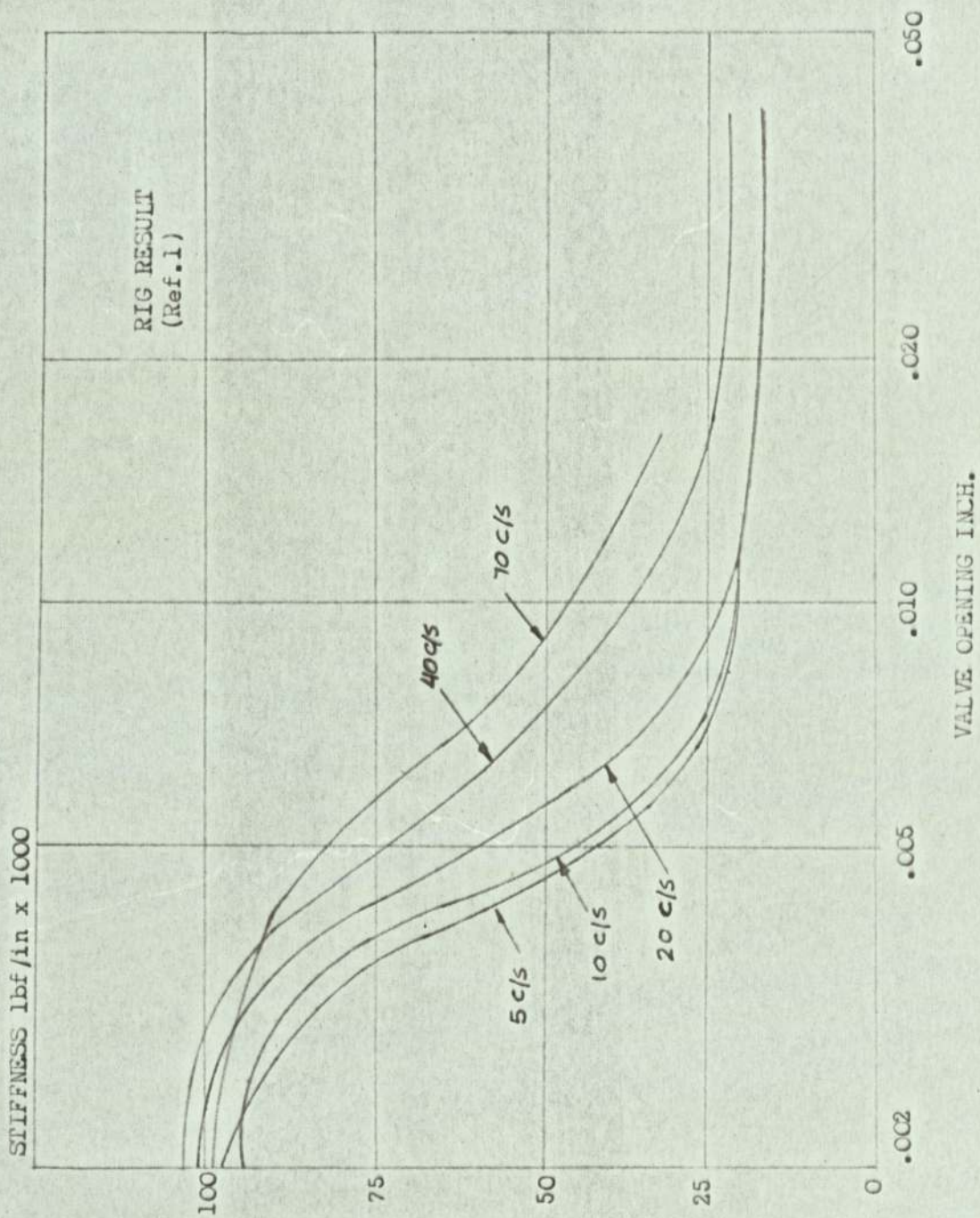
VARIATION OF IMPEDANCE WITH FREQUENCY  
COMPARISON OF ANALOGUE AND RIG RESULTS.



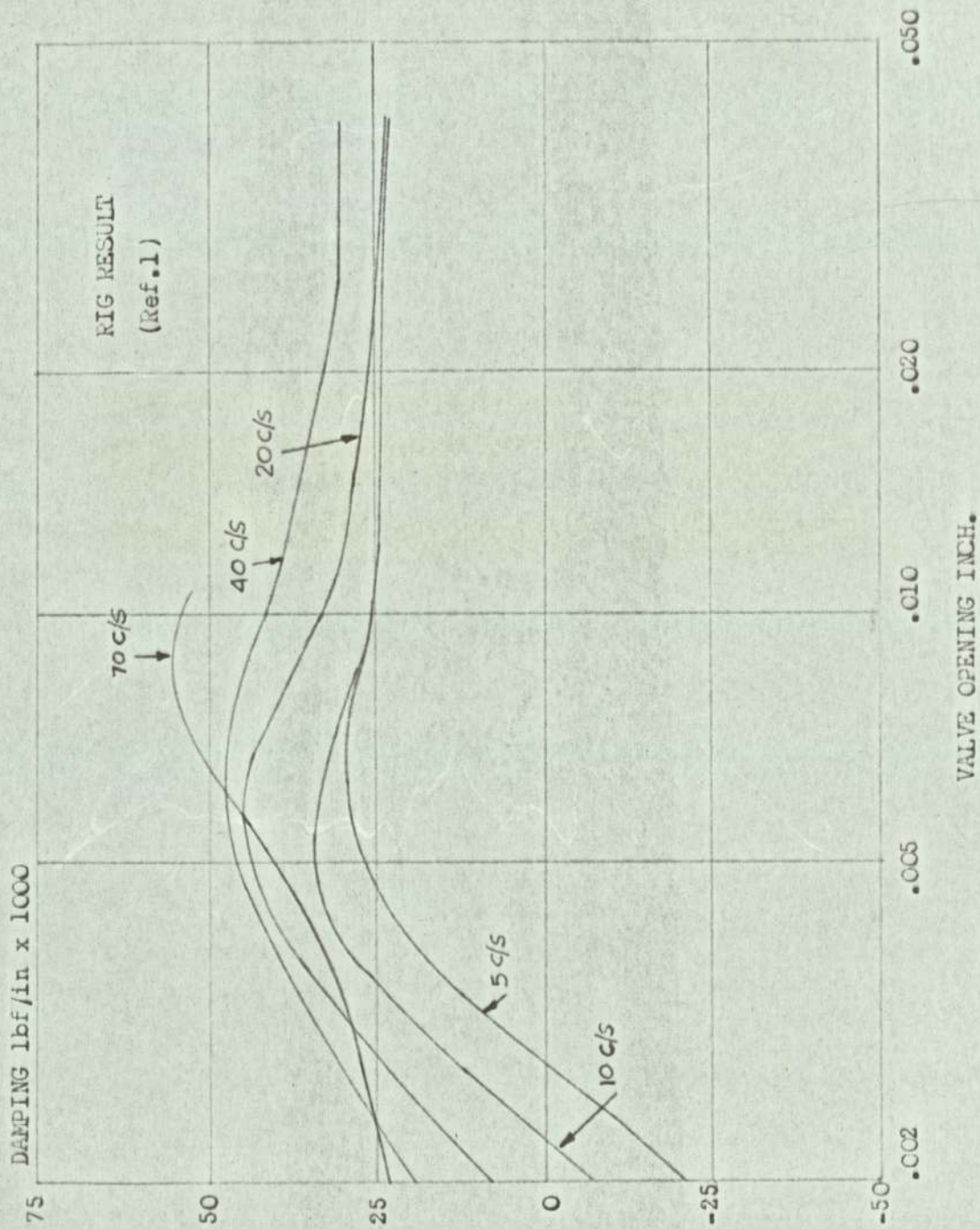
VARIATION OF STIFFNESS WITH FREQUENCY FOR CHANGES IN STATIC VALVE  
OPENING. PERTURBATION AMPLITUDE = ± .005 in.



VARIATION OF STIFFNESS WITH FREQUENCY FOR CHANGES IN  
STATIC VALVE OPENING. PERTURBATION AMPLITUDE =  $\pm .005$  in.

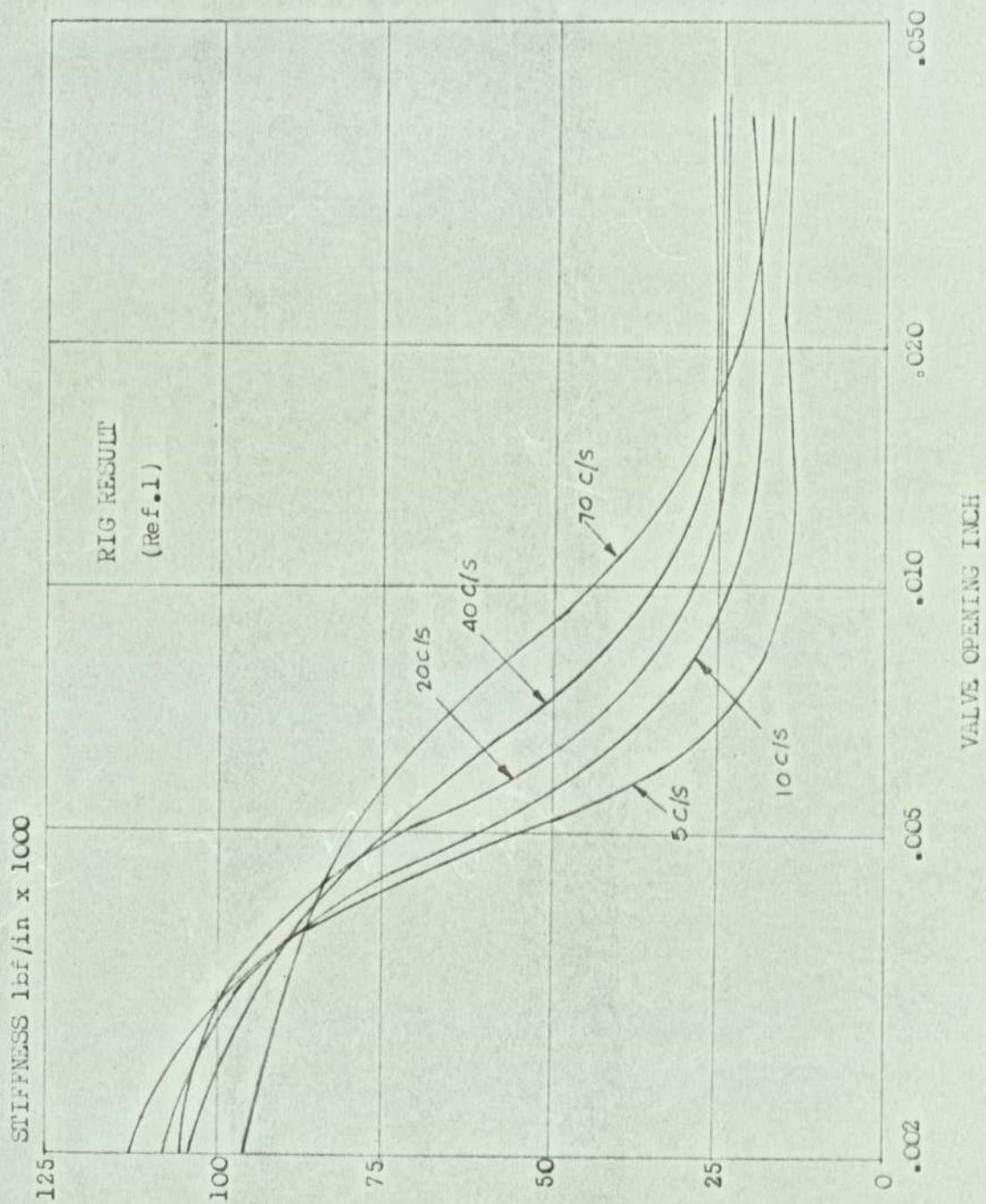


VARIATION OF STIFFNESS WITH VALVE OPENING  
PERTURBATION AMPLITUDE =  $\pm$  .002 in.

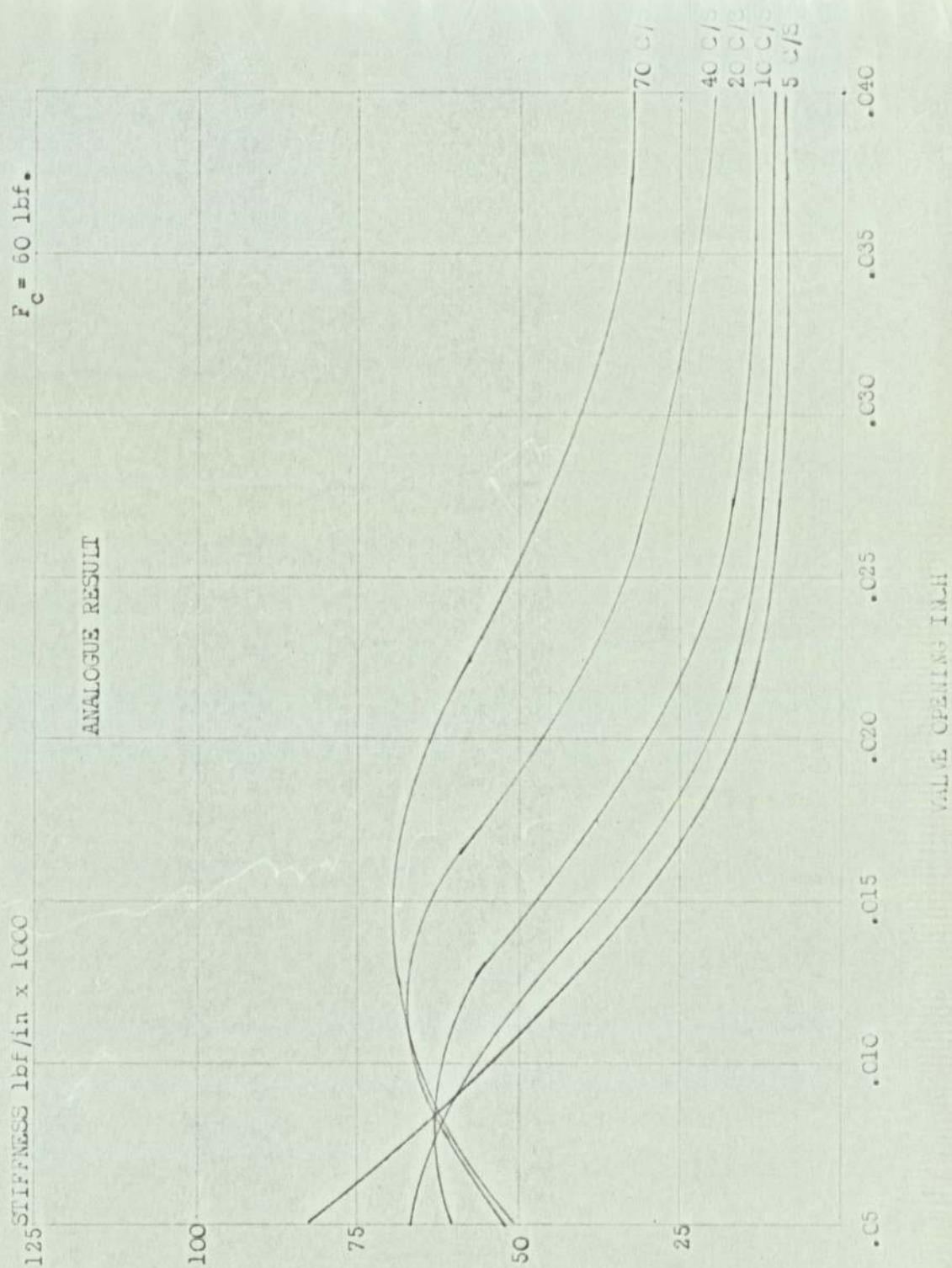


VARIATION OF DAMPING WITH STATIC VALVE OPENING

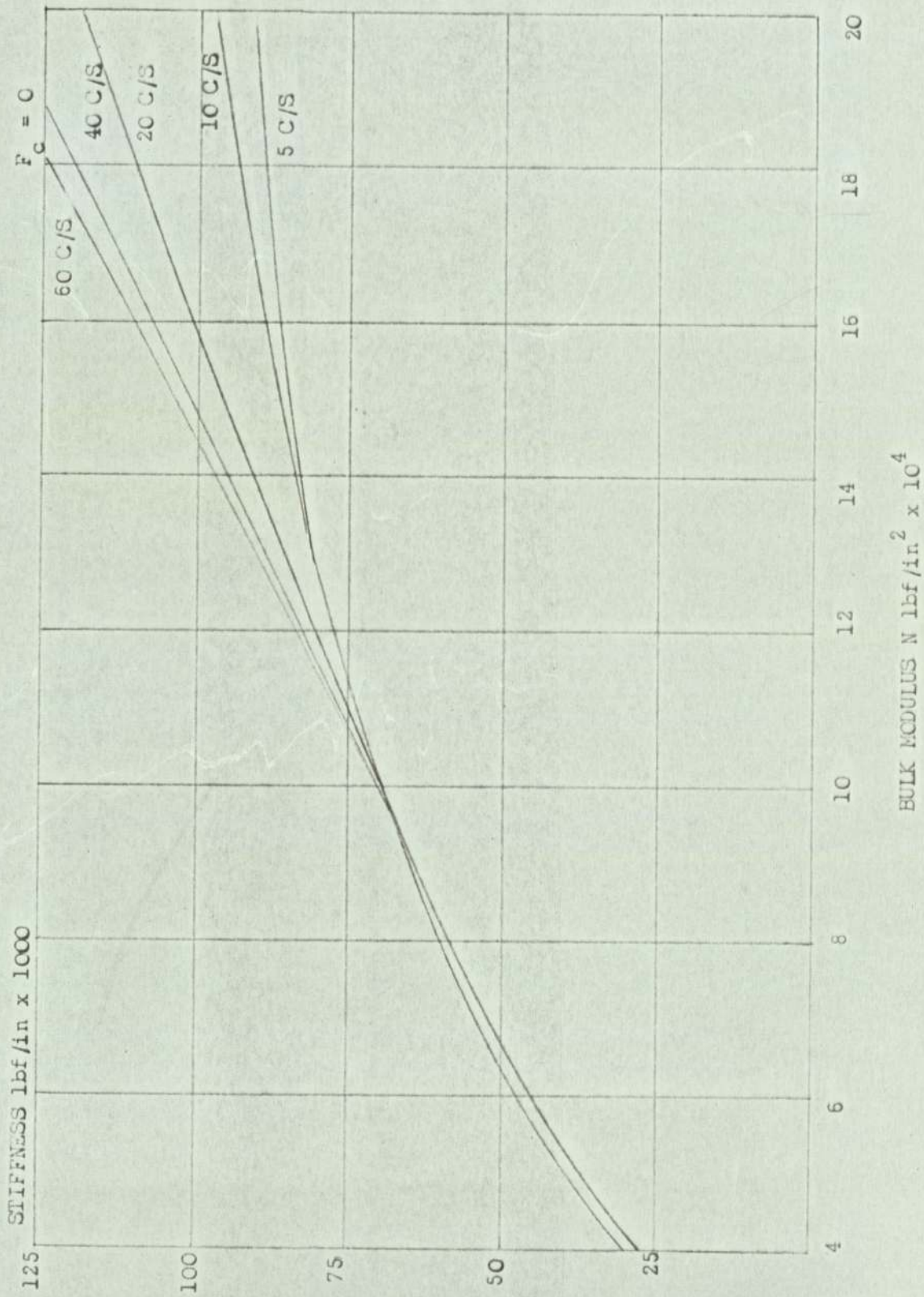
PERTURBATION AMPLITUDE =  $\pm$  .002 in.



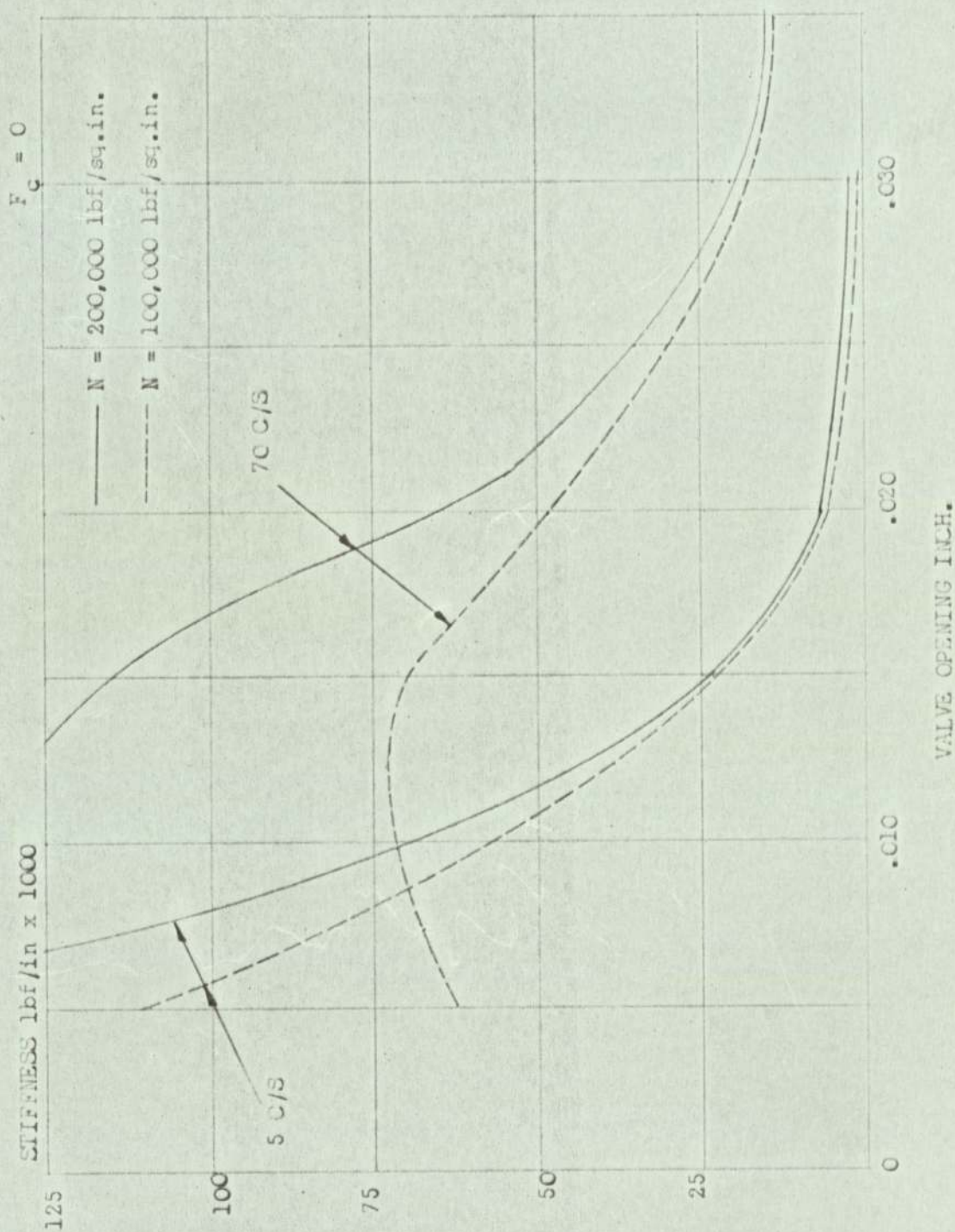
VARIATION OF STIFFNESS WITH STATIC VALVE OPENING  
 PERTURBATION AMPLITUDE =  $\pm$  .005 in.



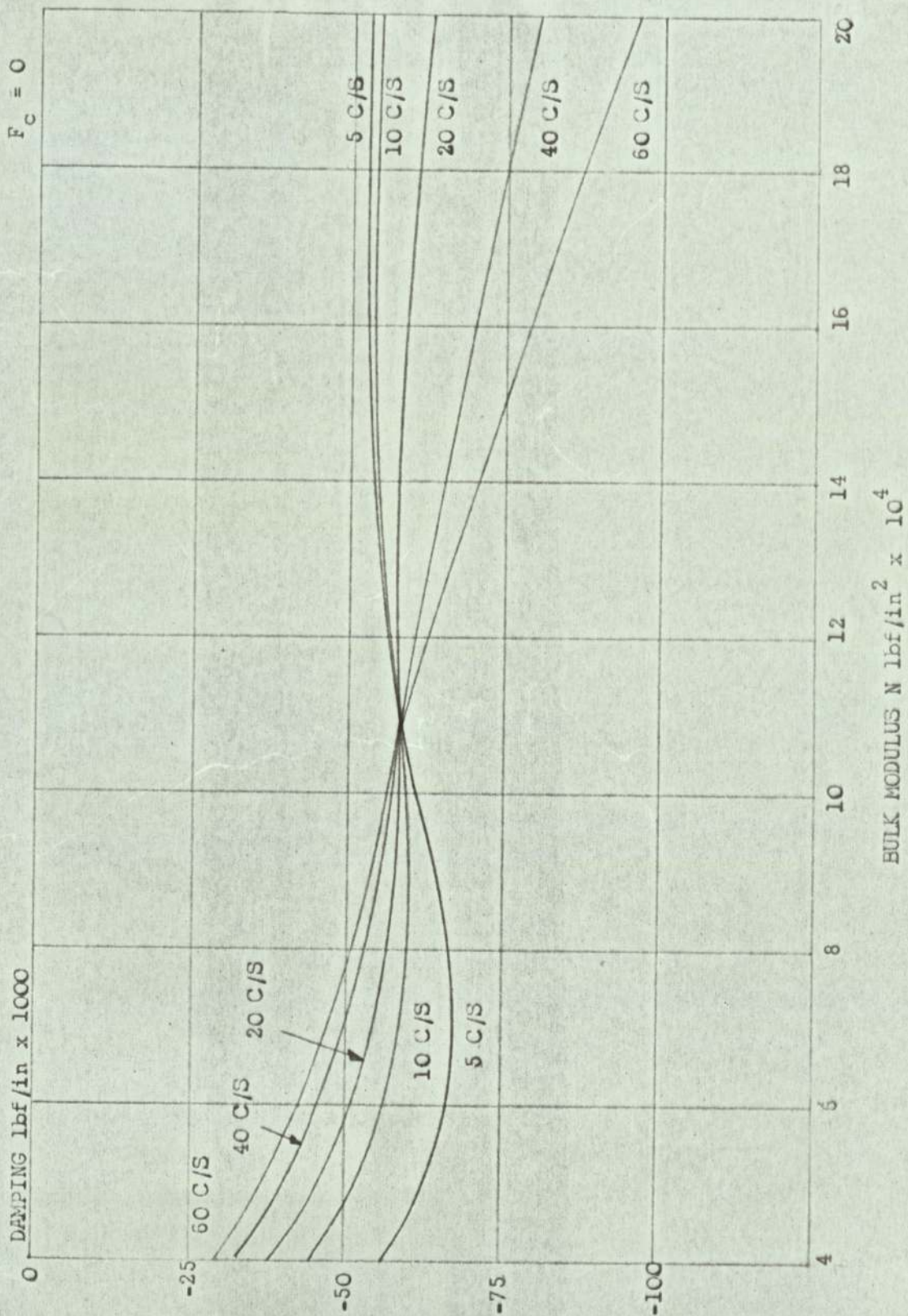
VARIATION OF STIFFNESS WITH STATIC VALVE OPENING  
PERTURBATION AMPLITUDE =  $\pm .005 \text{ in.}$



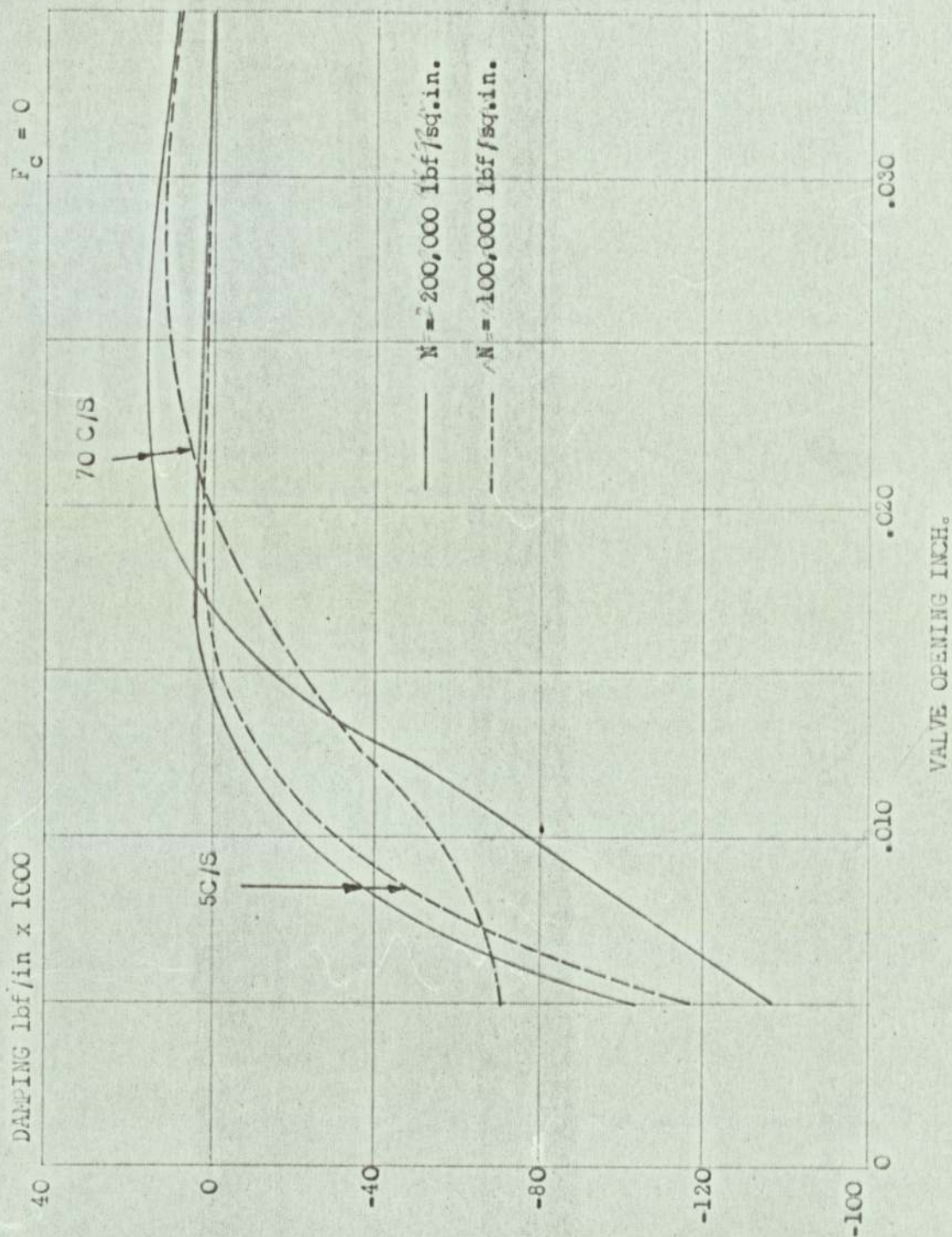
EFFECT OF BULK MODULUS ON STIFFNESS FOR CHANGES IN FREQUENCY. VALVE OPENING = .010 in. PERTURBATION AMPLITUDE = .005 in.



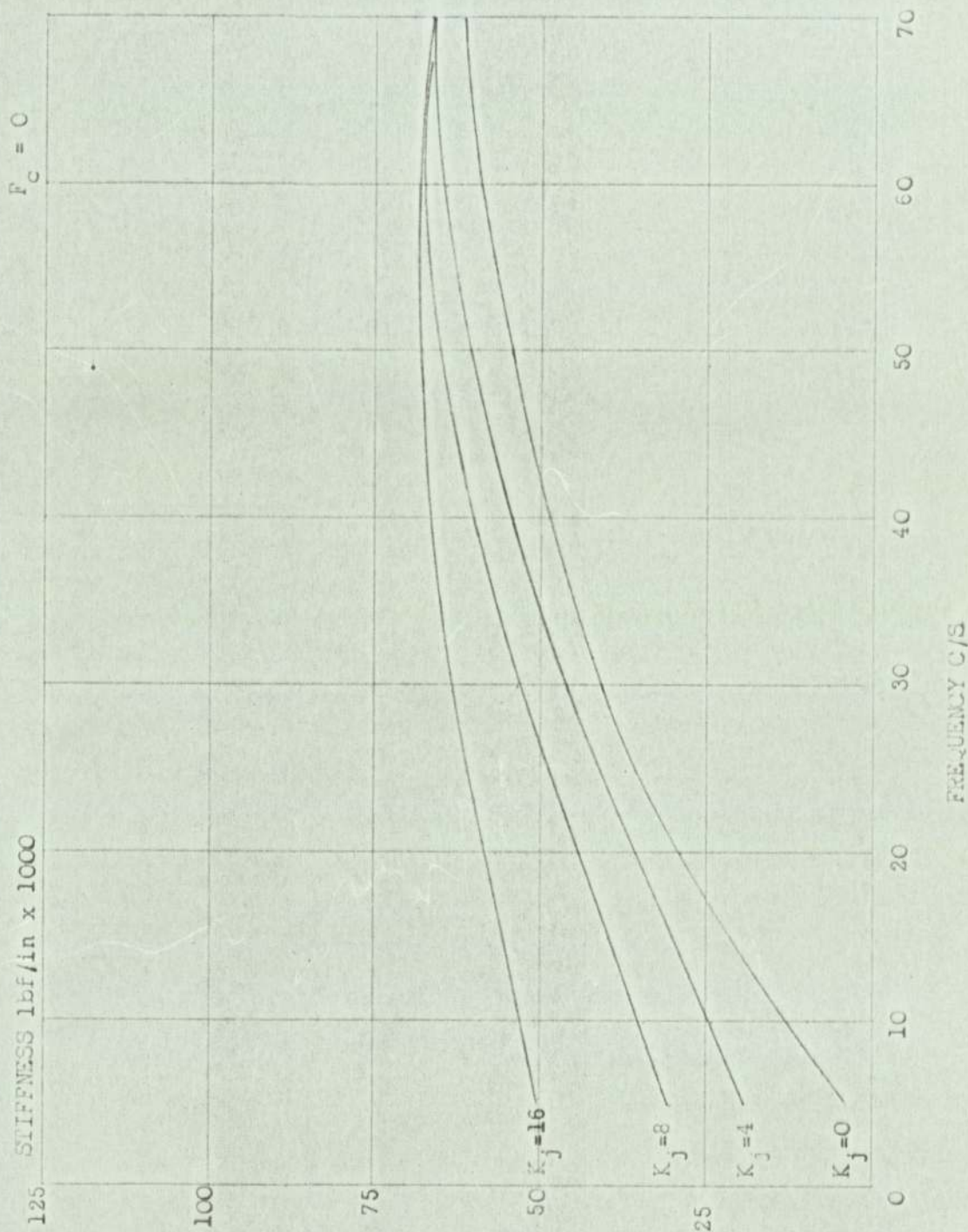
EFFECT OF BULK MODULUS ON STIFFNESS FOR CHANGES IN STATIC VALVE OPENING. PERTURBATION AMPLITUDE =  $\pm .003$  in.



EFFECT OF BULK MODULUS ON DAMPING FOR CHANGES IN FREQUENCY. VALVE OPENING = .010in. PERTURBATION AMPLITUDE =  $\pm .005$ in.



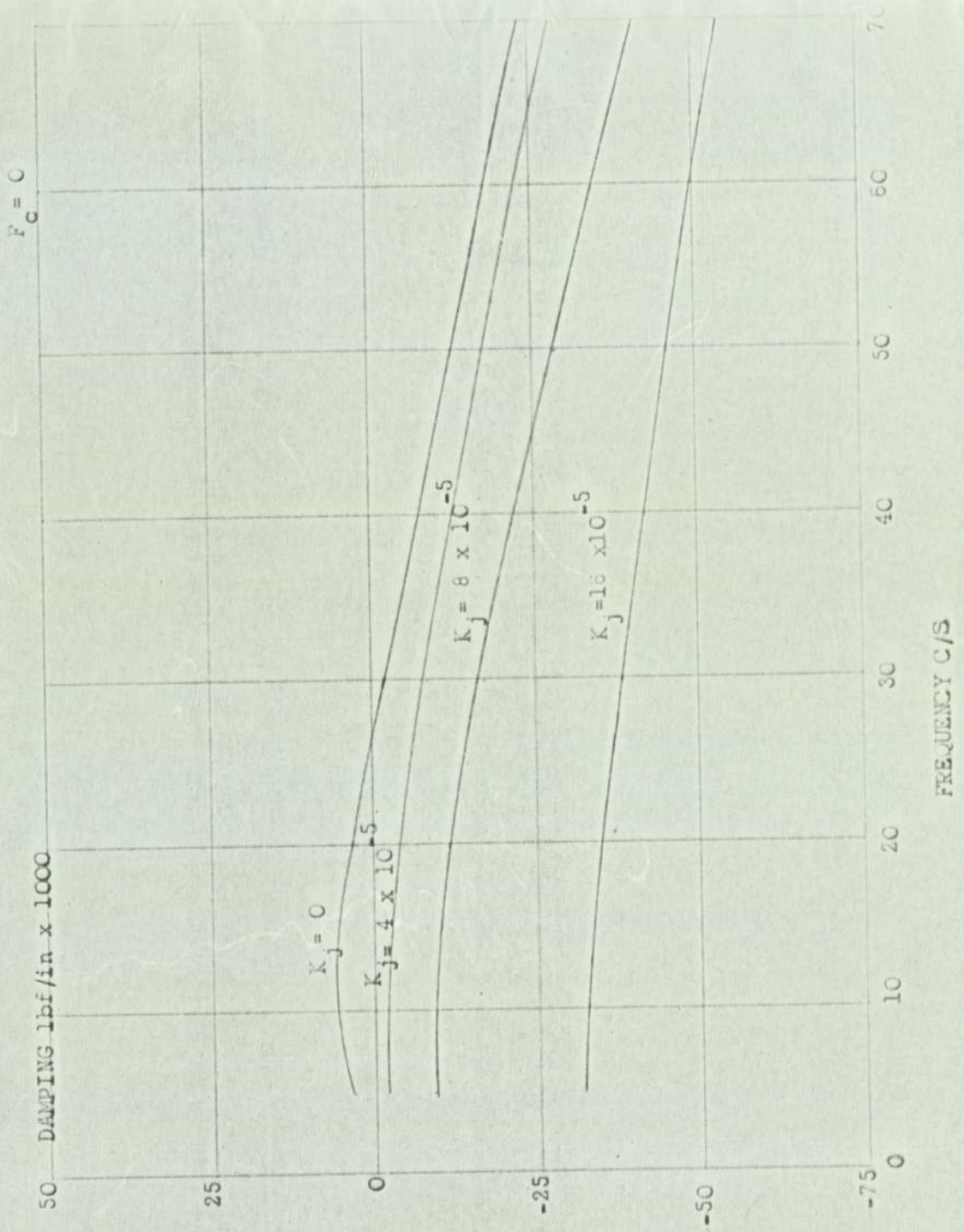
EFFECT OF BULK MODULUS ON DAMPING FOR CHANGES IN  
 STATIC VALVE OPENING. PERTURBATION AMPLITUDE =  $\pm .003$  in.



EFFECT OF LEAKAGE ON STIFFNESS STATIC VALVE OPENING = .015 in.

PERTURBATION AMPLITUDE =  $\pm$  .005 in.

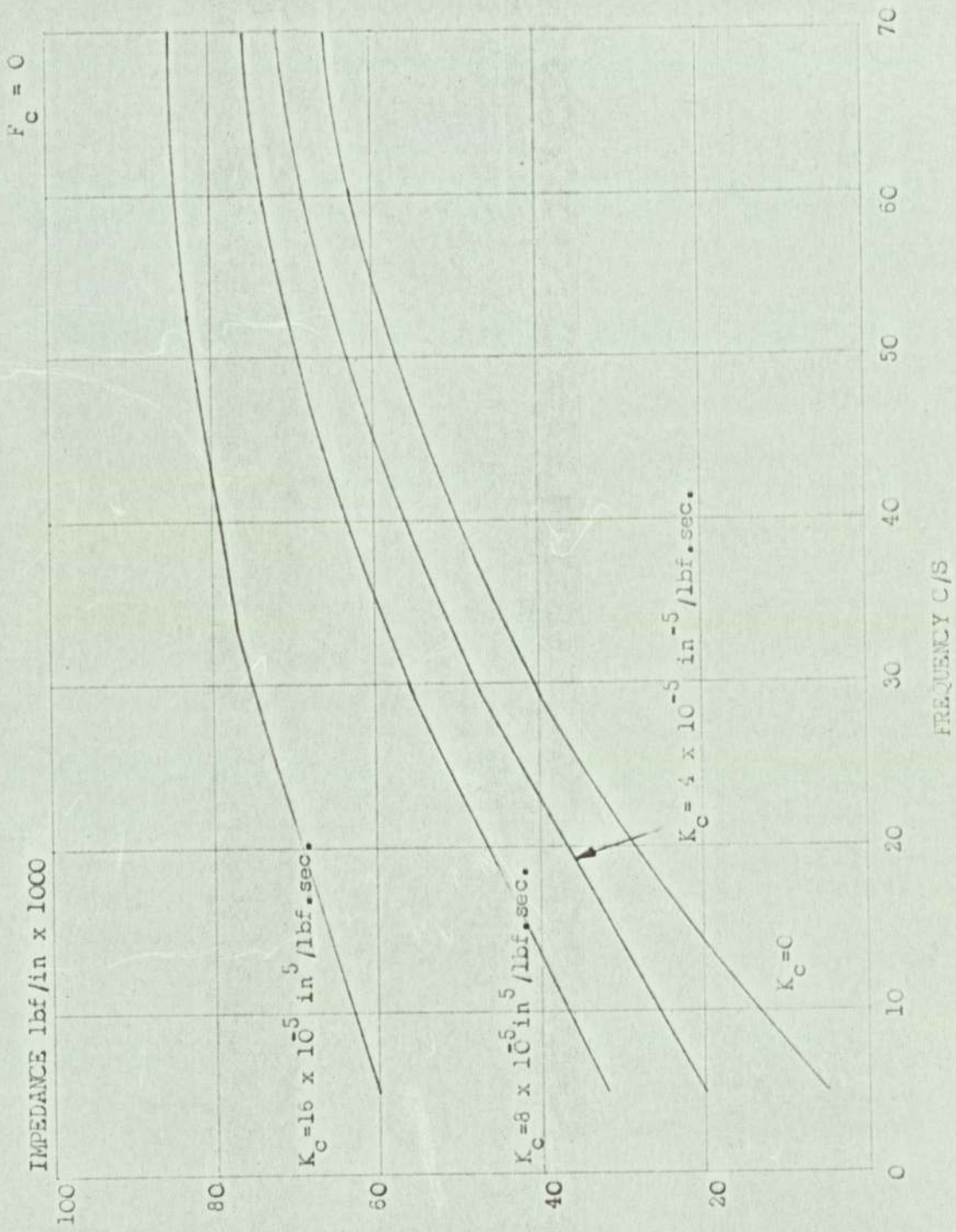
FIG.7.35



EFFECT OF LEAKAGE ON DAMPING. STATIC VALVE OPENING = .015 in.

PERTURBATION AMPLITUDE  $\bar{v} = \pm .005$  in.

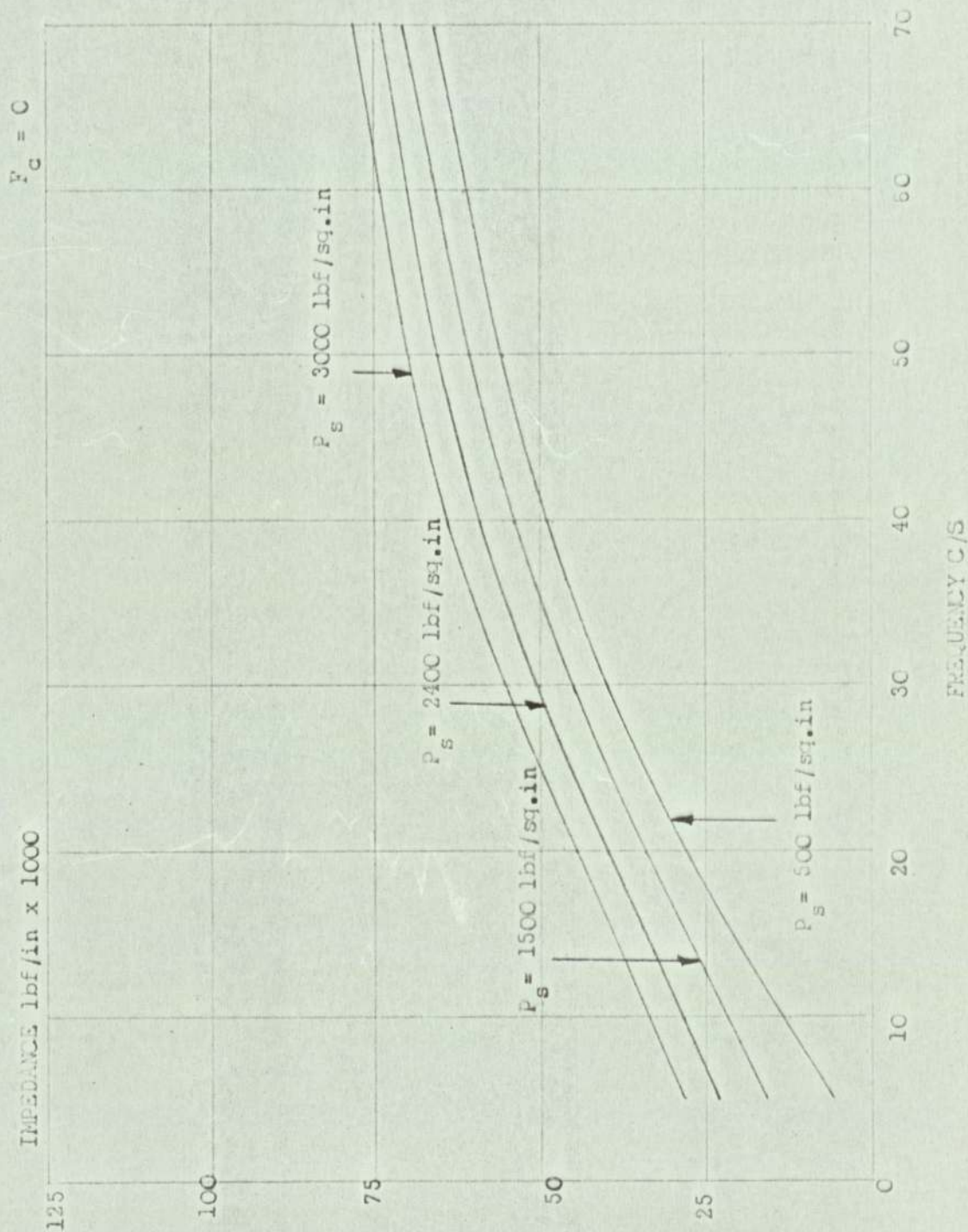
FIG.7.36



EFFECT OF LEAKAGE ON IMPEDANCE. STATIC VALVE OPENING = .015 in.

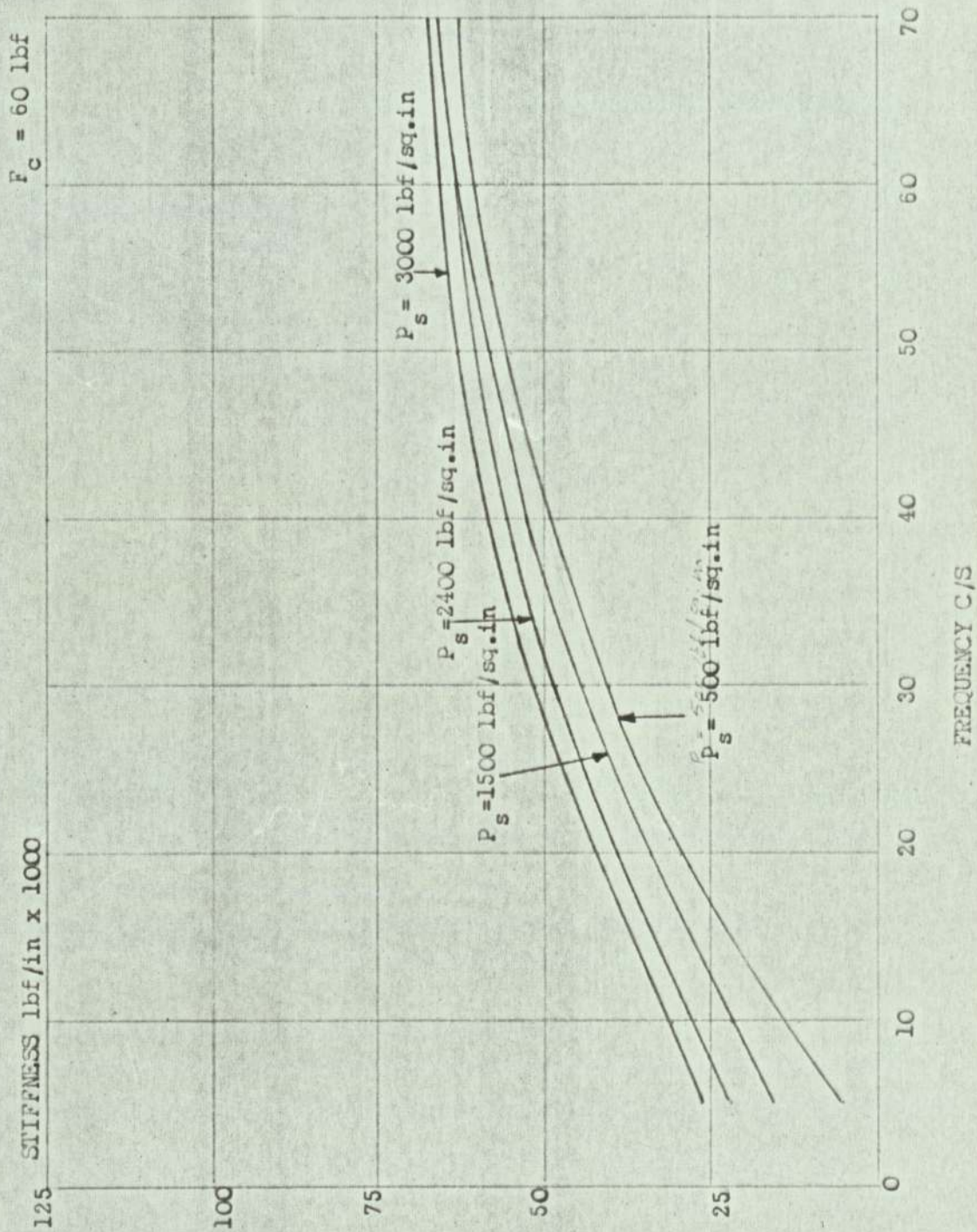
PERTURBATION AMPLITUDE =  $\pm$  .005 in.

FIG.7.37



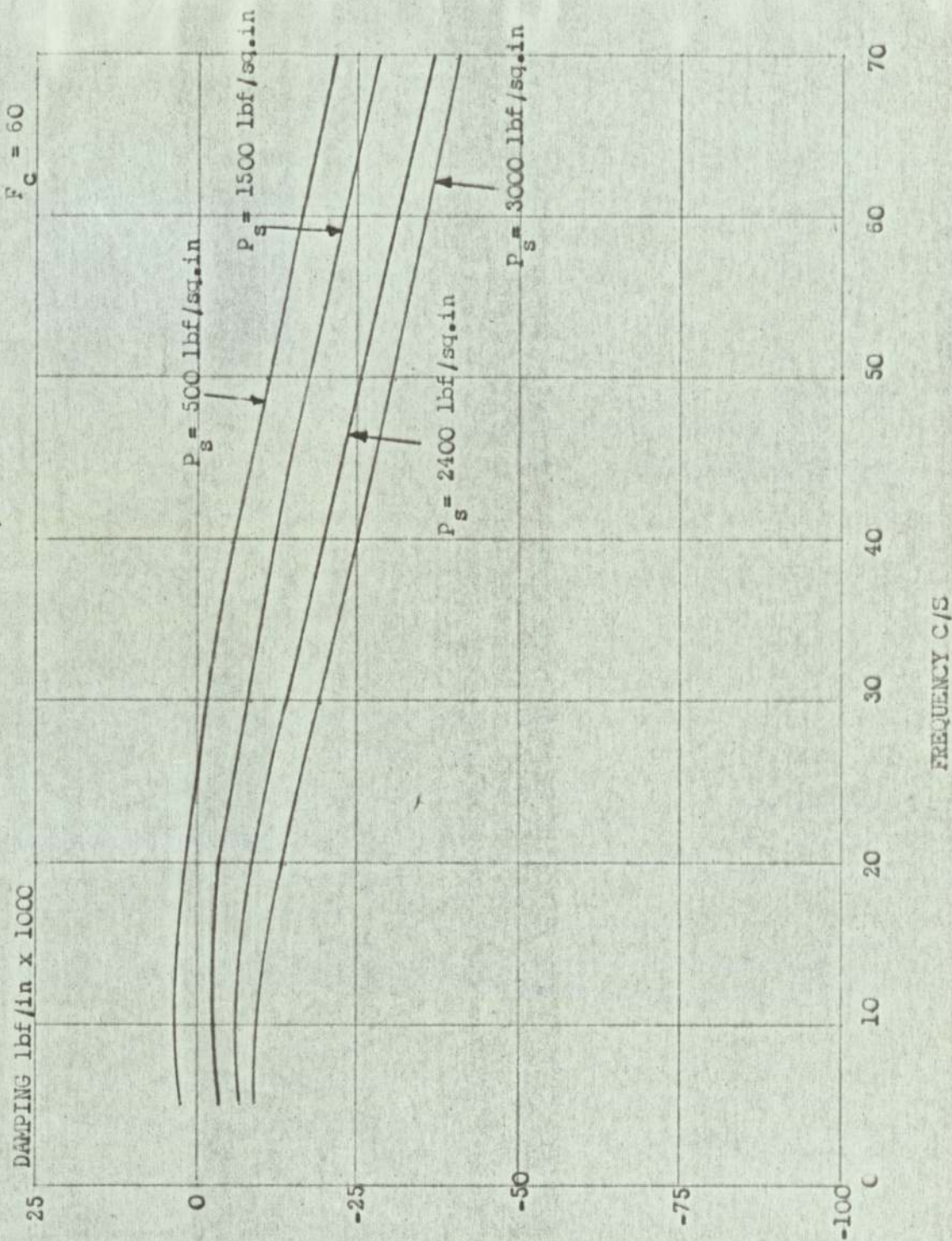
EFFECT OF SUPPLY PRESSURE ON IMPEDANCE

STATIC VALVE OPENING = .015 in. PERTURBATION AMPLITUDE = ± .005in.



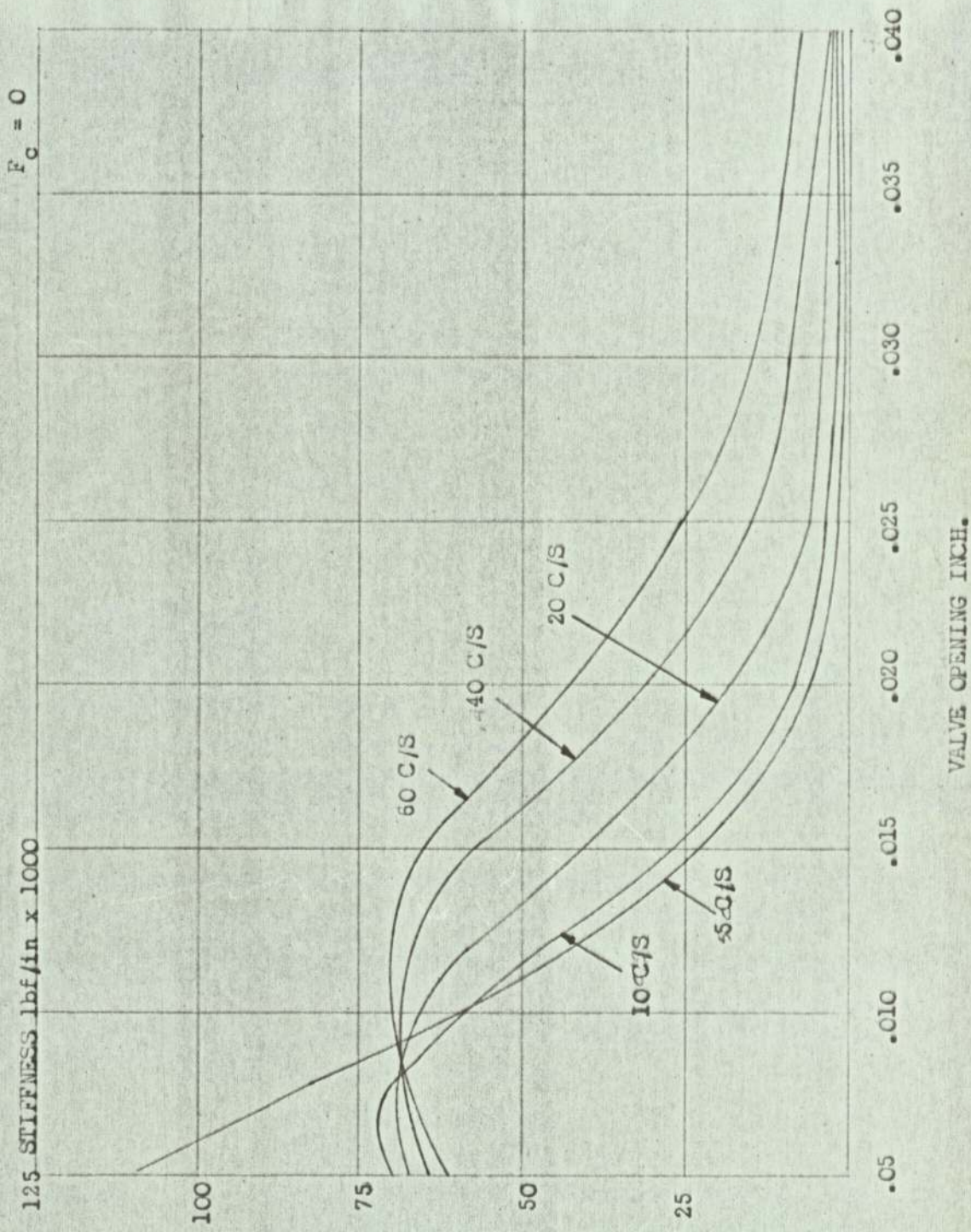
EFFECT OF SUPPLY PRESSURE ON STIFFNESS

STATIC VALVE OPENING = .015in. PERTURBATION AMPLITUDE =  $\pm$  .005in.



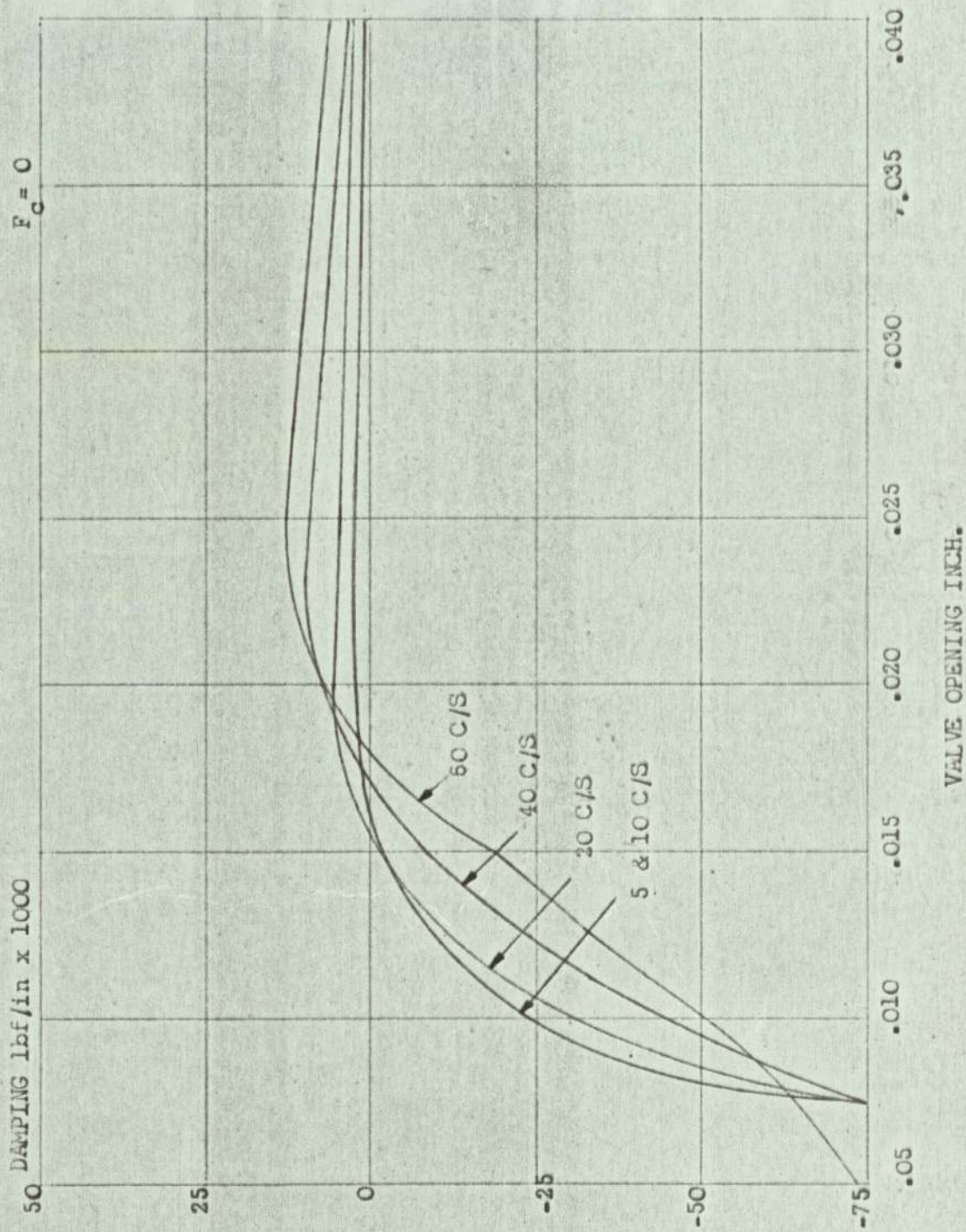
EFFECT OF SUPPLY PRESSURE ON DAMPING

STATIC VALVE OPENING = .015 in. PERTURBATION AMPLITUDE =  $\pm .005$  in.



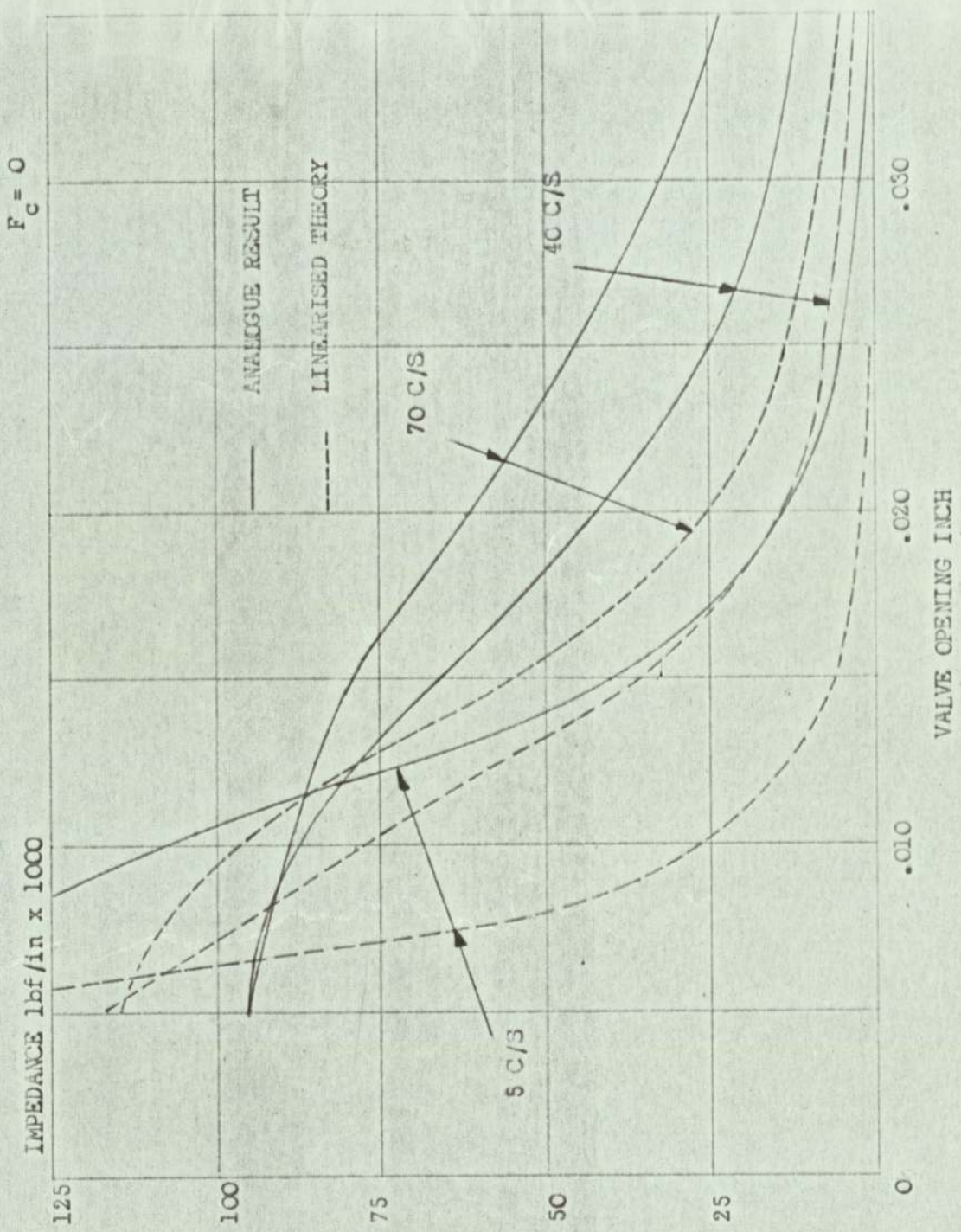
EFFECT OF STATIC VALVE OPENING ON STIFFNESS

PERTURBATION AMPLITUDE = ± .003in.

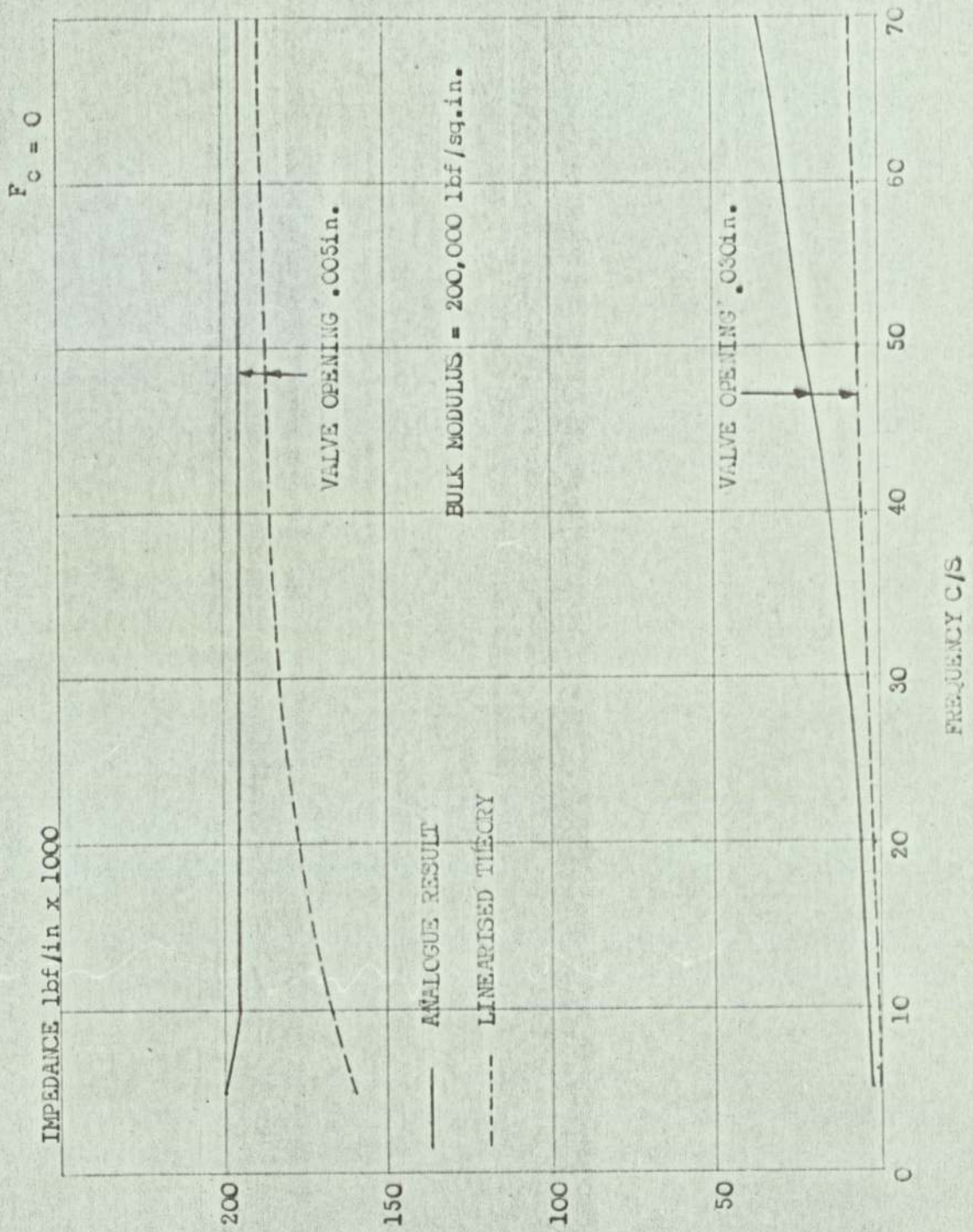


EFFECT OF STATIC VALVE OPENING ON DAMPING

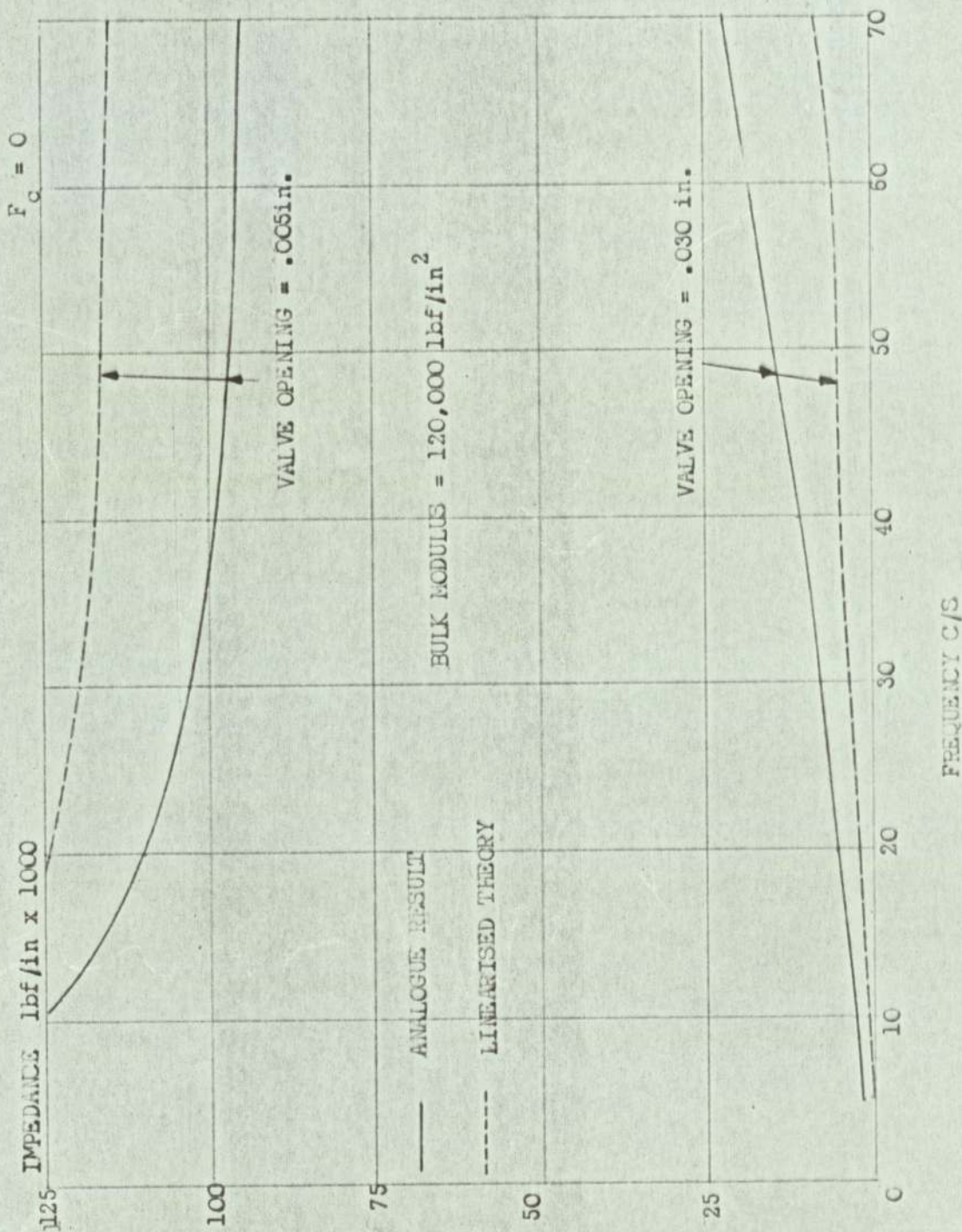
PERTURBATION AMPLITUDE =  $\pm .003$  in.



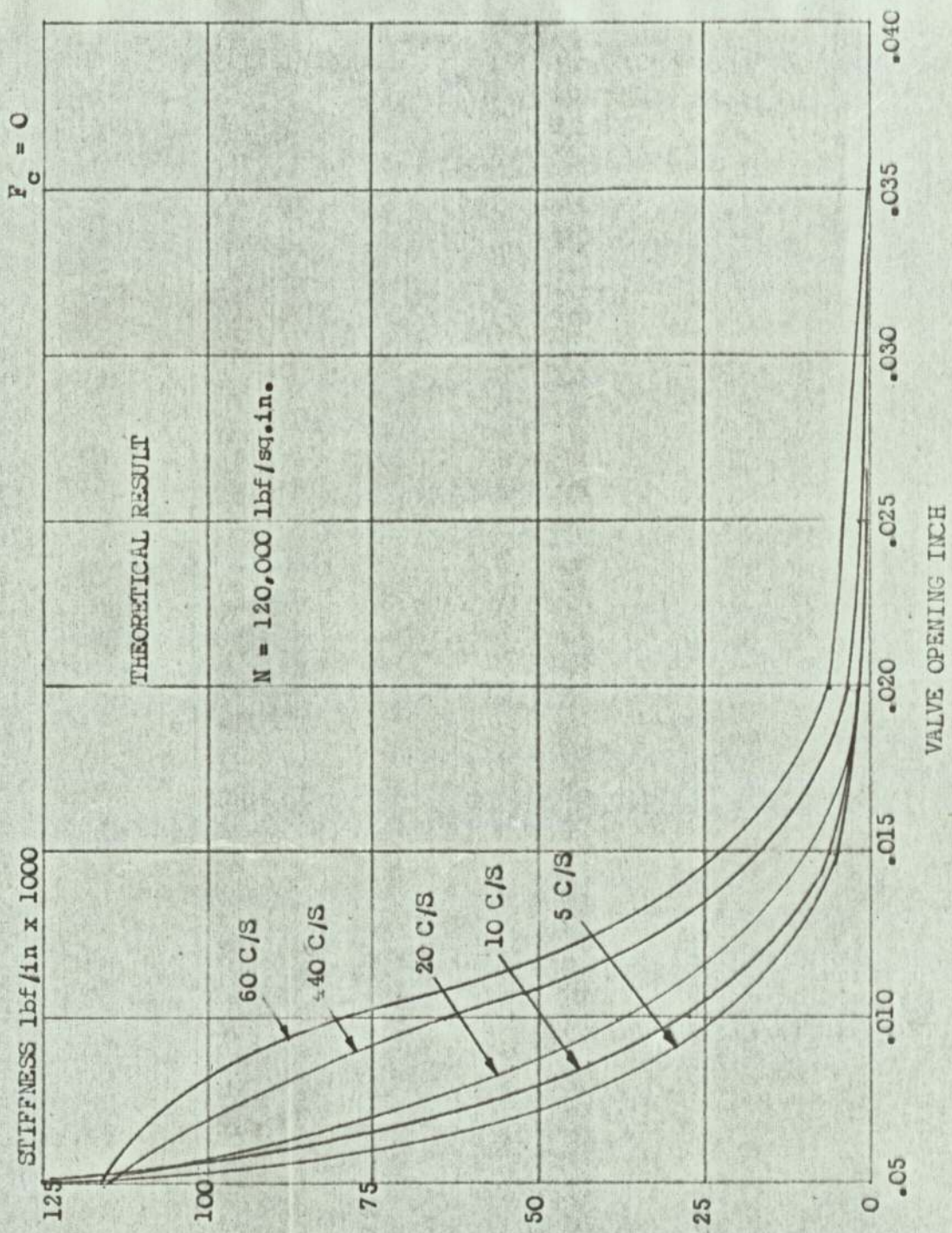
EFFECT OF STATIC VALVE OPENING ON IMPEDANCE  
COMPARISON OF ANALOGUE AND THEORETICAL RESULT.



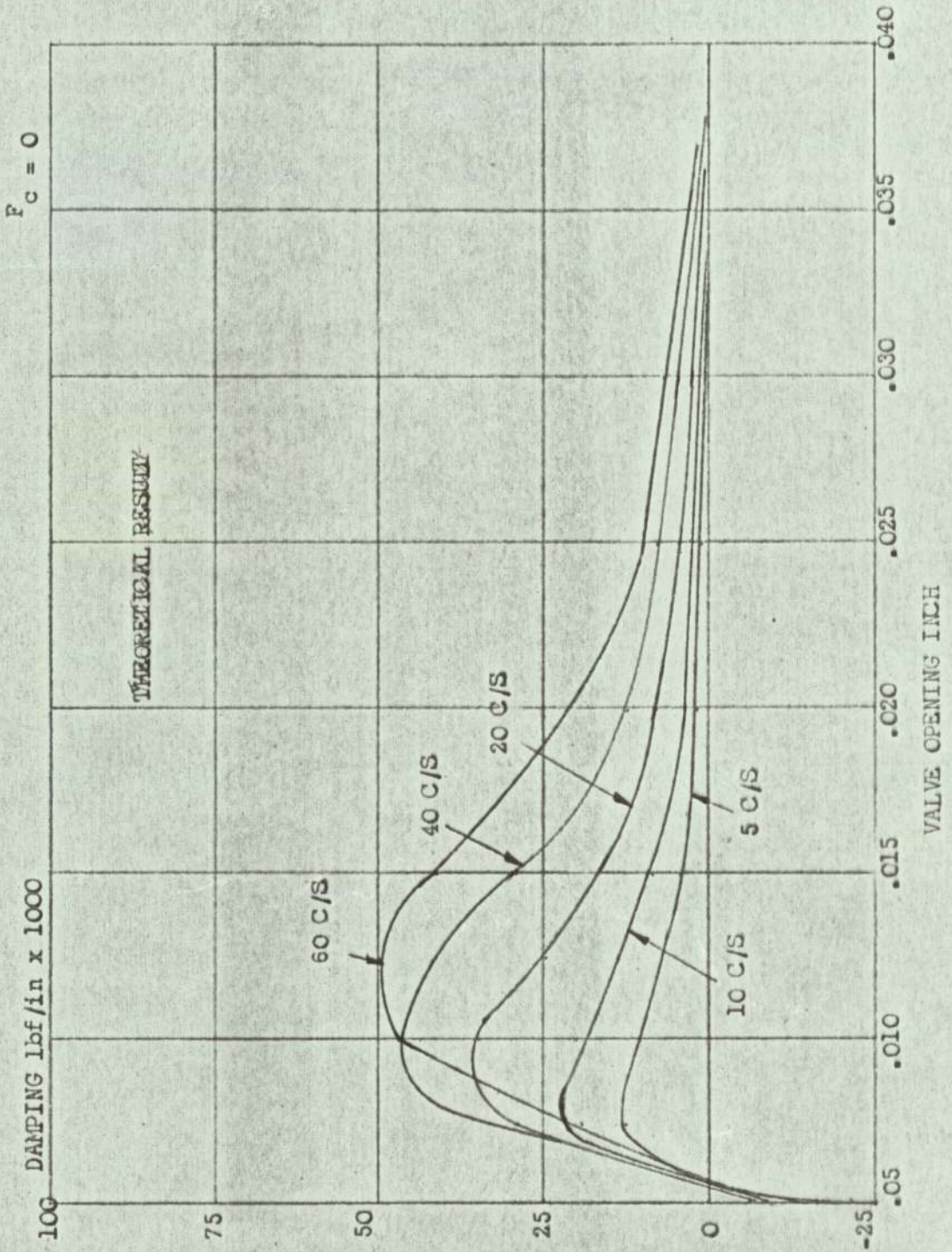
VARIATION OF IMPEDANCE WITH FREQUENCY AND VALVE OPENING  
COMPARISON OF ANALOGUE AND THEORETICAL RESULTS.



VARIATION OF IMPEDANCE WITH FREQUENCY AND VALVE OPENING  
COMPARISON OF ANALOGUE AND THEORETICAL RESULTS.

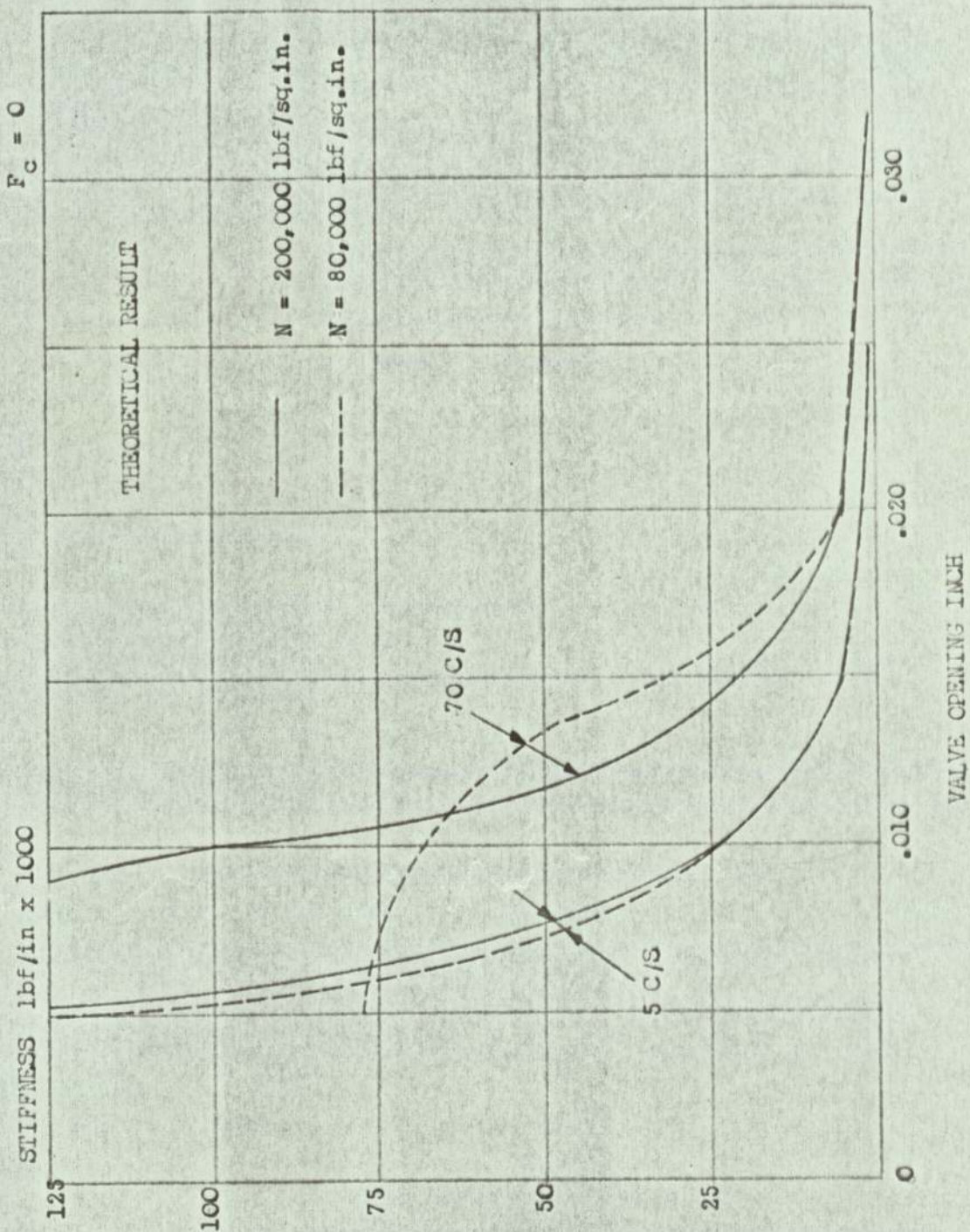


EFFECT OF STATIC VALVE OPENING ON STIFFNESS  
PERTURBATION AMPLITUDE<sup>+</sup> .005in.

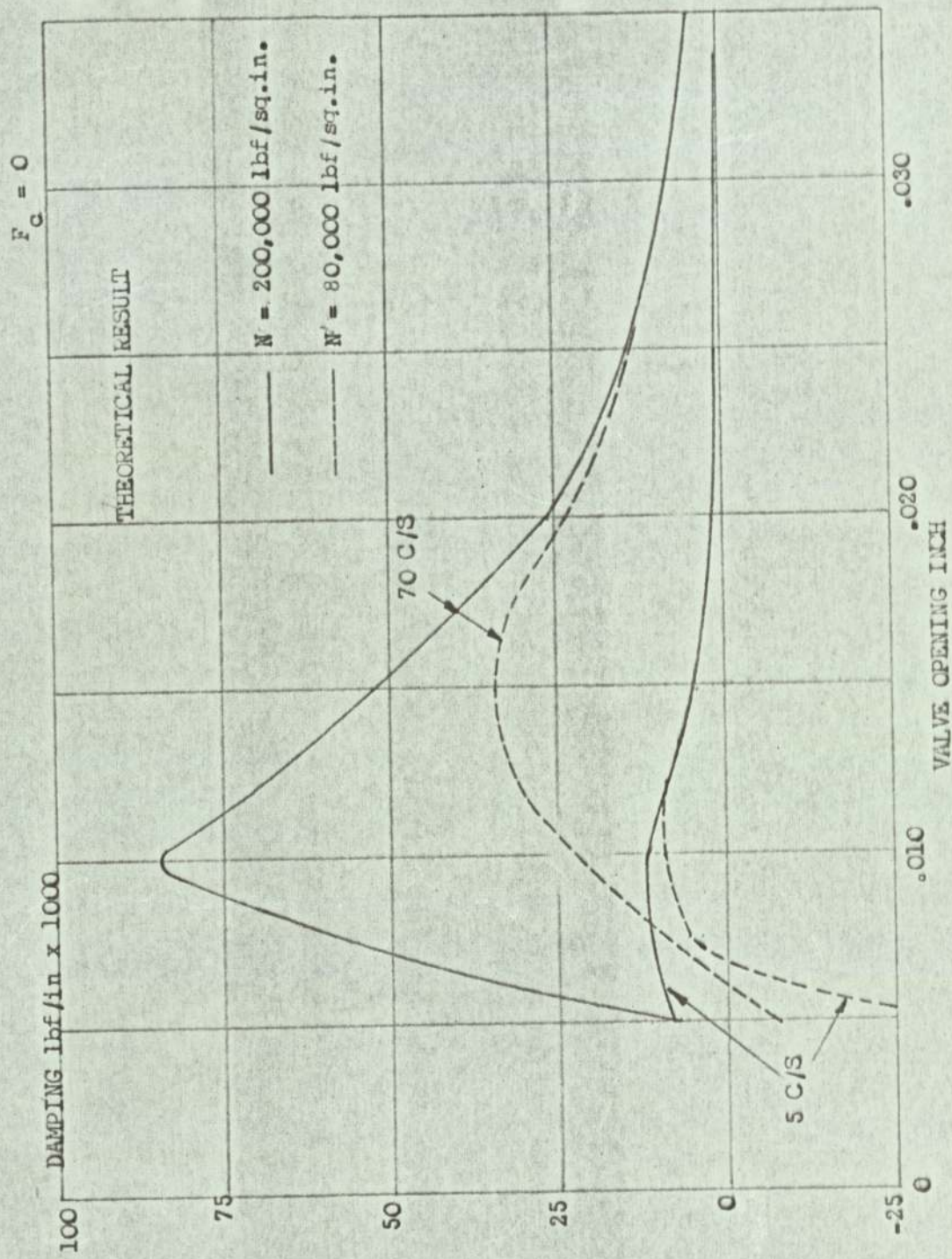


EFFECT OF STATIC VALVE OPENING ON DAMPING

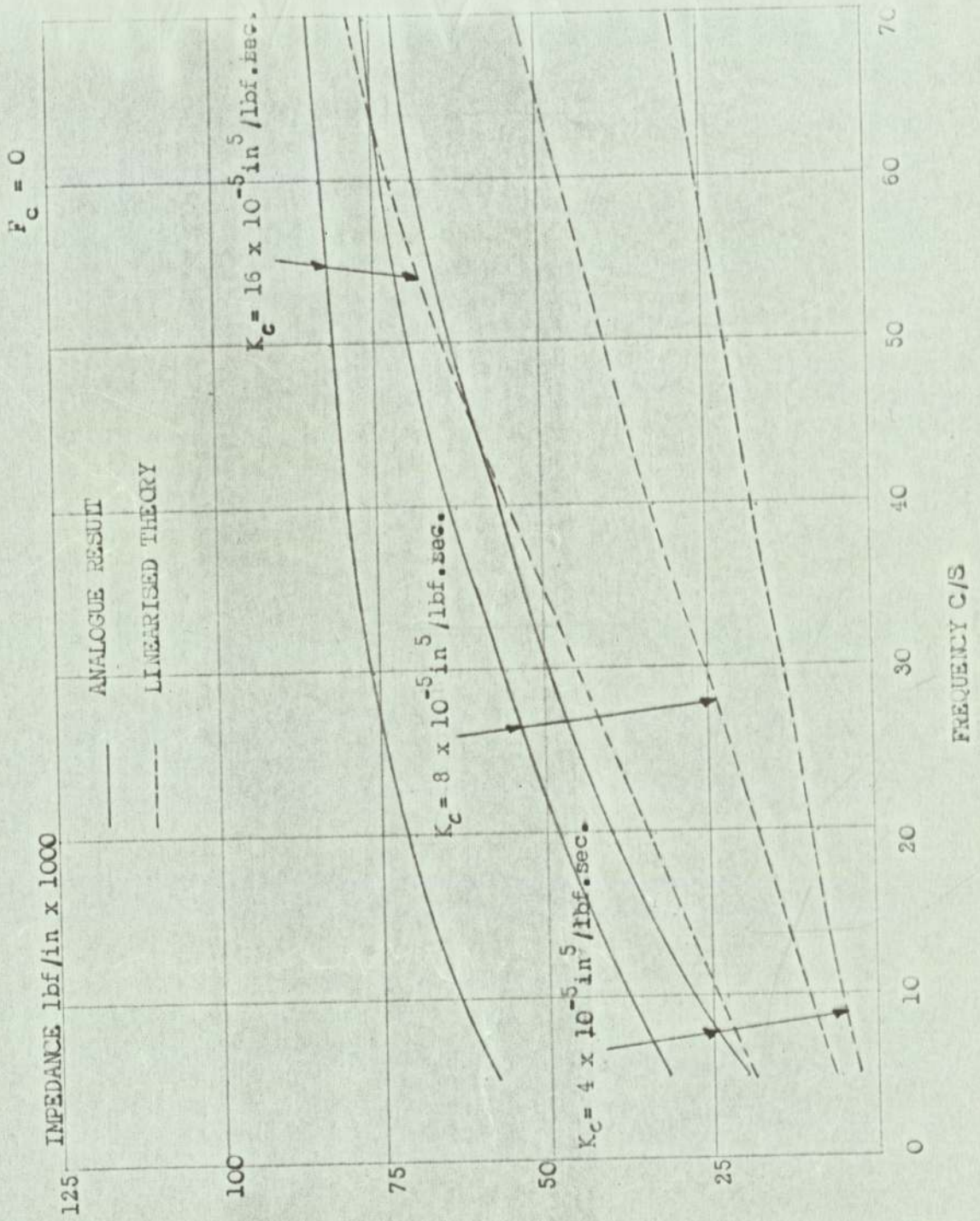
PERTURBATION AMPLITUDE =  $\pm .005$ in.



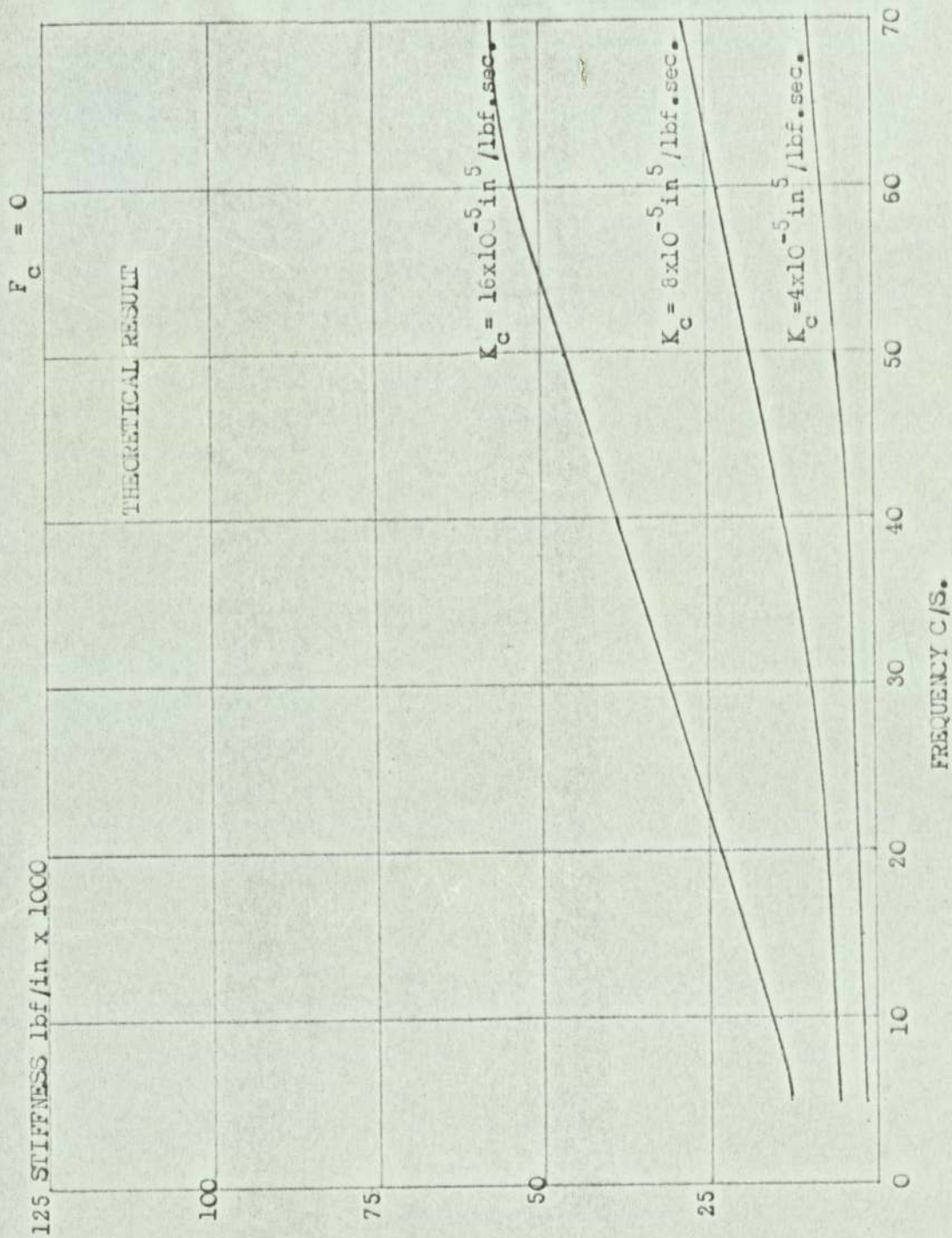
EFFECT OF BULK MODULUS ON STIFFNESS FOR CHANGES IN STATIC VALVE OPENING. PERTURBATION AMPLITUDE =  $\pm .005 \text{ in.}$



EFFECT OF BULK MODULUS ON DAMPING FOR CHANGES IN STATIC VALVE OPENING. PERTURBATION AMPLITUDE =  $\pm .005$  in.

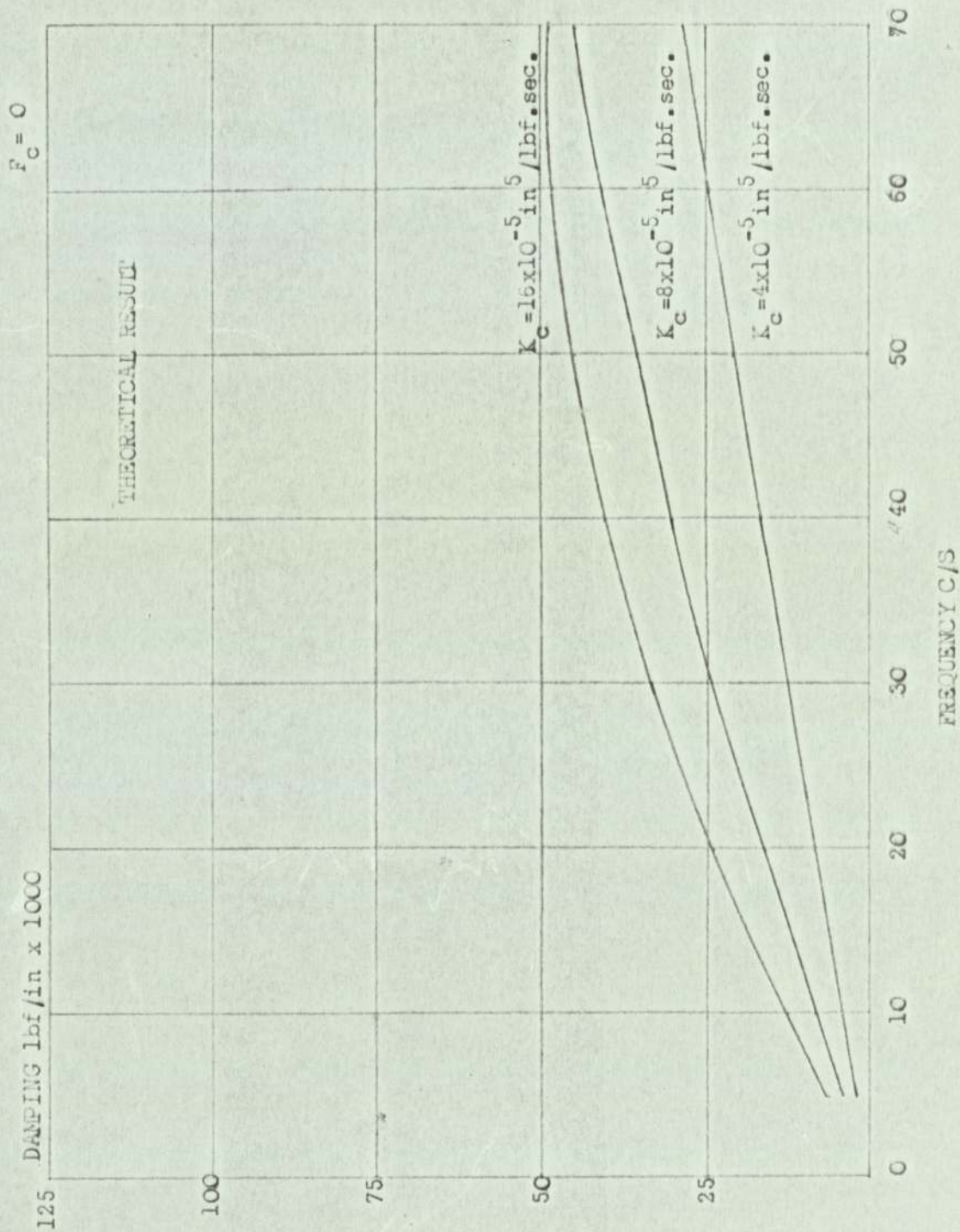


EFFECT OF LEAKAGE ON IMPEDANCE  
COMPARISON OF ANALOGUE AND THEORETICAL RESULT.



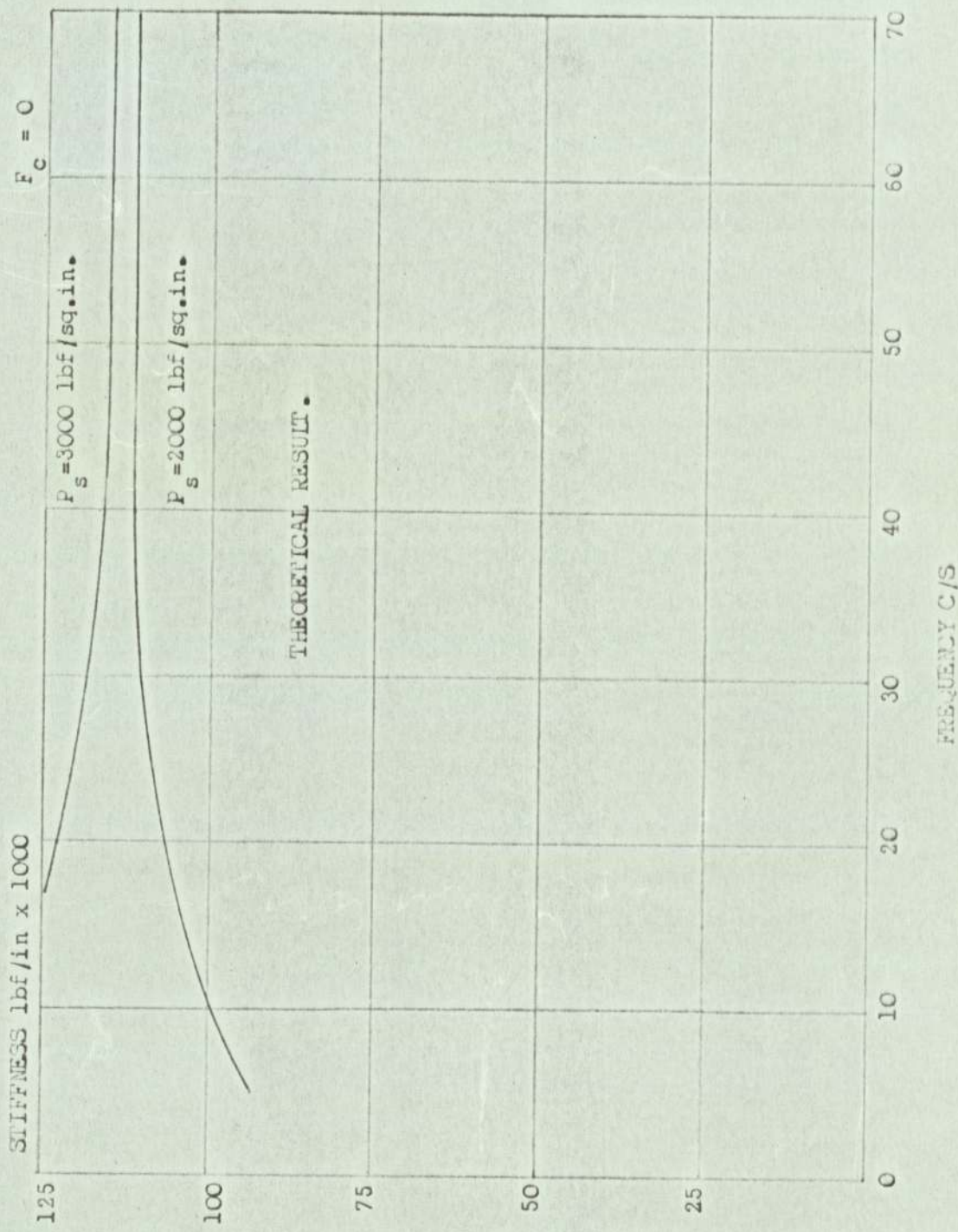
EFFECT OF LEAKAGE ON STIFFNESS STATIC VALVE OPENING = .015in.  
 PERTURBATION AMPLITUDE =  $\pm$  .005in.

FIG.7.51



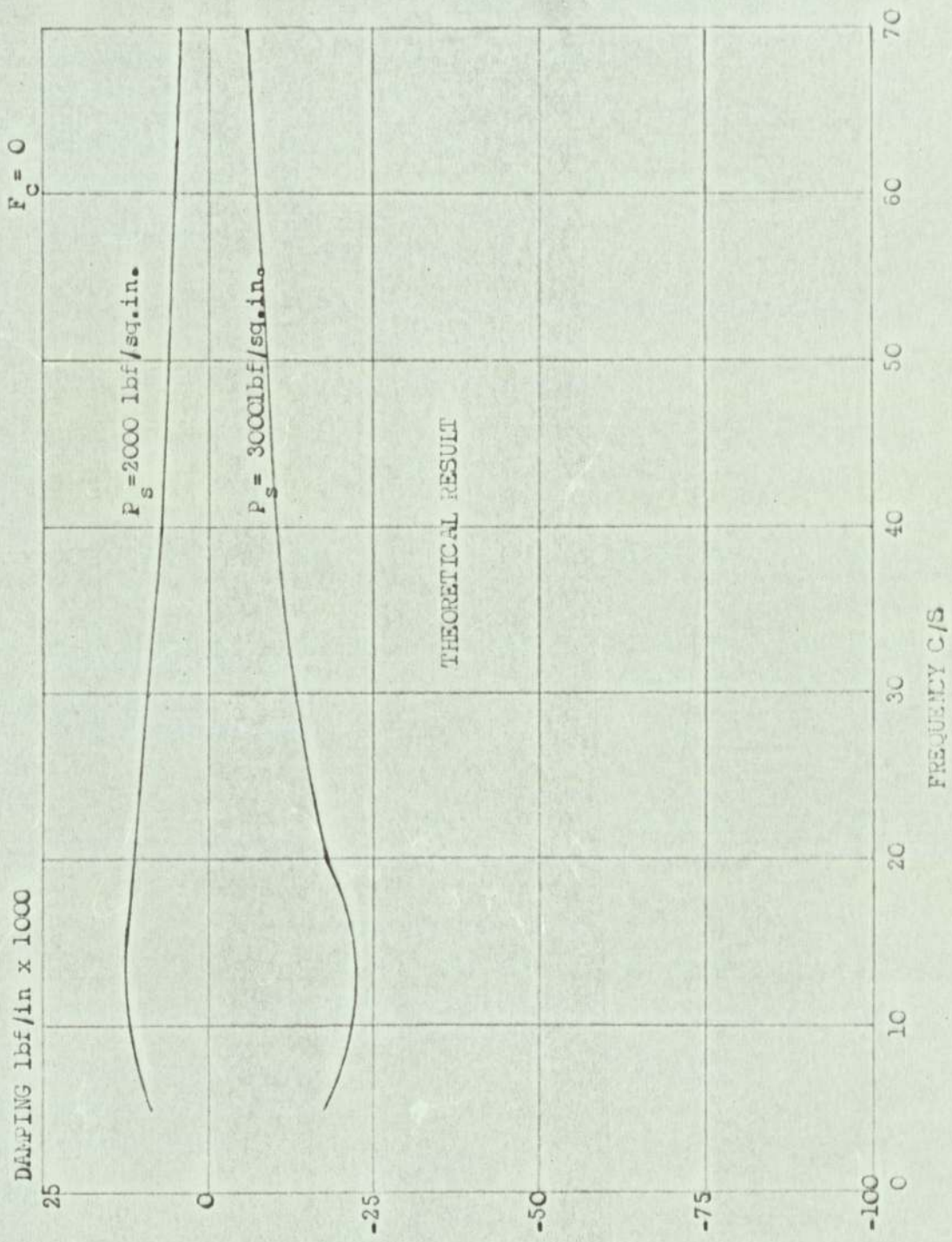
EFFECT OF LEAKAGE ON DAMPING. STATIC VALVE OPENING = .015 in.

PERTURBATION AMPLITUDE = .005 in.



EFFECT OF SUPPLY PRESSURE ON STIFFNESS.

STATIC VALVE OPENING = .005in. PERTURBATION AMPLITUDE =  $\pm$  .005in.



EFFECT OF SUPPLY ON DAMPING.

STATIC VALVE OPENING = .005in. PERTURBATION AMPLITUDE =  $\frac{1}{2}$  .005in.

CHAPTER 8

AN EXPERIMENTAL APPROACH FOR OBTAINING  
THE CONTROL SYSTEM IMPEDANCE BY THE  
SUB-SYSTEM TECHNIQUE.

CHAPTER 8

AN EXPERIMENTAL APPROACH FOR OBTAINING  
THE CONTROL SYSTEM IMPEDANCE BY THE  
SUB-SYSTEM TECHNIQUE.

<u>CONTENTS.</u>	<u>PAGE.</u>
8.1.      Notation.	106
8.2.      The Sub-System Technique.	108
8.3.      Impedance of the Sub-System.	110
8.4.      The Control System Impedance.	116

## CHAPTER 8

8.1 Notation.

The following notation has been used in this chapter.

C	Damping coefficient (lb-sec/in).
$F_1$	Force applied to the complex system at the mass $m_1$ and to the sub-system 'C' at station 1.
$F_{b2}$	Force applied to the sub-system 'B'.
$F_{c2}$	Force applied to the sub-system 'C' at station 2.
K	Spring gradient (lbf/in).
$M_{11}$	Driving point displacement mobility of the control system.
$M_{b22}$	Driving point displacement mobility of the sub-system 'B'.
$M_{c11}$	Driving point displacement mobility of the sub-system 'C' for excitation at station 1.
$M_{c21}$	Cross displacement mobility of the sub-system 'C' for excitation at station 1.
$M_{c12}$	Cross displacement mobility of sub-system 'C' for excitation at station 2.
$M_{c22}$	Driving point displacement mobility of the sub-system 'C' for excitation at station 2.
m	Mass (lbf.sec <sup>2</sup> /in).
$X_1$	Displacement of mass $m_1$ of the complex system for excitation at $m_1$ .
$X_{b22}$	Displacement of station 1 of the sub-system 'B'
$X_{c11}$	Displacement of station 1 of the sub-system 'C' for excitation at station 1.
$X_{c21}$	Displacement of station 2 of the sub-system 'C' for excitation.

- $X_{c12}$  Displacement of station 1 of the sub-system 'C' for excitation at station 2.
- $X_{c22}$  Displacement of station 2 of the sub-system 'C' for excitation at station 2.
- $Z_{11}$  Driving point impedance of the control system for excitation at mass  $m_1$ .

## 8.2. The Sub-System Technique.

It was mentioned earlier that it is not possible to determine the impedance of an aircraft control system consisting of the hydraulic servomechanism and the control surface by ground tests on the aircraft. The control system impedance can however, be determined by the sub-system technique. This method of vibration analysis is extensively made use of in determining the natural frequencies and response of aircraft structures (31), (32), (33) and (34). It essentially consists of dividing a complex system into a number of smaller systems or elements which readily lend themselves to analysis. The responses of the individual elements or sub-systems are then combined to yield the complex system response.

Consider the aircraft control system as shown in Fig.8.1. This is represented in block form by the complex system A which can be divided into two sub-systems B and C (Fig.8.2) representing the hydraulic servomechanism and the control surface respectively. It is required to determine the driving point impedance  $Z_{11}$  at  $X_1$  of the complex system A. If the sub-systems B and C are to be coupled the two conditions of equilibrium and compatibility must be satisfied. The equilibrium condition requires that the forces  $F_{b2}$  and  $F_{c2}$  remain in equilibrium with the exciting force  $F_1$  at  $X_1$  (Fig.8.2b), or in the absence of  $F_1$  these forces must balance each other, that is:-

$$F_{b2} + F_{c2} = F_1 \quad (8.1)$$

or

$$F_{b2} + F_{c2} = 0 \quad (8.2)$$

For the sub-systems to remain coupled the compatibility condition requires that

$$X_{b2} = X_{c2} = X_2 \quad (8.3)$$

For the sub-system C with the forces and displacements as shown in Fig.8.2b and using displacement mobilities:-

$$X_1 = M_{c11} F_1 + M_{c12} F_{c2} \quad (8.4)$$

$$X_2 = M_{c21} F_1 + M_{c22} F_{c2} \quad (8.5)$$

The sub-systems have been assumed to be linear and hence the principle of superposition of the motions due to forces  $F_1 \cos wt$  and  $F_{c2} \cos wt$  is applied.

For the sub-system B:-

$$X_{b2} = M_{b22} \cdot F_{b2} \quad (8.6)$$

but from equation (8.2)  $F_{b2} = F_{c2}$  and from equation (8.3)  $X_{b2} = X_2$ , therefore:-

$$X_2 = - M_{b22} \cdot F_{c2} \quad (8.7)$$

Substituting for  $X_2$  in equation (8.5):-

$$\begin{aligned} - M_b \cdot F_{c2} &= M_{c21} F_1 + M_{c22} F_{c2} \\ \text{or } F_{c2} &= - \frac{M_{c21} \cdot F_1}{M_{b22} + M_{c22}} \end{aligned} \quad (8.8)$$

Substituting equation (8.8) in equation (8.4) gives:-

$$X_1 = M_{c11} \cdot F_1 - \frac{M_{c12} M_{c21} \cdot F_1}{M_{b22} + M_{c22}}$$

Due to the reciprocal property of the system  $M_{c21} = M_{c12}$  and:-

$$M_{11} = \frac{X_1}{F_1} = M_{c11} - \frac{M_{c12}^2}{M_{b22} + M_{c22}} \quad (8.9)$$

Equation (8.9) represents the driving point displacement mobility of the complex system 'A' or the aircraft control system as shown in Fig.8.1. The driving point impedance on a displacement basis will simply be the inverse of mobility. In the following sections the aircraft control system is represented by an elastic system (Fig.8.3) which is divided into two sub-systems representing the hydraulic servo-mechanism and the control surface respectively as shown in Fig.8.4. The two sub-systems have been simulated on the analogue computer and their responses recorded on a magnetic tape. These responses have been combined using another analogue circuit to yield the control system impedance.

### 8.3. Impedance of the Sub-Systems.

#### 8.3.1 Impedance of the Control Surface.

The control surface is represented by the elastic system of Fig.8.4b. Due to the difficulty encountered in simulating a system free in space this system was attached to a support by means of a very light spring and a damper combination. The modified system is shown in Fig.8.5. With the forcing function applied to the lower mass the equations of motion are:-

$$m_2 \ddot{X}_{c21} + K_o X_{c21} + K_1 X_{c21} - K_1 X_{c11} + C_o \dot{X}_{c21} + C_1 \dot{X}_{c21} - C_1 \dot{X}_{c11} = 0 \quad (8.10)$$

$$m_1 \ddot{X}_{c11} + K_1 X_{c11} + C_1 \dot{X}_{c11} - K_1 X_{c21} - C_1 \dot{X}_{c21} = F \quad (8.11)$$

Writing  $F = F \exp j\omega t$ ,  $X = X \exp j\omega t$ ,  $K_1 = K_2 = K$ ,  $K_o = .04K$ ,

$$C_1 = C, C_o = .5C, m_1 = 1 \text{ and } m_2 = 2,$$

The equations of motion can be expressed as:-

$$(1.04K + 1.5 jcw - 2w^2) X_{c21} - (K + jcw) X_{c11} = 0 \quad (8.12)$$

$$- (K + jcw) X_{c21} + (K + jcw) X_{c11} = F \quad (8.13)$$

The denominator D for expressions for  $X_{c1}$  and  $X_{c2}$  can be obtained from equations (8.12) and (8.13):-

$$D = (1.04K + 1.5jcw - 2w^2) (K + jcw - w^2) - (K + jcw)^2 \quad (8.14)$$

$$\text{and } DX_{c11} = (1.04K + 1.5 jcw - 2w^2)F$$

$$\therefore X_{c11} = \frac{(1.04K + 1.5jcw - 2w^2)F}{(1.04K + 1.5jcw - 2w^2) (K + jcw - w^2) - (K + jcw)^2} \quad (8.15)$$

$$\text{similarly } DX_{c21} = (K + jcw)F$$

$$\text{and } X_{c21} = \frac{(K + jcw)F}{(1.04K + 1.5jcw - 2w^2) (K + jcw - w^2) - (K + jcw)^2} \quad (8.16)$$

With the forcing function applied to the upper mass ( $m_2$ ) the displacements are as follows:-

$$X_{c22} = \frac{(K + jcw - w^2)F}{(1.04K + 1.5jcw - 2w^2) (K + jcw - w^2) - (K + jcw)^2} \quad (8.17)$$

$$\text{and } X_{c12} = \frac{(K + jcw)^2 F}{(1.04K + 1.5jcw - 2w^2) (K + jcw - w^2) - (K + jcw)^2} \quad (8.18)$$

Note that the expressions for  $X_{c21}$  and  $X_{c12}$ , equations (8.16) and (8.18) are the same. This is due to the reciprocity of the system.

The natural undamped frequencies of this system are found to be 15 C/S and 70 C/S. The frequencies are obtained by equating to zero the equation (8.14) with a zero damping coefficient ( $C = 0$ ) which gives a quadratic in  $w^2$ .

Substituting the two frequencies in equations (8.15) to (8.18) the maximum value of displacement is found to be  $(7 \times 10^{-5} \cdot F)^{in}$ . Hence the maximum values of the variable are:-

$$F_{max} = 100 \text{ lb.}$$

$$X_{max} = 7 \times 10^{-3} \text{ in.}$$

$$\dot{X}_{max} = 3.1 \text{ in/sec.}$$

$$\ddot{X}_{max} = 1364 \text{ in/sec}^2.$$

#### Scale factor equations.

To convert the system variables into voltages for the analogue computer the following scale factor equations are used:-

$$F = \frac{100}{10} \left( \frac{\text{lb}}{\text{volt}} \right) F \quad (8.19)$$

$$X_{max} = \frac{7 \times 10^3}{10} \left( \frac{\text{in}}{\text{volt}} \right) X_{max}. \quad (8.20)$$

$$\dot{X}_{max} = \frac{3.1}{10} \left( \frac{\text{in}}{\text{sec. volt}} \right) \dot{X}_{max}. \quad (8.21)$$

$$\ddot{X}_{max} = \frac{1364}{10} \left( \frac{\text{in}}{\text{sec}^2 \text{ volt}} \right) \ddot{X}_{max}. \quad (8.22)$$

Substituting the scale factor equations together with the values of the masses, spring gradients and the damping coefficients in the equation of motion (8.10) and (8.11) gives:-

$$272.8 \ddot{X}_{c21} + 87.36X_{c21} - 84X_{c11} + 32.55\dot{X}_{c21} - 21.7\dot{X}_{c11} = 0 \quad (8.23)$$

$$13.64\ddot{X}_{c11} + 8.4X_{c11} - 8.4X_{c21} + 2.17\dot{X}_{c11} - 2.17\dot{X}_{c21} = F \quad (8.24)$$

The analogue computer diagram simulating the above equations is shown in Fig.8.6. The voltages representing the force  $F$  and the displacements  $X_{c11}$  and  $X_{c21}$  were recorded on a magnetic tape using the 14 track 'Ampex' tape recorder. To obtain the value of the displacement  $X_{c22}$  it is necessary to apply the force  $F$  at the mass  $m_2$  (Fig.8.5) and the equations (8.23) and (8.24) are modified as follows:-

$$27.28\ddot{X}_{c22} + 8.736X_{c22} - 8.4X_{c12} + 32.55\dot{X}_{c22} - 21.7\dot{X}_{c12} = F \quad (8.25)$$

$$136.4\ddot{X}_{c12} + 84X_{c12} - 84X_{c22} + 217\dot{X}_{c12} - 217\dot{X}_{c22} = 0 \quad (8.26)$$

On the analogue computer the above equations were established by removing the force  $F$  from amplifier 2 and applying it to amplifier 9 (Fig.8.6). In order to ensure no phase lag existed between  $X_{c22}$  and the previously recorded signals, the later were played through operational amplifiers and recorded again together with  $X_{c22}$  on other available tracks of the recorder. The force  $F$  for amplifier 9 was also derived using the recorded force signal. Each of the displacements was fed to the analysis equipment together with  $F$  to obtain the impedances  $Z_{c11}$ ,  $Z_{c21}$  and  $Z_{c22}$ . These impedances are plotted against frequency in Fig.8.7.

### 8.3.2 Impedance of the hydraulic servo.

The hydraulic servo is represented by the elastic system of Fig.8.4a which has two degrees of freedom resulting in co-ordinates  $X_{b1}$  and  $X_{b2}$ . With the forcing function applied at the co-ordinate  $X_{b2}$  the equations of motion for this system are:-

$$m_3 \ddot{X}_{b12} + K_3 X_{b12} + K_2 X_{b12} - K_2 X_{b22} + C_3 \dot{X}_{b12} + C_2 \dot{X}_{b12} - C_2 \dot{X}_{b22} = 0 \quad (8.27)$$

$$K_2 X_{b22} - K_2 X_{b12} + C_2 \dot{X}_{b22} - C_2 \dot{X}_{b12} = F \quad (8.28)$$

Solving these equations for the natural undamped frequency and displacements in the manner previously shown, the following values are obtained:-

Natural frequency	=	48 C/S
$X_{b12}$ (max)	=	$4.8 \times 10^{-5} \cdot F$ in
$X_{b22}$ (max)	=	$5.0 \times 10^{-5} \cdot F$ in

The maximum displacement for this system is the same order of magnitude as the displacement for the system representing the control surface. Hence the scale factors defined by equations (8.19) to (8.22) can be used. Substituting the scale factors and the values of coefficient in equations (8.27) and (8.28) gives:-

$$545.6 \ddot{X}_{b12} + 336 X_{b12} - 84 X_{b22} + 43.4 \dot{X}_{b12} - 21.7 \dot{X}_{b22} = 0 \quad (8.29)$$

$$8.4 X_{b22} - 8.4 X_{b12} + 2.17 \dot{X}_{b22} - 2.17 \dot{X}_{b12} = F \quad (8.30)$$

The analogue computer diagram simulating the above equations is shown in Fig.8.8. This system was simulated at the same time

as the system representing the control surface and hence the displacements  $X_{b22}$ ,  $X_{c11}$  and  $X_{c21}$  were simultaneously recorded. A plot of the impedance  $Z_{b22}$  is shown in Fig.8.9.

#### 8.4 The Control System Impedance.

The control system impedance has been determined by combining the measurements made on the sub-systems B and C and by direct measurement on the complex system 'A'.

##### 8.4.1 Combination of the Sub-System Responses.

The control system mobility,  $M_{11}$ , is defined by equation (8.9) as:-

$$\frac{X_1}{F_1} = M_{c11} - \frac{(M_{c12})^2}{M_{b22} + M_{c22}}$$

If the magnitude of the forces  $F_1$ ,  $F_{b2}$  and  $F_{c2}$  are equal then the control system mobility can be written in terms of displacements of the sub-systems:-

$$X_1 = X_{c11} - \frac{(X_{c12})^2}{X_{b22} + X_{c22}}$$

$$\frac{1}{X_1} = \frac{X_{b22} + X_{c22}}{X_{c11} (X_{b22} + X_{c22}) - (X_{c12})^2} \quad (8.31)$$

and the control system impedance which is the ratio of force to displacement can be expressed as:-

$$Z_{11} = \frac{F_1}{X_1} = \frac{(X_{b22} + X_{c22}) F_1}{X_{c11} (X_{b22} + X_{c22}) - (X_{c12})^2} \quad (8.32)$$

The control system impedance was computed in two stages using the previously recorded signals of force and sub-system displacements. The analogue computer diagram of Fig.8.10a combined the displacements as defined by the equation (8.31). The signals representing the numerator and the denominator of this equation were recorded on the tape. The force  $F$  was re-recorded to synchronise it with the combined displacements. The computer diagram of Fig.8.10b was used to multiply the numerator of equation (8.31) by the force  $F$  to give the numerator of the equation (8.32). Division of the numerator by the denominator was performed in the analysis equipment. The analysis equipment was driven by the frequency of the recorded Force signal which was fed to the sweep oscillator as a d.c. voltage proportional to frequency. This ensured that the dynamic filters in the analysis equipment were tuned to the frequency of the analogue computer signals. The control system impedance thus obtained is plotted against frequency in Fig.8.11.

#### 8.4.2 Impedance Measurements on the Complex System.

The equations of motion for the control system as represented by the complex system 'A' (Fig.8.3), with the forcing function applied to the mass  $m_1$ , are:-

$$m_3 \ddot{X}_3 + K_3 X_3 + K_2 (X_3 - X_2) + C_3 \dot{X}_3 + C_2 (\dot{X}_3 - \dot{X}_2) = 0 \quad (8.33)$$

$$m_2 \ddot{X}_2 - K_2 (X_3 - X_2) + K_1 (X_2 - X_1) - C_2 (\dot{X}_3 - \dot{X}_2) + C_1 (\dot{X}_2 - \dot{X}_1) = 0 \quad (8.34)$$

$$m_1 \ddot{X}_1 - K_1 (X_2 - X_1) - C_1 (\dot{X}_2 - \dot{X}_1) = F \quad (8.35)$$

The maximum values of the undamped natural frequency and the displacement are found to be 72 Hz and  $4F \times 10^{-5}$  in. This gives the maximum values for the variables as follows:-

$$F = 100 \text{ lbf.}$$

$$X = 4 \times 10^{-3} \text{ in.}$$

$$\dot{X} = 1.81 \text{ in/sec.}$$

$$\ddot{X} = 817 \text{ in/sec.}$$

and the scale factor equations become:-

$$F = \frac{100}{10} \quad \frac{\text{lbf}}{\text{volt}}$$

$$X = \frac{4 \times 10^{-3}}{10} \quad \frac{\text{in}}{\text{volt}}$$

$$\dot{X} = \frac{1.81}{10} \quad \frac{\text{in}}{\text{sec. volt.}}$$

$$\ddot{X} = \frac{817}{10} \quad \frac{\text{in}}{\text{sec.}^2 \text{ volt.}}$$

Substituting the scale factors and the coefficient values in the equations of motion gives:-

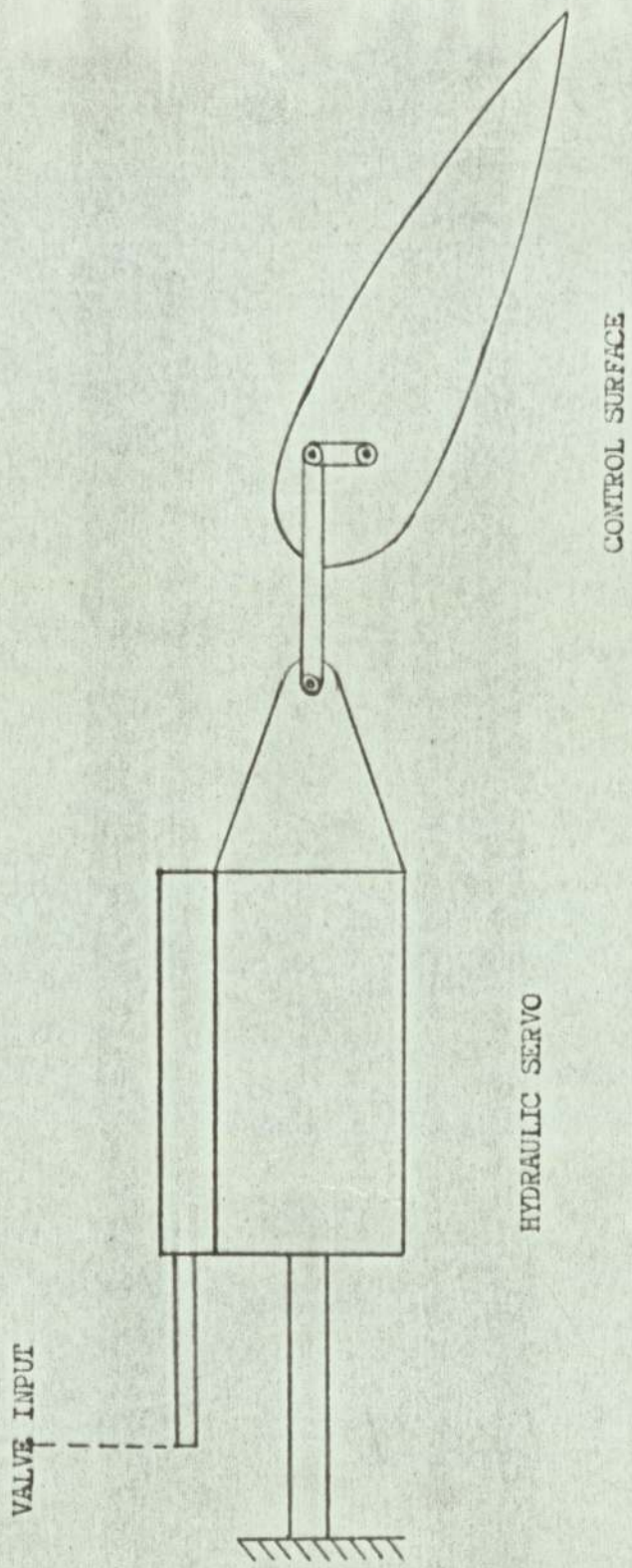
$$326.8 \ddot{X}_3 + 25.34 \dot{X}_3 - 12.67 \dot{X}_2 + 192X_3 - 48X_2 = 0 \quad (8.36)$$

$$163.4 \ddot{X}_2 - 12.67 \dot{X}_3 + 25.34 \dot{X}_2 - 12.67 \dot{X}_1 - 48X_3 + 96X_2 - 48X_1 = 0 \quad (8.37)$$

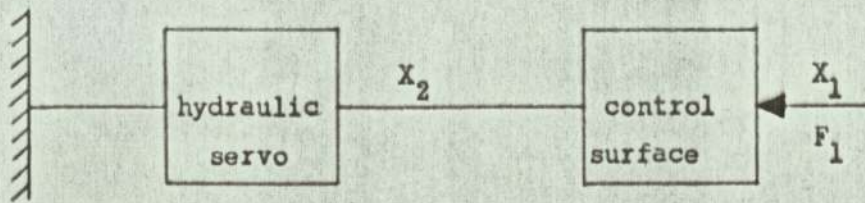
$$81.7 \ddot{X}_1 - 12.67 \dot{X}_2 + 12.67 \dot{X}_1 - 48X_2 + 48X_1 = 10F \quad (8.38)$$

The analogue computer diagram simulating the above equations is shown in Fig.8.12. The displacement  $X_1$  and the force were fed

to the analysis equipment to obtain the control system impedance  $Z_{11}$  (Fig 8.13). Figure 8.14 compares the control system impedance obtained by the sub-system technique and the direct excitation of the control system. The differences in the two methods are essentially due to the fact that elastic system representing the control surface was lightly attached to a support for the purpose of simulation.

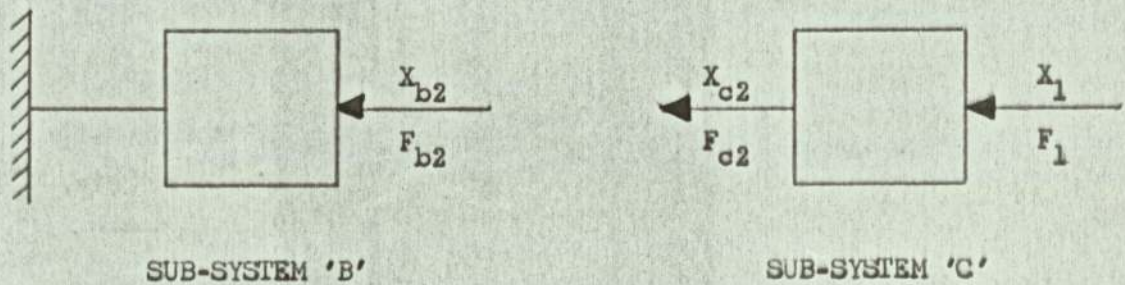


SCHEMATIC DIAGRAM OF AN AIRCRAFT CONTROL SYSTEM.



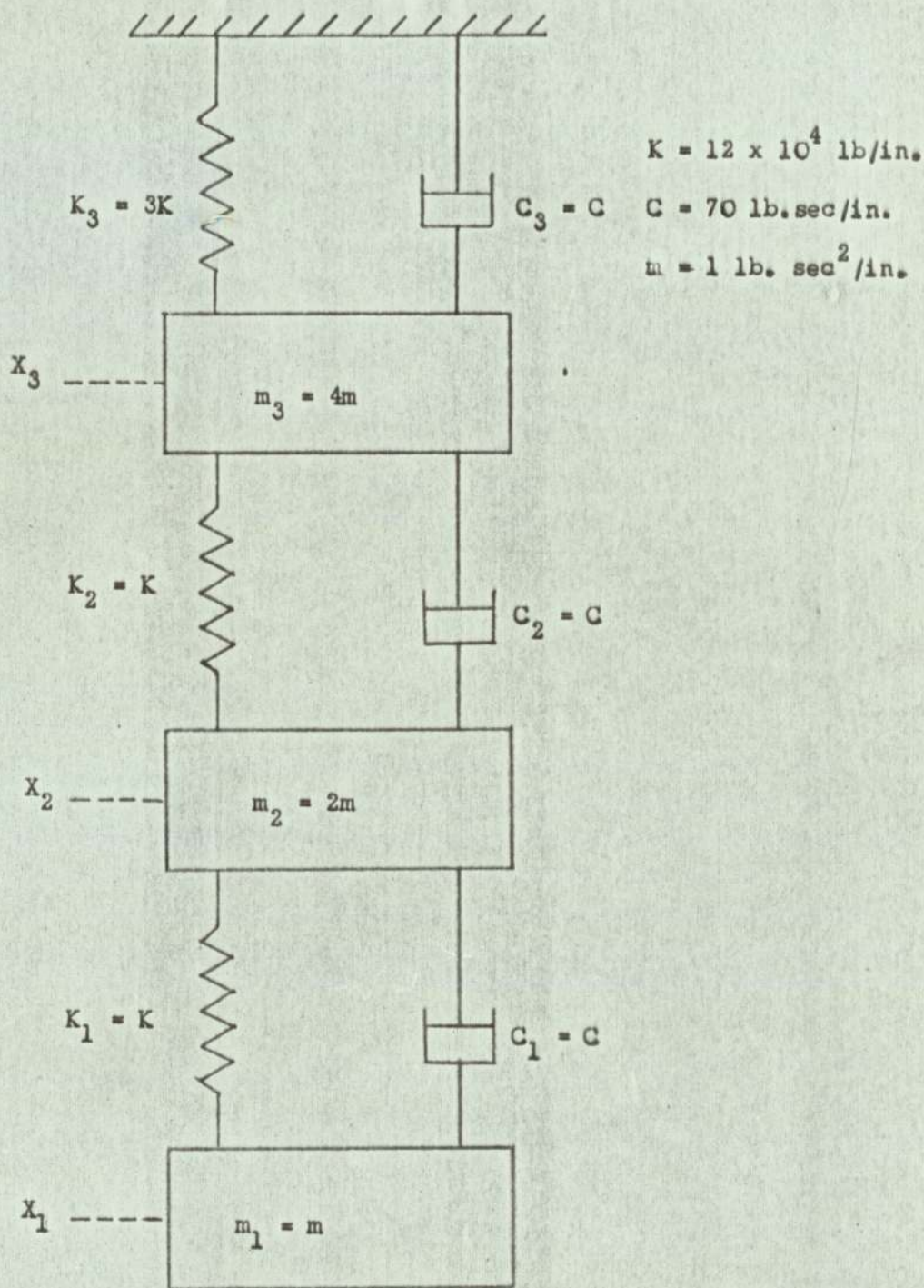
COMPLEX SYSTEM 'A'

a) BLOCK REPRESENTATION OF THE CONTROL SYSTEM



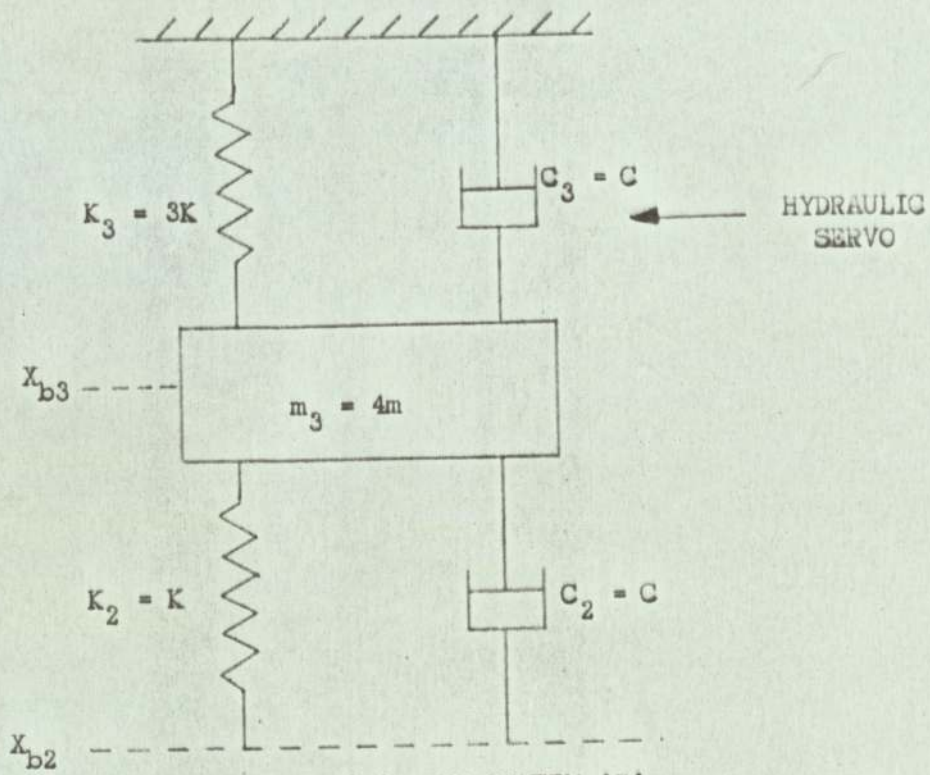
b) DIVISION OF THE COMPLEX SYSTEM INTO SUB-SYSTEMS

REPRESENTATION OF THE CONTROL SYSTEM BY THE SUB-SYSTEM TECHNIQUE

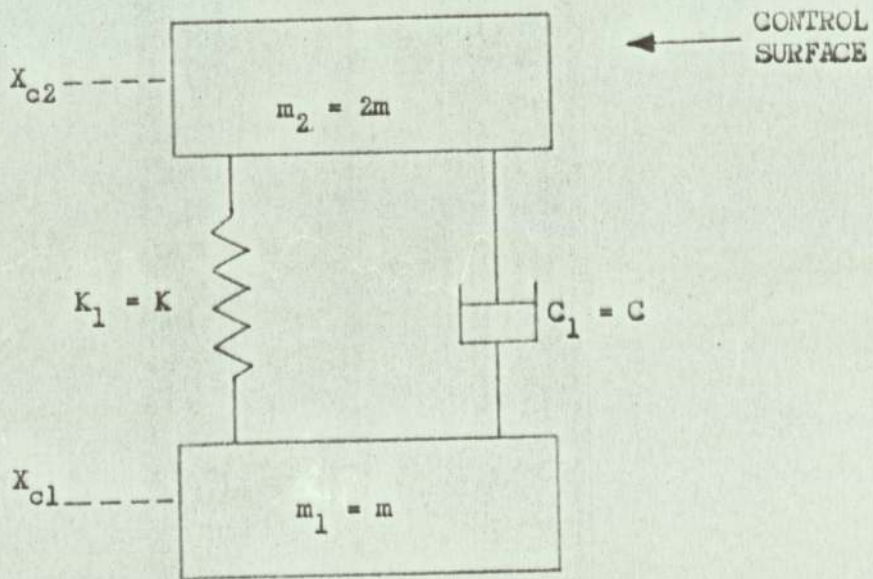


COMPLEX SYSTEM 'A'

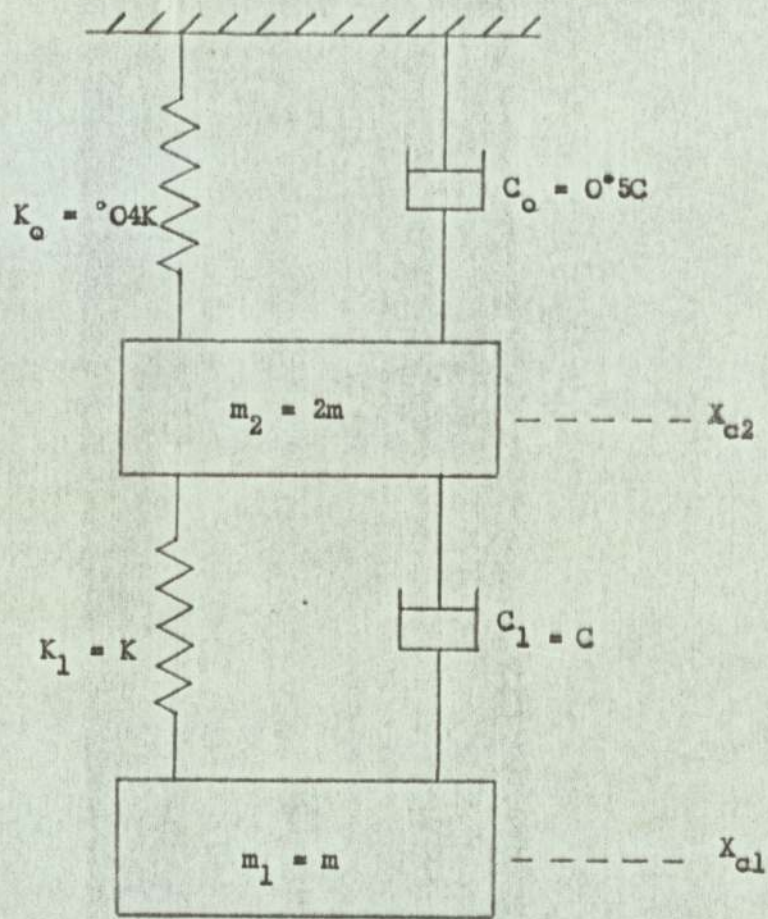
ELASTIC SYSTEM REPRESENTING THE AIRCRAFT CONTROL SYSTEM.



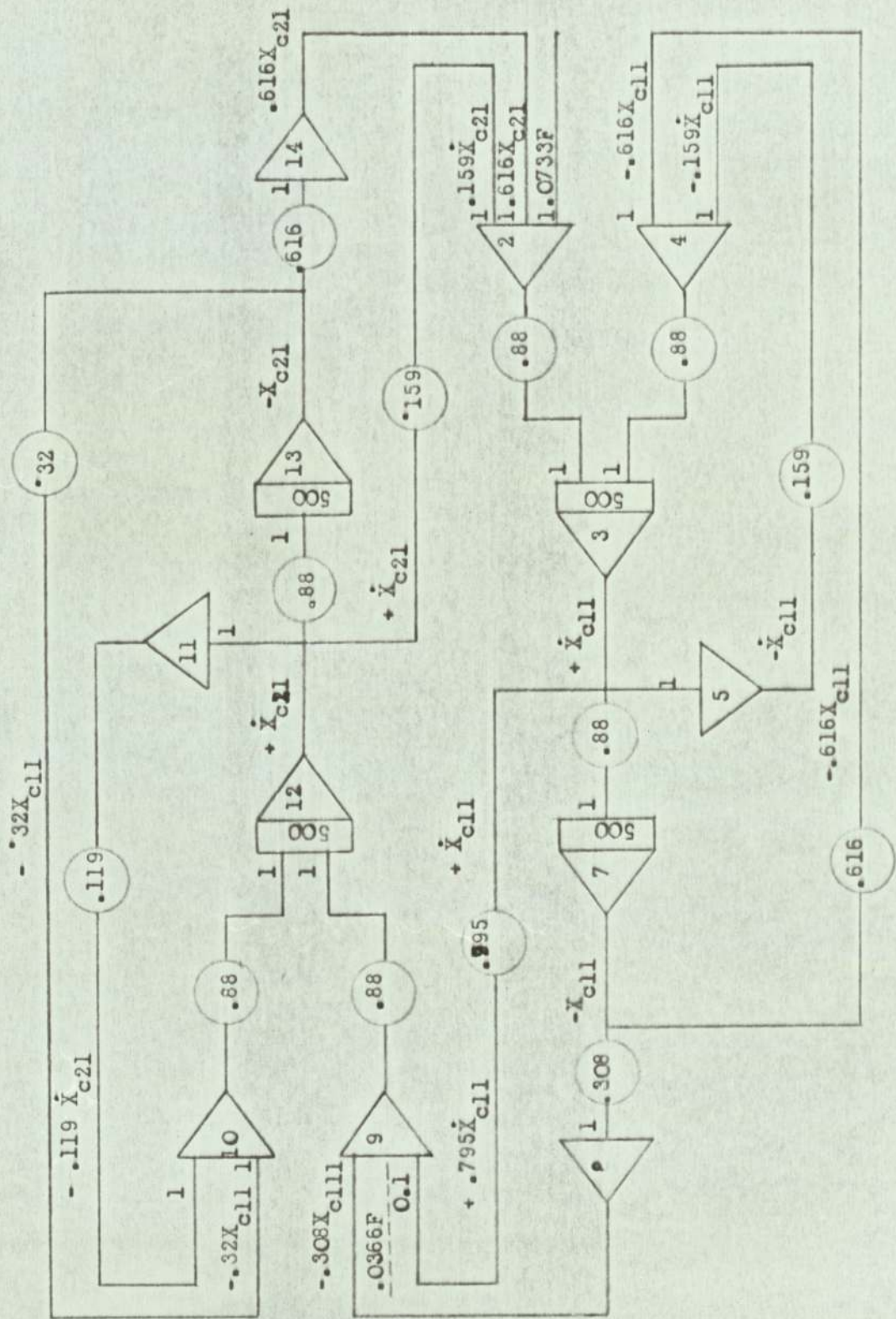
(a) SUB-SYSTEM 'B'



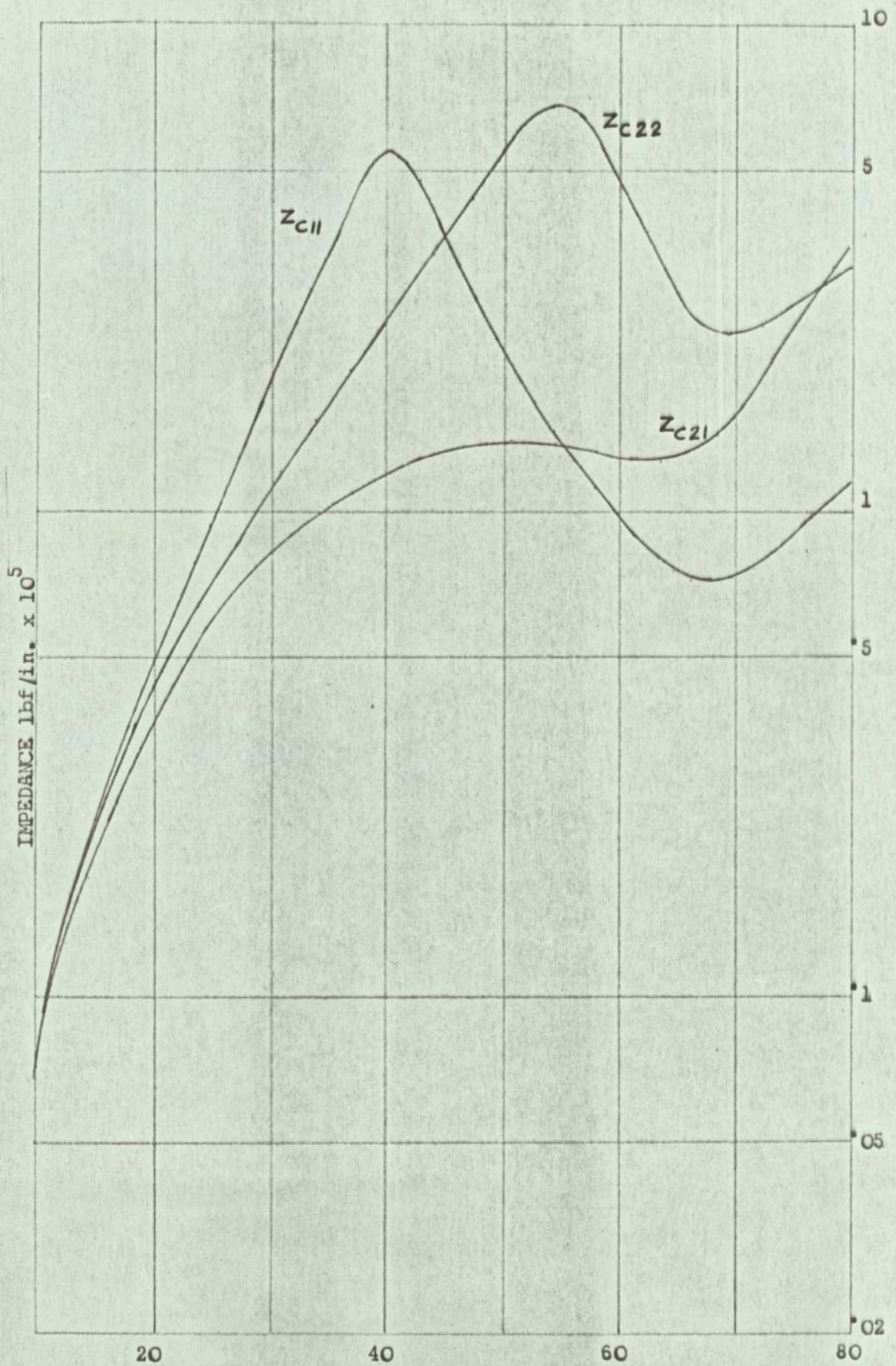
(b) SUB-SYSTEM 'C'



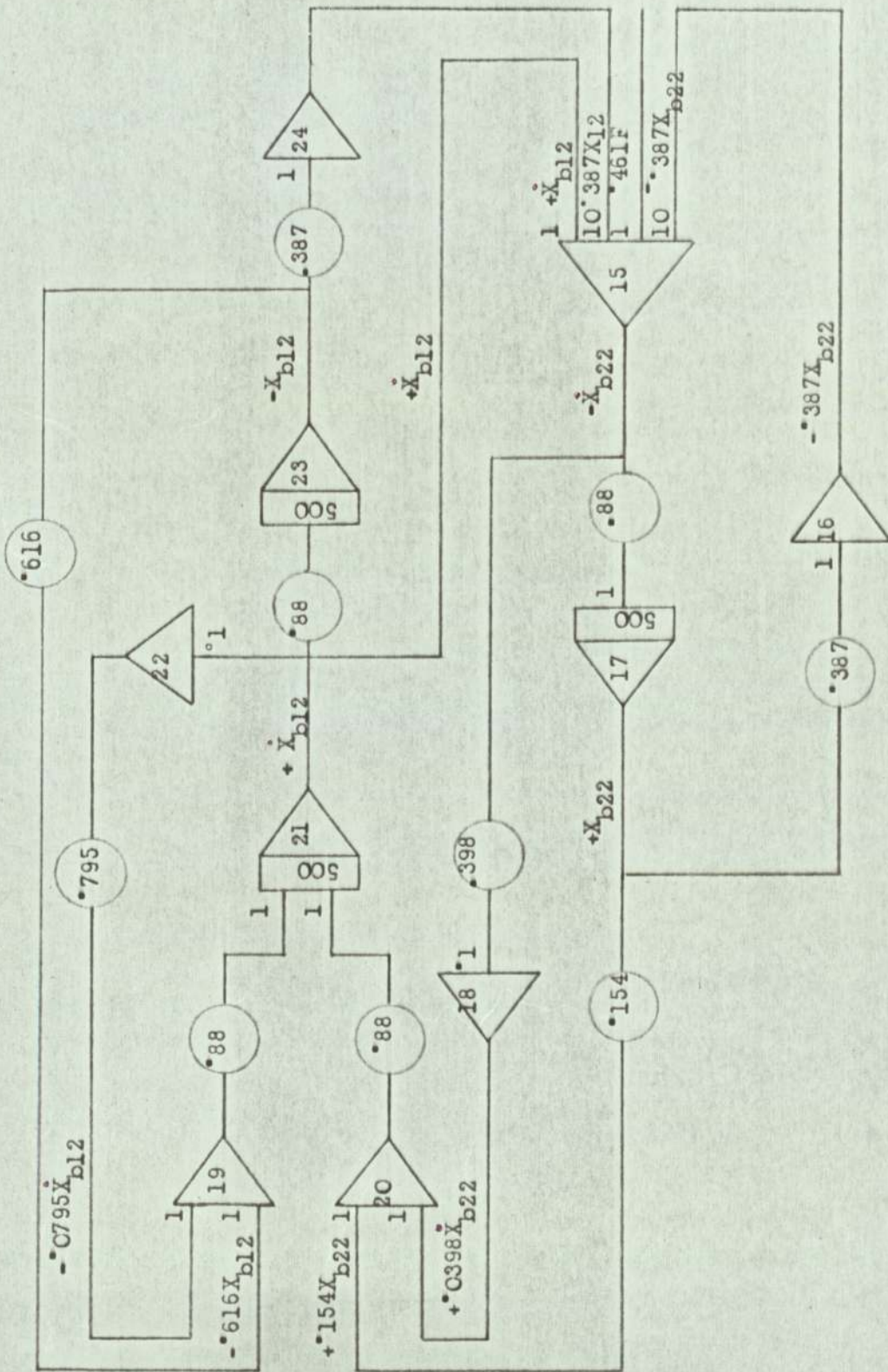
MODIFIED REPRESENTATION OF THE CONTROL SURFACE.



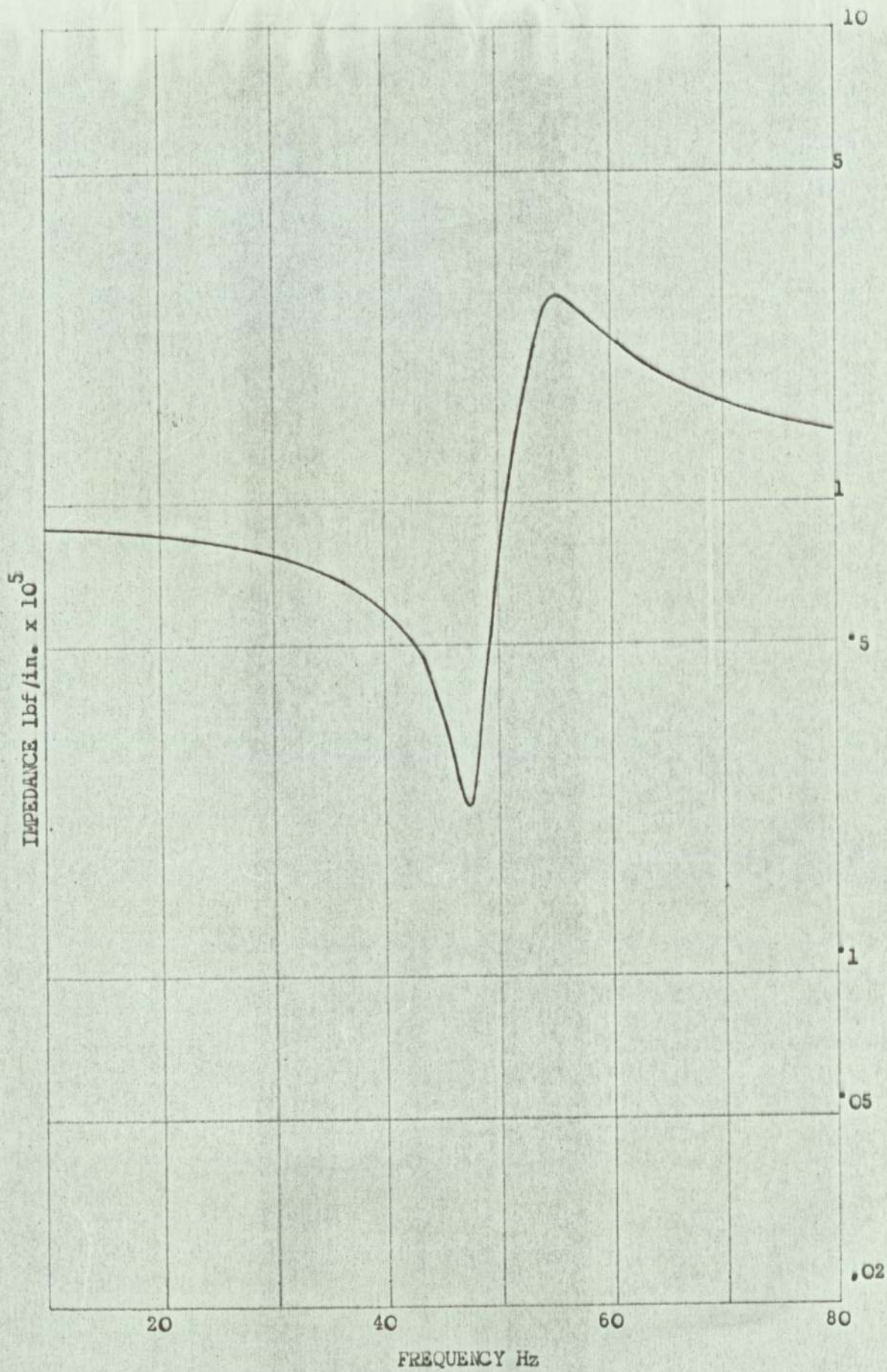
SIMULATION OF THE AIRCRAFT CONTROL SURFACE



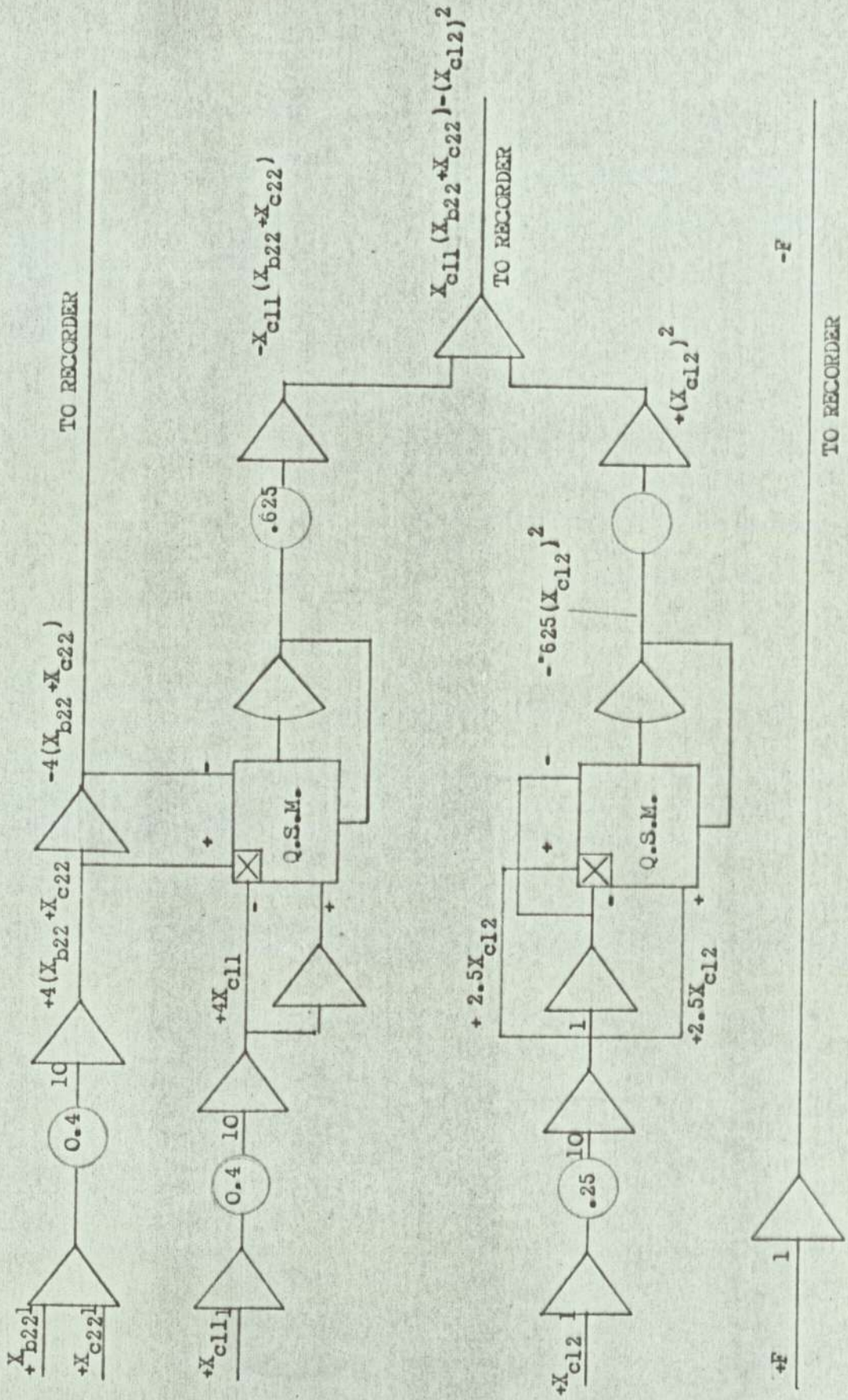
DIRECT AND CROSS IMPEDANCES OF THE CONTROL SURFACE



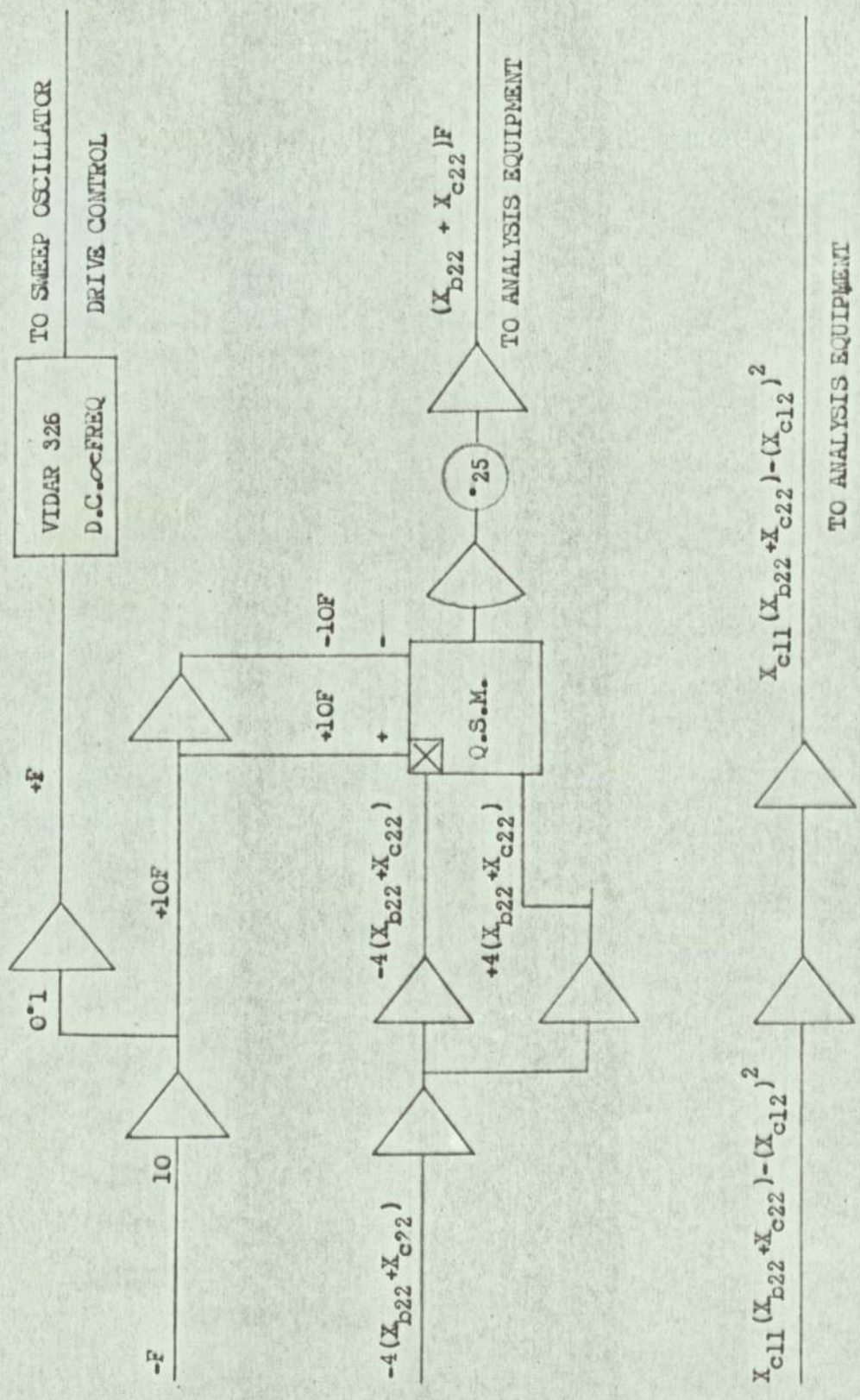
SIMULATION OF THE HYDRAULIC SERVOMECHANISM



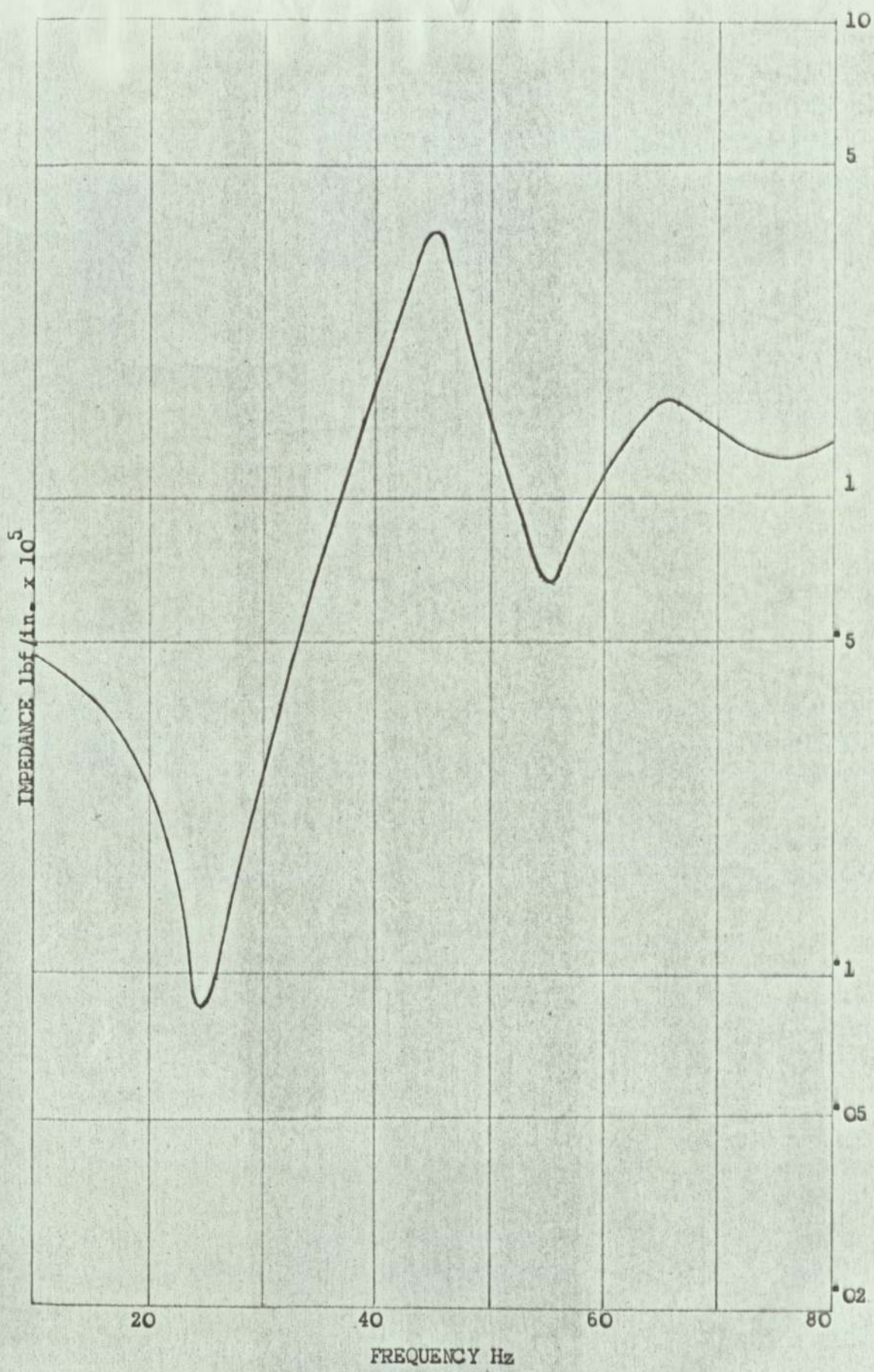
DIRECT IMPEDANCE OF THE HYDRAULIC SERVO



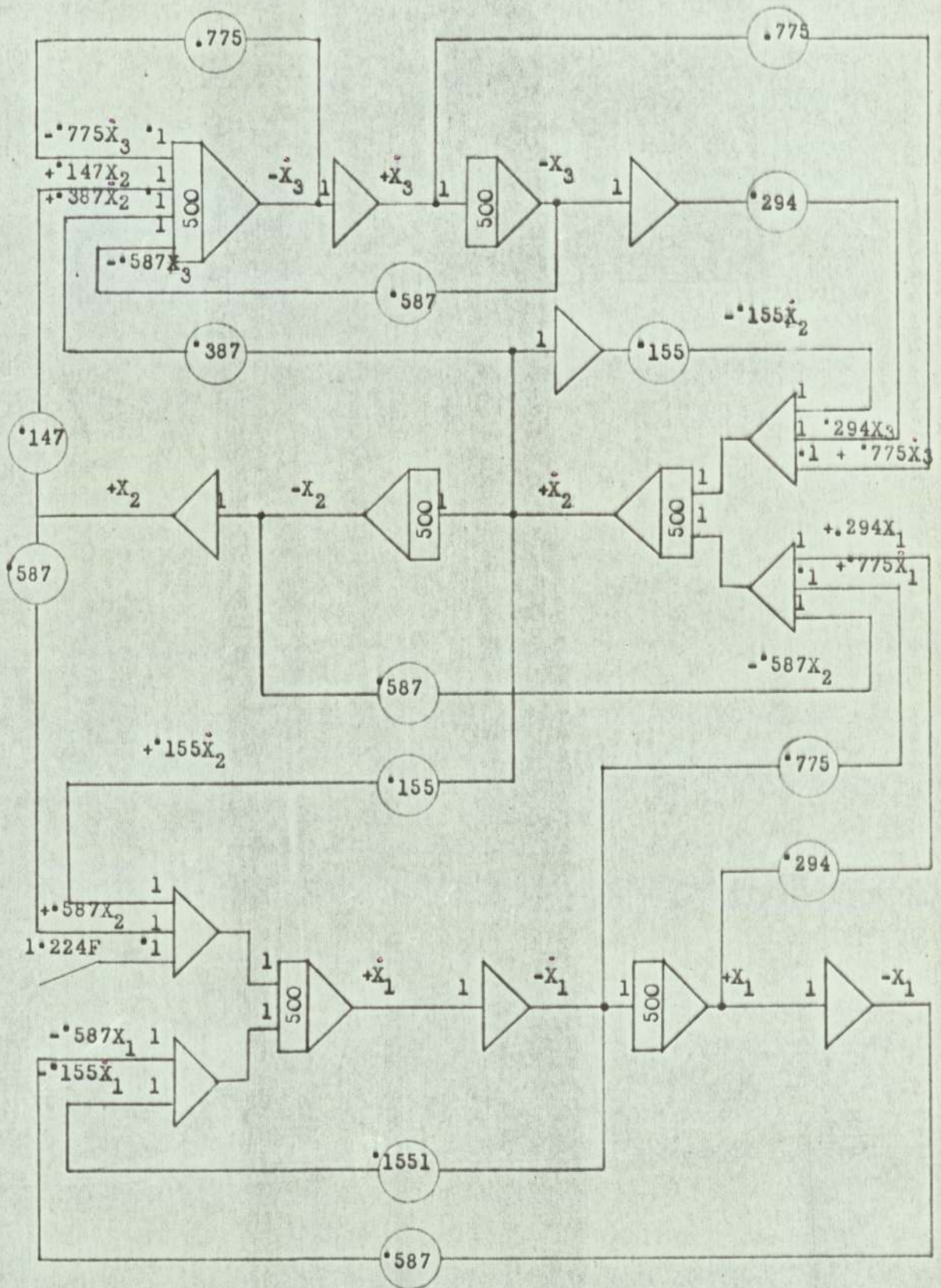
COMBINATION OF THE SUB-SYSTEM DISPLACEMENTS.



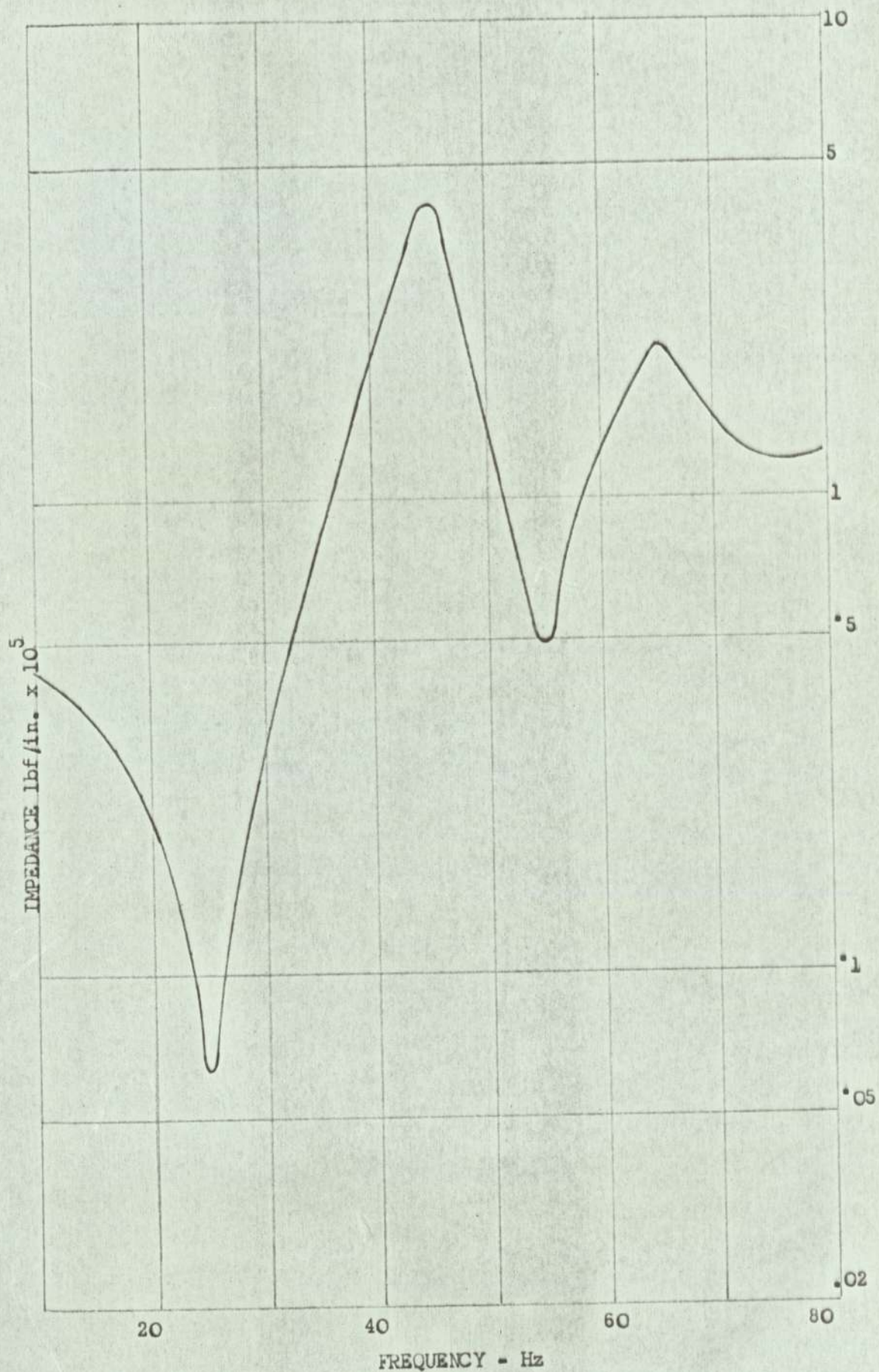
COMBINATION OF THE SUB-SYSTEM DISPLACEMENTS



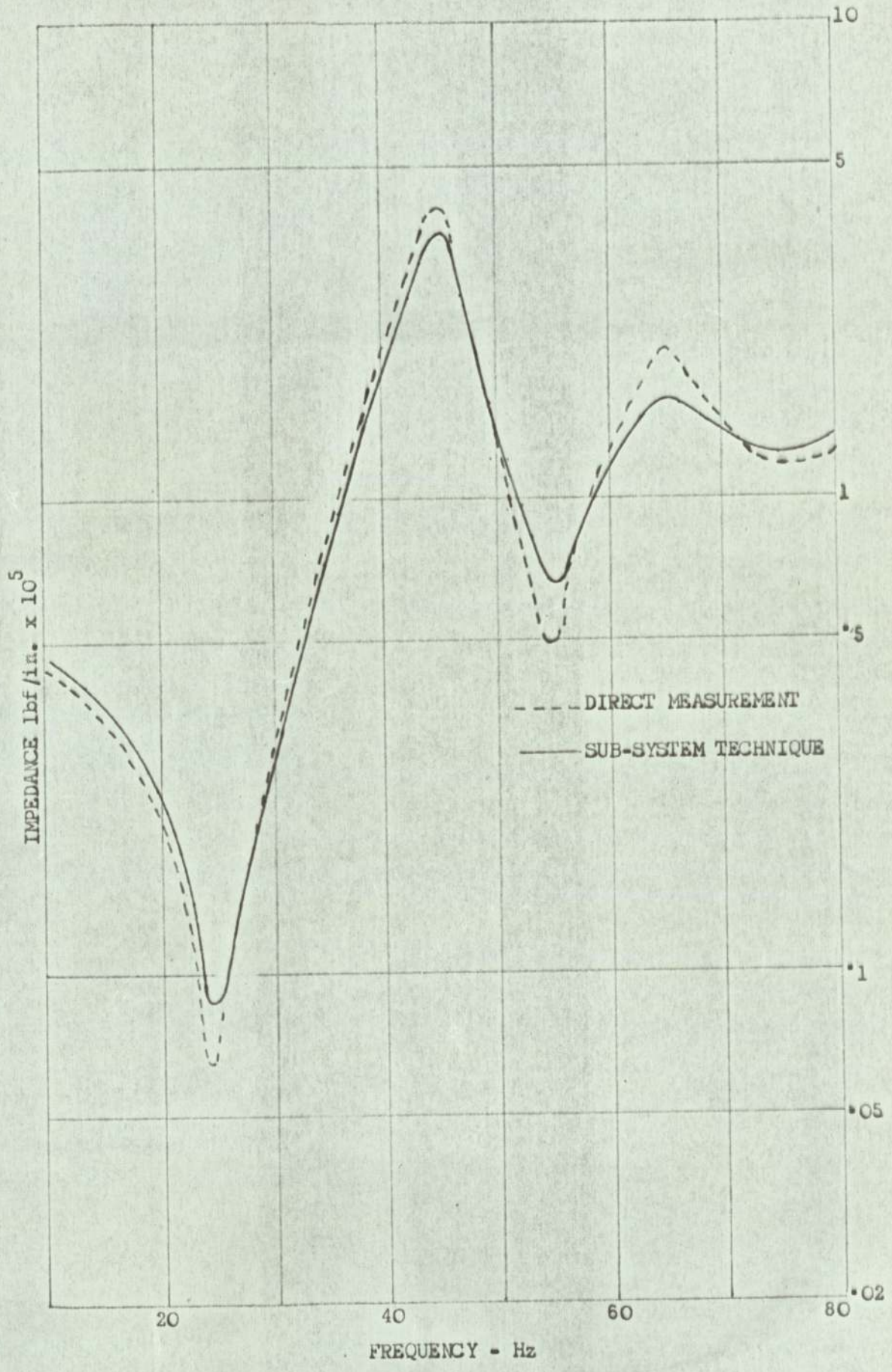
CONTROL SYSTEM IMPEDANCE BY THE SUB-SYSTEM METHOD



SIMULATION OF THE AIRCRAFT CONTROL SYSTEM



CONTROL SYSTEM IMPEDANCE BY DIRECT MEASUREMENT



CONTROL SYSTEM IMPEDANCE

CHAPTER 9.

CONCLUSIONS.

CHAPTER 9.

CONCLUSIONS.

<u>CONTENTS.</u>	<u>PAGE.</u>
9.1. Impedance Of The Servo For Small Valve Openings.	119
9.2. Impedance Of The Servo For Large Valve Openings.	119
9.3. The Effect Of Supply Pressure On Impedance.	119
9.4. Comparison Of The Analogue And The Rig Results.	120
9.5. Comparison Of The Analogue And The Theoretical Results.	121
9.6. The Impedance Of The Control System.	121

## CHAPTER 9

The results obtained from the analogue simulation of the hydraulic servomechanism and their comparison with the test rig and the theoretical results leads to the following conclusions.

### 9.1. Impedance Of The Servo For Small Valve Openings.

The low frequency impedance is mainly governed by the valve flow characteristics or the force-displacement relationship (Fig.6.4) which gives a large increase in the force for a small increase in the valve opening. Other parameters influencing the impedance are the coulomb friction which increases the damping, leakages which effect both the stiffness and the damping, and the value of the bulk modulus which contributes only to the stiffness.

The high frequency impedance tends to reach the value of the bulk modulus and is almost entirely governed by it. Coulomb friction increases the stiffness slightly at high frequencies.

### 9.2. Impedance Of The Servo For Large Valve Openings.

The low frequency impedance is influenced by all parameters except the bulk modulus. Both the leakage and the coulomb friction increase the stiffness and the damping. An increase in perturbation amplitude decreases both the stiffness and the damping.

The high frequency impedance is mainly influenced by the coulomb friction force which substantially increases both the stiffness and the damping. The leakage make a large contribution to the damping and the bulk modulus gives small increases in both stiffness and damping.

### 9.3. The Effect Of Supply Pressure On Impedance.

An increase in the supply pressure generally increases the impedance of the servo. It is, however, possible to increase the stiffness or the damping by changes in this parameter. By a careful

choice of the supply pressure a system can be made to have a fast response of better damping characteristics.

#### 9.4. Comparison Of the Analogue And The Rig Results.

A comparison between the analogue and the rig results shows a qualitative agreement for stiffness and damping in response to changes in the static valve opening and the perturbation amplitude. A quantitative agreement is shown to exist for the small valve openings. At large valve openings the analogue results generally give a higher value of impedance except at small valve openings, if the values of the bulk modulus, leakages and the coulomb friction force are constant. But by varying the values of these parameters in the simulation a quantitative agreement with the rig results can be obtained for any particular test conditions. This would suggest that the value of the coulomb friction force estimated for the hydraulic servo at 80lbf. is too high. Also the values of the bulk modulus and the leakage coefficient do not remain constant as the valve opening increases. The leakages are a function of the flow and the pressure drop in the system  $(\frac{dQ}{dP})$  which change with the valve opening. The bulk modulus is likely to change due to dilation of the jack body with the temperature and at low pressure the effects of air in the fluid can drastically reduce the bulk modulus. Values of N from 40,000lbf/sq.in. upwards have been used by different experimenters to allow for the effect of air in the fluid. From analogue simulation the following values for the various parameters are estimated for the physical system.

Coulomb friction force:- 30 - 40 lbf.

Bulk modulus N:- variable but having a value of about  
120,000 lbf/sq.in. at very small openings.

Leakage coefficient:- variable  $4-16 \times 10^{-5}$  in<sup>5</sup>/lbf.sec.

### 9.5. Comparison Of The Analogue And The Theoretical Results.

A qualitative agreement between the analogue and the theoretical results is seen to exist but the theoretical results give a very low value of the impedance at large valve openings which cannot be related to the physical system. The inclusion of coulomb friction may improve the theoretical results but makes the analysis more complicated.

### 9.6. The Impedance Of The Control System.

The sub-system technique presents a means of obtaining the control system impedance by separate measurements on the servo and the control surface structure. During this study it was possible to apply the same force levels to the elastic systems, representing the hydraulic servo and the control system, and hence displacement responses were manipulated to give the control system impedance. In practice, however, it will be necessary to apply different force levels to the sub-system in which case mobilities or impedances will have to be measured. These can then be combined either manually or on a digital computer.

REFERENCES

1. Penny, J.E.T. 'An Investigation of the Impedance of a Powered Flying Control System'. Thesis submitted for Ph.D at the University of Aston Birmingham. September, 1966.
2. Olson, H.F. 'Dynamic Analogies', D. Van Nostrand, New York, 1943.
3. Soroka, W.W. 'Analog Methods in Computation and Simulation', McGraw Hill, New York, 1954.
4. Guillemin, E.A. 'Introductory Circuit Theory', John Wiley & Sons, New York, 1953.
5. Skilling, H.H. 'Electrical Engineering Circuits', John Wiley & Sons, New York, 1957.
6. Firestone, F.A. 'The Mobility and Classical Impedance Analysis', American Institute of Physics Handbook, McGraw Hill, 1938.
7. Firestone, F.A. 'Twist Earth and Sky with Rod and Tube, The Mobility and Classical Impedance Analogies', J.A.S.A. 28, 1117-1153, 1956
8. Church, A.H. 'Mechanical Vibrations', John Wiley and Sons, 1963.
9. Bishop, R.E.D. 'The Analysis and Synthesis of Vibrating Systems', J. Royal Aero. Soc., Oct. 1954.
10. Duncan, W.J. 'Mechanical Admittances and Their Applications to Oscillation Problems', R & M. 2,000, 1947.

11. Rayleigh, Lord 'The Theory of Sound' Second Edition, Macmillan 1894.
12. McCloy, D. 'Graphical Analysis Of The Step Response of Hydraulic Servomechanism', Proc.Instn.Mech. Engrs. Vol.182, Part 1, No.12, 1967-68.
13. Butler, R. 'A Theoretical Analysis Of The Response of a Loaded Hydraulic Relay', Proc.Instn.Mech. Engrs. Vol. 173, No.6, 1959.
14. McRuer, D.T. 'An Analysis of Northrop Aircraft Powered Flight Controls', Northrop Aircraft Inc. 1949.
15. Conway, H.G.  
Collinson, E.G. 'An Introduction to Hydraulic Servomechanism Theory', Proc.Conf. Hydraulic Servomechanisms 1953, 1 (Instn.Mech.Engrs.)
16. Harpur, N.F. 'Some Design Considerations of Hydraulic Servo of Jack Type', Proc.Conf. Hydraulic Servomechanisms 1953, 41 (Instn.Mech.Engrs.).
17. Sung, C.B. 'Control of Inertial Loads by Hydraulic Servo-Systems Through Elastic Structures', Proc.Symp. Recent Mech.Engng.Dev.Automatic controls 196), 63 (Inst.Mech.Engrs ,London).
18. Williams, H. 'Effect of Oil Momentum Forces on the Performance of Electro-hydraulic Servomechanisms', Proc.Symp.Recent Mech.Engng.Dev.Automatic Control 1960,31 (Instn.Mech,Engrs.,London).
19. Lambert, T.H.  
Davies, R.M. 'Investigation of the Response of a Hydraulic Servomechanism with Inertial Load', J.Mech. Engng.Sci.1963,5, No.3, 281.

20. Glaze, S.G. 'Analogue Techniques and The Non-Linear Jack Servomechanism', Proc.Symp.Recent Mech. Engng.Dev. Automatic Control 1960.
21. Jackson, A.S. 'Analog Computation' McGraw Hill Book Company, 1960.
22. Korn G.A. 'Electronic Analog and Hybrid Computers', McGraw  
Korn, T.M. Hill, 1964.
23. Rogers, A.E. 'Analog Computation in Engineering Design  
Connolly, T.W. McGraw Hill.
24. Duncan, D.C. 'Characteristic of Precision Servo Computer  
Potentiometers', Trans. AIEE Conf. Feed-back  
Systems, Atlantic City, N.J. 1951.
25. Fisher, M.E. 'The Optimum Design of Quarter-Square Multipliers  
With Segmented Characteristics', J.Sci.Instr.  
34, Aug, 1957.
26. Angelo, E.I. 'An Electron-beam Tube for Analog Multi-  
plication', Rev.Sci.Instr., 25(3) March, 1954.
27. Savet, P.H. 'Analog Computing by Heat Transfer', Electronic  
Eng., Nov., 1960.
29. Fuchs, H. 'A Hall-effect Analog Multiplier',  
Electronic Eng., Nov., 1960.
29. Price, R. 'An FM-AM Multiplier of High Accuracy and  
Wide Range', MIT Research Lab. Electronics  
Tech.Rept. 213, Mass., Oct., 1951.
30. Ryder, J.D. 'Engineering Electronics', McGraw Hill.

31. Turner, M.J. 'Stiffness and Deflection Analysis of Complex Structures', J. Aero. Sci. Vol.23 No.9, 805-824, Sept., 1954.
32. Gladwell, G.M.I. 'Branch Mode Analysis of Vibrating Systems', J. Sound Vib. 1, 41-59 (1964).
33. Hurty, W.C. 'Dynamic Analysis of Structural Systems Using Component Modes'. J. A.I.A.A. Vol.3, No.4, 678-685, April, 1965.
34. Przemieniecki, J.S. 'Matrix Structural Analysis of Substructures', J. A.I.A.A., Vol.1, No.1, 138-147, Jan., 1963.

ACKNOWLEDGEMENTS.

The Author wishes to thank and acknowledge:

Professor E. Downham for his supervision, help and encouragement throughout the period of this investigation.

Dr. J.E.T. Penny for making available his experimental and theoretical results.

The members of the academic and technical staff of the Department of Mechanical Engineering for their help and co-operation.

His wife for the typing of the thesis and for the understanding shown by her throughout the period of this research.

CORRIGENDA

Page.

21 Equation (2.38) should read:-

$$Z_{21} = \frac{m_1 m_2 w^4 - [K_1 m_2 + K_2 (m_1 + m_2)] w^2 + K_1 K_2}{K_2}$$

34 Equation (3.5) should read:-

$$Q_1 = \frac{V_1}{N} \frac{dP}{dt} + A \frac{dX_0}{dt} + Q_{j1} + Q_{o1}$$

35 Equation (3.7) should read:-

$$E + e = X_1 - X_0 + x_1 - x_0$$

36 Equation (3.19) should read:-

$$\frac{dQ_{j1}}{dP_j} = \frac{dQ_{j2}}{dP_j} = C_{jp}$$

51 Line 13, "from and ..... interpreted" should read;=...

"form and hence easily interpreted"

52 Equation (4.2) should read:-

$$\therefore V_0 = \left( \frac{R_f}{R_1} V_1 + \frac{R_f}{R_2} V_2 \right) / R_f \left( \frac{1}{R_1} + \frac{1}{R_2} - \frac{1}{R_f} \right)$$

Page.

- 90 The fifth line from the bottom "The output .... that of  $X_o$ "  
should read, "The sign of the coulomb friction force is the same as  
that of  $X_o$ ."
- 98 Fourth line from the bottom "A change in the value of N from.....  
.... of frequency", should read:-  
A change in the value of N from 40,000 lbf/sq.in to 120,000 lbf/sq.in.  
makes very little difference to stiffness on a basis of frequency.
- 103 9th line from the bottom "value of stiffness for N = 80,000 lbf/sq.in"  
should read:-  
Value of stiffness for N = 80,000 lbf/sq.in becomes larger.
- Fig.7.11 The title should read:-  
Effect of bulk modulus on stiffness for changes in frequency, valve  
opening = .010 in. Perturbation amplitude =  $\pm$  .005in.
- 108 Line 19 "The equilibrium condition requires that the forces  
 $F_{b2}$  and  $C_{c2}$  remain....." should read:-  
The equilibrium condition requires that the forces  $F_{b2}$  and  $F_{c2}$   
remain....."

Page.

109 Line 10, substitute " $F_{b2} = -F_{c2}$ " for  $F_{b2} = F_{c2}$ .

111 Equation (8.18) The numerator should read:-

$$(K + j\omega)^2 \cdot F$$

-----